Universidad de Córdoba

Departamento de
Química Analítica

SISTEMAS ANALÍTICOS DE RESPUESTA RÁPIDA BASADOS EN EL ACOPLAMIENTO DIRECTO DE SOPORTES PLANOS Y TÉCNICAS INSTRUMENTALES

RAPID RESPONSE ANALYTICAL SYSTEMS BASED ON THE DIRECT COUPLING OF FLAT SUPPORTS AND INSTRUMENTAL TECHNIQUES

Tesis Doctoral

María del Carmen Díaz Liñán

Córdoba, 2021

TITULO: *Sistemas analíticos de respuesta rápida basados en el acoplamiento directo de soportes planos y técnicas instrumentales*

AUTOR: *María del Carmen Díaz Liñán*

Campus de Rabanales
Ctra. Nacional IV, Km. 396 A
14071 Córdoba

https://www.uco.es/ucopress/index.php/es/
ucopress@uco.es

SISTEMAS ANALÍTICOS DE RESPUESTA RÁPIDA BASADOS EN EL ACOPLAMIENTO DIRECTO DE SOPORTES PLANOS Y TÉCNICAS INSTRUMENTALES

LOS DIRECTORES

LUCENA RODRIGUEZ RAFAEL - 30836901L
Firmado digitalmente por LUCENA RODRIGUEZ RAFAEL - 30836901L
Fecha: 2021.10.27 09:05:25 +02'00'

Fdo. **Rafael Lucena Rodríguez**

Profesor Titular del Departamento de Química Analítica de la Universidad de Córdoba

LOPEZ LORENTE ANGELA INMACULADA - 45742775F
Digitally signed by LOPEZ LORENTE ANGELA INMACULADA - 45742775F
Date: 2021.10.26 20:06:00 +02'00'

Fdo. **Ángela Inmaculada López Lorente**

Profesora Contratada Doctora del Departamento de Química Analítica de la Universidad de Córdoba

Trabajo presentado para aspirar al Grado de Doctor en Ciencias

LA DOCTORANDA

DIAZ LIÑAN MARIA DEL CARMEN - 31015999Q
Firmado digitalmente por DIAZ LIÑAN MARIA DEL CARMEN - 31015999Q
Fecha: 2021.10.27 17:54:26 +02'00'

Fdo. **María del Carmen Díaz Liñán**

Graduada en Química

Rafael Lucena Rodríguez, Profesor Titular del Departamento de Química Analítica de la Universidad de Córdoba; **Ángela Inmaculada López Lorente,** Profesora Contratada Doctora del Departamento de Química Analítica de la Universidad de Córdoba,

EN CALIDAD DE:

Directores de la Tesis Doctoral presentada por la Graduada en Química, MARÍA DEL CARMEN DÍAZ LIÑÁN, titulada "Sistemas analíticos de respuesta rápida basados en el acoplamiento directo de soportes planos y técnicas instrumentales",

CERTIFICAN QUE:

1) El trabajo experimental de la Tesis Doctoral ha sido desarrollado en los laboratorios del Departamento de Química Analítica de la Universidad de Córdoba.

2) A nuestro juicio, reúne todos los requisitos exigidos a este tipo de trabajo.

3) María del Carmen Díaz Liñán es la primera autora de todos los trabajos científicos presentados en esta Tesis Doctoral. De acuerdo con la normativa de esta Universidad y los acuerdos internos del Grupo de Investigación, el primer autor es responsable de la realización del trabajo experimental y de la producción de la primera versión del manuscrito. Además, ha participado activamente en las reuniones periódicas con los supervisores para comprobar y discutir el progreso de la Tesis Doctoral.

Y para que conste y surta los efectos pertinentes, expiden el presente certificado en Córdoba, octubre de 2021.

LUCENA RODRIGUEZ RAFAEL - 30836901L
Firmado digitalmente por LUCENA RODRIGUEZ RAFAEL - 30836901L
Fecha: 2021.10.27 09:06:01 +02'00'

Rafael Lucena Rodríguez

LOPEZ LORENTE ANGELA INMACULADA - 45742775F
Digitally signed by LOPEZ LORENTE ANGELA INMACULADA - 45742775F
Date: 2021.10.26 20:05:26 +02'00'

Ángela Inmaculada López Lorente

TÍTULO DE LA TESIS: SISTEMAS ANALÍTICOS DE RESPUESTA RÁPIDA BASADOS EN EL ACOPLAMIENTO DIRECTO DE SOPORTES PLANOS Y TÉCNICAS INSTRUMENTALES

DOCTORANDO/A: María del Carmen Díaz Liñán

INFORME RAZONADO DEL/DE LOS DIRECTOR/ES DE LA TESIS

La doctoranda María del Carmen Díaz Liñán es Graduada en Química por la Universidad de Córdoba. Se incorporó al grupo de investigación durante el último curso, para la realización del Trabajo de Fin de Grado, en el que destacó por su implicación y trabajo, y que presentó obteniendo calificación de Sobresaliente. En los siguientes dos cursos realizó el Doble Máster en Profesorado de Enseñanza Secundaria Obligatoria y Bachillerato, Formación Profesional y Enseñanza de Idiomas y en Química Aplicada, obteniendo Matrícula de Honor en el Trabajo de Fin de Máster. A partir de ese momento se dedicó intensamente al trabajo experimental que le ha permitido la realización de la tesis doctoral, cuya Memoria se presenta para su defensa como compendio de publicaciones.

La tesis doctoral desarrolla sistemas analíticos de respuesta rápida, basados en el acoplamiento de fases sorbentes basadas en papel con técnicas tanto espectroscópicas como espectrométricas. En este contexto, se han propuesto diversos soportes basados en papel sin modificar, y papel modificado con distintos materiales, tales como polímeros de impresión molecular y nanomateriales. El trabajo experimental se ha divido en tres bloques experimentales, de acuerdo con las distintas modificaciones del papel. En el primer bloque se evalúa la capacidad sorbente intrínseca del papel de filtro para la extracción de aminas biogénicas de muestras de cerveza y su posterior determinación mediante espectrometría de masas por infusión directa. En un segundo bloque se muestran los resultados de la modificación de papel con polímeros de impresión molecular obtenidos mediante disolución del polímero, y que se acoplaron a fluorimetría así como espectrometría de masas. Por último, se evaluó el potencial de papel modificado con nanoflores de plata como sustrato dual para espectroscopia Raman amplificada en superficie y espectrometría de masas en la modalidad de *paper-spray*.

La realización de la investigación recogida en la Memoria que se presenta ha permitido a la doctoranda adquirir una sólida formación analítica, adiestrándose en el manejo de técnicas, tales como la espectrometría de masas, técnicas espectroscópicas como la espectroscopia de fluorescencia, espectroscopia infrarroja y Raman, así como técnicas microscópicas para la caracterización de los materiales. Además de la aplicación analítica de los desarrollos, se ha llevado a cabo la síntesis y caracterización de nuevos materiales, buscando la simplificación de los procesos, siguiendo así los principios de la Química Analítica Verde.

La investigación realizada ha dado lugar a cinco artículos científicos publicados en revistas de alto impacto, y a la publicación de dos capítulos de libro, más otro en vías de publicación. También han sido fruto de esta tesis doctoral cinco comunicaciones a Congresos nacionales e internacionales, tres de ellas orales/flash.

Además, la doctoranda ha participado activamente en la supervisión de dos Trabajos de Fin de Grado y un Trabajo de Fin de Máster. Asimismo, ha participado en diversas actividades de divulgación de la ciencia.

Cabe destacar la capacidad de trabajo de la doctoranda, tanto individual como en grupo, así como la responsabilidad y el alto grado de implicación. Durante el desarrollo de la tesis doctoral ha demostrado pensamiento crítico, autonomía, motivación y creatividad, lo que ha repercutido positivamente en el desarrollo de esta. Además, las habilidades de comunicación tanto escrita como oral de la doctoranda, no sólo en su lengua materna, sino también en inglés, son reseñables.

Finalmente, consideramos que la investigación desarrollada y recogida en esta Memoria, reúne todos los requisitos necesarios en cuanto a originalidad, innovación y calidad.

Por todo ello, se autoriza la presentación de la tesis doctoral.

Córdoba, a 26 de octubre de 2021

Firma del/de los director/es

LUCENA RODRIGUEZ RAFAEL - 30836901L

Firmado digitalmente por LUCENA RODRIGUEZ RAFAEL - 30836901L
Fecha: 2021.10.27 09:06:55 +02'00'

Fdo.: Rafael Lucena Rodríguez

LOPEZ LORENTE ANGELA INMACULADA - 45742775F

Digitally signed by LOPEZ LORENTE ANGELA INMACULADA - 45742775F
Date: 2021.10.26 20:04:46 +02'00'

Fdo.: Ángela Inmaculada López Lorente

PUBLICACIONES DE LA TESIS DOCTORAL

A continuación, se muestran los parámetros de calidad de las **publicaciones de la Tesis Doctoral**, obtenidos del Journal Citation Reports para la categoría de Química Analítica.

Capítulo	Revista	Año de publicación	Factor de impacto	Cuartil
1	Analytical Methods	2020	2.896	3
2	Journal of Chromatography A	2021	4.759	1
4	Sensors and Actuators B - Chemical	2019	7.460	1
5	Microchemical Journal	2021	4.821	1
7	Analytical and Bioanalytical Chemistry	2020	4.142	2

El artículo publicado en la revista *Analytical and Bioanalytical Chemistry*, correspondiente al Capítulo 7 de la Memoria, fue seleccionado como *"Paper in Forefront"* y pertenece a la colección *"ABC Highlights: authored by Rising Stars and Top Experts".*

Además, el Capítulo 3 de la Memoria se encuentra en vías de publicación y forma parte del libro *Analytical Sample Preparation with Nano- and other High-Performance Materials.* Asimismo, el Capítulo 6 se publicó en 2020 en el libro *Solid-Phase Extraction.*

ÍNDICE/INDEX

OBJETO

AIM

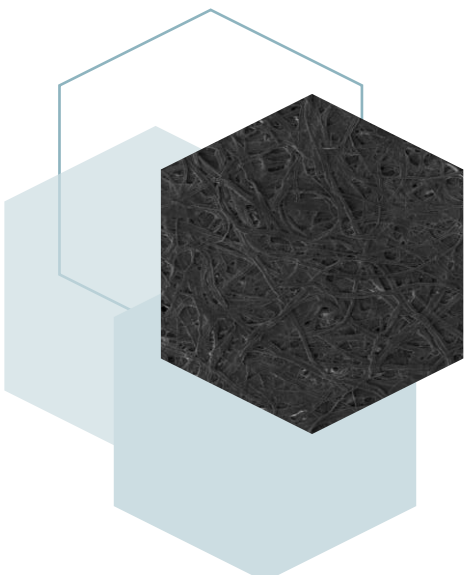

En las últimas décadas, la Química Analítica ha estudiado en profundidad el desarrollo de metodologías capaces de proporcionar resultados fiables de manera rápida para así responder a la creciente demanda informativa de la sociedad actual. En este contexto, la etapa de tratamiento de muestra se ha visto directamente afectada debido al tiempo que requiere y, además, por ser la principal fuente de error como consecuencia del alto grado de participación humana. La simplificación, miniaturización y automatización han sido las principales fuerzas impulsoras de la evolución del tratamiento de muestra en estos años. La aplicación de estas tres tendencias ha dado lugar a la aparición de las técnicas de microextracción. La reducción del consumo de reactivos, disolventes y energía, así como de los residuos generados, responden al compromiso social y medioambiental de la Química Verde y, al mismo tiempo, contribuyen al desarrollo de metodologías simples capaces de proporcionar resultados de calidad en un tiempo reducido.

Esta simplificación engloba, asimismo, a los materiales sorbentes empleados en las técnicas de microextracción. En esta línea, los dispositivos analíticos basados en papel han despertado un gran interés debido a las múltiples ventajas de este material como fase sorbente, entre las que destacan su flexibilidad, porosidad y bajo coste. Asimismo, en los últimos años, la modificación del papel con distintos materiales ha sido una tendencia estable que ha derivado en la mejora de la versatilidad de este soporte. La modificación del papel con polímeros o nanomateriales ha hecho posible el desarrollo de soportes planos con una elevada área superficial capaces de interaccionar con una gran variedad de analitos. No obstante, los procedimientos llevados a cabo para la modificación del papel a menudo son complicados y requieren un control muy estricto de las condiciones experimentales. Por este motivo, es necesario buscar alternativas capaces de solventar estas dificultades.

La simplificación de la etapa de tratamiento de muestra no supondría un gran avance si las técnicas instrumentales empleadas para la determinación de los analitos no estuviesen igualmente influenciadas por esta tendencia. En este sentido,

los soportes basados en papel han sido también muy útiles debido a su fácil manipulación y acoplamiento con técnicas instrumentales, como las técnicas espectroscópicas (fluorimetría, Raman, etc.) o la espectrometría de masas en la modalidad de *paper-spray*.

Teniendo en cuenta lo anteriormente expuesto, el objetivo principal de la Tesis Doctoral presentada en esta Memoria es el desarrollo de sistemas analíticos de respuesta rápida basados en el acoplamiento directo de soportes planos basados en papel con técnicas instrumentales, tales como la fluorimetría, la espectroscopia Raman y/o la espectrometría de masas. De este objetivo principal, surgen los siguientes objetivos específicos:

- Síntesis de soportes planos basados en papel compatibles con espectrometría de masas en la modalidad de infusión directa. Este objetivo se afronta en los **Bloques II y III** con el desarrollo de dos soportes planos basados en papel. En primer lugar, se ha explotado la capacidad sorbente intrínseca del papel **(Capítulo 2)**. En el segundo caso, se ha modificado papel de filtro con un polímero de impresión molecular para mejorar la selectividad en el aislamiento de los analitos **(Capítulo 5)**.
- Síntesis de soportes planos basados en papel compatibles con técnicas espectroscópicas. En el **Capítulo 3** de la Memoria se describe el empleo de sorbentes con una alta selectividad en diversas técnicas instrumentales. Por otro lado, se ha desarrollado un sustrato basado en papel modificado con un polímero de impresión molecular y se ha propuesto su acoplamiento con fluorimetría **(Capítulo 4)**.
- Síntesis de soportes planos basados en papel duales compatibles tanto con técnicas espectroscópicas como con espectrometría de masas. Esta investigación se desarrolla en el **Bloque IV** de la Memoria, donde se describen las tendencias sobre las membranas modificadas con nanomateriales **(Capítulo 6)**. Además, se llevó a cabo la modificación de un sustrato basado en papel con nanoflores de plata para la determinación de ketoprofeno en

muestra de saliva mediante espectroscopia Raman amplificada en superficie y espectrometría de masas ambiental en la modalidad de *paper-spray* **(Capítulo 7)**.

Por otro lado, también se han desarrollado los siguientes objetivos transversales durante el transcurso de la Tesis Doctoral:

- Caracterización de los soportes sintetizados mediante diversas técnicas instrumentales.
- Aplicación de los procedimientos desarrollados en el análisis de alimentos y muestras biológicas.

In the last decades, the development of methodologies able to provide rapid and reliable results has been deeply investigated in order to address the growing information demand of modern society. In this context, the sample preparation field is greatly concerning, since it is one of the most time-consuming steps and the main source of errors in the analytical procedure, due to the high level of human intervention. Simplification, automation and miniaturization have been the three main tendencies followed in the sample preparation field in the past years, leading to the rise of the microextraction techniques. Furthermore, the decrease of reagents, solvents and energy consumption agrees with the Green Chemistry principles and at the same time contributes to the development of methodologies capable of providing high-quality results in a shorter time.

The simplification also involves the materials used in the microextraction techniques. Paper-based analytical devices have emerged as a very promising material due to the advantages of paper as a sorbent, e.g., flexibility, porosity or cost-effectiveness. Likewise, the chemical modification of paper with different materials is a steady trend that has led to the increase of the versatility of this support. The modification of paper with polymers or nanomaterials has enabled the synthesis of flat supports with a high surface area able to interact with a wide variety of analytes. However, the procedures employed to carry out these modifications are usually tedious, and a strict control of the experimental conditions is mandatory. For this reason, it is of high importance searching for alternative methods that can overcome this drawback.

The simplification of the sample preparation step must consider not only the materials used, but also the instrumental techniques employed for the determination of the analytes. In this sense, paper-based analytical devices have been really useful due to their easy handling and coupling to instrumental techniques, such as spectroscopic techniques or paper-spray mass spectrometry.

Based on the foregoing, the foremost aim of this Doctoral Thesis is the development of rapid response analytical systems based on the coupling of paper-based flat

supports and instrumental techniques, such as fluorimetry, Raman spectroscopy or mass spectrometry, together with substrates that can be simultaneously employed in different techniques. The specific objectives derived from this general objective are as follows:

- Synthesis of paper-based flat supports compatible with direct infusion mass spectrometry. This research is detailed in **Blocks II and III**, where two paper-based flat supports are developed. On the one hand, the intrinsic sorbent capacity of non-modified cellulose was exploited in **Chapter 2**. On the other hand, the obtention of a molecularly imprinted paper is explained in **Chapter 5** of this Doctoral Thesis.
- Synthesis of paper-based flat supports compatible with spectroscopic techniques. The employment of selectivity enhanced sorbents with different instrumental techniques is described in **Chapter 3** of this Doctoral Thesis. Furthermore, a molecularly imprinted paper-based analytical device was developed and combined with fluorimetry **(Chapter 4)**.
- Synthesis of dual paper-based flat supports compatible with both spectroscopic techniques and mass spectrometry. The results of this study are shown in **Block IV**, where the current trends about particle loaded membranes are firstly described **(Chapter 6)**. On the other hand, the development of a silver nanoflower-coated paper for the determination of ketoprofen in saliva samples via Surface-enhanced Raman spectroscopy and ambient pressure mass spectrometry was carried out **(Chapter 7)**.

Additionally, the following specific objectives have been treated transversally throughout the entire Doctoral Thesis:

- Characterization of the supports obtained employing various instrumental techniques.
- Application of the developed procedures in the analysis of food products and biological samples.

BLOQUE I

INTRODUCCIÓN

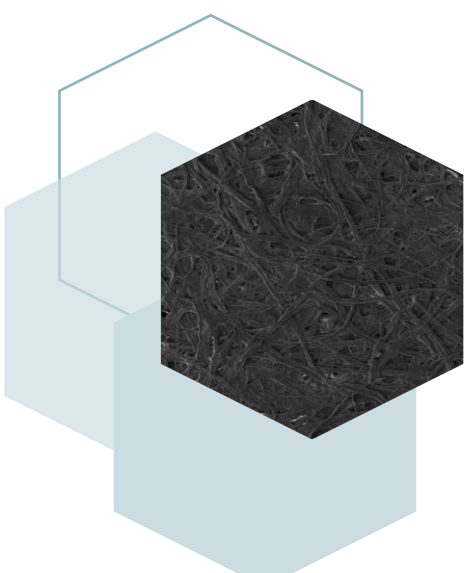

En los últimos años se ha hecho evidente la necesidad de desarrollar procedimientos de medida que proporcionen resultados rápidos y fiables. La Química Analítica ha hecho grandes esfuerzos por reducir el tiempo, así como la cantidad de reactivos y energía que emplea en el proceso de medida químico para así poder responder a esta demanda. La etapa crítica del proceso de medida químico es la toma y el tratamiento de muestra debido al alto grado de participación humana y a la cantidad de tiempo que requiere, aproximadamente el 80% del total. Sin embargo, es una etapa vital para la obtención de resultados debido a la incompatibilidad de la mayoría de los equipos con la matriz de la muestra o a la baja concentración a la que se encuentran los compuestos de interés. Además, no es un procedimiento generalizado para todas las muestras, sino que, dependiendo de su naturaleza, el tratamiento varía, lo que aumenta la complejidad de esta etapa.

Con frecuencia, se emplean técnicas de (micro)extracción durante el tratamiento de muestra con el objetivo de aislar y preconcentrar los compuestos de interés, a la vez que se eliminan las interferencias de la matriz de la muestra que dificultan la determinación de los analitos. En este contexto, el papel se ha convertido en un potente aliado de la Química Analítica debido a sus ventajas como fase sorbente, por ejemplo, su flexibilidad, bajo coste y porosidad. En este Bloque de la memoria de la Tesis Doctoral se recogen las últimas tendencias desarrolladas que tienen como eje central el papel y que suponen una mejora considerable para la etapa de tratamiento de muestra, así como las características de los distintos tipos de papel y las posibles modificaciones que se pueden llevar a cabo para aumentar su versatilidad.

Capítulo 1

Paper-based sorptive phases for microextraction and sensing

Analytical Methods, 12 (2020) 3074-3091

ROYAL SOCIETY OF CHEMISTRY

Analytical Methods
12 (2020) 3074–3091

Paper-based sorptive phases for microextraction and sensing

M. C. Díaz-Liñán, M. T. García-Valverde, R. Lucena*, S. Cárdenas, A. I. López-Lorente

Departamento de Química Analítica, Instituto Universitario de Investigación en Química Fina y Nanoquímica IUNAN, Universidad de Córdoba, Campus de Rabanales, Edificio Marie Curie, E-14071 Córdoba, Spain

The simplification of the analytical procedures, including cost-effective materials and detectors, is a current research trend. In this context, paper has been identified as a useful material thanks to its low price and high availability in different compositions (office, filter, chromatographic). Its porosity, flexibility, and planar geometry permit the design of flow-through devices compatible with most instrumental techniques. This article provides a general overview of the potential of paper, as substrate, on the simplification of analytical chemistry methodologies. The design of paper-based sorptive phases is considered in-depth, and the different functionalization strategies are described. Considering our experience in sample preparation, special attention has been paid to the use of these phases under the classical microextraction-analysis workflow, which usually includes a chromatographic separation of the analytes before their determination. However, the interest of these materials extends beyond this field as they can be easily implemented into spectroscopic and electrochemical sensors. Finally, the direct analysis of paper substrates in mass spectrometry, in the so-called paper-spray

technique is also discussed. This review is more focused on presenting ideas rather than the description of specific applications to draw a general picture of the potential of these materials.

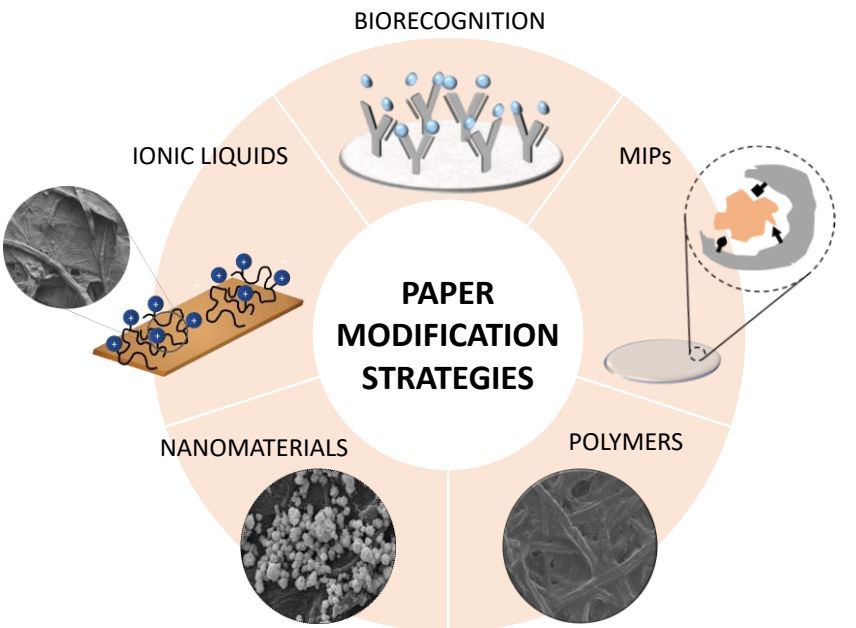

1. Introduction

Analytical Chemistry (AC) must answer the growing information demand of modern society as one of its main challenges. Although the information reliability is crucial, the speed at which this information is generated is essential to address the current global threats by rapid decision making, as the COVID-19 outbreak has demonstrated [1]. AC has become socially responsible and more conscious of its impact [2,3]. For example, analytical methodologies have been highly influenced by the Green Chemistry principles in the last decade, which has led to the downscale of the required resources (reagents, solvents, and energy) and the generated residues [4,5]. However, this impact goes beyond the environmental issues, as Prof. de la Guardia *et al.* suggest with the Democratic AC concept, [6] and AC must become more accessible and easier to be applied. This objective can only be achieved if simple methodologies, complemented by exhaustive and reliable methods, are developed. This simplification must involve not only the instrumentation [7] but also the materials [8] used to get the results.

Paper-based analytical devices (PADs) are currently attracting great attention due to their easy and rapid preparation, user-friendliness, cost-effectiveness, versatility, flexibility and portability, high porosity, biodegradability, biocompatibility and non-toxicity, among others [9]. All these properties result from the paper that is used as the substrate for the development of such devices. Depending on the application of the PADs, careful selection of the type of paper taking into account its characteristics (such as hydrophilicity, porosity, surface smoothness, cellulose content, and cost) is mandatory, as these characteristics will affect the final performance of the PAD. As will be further discussed, different types of paper have been described for the development of PADs, which include chromatographic paper, filter paper (i.e., that derived from cotton which accounts about 95% of cellulose), office paper [10] (which comprises about half of cellulose and other compounds like lignin or calcium carbonate), cardboard, and other types of papers such as nitrocellulose paper [11]. In this article, the potential of paper for the development of analytical devices is

presented from the perspective of a research group working on microextraction techniques. Initially, the role of paper as a substrate for the design of sorptive phases in solid-phase microextraction (SPME) will be presented, making emphasis on the versatility of the different materials. Also, paper-based analytical devices have been used together with spectroscopic [12], electrochemical [13], and, more recently, mass spectrometric detection [14], in different formats such as test strips, microchips or microfluidic [15] devices. In some of these approaches, the target compounds are isolated from the sample to the PADs, where the detection takes place, based on the same chemical interactions used in microextraction approaches. The scheme of these strategies is depicted in Fig. 1 and the content of these sections will be complemented with specific reviews of PADs.

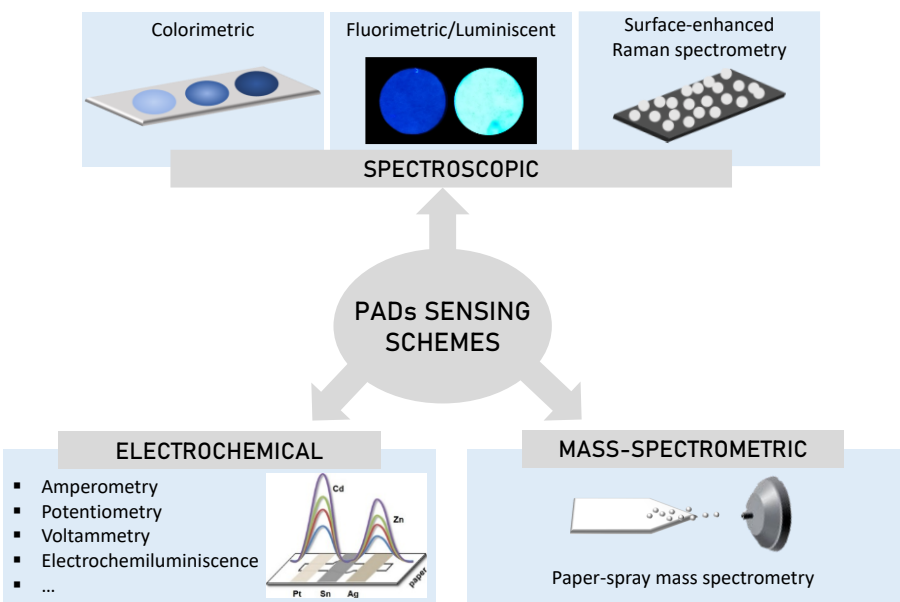

Figure 1. Scheme of those approaches that involve the isolation of the target compounds from the sample to the PADs where the detection takes place. They will be considered in depth in the last sections of the article.

2. Paper-based sorptive phases in microextraction

Although SPME is a consolidated technique in sample preparation, it is in constant evolution. Since its first proposal in 1989, the technique has evolved in different directions, including, among others, the synthesis of new extraction phases, [16] the design of new extraction formats [17,18] and the development of novel workflows [19,20]. In SPME the efficacy of the extraction, defined as the amount of analyte extracted (n_e), can be mathematically expressed as

$$n_e = \frac{K_{es} V_e V_s C_s}{K_{es} V_e + V_s} \qquad (1)$$

where K_{es} is the partition constant for the analyte that has an initial concentration in the sample of C_s; V_e is the volume of extraction phase, and V_s is the sample volume [21]. As it occurs in other extraction techniques, the SPME efficacy depends on the volume of the extraction phase. This relationship becomes even linear when the sample volume is very large ($V_s >> K_{es}V_e$).

$$n_e = K_{es} V_e C_s \qquad (2)$$

From this equation, it can be concluded that larger V_e would provide better sensitivity levels. However, in the in-fiber format, a larger V_e involves a thicker coating, which hinders the extraction kinetics. In fact, the time required to achieve a 95% extraction yield can be defined as

$$t_{95\%} = \frac{3\delta K_{es} d}{D} \qquad (3)$$

where *d* is the thickness of the coating, *D* is the diffusion coefficient of the analyte in a given coating, and δ is the thickness of the boundary layer. Thin-film microextraction (TFME) solves this compromise situation by changing the format of

the sorptive phase from a fiber to a planar substrate [22,23]. In planar geometry, a high V_e can be distributed on a larger surface, thus resulting in a thin coating.

In the last years, different materials including both commercial and lab-made ones, have been proposed as sorptive media in TFME [23,24]. In this context, cellulosic paper emerges as a suitable substrate for the fabrication of sorptive phases thanks to its high availability, low price, planar, and porous structure. This porous structure allows the design of thin sorptive coatings with a high superficial area which has a positive effect on the thermodynamics (high V_e in eqn (2)) and kinetics (low *d* in eqn (3)) of the extraction. The potential use of paper as a sorptive phase in microextraction was outlined at the end of the 1990s by Hurtubise and coworkers [25,26] who used Whatman 1PS paper for the isolation and preconcentration of polycyclic aromatic hydrocarbons (PAHs) from water. Whatman 1PS is commercially available as phases' separator in liquid–liquid extractions due to its hydrophobic character, provided by a stabilized silicone coating, which allows it to interact with the analyte by dispersion forces. In these initial publications, the analytes were directly detected, without elution, on the substrate by luminescent techniques. This approach envisioned the potential of paper for designing optical sensors.

Although unmodified paper can be used for the extraction of analytes [27], Ackerman and Hurtubise realized soon the possibility of anchoring sorptive phases on the paper taking advantage of its chemically rich surface, where several hydroxyl and some carbonyl groups can be found. In 2002 they scrutinized the dip-coating (which will be further discussed) and sol–gel techniques to immobilize some polysiloxanes over the paper substrate [28].

The modification of paper includes several strategies that can be classified into two main groups, namely: those involving a covalent immobilization of the sorptive phase and those based on the physical deposition of the phase over the paper.

Table 1. Paper-based sorptive phases in solid phase microextraction[a].

Paper substrate	Coating	Synthesis method	Analyte	Sample	Extraction approach	Instrumental technique	Reference
Whatman 1PS	Stabilized silicone	Commercial	Benzo(a)pyrene	Aqueous solution	Direct immersion	Fluorescence	[25]
Whatman 1PS	Stabilized silicone	Commercial	Polycyclic aromatic hydrocarbons	Aqueous solution	Direct immersion	Fluorescence and phosphorescence	[26]
Whatman	-	Commercial	8-Hydroxy-2'-deoxyguanosine	Urine	Direct immersion	CE-LIF	[27]
Whatman 1	Polysiloxanes	Sol-gel and dip-coating	Polar aromatic compounds and polycyclic aromatic	Aqueous solution	Direct immersion	Fluorescence and phosphorescence	[28]
Whatman	Hydroxil and phosphate groups	Mercerization and phosphorilation	Nickel	Water samples	Direct immersion	Scanometry	[29]
Whatman 44	Chrolosilanes and isocyanates	Covalent bonding	Natural strogenic hormones	Water samples	Direct immersion	LC-FD	[30]
Filter paper	1-Dodecylimidazolium	Covalent bonding	Bisphenol A	Sunflower oil	Direct immersion	LC-UV	[31]
Filter paper	Polydopamine	Covalent bonding	Nitrophenols	Vegetable oil	Direct immersion	LC-UV	[32]
Whatman 44	Aptamer	Covalent bonding after previous activation	Codeine	Urine	Direct immersion	ESI-IMS	[33]
Whatman 1	ZrO2	Sol-gel	Ribonucleosides	Urine	Direct immersion	Nano ESI-IMS	[34]

Table 1 (Contd.)

Paper substrate	Coating	Synthesis method	Analyte	Sample	Extraction approach	Instrumental technique	Reference
Filter paper	Functionalized ZnO nanorods	Hydrothermal treatment and covalent bonding	Phenylurea herbicides	Water sample	Direct immersion	LC-UV	[35]
Cellulose	Polypyrrole	Bulk synthesis and deposition into a planar format	DNA	Aqueous solutions	Electrochemical driven SPME	Fluorescence	[37]
Filter paper	Polystyrene	Dip-coating	Methadone	Urine	Pipette tip extraction	GC-MS	[39]
Filter paper	ZnO nanoparticles and polyamide	Dip-coating	Organophosphorous pesticides	Water samples	Direct immersion	GC-FID	[44]
Filter paper	Graphene oxide and polyamide	Dip-coating	Organophosphorous pesticides	Water samples	MEPS	GC-FID	[45]
Filter paper	Metal organic frameworks and chitosan	Dip-coating	Triazine herbicides	Water	Direct immersion	LC-MS/MS	[46]
Filter paper	Single wall carbon nanohorn	Dip-coating	Antidepressants	Urine	Pipette tip extraction	DI-MS	[47]
Filter paper	Polymeric ionic liquid	Dip-coating and covalent bonding	Anti-inflammatory drugs	Urine	Direct immersion	LC-MS/MS	[48]

[a] LC, liquid chromatography; GC, gas chromatography; CE, capillary electrophoresis; FD, fluorescence detection; UV, ultraviolet detection; ESI, electrospray; IMS, ion mobility spectrometry; LIF, laser induced fluorescence; MS, mass spectrometry, MS/MS, tandem mass spectrometry; FID, flame ionization detection; DI, direct immersion.

2.1. Paper-based sorptive phases prepared by the covalent immobilization of the coating

Paper, due to its high cellulose content, is a polar substrate that can interact with the target compounds by hydrogen-bonding [27], and cation exchange [29]. However, if the interaction with nonpolar or semipolar analytes is intended to be promoted, other coatings must be incorporated. The covalent immobilization of sorptive phases drives to very stable coatings, although it involves more complex synthetic routes in some cases. Saraji *et al.* evaluated the modification of paper with chlorosilanes and isocyanates for the extraction of some natural estrogenic hormones [30] demonstrating that those papers modified with phenylisocyanate provided a superior extraction performance as they combine different type of interactions (mainly dispersion forces and π–π) with the target analytes. This article is also relevant as it proposed synthetic routes like those employed for silica derivatization, thus indicating the high level of versatility than can be expected for paper coating. Up to date, this versatility has covered simple functional groups, polymers (both synthetic and natural ones), metal oxides, and nanoparticles (NPs). The main developments are included in Table 1 where the information is intentionally general to focus the attention on the usefulness of the substrates rather than in the specific instrumental techniques.

In 2017, Ye *et al.* proposed the immobilization of the ionic liquid 1-dodecylimidazolium to exploit its full sorption capacity [31]. The use of ionic liquids as solvents is somewhat limited by their viscosity that reduces the diffusion rate of the analytes. Their immobilization in a paper with a high surface (100 $m^2 \cdot g^{-1}$) increases the surface to volume ratio of the solvents improving the extraction kinetics. Interestingly, this article describes one of the limited applications of paper-based sorptive phases in non-polar matrices, where the π–π interactions with the target analyte (bisphenol A) are boosted. The same research group proposed the immobilization of polydopamine for the extraction of nitrophenols in oil [32]. The synthesis of the coating is straightforward as it only requires the incubation of the

paper in a dopamine solution at pH 8.5. The modification generates a rougher surface.

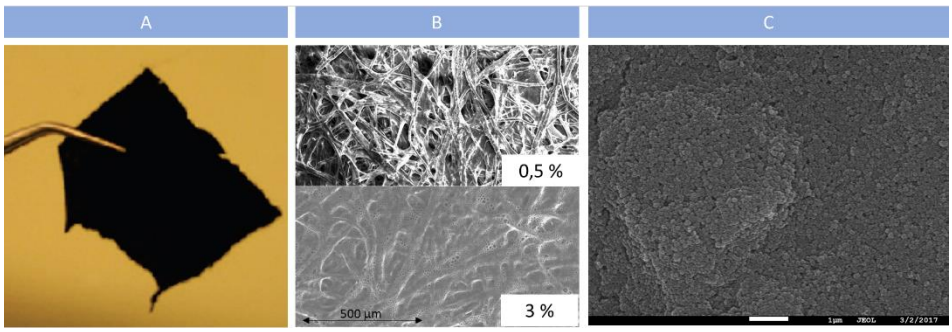

Figure 2. (A) Picture of conductive paper synthesized by the chemical modification of cellulose with a polypyrrole coating. Reproduced from ref. [36] with permission from American Chemical Society, copyright 2008. (B) Scanning electron micrographs of a paper coated with a 0.5% and 3% of polystyrene. Adapted from ref. [39] with permission from Elsevier, copyright 2017; (C) scanning electron micrograph of a paper coated with a suprastructure of single wall carbon nanohorns. Reproduced under the terms of the Creative Commons Attribution License from ref. [47].

The use of selectivity enhanced polymers can be essential in microextraction, where the amount of sorptive phase is reduced. In this sense, the limited capacity is saved for the analyte avoiding the retention of matrix components. Aptamers, which are DNA molecules artificially selected to bind a specific target analyte, have also been immobilized in paper for the selective extraction of codeine [33]. The high selectivity of the extraction allowed to circumvent the chromatographic separation since the analytes are directly measured by ion mobility spectrometry.

Paper can also be modified with metal oxides and NPs. Wan *et al.* coated paper with a thin layer of ZrO_2 via a sol–gel reaction. The selective interaction of this oxide with diol containing compounds allowed the extraction of some ribonucleosides from urine and their simple determination by nano electrospray ionization (nano ESI) emitters and tandem mass spectrometry [34]. Also, Saraji and coworkers have

proposed the synthesis of ZnO nanorods modified with phenylcarbamate for the extraction of phenylurea herbicides [35].

In all the above-described examples, the sorptive phase is prepared by the direct modification of paper, which maintains its planar structure during the synthesis. In our experience, this method can be somewhat problematic in some cases due to the slow diffusion of the reagents from the bulk solution to the paper surface. This limitation can be avoided if micro- or nanocellulose is used as the precursors since these materials can be easily dispersed in the reaction medium, guarantying a good functionalization. Once the cellulose has been modified, it can be transformed into a planar substrate by simple deposition [36]. Razak *et al.* applied this strategy to prepare a conductive paper based on a polypyrrole coating [37]. The paper, whose structure is similar to that presented in Fig. 2A, is used as a working electrode in electro mediated SPME where the ion exchange capacity can be modulated playing with the applied voltage. In fact, this material provided a rapid extraction and release of DNA, reducing the equilibration time from hours to minutes.

2.2. Paper-based sorptive phases prepared by the physical deposition of the coating

Paper-based sorptive phases can be easily synthesized by the dip-coating method [38] using a solution or dispersion containing the actual sorptive phase as the precursor. The following applications are all included in Table 1 that tries to draw the general picture of the potential of paper-based sorptive extraction. In 2017 our research group evaluated this strategy using commercial polystyrene (PS) as the extraction phase [39]. The procedure consists of two consecutive and straightforward steps that can be repeated several times until the desired coating thickness is achieved. In the first step, a paper segment is immersed in a chloroformic solution containing PS at a concentration of 3% w/v. Later, in a second step, the paper is collected and dried, and the evaporation of the solvent creates a thin film of the PS over the paper surface. The dip-coating technique allows

exploiting the fibrous structure of the paper, although this aspect depends on the appropriate concentration of the precursor and the number of dips. Fig. 2B shows the scanning electron microscopy pictures of two phases prepared at different concentrations of PS. While the fibrous structure of the paper is maintained for a PS concentration of 0.5% (w/v), the surface becomes smoother for a PS concentration of 3% (w/v). The compromise between a high superficial area and a high sorption capacity must be therefore optimized in each application. In the aforementioned approach, the thin film microextraction was done by introducing a segment of the modified paper in a pipette tip and using the pipette as a pumping system. Although this procedure is quite simple and very convenient for bioanalysis, the percentage of the sample that gets close contact with the paper is low, thus reducing the real potential of the approach.

The dip-coating technique can be easily adapted to other polymers, if an appropriate solvent is found, and their combination with nanoparticles. This combination, usually named as polymeric nanocomposites, shares in a synergic way the properties of both the polymer and the nanomaterials [40]. Our group proposed in 2018 a functional paper containing a nanocomposite of polyamide and TiO_2 NPs where the sorption capacity of the polymer is combined with the photocatalytic features of the nanomaterial [41] In this general dip-coating procedure, the evaporation of the solvent step can be substituted by a simple solvent changeover, as it has been described for other polymeric nanocomposites [42,43]. Ayazi *et al.* have applied this alternative to synthesizing polymeric nanocomposite coatings based on polyamides and containing ZnO NPs [44] and graphene oxide [45]. In this case, the precursor medium is obtained by dispersing the nanomaterial in a solution of the polyamide in formic acid. The paper is then immersed in this solution and subsequently introduced in water. The solvent changeover induces the gelation of the polyamide, since it is insoluble in water, around the NPs thus creating the coating. Once synthesized, these papers can be applied under different workflows. The simplest one consists of the incubation of the paper into the sample solution

[44] but these phases are also compatible with the microextraction in packed sorbent technique (MEPS) [45]. MEPS has important benefits related to its potential automation and its efficiency as the sample is forced to pass through the sorptive phase. In this interesting approach, the paper is cut in a circular shape (the internal diameter must fit with the syringe internal diameter) and packed between two polypropylene frits. In this context, chitosan has also been proposed as an adhesive element for the immobilization of metal–organic frameworks on paper for the extraction of triazine herbicides [46].

In the polymeric nanocomposite coating, the polymer plays a crucial role in the mechanical stabilization of the NPs. In fact, it entraps the NPs, avoiding their leaching during the extraction. However, the synthesis of pure NPs coatings has also been proposed. In this sense, Ríos-Gómez *et al.* described the synthesis of a monolithic carbon paper based on the physical immobilization of single-wall carbon nanohorns (SWCNHs) for the extraction of several antidepressant drugs from urine [47]. This work takes advantage of the ability of SWCNHs to form ordered nanometric aggregates, called dahlia, in solution. These aggregates can be assembled into suprastructures of high mechanical stability when the solvent is evaporated. Fig. 2C shows the SEM picture of this suprastructures phase over a paper surface. The aggregates confer the paper with a porous coating, which clearly increases the extraction efficiency.

The dip coating and the covalent immobilization of the sorptive phase have also been combined for the synthesis of paper coated with polymeric ionic liquids (PIL). The procedure involves the immersion of the paper in an aqueous solution of PIL followed by its the thermal curation at 150 °C [48]. The thermal treatment is not aimed only to achieve the evaporation of water but also allows the interaction of the aminated polymer with some free carbonyl groups in the cellulose structure thus allowing the covalent anchoring of the PIL. PIL-paper has been applied to the extraction of some anti-inflammatory drugs from biofluid taking advantage of the dual interaction (hydrophobic and anion exchange) of the sorptive phase.

3. Paper-based spectroscopic sensors

Spectroscopic detection is one of the straightforward methods for the determination of compounds. This technique is widely used in diverse fields due to its multiple advantages. On the one hand, it is a rapid and direct technique, providing reproducible and reliable results within seconds or a few minutes [49–51]. On the other hand, the wide variety of spectroscopic detectors that exist nowadays include many portable devices, thus having the opportunity to perform on-site measurements [52]. Furthermore, common spectroscopic detectors are user-friendly [52]. In the last years, spectroscopic detection, specifically colorimetric detection, has encountered a very useful tool in smartphones due to the possibility to integrate the intake of results as well as the readout in the same device, while being also a lightweight platform [52,53].

The use of paper as the substrate for spectroscopic sensing broadens the application scope of this technique due to the combination of its multiple advantages as a substrate and the already mentioned advantages of spectroscopic detection, thus having a synergistic relation between both. Paper provides with superior stability [54,55], easier handling and flexibility [54,56] to the sensor which facilitates its incorporation to other instrumental devices [57]. It provides a bright, high-contrast, colorless background [54], which is of high importance in optical sensing, since most of these sensors are based on color-change reactions or the emergence of fluorescence. Also, the paper coating can act as an extractant phase, preconcentrating the analytes and, thus, improving the sensitivity [50,53]. Besides, since paper can be easily modified via deposition of compounds (Fig. 3), immobilization of nanostructures [58] or polymers [57], it is possible to develop a specific sensor for almost any compound. Regarding this, gold and silver nanoparticles or quantum dots (QDs) are widely used as signal reporters due to their inherent optical properties [59] while polymers can act as an extractant component or a net for the immobilization of the nanostructure. The illumination in the optical PADs plays a key role since it may cause variations in color intensity and

hue [54], and it is usual to perform the measurements inside a controlled light box or making further image treatment.

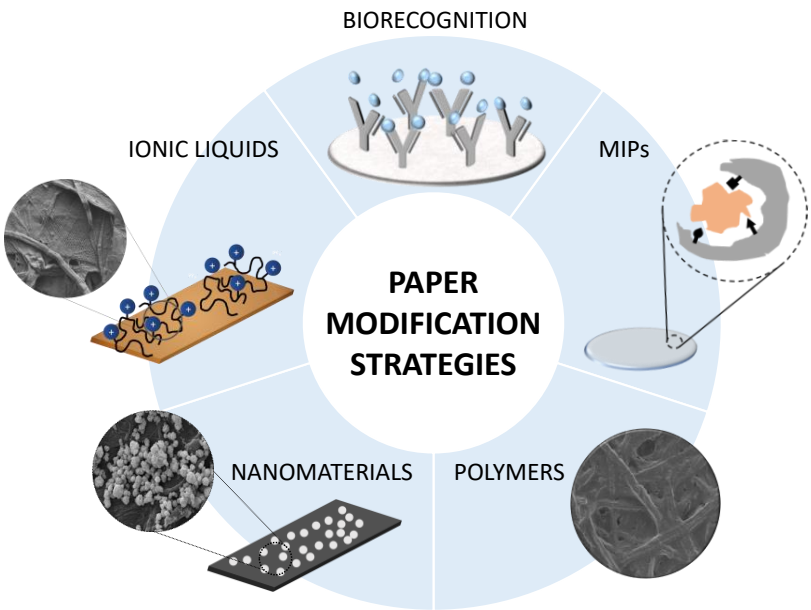

Figure 3. Modification of the surface of paper with different materials, namely nanomaterials, polymers, molecularly imprinted polymers (MIPs), biomolecules such as antibodies or aptamers, ionic liquids, among others.

While most of the spectroscopic sensors are based on photometrical and fluorescent detection, other spectroscopic techniques have made their way to the top in the last years, being surface enhanced Raman spectroscopy (SERS) an example. This technique is based on the enhancement of Raman scattering of molecules adjoining metallic nanostructures, e.g., gold and silver nanoparticles [60]. Silicon is typically used as substrate in SERS approaches, nevertheless, the advantages of paper have outshined those of silicon [54]. For instance, hydrophilicity plays a critical role, since the solution containing the nanoparticles can be easily transferred to the paper by

simple immersion [61]. Furthermore, the porous structure of paper allows the immobilization of nanoparticles throughout the entire net, whereas in silicon they can only occupy the surface where they are deposited, thus leading to more sensitive sensors.

This section aims to discuss the recent advances in paper-based spectroscopic sensors, more specifically colorimetric and fluorescence. Furthermore, paper-based sensors coupled with other spectroscopic techniques will also be discussed.

3.1. Colorimetric PADs

Paper-based colorimetric sensors are widely used nowadays due to its rapid response and visual readout [55], providing reliable results even in naked-eye screening tests [49], e.g., pH strips [55,62], pregnancy tests [55], urine infection detection [62], etc. Furthermore, when coupled to optical detectors, it is possible to quantify the color intensity [49,50,54]. Thepchuay *et al.* synthesized the first paper-based biosensor for the direct quantification of ethanol content in whole blood via specific enzymatic colorimetric detection involving alcohol oxidase (AOX), horseradish peroxidase (HRP) and 2'-azino-bis(3-ethylbenzothiazoline-6-sulfonic acid) diammonium salt (ABTS) [63]. A device consisting of two layers of filter paper held together by a double-sided mounting tape, which has a circular disc cut out, i.e., the headspace, was designed. The reagent is deposited on one layer and the sample onto the opposite layer, and then both are covered with sticky tape. The diffusion of ethanol across the thin headspace led to the color change of ABTS from light to dark green, and the surface was photographed with a professional camera to obtain the mean value of the color intensity, which was then employed for analysis. This portable, low cost, and disposable device allows readout within 5 min, which is suitable for roadside and toxicological tests.

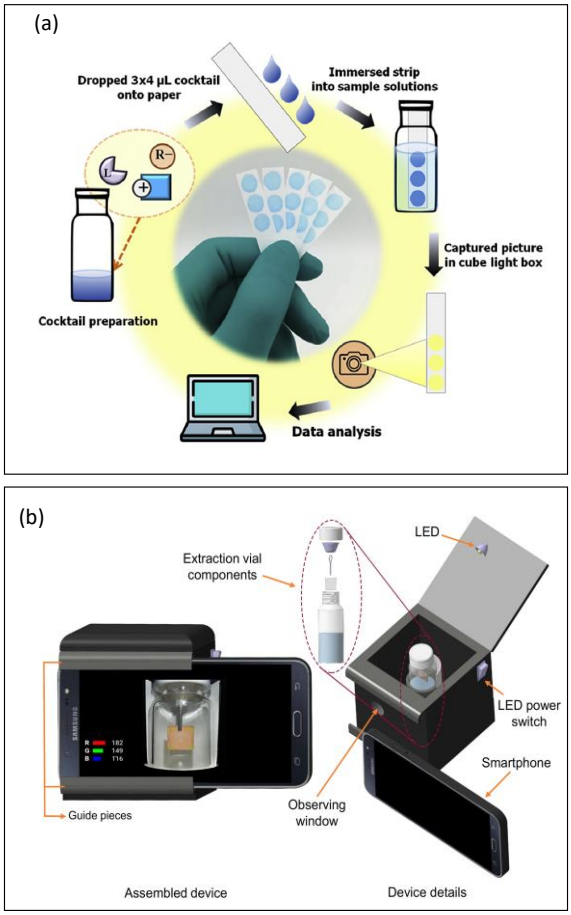

Figure 4. (a) Schematic illustration of the fabrication of a colorimetric sensor for the determination of Ag^{+} and Hg^{2+} via reaction with chromoionophore XIV. Reproduced from ref. [64] with permission from Elsevier, copyright 2020; and (b) illustration of the experimental setup employed in the determination of sulfite in food samples. Reproduced from ref. [53] with permission from Elsevier, copyright 2019.

Heavy metals comprise an important problem regarding pollution, especially mercury and silver ions, which are pollutants present in water, soil, food, and cleaning products. Phichi *et al.* developed a PAD based on bulk ion-selective optodes

for the determination of these pollutants in different water sources and cleaning products [64]. As observed in Fig. 4a, the mix of the reagents, containing chromoionophore XIV, was dried onto the paper strip, resulting in the apparition of blue color from the protonated form of this compound. Then, the strip was immersed in the sample, resulting in a color change from blue to yellow, the deprotonated form of the chromoionophore XIV. The colored surface was then photographed with a professional camera in a light box to control the ambient light of the pictures. The developed sensor was employed for the determination of mercury in different water samples and silver in cleaning products containing silver nanoparticles, showing a good response (selectivity and sensitivity) even in samples where both analytes were present. Along with heavy metals, water contamination with arsenic has also become a major issue. Pena-Pereira *et al.* developed a non-instrumental approach for the arsenic speciation in water based on the color change produced upon reaction with silver nitrate [65]. Silver nitrate was deposited onto a PAD, which was then exposed to the headspace above the sample, thus obtaining a colored product that was scanned and analyzed with an image treatment software. Following a similar approach, Saraji and Bagheri synthesized a PAD modified with chloramine-T/pyridinebarbituric acid for the determination of cyanide in water samples via headspace microextraction combined with digital image analysis [50]. The method allowed the determination of this pollutant not only from standards but also from colored and turbid water samples.

Recently, smartphones have become a perfect option for rapid and inexpensive analyses, since the processing unit, readout, user input, and sensor are integrated altogether in the same device. However, the low selectivity and sensitivity of these devices as detection systems limit their application in analytical methodologies. In this sense, Shahvar *et al.* developed a PAD for the determination of sulfite in food samples via headspace microextraction and smartphone-based detection [53]. The PAD was impregnated with a solution containing 1,10-phenathroline and Fe(III) and exposed to the headspace above the sample. Upon acidification of the sample, the

existent sulfite was converted to sulfur dioxide, this compound reducing the Fe(III) present in the PAD to Fe(II). Transition metals like Fe(II) can form complexes with phenanthroline via interaction with the nitrogen present in its structure. The formation of the complex $[Fe(phen)_3]^{2+}$, the counter anion being the sulphate ions formed during the reaction, led to a red color. The color intensity of the surface of the PAD was photographed and the picture was treated with a smartphone and an RGB analyzer software installed on the same device as depicted in Fig. 4b.

Infectious diseases are a significant concern in every country since they are rapidly spread. With the recent crisis of COVID-19, the interest in the development of cheap and rapid sensors has increased to an even greater extent, considering the importance of an early diagnosis. In this sense, colorimetric paper-based sensors are again one of the best options for the performance of simple and rapid assays. Furthermore, as already mentioned, gold nanoparticles (AuNPs) along with silver nanoparticles (AgNPs) have attracted increasing attention due to their optical properties. Considering the importance of the detection of specific DNA sequences of infectious diseases, Teengam *et al.* synthesized a multiplex colorimetric PAD based on the aggregation of AuNPs for the simultaneous detection of middle east respiratory syndrome coronavirus (MERS-CoV), M. tuberculosis (MTB) and human papilloma virus (HPV) via color-change detection [66]. AuNPs were immobilized in the PADs, which experienced aggregation upon addition of the sample, thus leading to the emergence of a brownish color. The color intensity was measured using an image treatment software. The results showed that this colorimetric PAD could be a low-cost and disposable alternative tool for the rapid screening and early-stage detection of infectious diseases.

3.2. Fluorescence PADs

Fluorescence detection is also widely considered in the design of optical sensors. The modification of the PADs with fluorescent compounds such as QDs, can broaden their application scope since it is possible to develop tunable fluorescence sensors.

Regarding this, Qiu *et al.* synthesized a PAD for the detection of carcinoembryonic antigen (CEA) [58], which is a biomarker employed for diagnosis and treatment of cancer. For this purpose, a PAD was modified with glucose oxidase (GOD) and CdTe/CdSe QDs, the fluorescent component. This process was carried out by making a gate-like method involving aptamer-functionalized mesoporous silica nanoparticles (MSNs) loaded with glucose molecules. Glucose molecules gated in the pores of MSNs were released upon the introduction of the target CEA in the detection cell and oxidized by GOD to produce gluconic acid and hydrogen peroxide, the latter quenching the fluorescence of the QDs. The fluorescence intensity of the paper was determined qualitatively by naked eye and a smartphone and quantitatively using a spectrofluorometer. Moreover, Yu *et al.* developed a paper-based microsensor for the determination of the water content in solid pharmaceuticals based on the fluorescence of lanthanide metal– organic framework (MOF) Eu-dipicolinic acid/2-aminopththalic acid (Eu-DPA/PTA-NH_2) [67]. The fluorescence intensity of PTANH_2 increases with the water content in the MOF, while the fluorescence intensity of the lanthanide decreases, thus leading to a fluorescence color change from red to blue under 254 nm UV light. The paper was modified by immersion in the aqueous solution of Eu-DPA/PTA-NH_2 and was employed as a headspace sensor of water, the fluorescence intensity being recorded by a smartphone upon excitation with UV light. The as-synthesized device can be used for the accurate water assay in solid samples, as it provides a sensitive response, while being also a portable, long-term stable, rapid sensor. Furthermore, Petruci *et al.* developed a PAD for the *in situ* determination of gaseous hydrogen sulfide based on the quenching of the fluorescence of fluorescein mercury acetate (FMA) [68]. FMA was drop-casted onto the surface of the PAD, which was then positioned in the detection system, consisting of a 470 nm light-emitting diode (LED) and a microfiber optic USB spectrometer. Upon reaction with hydrogen sulfide, FMA fluorescence intensity was quenched, the decrease being measured by the detection system. Using a miniaturized display, it was possible to develop a device capable of performing the gas sampling and the analytical signal acquisition within seconds,

thus being a suitable approach for the determination of this compound in a real-world environment.

As previously mentioned, common filter paper can be easily modified with different solid compounds, such as nanostructures and polymers, thus obtaining devices that combine the properties of the cellulosic substrate and the immobilized material. Regarding this, a molecularly imprinted PAD was recently synthesized by our group via a polymerization-free synthesis for the determination of quinine (Fig. 5) [57]. The synthesis of the molecularly imprinted polymer (MIP) was achieved by the dissolution of the polymer, i.e., nylon-6, in formic acid and addition of the template molecule to the solution. This procedure for the preparation of MIPs is not only cost-effective but also speedier, and eco-friendlier as compared to those methods that carry out the entire polymerization process since lower amounts of reagents are used. Furthermore, the use of filter paper not only made the synthesis process of the sensor simpler and inexpensive, it also made it easy to be incorporated to the fluorimeter cell via a custom-built magnetic piece that held the PAD. The developed MIP-PAD showed affinity towards quinine even in the presence of a similar fluorescent molecule, i.e., norfloxacin. The as-synthesized sensor opens a wide range of opportunities in further investigations, as it is an easy and rapid way to prepare these useful materials.

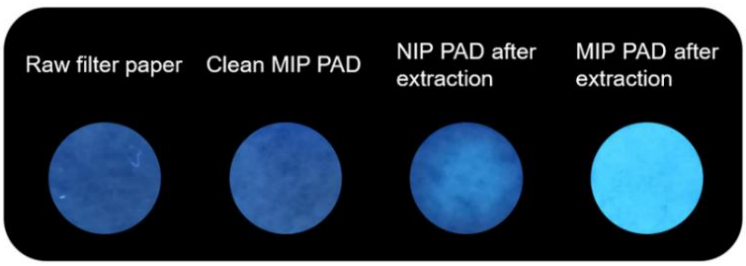

Figure 5. Comparison of the extraction capacity of quinine of MIP and NIP PADs from a 10 mg L^{-1} solution. Reproduced from ref. [57] with permission from Elsevier, copyright 2019.

3.3. Surface-enhanced Raman spectroscopy PADs

As aforementioned, SERS technique has raised attention in the last years. This technique not only can provide the fingerprint of almost any compound within a few seconds but also quantify the amount of analyte in a certain substrate. PAD-based SERS substrates have outshined other commonly used substrates since they are disposable and flexible enough to be suitable for sample collection. Restaino *et al.* developed an inkjet-printed paper dipstick for the determination of sulfapyridine via SERS detection [69]. The dipsticks were printed using a previously prepared ink containing AgNPs and then immersed into the analyte solution. After a certain amount of time, the dipstick is removed from the sample, and spectra are then recorded on various locations throughout the entire printed surface of the dipstick. This AgNP-based PAD can detect concentrations of sulfapyridine within therapeutic levels and can be stored for several days.

The SERS intensity relies on various factors related to the nanoparticles, being the shape one of the most important variables. It has been confirmed that the electromagnetic field surrounding nanoparticles with sharp edges or tips is significantly higher compared to those with planar surfaces [70]. In this sense, a silver nanoflower-coated paper was synthesized by our group as a dual substrate for the determination of ketoprofen via SERS and ambient pressure mass spectrometry [61]. The paper was modified with silver and ethylenediamine, which acts as a bridge between the former silver layer and the silver nano-flowers (AgNFs) that are incorporated by immersion of the paper in the solution containing the nanoflowers. Upon swabbing of ketoprofen deposited and dried in a glass slide, SERS spectra were recorded, using the band appearing at 1000 cm^{-1} for the quantification of the analyte.

4. Electrochemical paper-based analytical devices

The coupling the PADs to electrochemical detection provides low cost and versatile analytical platforms—the so-called ePADs—with enhanced limits of detection as

compared PADs with colorimetric detection, and high selectivity. Moreover, ePADs are suitable for miniaturization and in-field application [10], for example coupled to a mobile phone for potentiostatic control [71]. Since the publication in 2009 of Dungchai *et al.* [72] about electrochemical detection with paper-based microfluidics (mPADs), numerous developments in this field have been reported, paper being used for the design of amperometric, voltammetric [73], potentiometric [74], impedimetric and electrochemiluminescence sensors [75,76], among others. A comprehensive review of the different ePADs reported is out of the scope of this revision article, while recent reviews summarize fabrication methods and applications of ePADs [10,11,77,78], and more information of their application for detection of biomarkers can be found elsewhere [79].

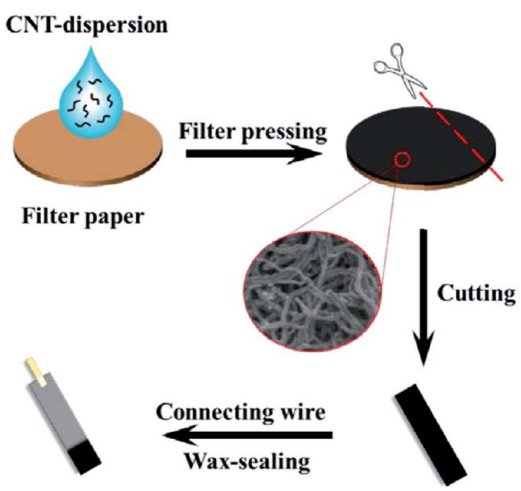

Figure 6. Scheme of the fabrication of a paper-based analytical device via drop-casting of filter paper with carbon nanotubes. Reproduced from ref. [83] with permission from John Wiley and Sons, copyright 2018.

Paper is intrinsically a nonconductive material; thus, modification of the surface is mandatory for electrochemical applications. The network of cellulose fibers of paper is the base for immobilization of conductive materials forming the electrodes, e.g., via painting with conductive substances (e.g., conductive carbon ink), which can easily adsorb onto the fibers of the paper, screen printing [80], pencil drawing [81], sputtering, laser-scribing, etc. [10]. Among them, drop-casting of different materials, e.g., metal–organic frameworks (MOFs) [82], and nanomaterials is widely used in order to improve the performance of the paper-based electrode, e.g., modification with carbon nanotubes (CNTs) [83], as shown in Fig. 6, metal nanoparticles (e.g., AuNPs [84], Fe_3O_4 [85]), as well as the combination of different nanoparticles e.g., gold nanoparticles (AuNPs) and CNTs [86], via sputtering of AuNPs on commercial art paper, later modified with multiwalled CNTs for the determination of bisphenol A; as well as copper nanoparticles and graphene [87] for NOx gas sensing, among others. The incorporation of metal NPs leads to an enhancement in both the surface area of the electrode and the conductivity, thus amplifying the signal [88]. In addition to nanomaterials, other mediators such as metallophthalocyanine have been reported for electrode modification. In this sense, Nantaphol *et al.* [73] developed an electrochemical paper-based device using cobalt phthalocyanine (CoPc) in order to enhance the oxidation of 8-hydroxyquinoline (8-HQ), which was studied by using cyclic voltammetry and square-wave voltammetry. This ePAD has been applied to the determination of 8-HQ in cosmetic samples. Furthermore, a combination of CoPc, graphene, and ionic liquid has been used for the development of a disposable paper-based sensor for the detection of glucose [89]. The presence of graphene and ionic liquid, due to excellent properties such as high ionic conductivity improves the performance of the sensor.

Electrochemical PADs have been coupled to microextraction techniques, such as headspace liquid-phase microextraction (HLPME) [90], gas-diffusion microextraction (GDME) [91] and paper-supported thin-layer ion transfer voltammetry [92]. The coupling of ePADs with microextraction simplifies the

process and enables a fast sample preparation of complex matrices, at the same time that the electrochemical detection with the disposable PADs makes the procedure cost-effective. A miniaturized procedure for the determination of hydrogen sulfide in fuel oil samples has been developed based on the use of HLPME coupled to a PAD comprised of hydrophobic zones of sample and supporting electrolyte connected by a hydrophilic channel (Fig. 7a–c) [90]. The ePAD consists of a nickel working, platinum auxiliary, and Ag/AgCl reference electrodes. Sulfide ions were first separated and extracted from fuel via HLPME and subsequently detected via cyclic voltammetry.

In addition, a paper-based analytical sensor for sulphite analysis in beverages has been developed via laser-pyrolysis of common paperboard in order to produce conductive carbon material electrode [91]. The ePAD was combined with a GDME unit and subsequent square-wave voltammetric analysis (Fig. 7d and e). The GDME step provides the advantages of microextraction, such as improved sensitivity, and leads to the extraction of volatile and semi-volatile compounds. SO_2 diffuses through the membrane and is entrapped in an acceptor solution. Moreover, Ding *et al.* [92] have reported the so-called paper-supported thin sample layer voltammetry for the determination of ions such as tetrabutylammonium chloride and potassium. The setup combines paper sampling and a commercial electrode with an ion-selective membrane. Cyclic voltammetry is used to modulate the ion transfer across the membrane.

In the case of sensors using PADs, sample treatment such as mixing, (micro)extraction, separation, etc. are usually integrated into the PAD platform, which will determine its portability and ability for on-site measurements. Both 2D and 3D electrochemical sensors based on paper have been reported, the first comprising the three electrodes onto a single piece of paper, while in 3D sensors the paper is folded as origami structures, so that the electrodes are in different parts of the paper. Liu *et al.* [93] for example, have reported a self-powered origami PAD with a pop-up structure for adenosine 5'-triphosphate triggered by glucose oxidase

reaction and differential pulse voltammetry detection. Moreover, an origami design has also been applied to the determination of NOx gas, integrating the gas adsorbent and electrochemical detection zone through differential pulse voltammetry in a single paper device [87]. Moreover, the so-called Janus ePADs allow for multiple electrochemical experiments from a single sample [94]. A Janus ePAD has been recently reported for simultaneous detection of Cd, Pb, Cu, Fe, and Ni by conducting square-wave anodic stripping voltammetry and square-wave cathodic stripping voltammetry [95]. Another 3D-ePAD, comprising Fe_3O_4 and Au NPs to create nano-sized MIPs, has been described for the determination of serotonin [85].

As described in more detail above, different types of paper can be used for the development of PADs, such as filter or chromatographic paper among others. For example, an ePAD composed of Whatman SG81 chromatographic paper coupled to 3D-printed electrodes has been fabricated and applied to the electrochemical detection of dexamethasone and prednisolone [96]. The analytes are first separated in the chromatographic paper taking into account their different partition coefficient for chromatographic separation using a mobile phase, and the separated analytes were subsequently quantified by differential pulse voltammetry on the printed electrodes within the paper. Thus, this platform combines the separation and detection steps in the same PAD, which opens the door to rapid, cost-effective and on-site quantitative detection.

In order to improve the selectivity of the measurements and prevent interferences from the sample matrix, recognition elements can be attached to the paper surface, such as antibodies, aptamers or molecular imprinted polymers. PADs, in general, and ePADs among them, are useful for biodetection, as paper is a convenient platform for the immobilization of antibodies. Silva *et al.* [97] have reported the development of an ePAD for the label-free potentiometric immunosensing detection of Salmonella typhimurium. They employed two different functionalization strategies, based on the one hand, on the direct conjugation of antibodies to a polymer membrane, and, on the other hand, the use of intermediate layers of

polyamidoamine dendrimer with an ethylenediamine core. Moreover, a paper-based immunocapture assay for the determination of ethinylestradiol (EE2) has been reported, comprising the modification of paper microzones with silica NPs and anti-EE2 specific antibodies [98]. Firstly, preconcentration of the analyte takes place, and the paper microzones are then placed onto a screen-printed electrode modified with reduced graphene.

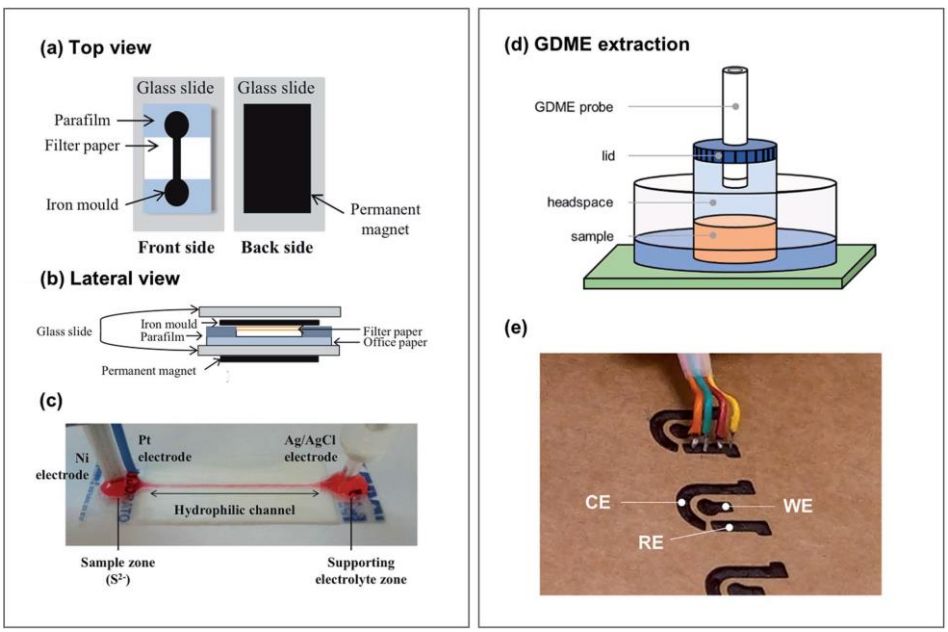

Figure 7. Scheme (a) top view, and (b) lateral view of the paper-based analytical device for the determination of hydrogen sulfide coupled to HLPME. (c) Photograph of the paper-based analytical device. Scheme of the laser-pyrolyzed electrochemical paper-based analytical sensor for sulphite analysis: (d) gas-diffusion microextraction (GDME) unit, and (e) photograph of the electrodes fabricated via room-temperature laser pyrolysis for square-wave voltammetric analysis. Pictures (a–c) are reproduced from ref. [90] with permission from Elsevier, copyright 2018; pictures (d and e) are reproduced from ref. [91] under the terms of the Creative Commons Attribution License.

An alternative to biorecognition for improving the selectivity in the extraction and detection of the target analytes is the use of MIPs which are less expensive than antibodies, more robust and easier to produce. For example, MIPs on a movable valve microfluidic ePAD have been exploited for the detection of biomarkers [99], directly detecting antigens without the need of antibodies, which decreases the cost of analysis as well as washing steps and antibody preservation duties. In addition, Kamel *et al.* [74] have developed an ultra-low-cost, disposable paper-based potentiometric sensor for the determination of BPA based on the use of molecularly imprinted nanobeads coupled to the electrode. The molecularly imprinted nanobeads are dispersed in the polymeric membrane potentiometric sensor based on chromatography paper, and they act as recognition receptors towards BPA.

Last but not least, paper-based dual detection devices combining electrochemical detection with other techniques such as spectroscopy have been reported. For example, an ePAD consisting of office paper modified with AuNPs has been reported for both electrochemical and SERS determination of drugs such as cocaine [100]. The reported ePADs are single-use, with a high electroactive area and dual detection, enabling the determination of both electroactive and non-electroactive compounds.

5. Paper spray mass spectrometry (PS-MS)

Mass spectrometry is a powerful tool for the analysis of complex mixtures, being one of the most sensitive analytical techniques currently available. Among other modalities, ambient ionization techniques, such as desorption electrospray ionization (DESI) and direct analysis in real-time (DART), have sparked interest since they allow the direct ionization of the analytes avoiding sample preparation [101]. Paper spray (PS) method combines the characteristics of conventional ESI and ambient ionization techniques, allowing fast chemical screening at high sensitivity with slight sample requirements. Additionally, quantitative results may be obtained with the utilization of internal standards [102]. PS-MS consists of the deposition of a minimal amount of sample (<10 mL) on a paper substrate, which is

placed in front of the MS inlet. The electrospray is produced with the application of a high voltage (3–5 kV) along with a small volume of solvent (10–50 mL) for moistening the substrate, creating an electric field at the end of the paper [103]. Charged droplets are produced as a consequence of the coulombic force, being subsequently desolvated generating dried ions. Pure methanol, or with a minor proportion of water, and the common ESI additives, are typically used as the wetting solution. Wet paper is conductive, and the fibrillar structure of cellulose acts as microchannels for the liquid transport, including carried analytes by the wetting solution [104]. This material provides many advantages to the PS modality including large commercial availability at low cost as well as a great variety of products with different pore size, thickness, weight, etc. These properties have a decisive impact on the ionization efficiency and the release of target compounds from complex matrices and the diffusion of the analytes through the substrate, which is related to the analyte recovery [105]. Therefore, different types of papers have been tested as PAD, *viz*. filter paper with different pore sizes as well as print, silica-coated, glass fiber, and chromatographic papers. It has been proven that papers with smaller pore size and thicker paper stock produce a reduction of recovery while increasing ionization efficiency [106]. Filter and chromatographic papers have shown better performance, thus being the most commonly used.

Additionally, due to the malleability of this material, PADs may be easily adapted to fit the needs of the study. For this reason, PADs are commonly cut to triangular shapes in order to increase the strength of the electric field, enhancing the formation of the spray [107]. Slight variations in the macroscopic angle of the PAD may affect the total spray current, changing the electric field intensity at the tip and therefore leading to differences in signal intensities [104]. Furthermore, wetting solvent as well as sample position on the paper substrate are found to affect ion suppression and recovery [108]. Several studies have been carried out to elucidate the influence of the position of the tip directed to the MS inlet. Although an accurate positioning is not required for the correct implementation of PS [102], it has been noted a

relationship between the tip angle and the positioning of the PAD. In this manner, the larger the angle, the shorter the critical distance needed to produce the spray [109]. All these considerations need to be taken into account to accomplish proper performance.

There are different ways of deposition of the sample, viz. analytes may be preloaded on the paper substrate, added with a wetting solution or swabbed from sample surfaces [102]. Since its first approach in 2010 by Cooks and Ouyang's groups, there is a steady increase in the development of tools and analytical methodologies involving PS-MS. Owing to the porous characteristics of paper, it has been used for the determination of therapeutic drugs in whole dried blood samples, being directly analyzed on the storage medium [101]. Similarly, PS-MS has been used for the determination of illicit chemicals compounds like steroids, drugs and explosives, small organic compounds like peptides, proteins, nucleotides, and phospholipids in different complex matrices like food, urine, blood, and tissue [102]. Moreover, the technique may be applied to study reactions and identify intermediates [110]. In this way, PADs have been modified with nanoparticles that act as catalysts of different processes [111]. One of the main advantages in all these applications is the short time required analysis time (~1 min), which is dependent on the volume of the wetting solvent.

In the last years, different approaches have been developed for expanding the applicability of PS-MS. Fig. 8 shows some of these examples, such as the fabrication of cartridges for integrating solid-phase extraction column (Fig. 8a) or solvent reservoirs to prolong the spray generation from the paper tip (Fig. 8b) [107,112,113]. On this account, 3D-printers are being a very useful tool in this field due to the possibility of creating holding devices for samples/PADs as well as controlling the reproducibility between sample loadings (Fig. 8c and d) [106,114]. Dowling *et al.* developed an on-cartridge paper spray for the rapid screening of pharmaceuticals in soil samples (Fig. 8e) [115]. Likewise, high-throughput platforms to accommodate multiple PADs (Fig. 8f) have been developed [116]. Apart

from that, different approaches have been raised by modifying the surface of PADs with a wide variety of functional groups, improving the versatility of PS-MS. On one side, PADs have been modified to enhance the spray formation, being possible the reduction of the applied voltage as well as the enhancement of the sensitivity. An example of this enhancement was observed modifying PADs with silver nanoflowers providing better sensitivity than that obtained with bare paper [61]. Other materials like zirconia [117], polystyrene microspheres [118], metal–organic frameworks [119] and CNTs have also been applied to efficiently coat the PADs. CNTs have been used to enhance the paper electrical conductivity reducing the spray voltage to 3 V, using an external battery [120]. Similarly, mesoporous graphene foams (MGF) have also been used to modify PADs allowing the reduction of the spray voltage to 2.4 kV [105]. The hydrophobic modification of PADs with polymers [121] or using a silanization process, as well as the creation of paraffin barriers [122], avoid the spread of analyte over the entire surface of the paper substrate, improving quantitative analyses using PS-MS. Liu *et al.* proposed the modification of PADs with 1-[3-(trimethoxysilyl)propyl]urea to reduce ionization suppression caused by anions and highly polar compounds in the negative mode ionization of MS [123].

Although in most of the cases samples are directly analyzed, in many instances sample treatment is an unavoidable step. The complexity of matrix or even the low concentration in which analytes are found in different samples, considerably decreases the efficiency of PS-MS [124]. For this reason, some strategies have been proposed in this way to increase the specificity of PS-MS, enhancing the accuracy and precision of the method. Due to the physical characteristics of PADs, they may act as solid supports for microsolid phase extraction (m-SPE) as well as substrate for PS. An example of this combination is the coating of paper with MIPs, which have been used as selective substrates to enhance the sensitivity in the determination of different metabolites in biological samples [125,126]. Similarly, a combination of aptamers and carbon nanomaterials coated PADs have been proposed for the

determination of drugs of abuse in plasma and saliva samples [127]. Recently, supramolecular microextraction has also been used as a remediation in the analysis of tricyclic antidepressants in urine [128]. In all cases, the improvement in the sensitivity of the technique in comparison with bare paper demonstrates the potential of microextraction in combination with PS-MS.

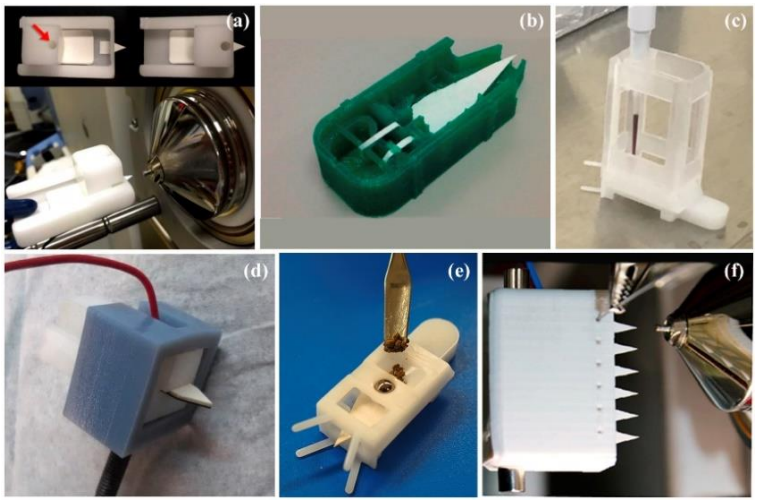

Figure 8. 3D-printed designs for PS-MS. (a) Disposable SPE cartridge for complex matrices. Reproduced from ref. [107] with permission from American Chemical Society, copyright 2015; (b) cartridge for continuous solvent supply. Reproduced from ref. [113] with permission from American Chemical Society, copyright 2014; (c and d) devices to reduce the variability from the repeated analyses. Picture c reproduced from ref. [114] under the terms of the Creative Commons Attribution License from reference. Picture d reproduced from ref. [106] with permission from Elsevier, copyright 2018; (e) on-cartridge device intended for the direct analysis of solid samples. Reproduced from ref. [115] with permission from Elsevier, copyright 2020; (f) 3D-printed holder to achieve high throughput detection. Reproduced from ref. [116] with permission from American Chemical Society, copyright 2019.

Table 2 summarizes the applications mentioned throughout the entire review that comprise certain modification of the paper substrate and the coupling with different detection systems, i.e., spectrometric, electrochemical and PS-MS.

Table 2. Highlighted examples of surface-modified paper substrates coupled to different detection systems[a]

Paper substrate	Modification	Analyte	Sample	Detection system	Reference
Whatman 44	Pyridine-barbituric acid	Cyanide	Water samples	Digital image analysis	[50]
Blue ribbon filter 589/3	Fe(III), 1,10-phenanthroline and acetate buffer	Sulfite	Food samples	Smartphone-based sensing	[53]
Filter paper	MIP	Quinine	Soda drink	Fluorimetry	[57]
Grade GF/C Whatman glass microfiber filters	CdTe/CdSe quantum dots and glucose oxidase	Carcinoembryonic antigen	Human serum samples	Fluorimetry	[58]
Filter paper	Silver nanoflowers	Ketoprofen	Human saliva samples	SERS and PS-MS	[61]
Whatman 4	ABTS, alcohol oxidase and horse radish peroxidase	Ethanol	Whole blood samples	Digital image analysis	[63]
Whatman 42	Ion selective optode	Ag^{+} and Hg^{2+}	Water samples and cleaning products	Digital image analysis	[64]
Whatman 3	Silver nitrate	Arsenic	Water samples	Digital image analysis	[65]
Whatman 1	AgNPs and acpcPNA probe	MERS-CoV, MTB and HPV oligonucleotides	DNA target	Digital image analysis	[66]
Filter paper	Eu-dipicolinic acid/2-aminopththalic acid	Water content	Solid pharmaceuticals	Ratiometric chromaticity	[67]
Whatman 41	Fluorescein mercury acetate and ethylene glycol	Hydrogen sulfide	Air	Fluorimetry	[68]
Chromatography paper	Molecularly imprinted nanobeads	Bisphenol A	Plastic samples	Potentiometry	[74]
Paper electrode	Hierarchical assembled nanomaterials and	microRNA	Serum samples	CV, EIS and SWV	[82]
Filter paper	Carbon nanotubes	Neurochemicals	Brain microdialysate	EIS, CV, amperometry	[83]
Filter paper	Fe_3O_4@Au NPs coated with MIPs	Serotonin	Pharmaceutical capsules, urine samples	LSV	[85]
Commercial art paper	AuNPs and carbon nanotubes	Bisphenol A	Plastic samples	LSV	[86]
Whatman 1	Cu NPs	NOx gas	Air and exhaust gases from cars	DPV	[87]
Paper	Cobalt phthalocyanine, graphene and ionic liquid	Glucose	Honey, white wine and human serum	CV	[89]
Whatman chromatography paper no. 2	Pop-up origami (DNA1-aptamer-DNA2-GOx modified)	Adenosine 5'-triphosphate (ATP)	-	DPV/ supercapacitor amplified signal	[93]

Table 2 (Contd.)[a]

Paper substrate	Modification	Analyte	Sample	Detection system	Reference
Whatman chromatography paper no. 4	Electrochemically reduced graphene oxide (RGO)	Norepinephrine, serotonin, p-aminophenol	-	DPV	[94]
Whatman SG81 chromatography paper	Silica coated	Dexamethasone and prednisolone	Herbal medicines	DPV	[96]
Filter paper	Antibodies	Salmonella typhimurium	Apple juice	Potentiometric immunosensor	[97]
Whatman chromatography paper No. 1	MIPs	Carcinoembryonic antigen	-	DPV	[99]
Office paper	AuNPs	Cocaine	Seized street cocaine sample	Electrochemistry + SERS	[100]
Chromatography paper	Mesoporous graphene foams	Amphetamine	Saliva		[104]
Filter paper	Zirconia	Therapeutic drugs	DBS		[117]
Filter paper	Polystyrene microspheres	Proteins and peptides	PBS and Tris buffer solutions and DBS		[118]
Filter paper	MOF	Therapeutic drugs	DBS		[119]
Filter paper	CNTs	Pesticides	Fruit surfaces		[120]
Whatman 1	Organosiloxane polymers	Narcotic drugs	Water and urine	PS-MS	[121]
Whatman 1	Paraffin	HMF and sugars	Hydrolysis liquor		[122]
Chromatography paper	Urea	Salicylic acis and terpene lactones	Urine and Egb		[123]
Cellulose	MIP	Dopamine, sarcosine and butvric acid	Urine		[125]
Cellulose	MIP	Cocaine	Oral fluids		[126]
Whatman filter paper	Aptamers-CNMs	Drugs of abuse	Plasma and saliva		[127]

[a]MIP = molecularly imprinted polymer; SERS = surface enhanced Raman spectroscopy; PS-MS = paper spray mass spectrometry; ABTS = 20-azino-bis(3-ethylbenzothiazoline-6-sulfonic acid) diammonium salt; acpcPNA = D-proline/2-aminocyclopentanecarboxylic acid; MERS-CoV = middle east respiratory syndrome coronavirus; MTB = Mycobacterium tuberculosis; HPV = human papillomavirus; MOF = metal organic framework; CV = cyclic voltammetry; DPV = differential pulse voltammetry; EIS = electrochemical impedance spectroscopy; LSV = linear sweep voltammetry; SWV = square wave voltammetry; SWASV = square-wave anodic stripping voltammetry; SWCSV = square-wave cathodic stripping voltammetry; DBS = dried blood spots; PBS = phosphate buffered saline; HMF = hydroxymethylfurfural; EGb = Ginkgo biloba extract; CNMs = carbon nanomaterials.

6. Conclusions

The information demands of our society have prompted the development of rapid analytical devices capable of providing information in a short period, using cost-effective detectors and materials in order to extend the applicability of these devices to a higher population, not only in developed countries but also in less-favored and remote areas of low- and middle-developed countries. Current trends in AC are geared towards miniaturization, automation, and portability of analytical systems and methods, in the seek of reducing sample amounts and speeding the achievement of information, e.g., in the so-called point-of-care (POC) diagnosis tests. This review article has focused on the development of paper-based analytical devices, owing to the advantages of paper as a platform such as low cost, availability, porosity, surface modification, already discussed along with the manuscript.

A great variety of papers of different nature have been described for the development of such PADs (e.g., chromatographic, filter, office papers, among others) which are coupled to different sensing schemes both spectroscopic, electrochemical or even mass spectrometry. Moreover, the use of paper as sorptive phase has boosted the development of thin-film microextraction, the functionalization of the paper surface extending the versatility of the technique. In fact, the functionalization of the surface of paper with a wide variety of materials has opened the door to the use of paper as a platform in a variety of sensors, ranging from e.g., colorimetric, fluorometric, to electrochemical. On the one hand, the combination of paper with both natural and synthetic polymers improves the extraction capability of paper, while the attachment of nanomaterials enables further sensing schemes with improved sensitivity and selectivity. On the other hand, the suitability of paper in biosensing and clinical diagnosis relies on the wide variety of biomolecules that can be bound at the surface of paper, i.e., antibodies, aptamers, etc., which provides with selective platforms suitable for addressing current challenges of our society. While many diagnostic tests based on paper are already widespread, e.g., pregnancy tests, glucose sensing, it is envisaged that modified paper strip sensors will lead the trends

in the development of sensing schemes in AC in the next future.

In summary, PADs can be applied in different formats in the analytical chemistry field. The combination of paper-based sorptive phases with chromatographic techniques allows the development of rearguard analytical methods, while paper-based sensors can be used as rapid screening alternatives. Both approaches are not antagonistic since they can be even combined in the so-called vanguard/rearguard approaches. Also, the direct analysis of paper-based phases with MS is powerful in those contexts (for example, clinical tests) where rapid and reliable information is needed.

The combination of PADs with cell phone technology [129,130] and 3D-printing [131] defines a fascinating research context where new and worldwide accessible platforms will appear in the next years.

Conflicts of interest

There are no conflicts to declare.

Acknowledgements

The financial support of the Spanish Ministry of Economy and Competitiveness through the grant CTQ2017-83175R made this research possible. This article is based upon work from the Sample Preparation Task Force and Network, supported by the Division of Analytical Chemistry of the European Chemical Society.

References

[1] C. Sheridan, Nat. Biotechnol., 2020, 38(5), 515–518.

[2] M. Valcárcel and R. Lucena, TrAC, Trends Anal. Chem., 2012, 31, 1–7.

[3] M. Valcárcel, G. D. Christian and R. Lucena, Anal. Chem., 2013, 85, 6152–6161.

[4] M. de la Guardia and S. Garrigues, Handbook of Green Analytical Chemistry, 2012.

[5] A.Gałuszka, Z. Migaszewski and J. Namiésnik, TrAC, Trends Anal. Chem., 2013, 50, 78–84.

[6] F. Chemat, S. Garrigues and M. de la Guardia, Current Opinion in Green and Sustainable Chemistry, 2019, 19, 94–98.

[7] Š. Kubínová and J. Šlégr, J. Chem. Educ., 2015, 92, 1751–1753.

[8] G. Mafra, M. T. García-Valverde, J. Millán-Santiago, E. Carasek, R. Lucena and S. Cárdenas, Separations, 2020, 7, 2.

[9] T. Ozer, C. McMahon and C. S. Henry, Annu. Rev. Anal. Chem., 2020, 13, DOI: 10.1146/annurev-anchem-061318-114845.

[10] V. N. Ataide, L. F. Mendes, L. I. L. M. Gama, W. R. de Araujo and T. R. L. C. Paixão, Anal. Methods, 2020, 12, 1030–1054.

[11] W. J. Paschoalino, S. Kogikoski, J. T. C. Barragan, J. F. Giarola, L. Cantelli, T. M. Rabelo, T. M. Pessanha and L. T. Kubota, ChemElectroChem, 2019, 6, 10–30.

[12] C.-C. Huang, C.-Y. Cheng and Y.-S. Lai, Trends Food Sci. Technol., 2020, 100, 349–358.

[13] E. Noviana and C. S. Henry, Curr. Opin. Electrochem., 2020, 23, 1–6.

[14] E. M. McBride, P. M. Mach, E. S. Dhummakupt, S. Dowling, D. O. Carmany, P. S. Demond, G. Rizzo, N. E. Manicke and T. Glaros, TrAC, Trends Anal. Chem., 2019, 118, 722–730.

[15] S. R. Chinnadayyala, J. Park, H. T. N. Le, M. Santhosh, A. N. Kadam and S. Cho, Biosens. Bioelectron., 2019, 126, 68–81.

[16] H. Piri-Moghadam, M. N. Alam and J. Pawliszyn, Anal. Chim. Acta, 2017, 984, 42–65.

[17] R. Jiang and J. Pawliszyn, TrAC, Trends Anal. Chem., 2012, 39, 245–253.

[18] G. A. Gómez-Ríos and J. Pawliszyn, Angew. Chem., Int. Ed., 2014, 53, 14503–14507.

[19] G. A. Gómez-Ríos and M. F. Mirabelli, TrAC, Trends Anal. Chem., 2019, 112, 201–211.

[20] A. Napylov, N. Reyes-Garces, G. Gomez-Rios, M. Olkowicz, S. Lendor, C. Monnin, B. Bojko, C. Hamani, J. Pawliszyn and D. Vuckovic, Angew. Chem., Int. Ed., 2020, 59, 2392–2398.

[21] J. Pawliszyn, in Handbook of Solid Phase Microextraction, Elsevier, 2012, pp. 13–59.

[22] I. Bruheim, X. Liu and J. Pawliszyn, Anal. Chem., 2003, 75, 1002–1010.

[23] Y. A. Olcer, M. Tascon, A. E. Eroglu and E. Boyacı, TrAC, Trends Anal. Chem., 2019, 113, 93–101.

[24] R. V. Emmons, R. Tajali and E. Gionfriddo, Separations, 2019, 6, 39.

[25] J. Chen and R. J. Hurtubise, Talanta, 1998, 45, 1081–1087.

[26] A. H. Ackerman and R. J. Hurtubise, Appl. Spectrosc., 1999, 53, 770–775.

[27] X. Meng, Q. Liu and Y. Ding, Electrophoresis, 2017, 38, 494–500.

[28] A. H. Ackerman and R. J. Hurtubise, Anal. Chim. Acta, 2002, 474, 77–89.

[29] A. R. Allafchian, B. Farajmand and A. J. Koupaei, Bull. Environ. Contam. Toxicol., 2018, 100, 529–535.

[30] M. Saraji and B. Farajmand, J. Chromatogr. A, 2013, 1314, 24–30.

[31] C. Ye, C. Liu, S. Wang and Z. Wang, Anal. Sci., 2017, 33, 229–234.

[32] C. Ye, Y. Wu and Z. Wang, RSC Adv., 2016, 6, 9066–9071.

[33] Z. Hashemian, T. Khayamian and M. Saraji, Anal. Bioanal. Chem., 2015, 407, 1615–1623.

[34] L. Wan, H. Zhu, Y. Guan and G. Huang, Talanta, 2017, 169, 209–215.

[35] M. Saraji and N. Mehrafza, RSC Adv., 2017, 7, 50210–50215.

[36] A. Mihranyan, L. Nyholm, A. E. G. Bennett and M. Strømme, J. Phys. Chem. B, 2008, 112, 12249–12255.

[37] A. Razaq, G. Nyström, M. Strømme, A. Mihranyan and L. Nyholm, PLoS One, 2011, 6, e29243.

[38] J. Ríos-Gómez, R. Lucena and S. Cárdenas, LCGC Europe, 2020, 33, 60–66.

[39] J. Ríos-Gómez, R. Lucena and S. Cárdenas, Microchem. J., 2017, 133, 90–95.

[40] E. M. Reyes-Gallardo, R. Lucena, S. Cárdenas and M. Valcárcel, Bioanalysis, 2015, 7, 1723–1730.

[41] J. Ríos-Gómez, B. Ferrer-Monteagudo, ´A. I. López-Lorente, R. Lucena, R. Luque and S. Cárdenas, J. Cleaner Prod., 2018, 194, 167–173.

[42] E. M. Reyes-Gallardo, R. Lucena, S. Cárdenas and M. Valcárcel, Microchem. J., 2016, 124, 751–756.

[43] E. M. Reyes-Gallardo, R. Lucena and S. Cárdenas, RSC Adv., 2017, 7, 2308–2314.

[44] Z. Ayazi, F. Shekari Esfahlan and Z. Monsef Khoshhesab, Anal. Methods, 2018, 10, 3043–3051.

[45] Z. Ayazi, F. Shekari Esfahlan and P. Matin, Int. J. Environ. Anal. Chem., 2018, 98, 1118–1134.

[46] Y. Jiang, P. Ma, H. Piao, Z. Qin, S. Tao, Y. Sun, X. Wang and D. Song, Microchim. Acta, 2019, 186, 742.

[47] J. Ríos-Gómez, B. Fresco-Cala, M. García-Valverde, R. Lucena and S. Cárdenas, Molecules, 2018, 23, 1252.

[48] J. Ríos-Gómez, M. T. García-Valverde, A. I. López-Lorente, C. Toledo-Neira, R. Lucena and S. Cárdenas, Anal. Chim. Acta, 2020, 1094, 47–56.

[49] C. Parolo and A. Merkoçi, Chem. Soc. Rev., 2013, 42, 450– 457.

[50] M. Saraji and N. Bagheri, Sens. Actuators, B, 2018, 270, 28– 34.

[51] F. B. Kamal Eddin and Y. Wing Fen, Sensors, 2020, 20, 1039.

[52] W. R. de Araujo, T. M. G. Cardoso, R. G. da Rocha, M. H. P. Santana, R. A. A. Muñoz, E. M. Richter, T. R. L. C. Paixão and W. K. T. Coltro, Anal. Chim. Acta, 2018, 1034, 1–21.

[53] A. Shahvar, M. Saraji, H. Gordan and D. Shamsaei, Talanta, 2019, 197, 578–583.

[54] E. W. Nery and L. T. Kubota, Anal. Bioanal. Chem., 2013, 405, 7573–7595.

[55] V. Scognamiglio and F. Arduini, TrAC, Trends Anal. Chem., 2019, 120, 115642.

[56] A. M. López-Marzo and A. Merkoçi, Lab Chip, 2016, 16, 3150–3176.

[57] M. C. Díaz-Liñán, A. I. López-Lorente, S. Cárdenas and R. Lucena, Sens. Actuators, B, 2019, 287, 138–146.

[58] Z. Qiu, J. Shu and D. Tang, Anal. Chem., 2017, 89, 5152–5160.

[59] X. Ge, A. M. Asiri, D. Du, W. Wen, S. Wang and Y. Lin, TrAC, Trends Anal. Chem., 2014, 58, 31–39.

[60] G. Zhu, X. Yin, D. Jin, B. Zhang, Y. Gu and Y. An, TrAC, Trends Anal. Chem., 2019, 111, 100–117.

[61] M. C. Díaz-Liñán, M. T. García-Valverde, A. I. López- Lorente, S. Cárdenas and R. Lucena, Anal. Bioanal. Chem., 2020, 412(15), 3547–3557.

[62] L. Liu, D. Yang and G. Liu, Biosens. Bioelectron., 2019, 136, 60–75.

[63] Y. Thepchuay, T. Sonsa-ard, N. Ratanawimarnwong, S. Auparakkitanon, J. Sitanurak and D. Nacapricha, Anal. Chim. Acta, 2020, 1103, 115–121.

[64] M. Phichi, A. Imyim, T. Tuntulani and W. Aeungmaitrepirom, Anal. Chim. Acta, 2020, 1104, 147–155.

[65] F. Pena-Pereira, L. Villar-Blanco, I. Lavilla and C. Bendicho, Anal. Chim. Acta, 2018, 1011, 1–10.

[66] P. Teengam, W. Siangproh, A. Tuantranont, T. Vilaivan, O. Chailapakul and C. S. Henry, Anal. Chem., 2017, 89, 5428–5435.

[67] L. Yu, Q. Zheng, H. Wang, C. Liu, X. Huang and Y. Xiao, Anal. Chem., 2020, 92, 1402–1408.

[68] J. F. d. S. Petruci and A. A. Cardoso, Anal. Chem., 2016, 88, 11714–11719.

[69] S. M. Restaino, A. Berger and I. M. White, in Biosensors and Biodetection. Methods in Molecular Biology, ed. B. Prickril and A. Rasooly, Humana Press, New York, NY, 2017, 525–540.

[70] R. F. Aroca, Phys. Chem. Chem. Phys., 2013, 15, 5355.

[71] J. L. Delaney, E. H. Doeven, A. J. Harsant and C. F. Hogan, Anal. Chim. Acta, 2013, 790, 56–60.

[72] W. Dungchai, O. Chailapakul and C. S. Henry, Anal. Chem., 2009, 81, 5821–5826.

[73] S. Nantaphol, W. Jesadabundit, O. Chailapakul and W. Siangproh, J. Electroanal. Chem., 2019, 832,

480–485.

[74] A. H. Kamel, X. Jiang, P. Li and R. Liang, Anal. Methods, 2018, 10, 3890–3895.

[75] S. Ge, J. Zhao, S. Wang, F. Lan, M. Yan and J. Yu, Biosens. Bioelectron., 2018, 102, 411–417.

[76] X. Sun, B. Li, C. Tian, F. Yu, N. Zhou, Y. Zhan and L. Chen, Anal. Chim. Acta, 2018, 1007, 33–39.

[77] E. Noviana, C. P. McCord, K. M. Clark, I. Jang and C. S. Henry, Lab Chip, 2020, 20, 9–34.

[78] T. Gebretsadik, T. Belayneh, S. Gebremichael, W. Linert, M. Thomas and T. Berhanu, Analyst, 2019, 144, 2467–2479.

[79] M. Gutiérrez-Capitán, A. Baldi and C. Fernández-Sánchez, Sensors, 2020, 20, 967.

[80] S. Cinti, L. Fiore, R. Massoud, C. Cortese, D. Moscone, G. Palleschi and F. Arduini, Talanta, 2018, 179, 186–192.

[81] N. Dossi, R. Toniolo, F. Terzi, E. Piccin and G. Bontempelli, Electrophoresis, 2015, 36, 1830–1836.

[82] R. Tian, Y. Li and J. Bai, Anal. Chim. Acta, 2019, 1058, 89–96.

[83] H. Qin, Z. Zhu, W. Ji and M. Zhang, Electroanalysis, 2018, 30, 1022–1027.

[84] X.-M. Bi, H.-R. Wang, L.-Q. Ge, D.-M. Zhou, J.-Z. Xu, H.-Y. Gu and N. Bao, Sens. Actuators, B, 2018, 260, 475–479.

[85] M. Amatatongchai, J. Sitanurak, W. Sroysee, S. Sodanat, S. Chairam, P. Jarujamrus, D. Nacapricha and P. A. Lieberzeit, Anal. Chim. Acta, 2019, 1077, 255–265.

[86] H. Li, W. Wang, Q. Lv, G. Xi, H. Bai and Q. Zhang, Electrochem. Commun., 2016, 68, 104–107.

[87] K. Pungjunun, S. Chaiyo, N. Praphairaksit, W. Siangproh, A. Ortner, K. Kalcher, O. Chailapakul and E. Mehmeti, Biosens. Bioelectron., 2019, 143, 111606.

[88] V. B. C. Lee, N. F. Mohd-naim, E. Tamiya and M. U. Ahmed, Anal. Sci., 2018, 34, 7–18.

[89] S. Chaiyo, E. Mehmeti, W. Siangproh, T. L. Hoang, H. P. Nguyen, O. Chailapakul and K. Kalcher, Biosens. Bioelectron., 2018, 102, 113–120.

[90] D. Nechaeva, A. Shishov, S. Ermakov and A. Bulatov, Talanta, 2018, 183, 290–296.

[91] A. Bezerra Martins, A. Lobato, N. Tasić, F. J. Perez-Sanz, P. Vidinha, T. R. L. C. Paixão and L. Moreira Gonçalves, Electrochem. Commun., 2019, 107, 106541.

[92] J. Ding, T. Cherubini, D. Yuan and E. Bakker, Sens. Actuators, B, 2019, 280, 69–76.

[93] Y. Liu, K. Cui, Q. Kong, L. Zhang, S. Ge and J. Yu, Biosens. Bioelectron., 2020, 148, 111839.

[94] S. Nantaphol, A. A. Kava, R. B. Channon, T. Kondo, W. Siangproh, O. Chailapakul and C. S. Henry, Anal. Chim. Acta, 2019, 1056, 88–95.

[95] J. Mettakoonpitak, J. Volckens and C. S. Henry, Anal. Chem., 2020, 92, 1439–1446.

[96] V. Primpray, O. Chailapakul, M. Tokeshi, T. Rojanarata and W. Laiwattanapaisal, Anal. Chim. Acta, 2019, 1078, 16–23.

[97] N. F. D. Silva, C. M. R. Almeida, J. M. C. S. Magalhães, M. P. Gonçalves, C. Freire and C. Delerue-Matos, Biosens. Bioelectron., 2019, 141, 111317.

[98] M. L. Scala-Benuzzi, J. Raba, G. J. A. A. Soler-Illia, R. J. Schneider and G. A. Messina, Anal. Chem., 2018, 90, 4104–4111.

[99] J. Qi, B. Li, N. Zhou, X. Wang, D. Deng, L. Luo and L. Chen, Biosens. Bioelectron., 2019, 142, 111533.

[100] W. A. Ameku, W. R. de Araujo, C. J. Rangel, R. A. Ando and T. R. L. C. Paixão, ACS Appl. Nano Mater., 2019, 2, 5460–5468.

[101] H. Wang, J. Liu, R. G. Cooks and Z. Ouyang, Angew. Chem., Int. Ed., 2010, 49, 877–880.

[102] J. Liu, H. Wang, N. E. Manicke, J.-M. Lin, R. G. Cooks and Z. Ouyang, Anal. Chem., 2010, 82, 2463–2471.

[103] F. Bianchi, N. Riboni, V. Termopoli, L. Mendez, I. Medina, L. Ilag, A. Cappiello and M. Careri, J. Anal. Methods Chem., 2018, 2018, 1–24.

[104] C.-H. Lin, W.-C. Liao, H.-K. Chen and T.-Y. Kuo, Bioanalysis, 2014, 6, 199–208.

[105] J. Ji, L. Nie, L. Liao, R. Du, B. Liu and P. Yang, J. Chromatogr. B, 2016, 1015–1016, 142–149.

[106] B. J. Bills, J. Kinkade, G. Ren and N. E. Manicke, Forensic Chemistry, 2018, 11, 15–22.

[107] C. Zhang and N. E. Manicke, Anal. Chem., 2015, 87, 6212–6219.

[108] C. Vega, C. Spence, C. Zhang, B. J. Bills and N. E. Manicke, J. Am. Soc. Mass Spectrom., 2016, 27, 726–734.

[109] N. E. Manicke, B. J. Bills and C. Zhang, Bioanalysis, 2016, 8, 589–606.

[110] S. Bag, P. I. Hendricks, J. C. Reynolds and R. G. Cooks, Anal. Chim. Acta, 2015, 860, 37–42.

[111] S. Banerjee, C. Basheer and R. N. Zare, Angew. Chem., Int. Ed., 2016, 55, 12807–12811.

[112] H. V. Pereira, V. S. Amador, M. M. Sena, R. Augusti and E. Piccin, Anal. Chim. Acta, 2016, 940, 104–112.

[113] G. I. Salentijn, H. P. Permentier and E. Verpoorte, Anal. Chem., 2014, 86, 11657–11665.

[114] J. McKenna, E. S. Dhummakupt, T. Connell, P. S. Demond, D. B. Miller, J. Michael Nilles, N. E. Manicke and T. Glaros, Analyst, 2017, 142, 1442–1451.

[115] S. Dowling, E. M. McBride, J. McKenna, T. Glaros and N. E. Manicke, Forensic Chemistry, 2020, 17, 100206.

[116] Y. Yang, H. Liu, Z. Chen, T. Wu, Z. Jiang, L. Tong and B. Tang, Anal. Chem., 2019, 91, 12874–12881.

[117] Y. Zheng, Q. Wang, X. Wang, Y. Chen, X. Wang, X. Zhang, Z. Bai, X. Han and Z. Zhang, Anal. Chem., 2016, 88, 7005–7013.

[118] J. Li, Y. Zheng, W. Mi, T. Muyizere and Z. Zhang, Anal. Methods, 2018, 10, 2803–2811.

[119] X. Wang, Y. Zheng, T. Wang, X. Xiong, X. Fang and Z. Zhang, Anal. Methods, 2016, 8, 8004–8014.

[120] R. Narayanan, D. Sarkar, R. G. Cooks and T. Pradeep, Angew. Chem., Int. Ed., 2014, 53, 5936–5940.

[121] M. T. Dulay and R. N. Zare, Rapid Commun. Mass Spectrom., 2017, 31, 1651–1658.

[122] T. C. Colletes, P. T. Garcia, R. B. Campanha, P. V. Abdelnur, W. Romão, W. K. T. Coltro and B. G. Vaz, Analyst, 2016, 141, 1707–1713.

[123] J. Liu, Y. He, S. Chen, M. Ma, S. Yao and B. Chen, Talanta, 2017, 166, 306–314.

[124] L. Di Donna, D. Taverna, S. Indelicato, A. Napoli, G. Sindona and F. Mazzotti, Food Chem., 2017, 229, 354–357.

[125] T. P. P. Mendes, I. Pereira, M. R. Ferreira, A. R. Chaves and B. G. Vaz, Anal. Methods, 2017, 9, 6117–6123.

[126] L. S. Tavares, T. C. Carvalho, W. Romão, B. G. Vaz and A. R. Chaves, J. Am. Soc. Mass Spectrom., 2018, 29, 566–572.

[127] T. Zargar, T. Khayamian and M. T. Jafari, Microchim. Acta, 2018, 185, 103.

[128] F. M. de Oliveira, G. L. Scheel, R. Augusti, C. R. T. Tarley and C. C. Nascentes, Anal. Chim. Acta, 2020, 1106, 52–60.

[129] E. Aydindogan, E. Guler Celik and S. Timur, Anal. Chem., 2018, 90, 12325–12333.

[130] M. Rezazadeh, S. Seidi, M. Lid, S. Pedersen-Bjergaard and Y. Yamini, TrAC, Trends Anal. Chem., 2019, 118, 548–555.

[131] B. Gross, S. Y. Lockwood and D. M. Spence, Anal. Chem., 2017, 89, 57–70.

BLOQUE II

PAPEL COMO SORBENTE EN QUÍMICA ANALÍTICA

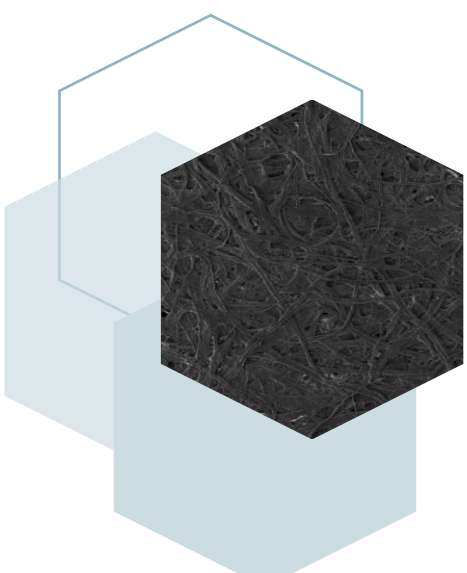

En los últimos años, se han explotado las ventajas del papel como soporte. Este material presenta numerosas ventajas, como por ejemplo flexibilidad, estabilidad mecánica y bajo coste; pero, además, es posible modificarlo químicamente, lo que aumenta su versatilidad como sorbente.

Sin embargo, el papel sin modificar, gracias a su naturaleza celulósica, puede establecer interacciones con diferentes compuestos, como por ejemplo las aminas. Los puentes de hidrógeno juegan un papel esencial en la interacción entre las cadenas de celulosa, lo que permite su empaquetamiento en fibras. Algunas aminas son capaces de romper estos enlaces y formar nuevos puentes de hidrógeno con las cadenas de celulosa [1]. En este Bloque de la memoria de la Tesis Doctoral se presenta el uso de papel de filtro para la extracción de siete aminas biogénicas de muestras de cerveza **(Capítulo 2).**

La metodología desarrollada en este Bloque supone un gran avance en la dirección de la Química Analítica verde [2] y la Química Analítica blanca [3], pues se minimiza el consumo de reactivos, disolventes y energía al no ser necesaria la modificación del papel. Asimismo, el análisis directo de los eluidos mediante espectrometría de masas usando la técnica de infusión directa permite acelerar la generación de resultados.

[1] D. Sawada, Y. Nishiyama, L. Petridis, R. Parthasarathi, S. Gnanakaran, V.T. Forsyth, M. Wada, P. Langan, Structure and dynamics of a complex of cellulose with EDA: insights into the action of amines on cellulose, Cellulose 20 (2013) 1563-1571.

[2] A. Gałuszka, Z. Migaszewski, J. Namieśnik, The 12 principles of green analytical chemistry and the significance mnemonic of green analytical practices, TrAC Trends Anal. Chem. 50 (2013) 78–84.

[3] P.M. Nowak, R. Wietecha-Posłuszny, J. Pawliszyn, White analytical chemistry: an approach to reconcile the principles of green analytical chemistry and functionality, TrAC Trends Anal. Chem. (2021) 116223.

Capítulo 2

Unmodified cellulose filter paper, a sustainable and affordable sorbent for the isolation of biogenic amines from beer samples

Journal of Chromatography A, 1651 (2021) 462297

Journal of Chromatography A
1651 (2021) 462297

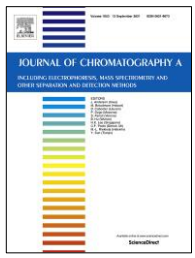

Unmodified cellulose filter paper, a sustainable and affordable sorbent for the isolation of biogenic amines from beer samples

M.C. Díaz-Liñán, R. Lucena*, S. Cárdenas, A.I. López-Lorente

Affordable and Sustainable Sample Preparation (AS2P) Research Group. Departamento de Química Analítica, Instituto Universitario de Investigación en Química Fina y Nanoquímica IUNAN, Universidad de Córdoba, Campus de Rabanales, Edificio Marie Curie, E-14071 Córdoba, Spain

While current trends in Green Analytical Chemistry aim at reducing or simplifying sample treatment, food usually comprises complex matrices where direct analysis is not possible in most cases. In this context, sample treatment plays a pivotal role. Biogenic amines are naturally formed in many foodstuffs due to the action of microorganisms, while their presence has been associated with adverse health effects. In this work, the extraction of seven biogenic amines (cadaverine, histamine, phenylethylamine, putrescine, spermidine, spermine, and tyramine) from beer samples has been simplified using laboratory filter paper as sorbent without any further modification. The analysis of the eluates by direct infusion mass spectrometry reduces the time of analysis, increasing the sample throughput. This simple but effective method enabled the determination of the analytes with limits of detection as low as 0.06 mg L^{-1} and relative standard deviations better than 11.9%. The suitability of the method has been assessed by analyzing eight different types of beers by the standard addition method.

Keywords: Biogenic amines, Filter paper, Direct infusion mass spectrometry, Cellulose.

1. Introduction

Biogenic amines (BAs) are compounds with a low molecular weight present in living organisms' cells and associated with metabolic processes [1]. They can also be detected in various foods and beverages containing free amino acids due to the action of microorganisms with decarboxylase activity and convenient circumstances for bacterial production [2]. Although BAs play an important role in different physiological activities, a high intake of these compounds may result in adverse health effects, such as headaches, arrhythmias, and alterations of blood pressure, among other consequences [3]. For this reason, the determination of BAs content in food is of high importance. Foodstuff obtained through microbial-mediated fermentation may possess high amounts of BAs, while vegetable-type foods are generally considered products with low BAs content [4]. Regarding legal limits, only histamine has been strictly restricted since it can cause so-called scombroid poisoning [5]. Depending on the fish product, the European Union has established a maximum amount of histamine of 400 $mg \cdot kg^{-1}$ [6], while in beverages, it is recommended a concentration below 2 $mg \cdot L^{-1}$ [7]. As for other BAs, such as cadaverine, putrescine, or spermidine, among others, no limits have been established, although ranges of 100–800 $mg \cdot kg^{-1}$ and 30 $mg \cdot kg^{-1}$ for tyramine and phenylethylamine, respectively, were suggested a few decades ago as safe limits [7]. Nevertheless, it is crucial to monitor the accumulation of BAs since they have a synergistic effect on the toxicological outcome of other compounds. Also, some BAs can form carcinogenic nitrosamines via interaction with nitrites [8].

Different techniques have been employed for the determination of BAs in foods and beverages, including thin-layer chromatography [9, 10], capillary electrophoresis [11, 12], and gas and liquid chromatography coupled to different detectors [13–16]. Among all of them, liquid chromatography (LC) coupled to mass spectrometry (MS) or ultraviolet-visible spectroscopy is the most employed. To avoid low sensitivity or tailing peaks due to the high polarity of BAs, derivatization is usually carried out [17–19]. However, this process is time-consuming and can affect the recoveries of

the analytes [20]. On the other hand, food samples are complex which make sample preparation almost unavoidable.

The Green Analytical Chemistry (GAC) advocates for direct analysis, avoiding any sample preparation [21]. The recently defined White Analytical Chemistry (WAC) concept reconciles the GAC principles with the primary objective of Analytical Chemistry [22], the obtaining of reliable chemical information. Sample preparation is accepted under the WAC umbrella if it is needed to solve an analytical problem. The development of efficient sample preparation procedures, which fit the analytical problem under evaluation while having a low environmental impact, can be defined as the main aim in the scenario defined by GAC and WAC. The use of natural materials in sample preparation is a clear trend [23, 24]. In this context, paper has been gaining attention due to its multiple advantages. On the one hand, it is mechanically stable [25], which in turn facilitates the coupling of this material with instrumental techniques such as MS [26, 27], surface-enhanced Raman spectroscopy [26, 28], or fluorimetry [29]. Furthermore, it enables the spontaneous fluidic transport of compounds, reducing the amount of sample and reagents used. Also, it is a widely accessible and cost-effective material.

In this work, a fast and straightforward method for the determination of seven biogenic amines in beer samples is proposed. The analytes are isolated from the sample using unmodified cellulose filter paper as sorbent. The extraction does not require any complex apparatus since the samples are incubated with the sorbent for 45 min under continuous agitation. The analytes are quantified via direct infusion MS. The suitability of the method was evaluated by analyzing eight commercial beer samples, obtaining concentration values similar to those previously described in other works.

2. Materials and methods

2.1. Reagents

Unless otherwise specified, all reagents were obtained from Sigma-Aldrich (Madrid, Spain) with an analytical grade or better. Stock solutions of cadaverine (CAD), histamine (HIS), phenylethylamine (PHE), putrescine (PUT), spermidine (SPD), spermine (SPR) and tyramine (TYR) were prepared in HCl 0.1 mol·L^{-1} at a concentration of 10,000 mg·L^{-1} and stored in the dark at 4 °C. Working solutions were prepared at the appropriate concentration by dilution of the stock in HCl 0.1 mol·L^{-1} or beer sample. Hexamethylenediamine (HMDA) was employed as the internal standard (IS) and was added to the sample before extraction. Fig. 1 depicts the structure of all the amines employed in this work, including the IS. During the optimization of pH and ionic strength, 1 mol·L^{-1} solutions of NaOH and Na_2SO_4 were used, respectively, for the standards and sample adjustments.

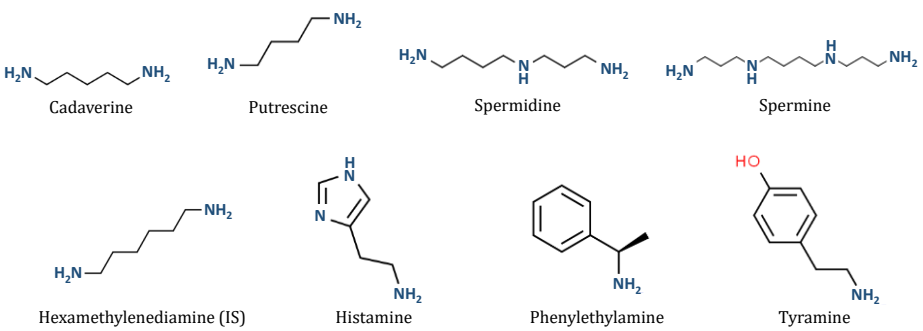

Figure 1. Chemical structure of the biogenic amines and the internal standard employed in this work.

Milli-Q water (Millipore Corp., Madrid, Spain), LC-MS-quality formic acid and LC-MS-quality acetonitrile were used as the carrier phase for direct infusion mass spectrometric analysis.

For the extraction of the analytes, common filter paper (i.e., Filter-Lab 42×52 cm, with a density of 73 g·cm^{-2}) was employed as sorbent.

The different beer samples were obtained from a local market.

2.2. Extraction procedure

This research aimed to design a straightforward and rapid analytical method to determine biogenic amines in beer. For simplicity, external calibration was selected as the first approach. The standards were prepared using an aqueous media containing 5% of ethanol to mimic a conventional beer matrix. The pH and the ionic strength (expressed as electrical resistivity) were fixed at 4.34 and 7.9·10^{-4} μΩ·cm, respectively. For the extraction, 1 mL of the standard, containing the IS at 1 mg·L^{-1}, was placed in an Eppendorf tube and incubated with a paper strip (1.5 ×0.5 cm) for 45 min under vigorous agitation in an orbital stirrer. Later, the paper strip was rinsed with Milli-Q water for 5 min and finally eluted with 0.5 mL of a 0.1% formic acid in methanol/water 60:40 mixture for 5 min in an orbital stirrer.

As the external calibration model did not provide acceptable relative recoveries, the standard addition method was finally selected. Initially, beer samples were ultrasonically degassed. The samples were spiked with the analytes at the required concentration, adding the IS at 0.5 mg·L^{-1}. Finally, the samples were extracted following the same procedure previously described for external calibration standards.

2.3. Mass spectrometry measurements

Direct infusion mass spectrometry was carried out using an Agilent 1260 Infinity HPLC system (Agilent, Palo Alto, CA, USA) arranged with an autosampler and a binary high-pressure pump. 10 μL of the standards or sample extracts were directly injected in a carrier phase composed of 0.1% formic acid in Milli-Q water (solvent A) and 0.1% formic acid in LC-MS-quality acetonitrile (solvent B) in an 85/15 v/v%

proportion. The flow rate was 0.3 mL·min^{-1}, and the analysis time was 2 min.

For analyte detection and quantification, an Agilent 6420 triple quadrupole MS with an electrospray source was employed. The different mass spectrometer settings were optimized to increase the selected reaction monitoring (SRM) signal. The selected values were 7 L·min^{-1} flow using a temperature of 300 °C of the drying gas, i.e., nitrogen with 99.9% purity. The nebulizer pressure was kept at 30 psi, while the voltage of the capillary was set to 4000 V in positive mode. A 1 mg·L^{-1} solution of standards in Milli-Q water was directly infused in the mass spectrometer to optimize the instrumental parameters for the MS/MS determination of the analytes and the IS. These parameters are specified in Table S1 (supplementary material). Finally, for data analyses, Agilent MassHunter Software (version B.06.00) was used.

3. Results and discussion

In the last years, our research group has studied in detail the design of new paper-based sorptive phases for the extraction of different analytes from food [29], biological [30, 31], and environmental matrices [32]. In these materials, the paper acts as a support of the actual sorptive phase that can be a polymer [29–31], a nanoparticle [33] or a combination of both [26, 32]. These coatings provide an enhancement of the sorptive capacity and or selectivity of the materials.

Metallic silver can interact selectively with amines [34]. The modification of paper with metallic silver, which can be easily developed by immersing the paper into a silver nitrate solution followed by UV curing [26], was our initial objective. However, during the first experiments, a high background extraction of the amines, in the absence of metallic silver, was observed. These results suggested the ability of unmodified paper to interact with amines. H-bonding plays a critical role in stacking cellulose chains, thus permitting their packing into fibers [35]. The disruption of the H-bonding pattern of cellulose by some amines, like ethylene diamine, has been reported [36], providing insight into the mechanism for extracting BAs from beer samples. In fact, the use of unmodified cellulose to extract amine-containing

molecules can be found in the literature [37].

3.1. Evaluation of the variables that affect the extraction

The different variables that could influence the extraction efficiency and, thereby, the signal obtained in the mass spectrometry measurements, were studied following a univariate approach. Each beer sample has a characteristic ethanol content, pH, and ionic strength. For this reason, these chemical variables were evaluated in detail. The extraction kinetics was also evaluated to boost the sensitivity of the determination.

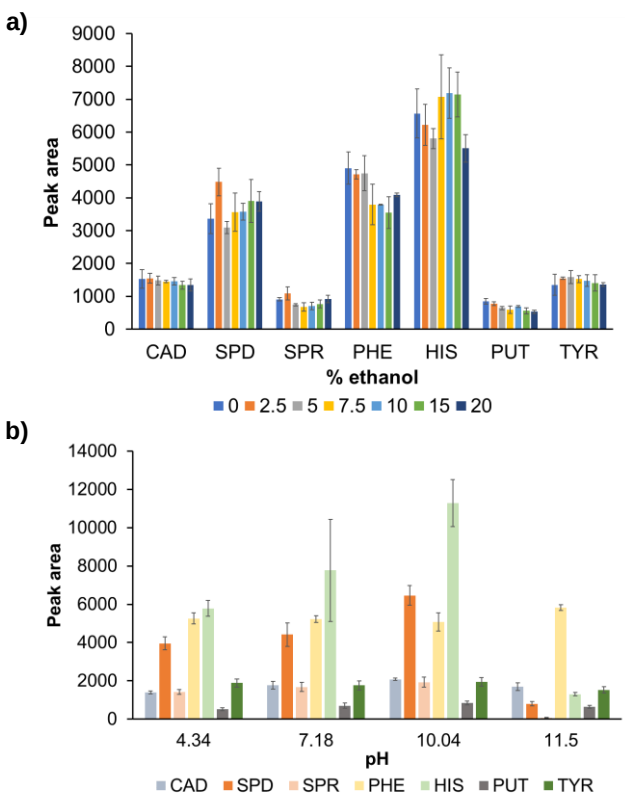

Figure 2. Effect of (a) % of ethanol and (b) pH on the peak areas of the analytes after extraction from an aqueous solution with the analytes present at a concentration of 500 $\mu g \cdot L^{-1}$.

Firstly, the effect of the ethanol content was examined in the interval 0–20%. As can be observed in Fig. 2a, there are no significant differences in the range studied. However, an analysis of variance (ANOVA) was carried out to fully demonstrate this point. The results revealed that there are no significant differences ($F<F_{crit}$) in the signals in the range studied for all the analytes except for PUT, in which the F-value was slightly superior to the F_{crit}-value. Considering this result, the ethanol content was fixed at 5% for standards to mimic the beer samples matrix.

The extraction pH was studied because it affects the ionization state of both the analytes and the sorbent in solid-phase extraction procedures. The pH was studied in a range from 4.34 (lower value of the analyzed beers) to 11.5. As can be seen in Fig. 2b, the signals of SPD and HIS were positively affected by the pH. However, the signal for SPR was negatively affected at a very basic pH. For the remaining analytes (namely, CAD, PHE, PUT and TYR) no significant differences were observed in the range of pH investigated. Considering these results, a pH value of 4.34 was selected as optimum since it provided the best reproducibility while maintaining a good signal. Furthermore, all the beer samples have a similar pH value, thus avoiding further altering the matrix.

The effect of ionic strength was evaluated, using the electrical resistivity as the parameter, in the range from 18 μΩ·cm (Milli-Q water) to $3.5 \cdot 10^{-4}$ μΩ·cm. As can be discerned from Fig. 3, the best results were obtained without the addition of any electrolyte to the medium. Note that the x-axis is represented in a decreasing resistivity scale since resistivity drops when the ionic strength increases. The optimum extraction condition is not realistic for sample analysis as samples present ionic strength. The electrical resistivity of several beer samples was measured, and the lower resistivity value (higher ionic strength) resulted in being $7.9 \cdot 10^{-4}$ μΩ·cm. This value was selected as the optimum as it permits the adjustment of the samples, adding an electrolyte, before their processing.

The extraction time was studied in the range of 15–60 min. No significant differences were found in the range investigated for all the analytes except for SPD,

which increases up to 45 min (Fig. S1). An analysis of variance was performed to verify this point. As expected, all the F-values were lower than the F_{crit}-values, thus confirming that there are no significant differences in the signals of the analytes in all the range studied, except for SPD in which the F-value was superior to the F_{crit}-value. Therefore, 45 min was selected as the optimal extraction time. Although it is a relatively long time, many samples can be simultaneously extracted in the orbital stirrer allowing a high sample throughput. Also, the precision values are better at 45 min compared to 15 min.

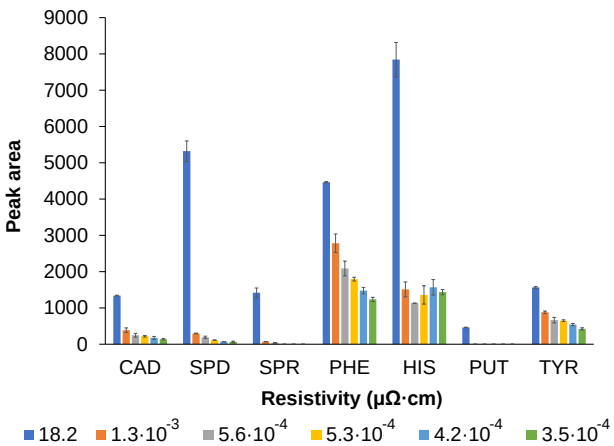

Figure 3. Effect of the ionic strength (expressed as electrical resistivity) on the extraction of the analytes from 500 μg·L^{-1} aqueous solutions.

3.2. Analytical evaluation by an external calibration model

A calibration graph was built using standard solutions containing the analytes at concentrations between 0.2 and 10 mg·L^{-1} and the IS at 1 mg·L^{-1}. To simulate a general beer matrix, the standards contained 5% ethanol. Also, the pH and ionic strength of standards were fixed at the optimized value. The ratio (areas of the analyte)/(area of IS) was represented versus the concentration. Data were adjusted to linear models obtaining R^2 values ranging from 0.983 to 0.998. The limit of

detection (LOD), obtained from a signal to noise ratio (S/N) of 3, was 0.06 mg·L^{-1} for all the analytes, PUT excepted (0.18 mg·L^{-1}). The limit of quantification (LOQ) for each analyte, obtained from a S/N of 10, resulted to be 0.2 mg·L^{-1} for all the analytes, PUT excepted (0.6 mg·L^{-1}). The precision, expressed at relative standard deviation (n=3), at 2.5 mg·L^{-1} varied between 0.7 and 11.9%. The data are summarized in Table 1 and the calibration graphs are shown in Fig. S2.

The application of these models to the analysis of real samples was not satisfactory since the relative recoveries were far from being quantitative. In fact, the slopes of the calibration curves obtained for standards and spiked beer samples were statistically different. For this reason, the addition standard method was selected.

Table 1. Analytical figures of merit of the external calibration model. For building the model, solutions containing the target analytes and the internal standards were extracted, the final extracts being analyzed by direct infusion MS.

Analyte	LOD (mg·L^{-1})	LOQ (mg·L^{-1})	Linear range (mg·L^{-1})	R^2	RSD (%)
Cadaverine	0.06	0.2	LOQ-10	0.995	9.5
Histamine	0.06	0.2	LOQ-10	0.991	6.7
Phenylethylamine	0.06	0.2	LOQ-10	0.998	0.7
Putrescine	0.18	0.6	LOQ-10	0.983	6.6
Spermidine	0.06	0.2	LOQ-10	0.990	11.9
Spermine	0.06	0.2	LOQ-10	0.996	8.6
Tyramine	0.06	0.2	LOQ-10	0.996	2.9

LOD: limit of detection, LOQ: limit of quantification, RSD: relative standard deviation

3.3. Addition standard method analysis of beer samples

The reliability of the method was evaluated through the analysis of eight commercial beer samples obtained from a local market in Córdoba, Spain. The addition standard calibration graphs are shown in Fig. S3. All the analytes were detected in the eight beer samples, except for HIS and PHE, which were below the LOD in several samples. As can be observed in Table 2, CAD, PUT and TYR were the

most abundant amines in all the samples, ranging from 0.55 to 1.13 mg·L^{-1}, 3.25 to 15.10 mg·L^{-1} and 0.64 to 3.75 mg·L^{-1}, respectively.

Table 2. Analysis of beer samples by the addition standard methods. The samples were ultrasonic degassed and extracted using paper as sorptive phase. The extracts are analyzed by direct infusion MS.

Beer sample		**Biogenic amine content (mg·L^{-1})**						
Type	% alcohol	Cadaverine	Histamine	Phenylethylamine	Putrescine	Spermidine	Spermine	Tyramine
Lager Pilsen	5	0.55 ± 0.07	< LOD	< LOD	4.47 ± 0.08	0.41 ± 0.04	> LOD <LOQ	0.66 ± 0.08
Oktoberfest-Märzen	7.2	0.9 ± 0.1	> LOD <LOQ	< LOD	6 ± 1	0.55 ± 0.05	0.39 ± 0.02	0.81 ± 0.03
Dark Lager	5.9	1.13 ± 0.03	> LOD <LOQ	< LOD	4.9 ± 0.4	0.46 ± 0.01	0.20 ± 0.01	0.93 ± 0.02
Weissbier	5	1.1 ± 0.1	0.22 ± 0.02	> LOD <LOQ	3.4 ± 0.4	1.38 ± 0.09	0.34 ± 0.02	3.7 ± 0.2
Dark abbey Belgium	6	0.62 ± 0.07	> LOD <LOQ	< LOD	Above the linear range	> LOD <LOQ	> LOD <LOQ	1.2 ± 0.2
Dark wheat beer	5.3	1.11 ± 0.08	0.27 ± 0.01	> LOD <LOQ	6.6 ± 0.7	0.46 ± 0.02	> LOD <LOQ	0.64 ± 0.04
Lager 0.0	0	1.1 ± 0.1	> LOD <LOQ	< LOD	5.2 ± 0.3	0.60 ± 0.05	0.27 ± 0.05	0.73 ± 0.09
Blond abbey	8.5	0.7 ± 0.1	> LOD <LOQ	< LOD	3.2 ± 0.3	0.22 ± 0.02	> LOD <LOQ	1.5 ± 0.2

LOD: limit of detection, LOQ: limit of quantification

Furthermore, SPD and SPR varied from 0.22 to 1.38 mg·L^{-1} and 0.20 to 0.39 mg·L^{-1}, respectively. As can be observed in Table 3, the LOQs reported in previous works for the determination of biogenic amines in food matrices are generally below the LOQs reported in this work. However, all the approaches involve chromatography and longer analysis time are required. Considering that biogenic amines are usually found at relatively high concentration levels, the previous step of chromatography has been avoided in this work and reasonable concentration levels have been obtained with direct infusion of the analytes compared to those observed in Table 3, thus demonstrating the suitability of the method for the determination of these compounds in beer samples [19, 38].

Table 3. Comparison of the proposed method with other counterparts proposed in the literature to determine biogenic amines in beer samples.

Biogenic amine	Sample matrix	Sample pretreatment	Extraction method	Technique	LOD ($\mu g \cdot L^{-1}$)	LOQ ($\mu g \cdot L^{-1}$)	Ref.
TRP, PHE, PUT, CAD, HIS, TYR, SPD and SPM	Wine and beer	Degasification, treatment with PVPP, derivatization and filtration	-	HPLC-fluorescence	30-180	200-590	[19]
PA , DMA , EA , DEA , MA , TRP, CAD, SPM, PHE, TYR, PUT, HIS, BA , HEA , isoPA , SPD and AGM	Beer	Degasification and 1 + 9 v/v dilution	-	RPLC-MS	0.54-4.30	1.6-13.0	[17]
SPM, SPD, TYR, HIS, PHE and TRP	Beer and milk	pH adjustment, filtration and derivatization (beer)	MIL-DLLME	HILIC-MS HPLC-UV-Vis	12-94 0.51-1.49	35-290 1.70-4.93	[39]
PUT, AGM, CAD, ETA, HIS, TRP, TYR and PHE	Beer	Sonication, filtration and derivatization	-	UHPLC-fluorescence	7-206	22-681	[40]
CAD, SPM, PHE, SPD, TYR, HIS, PUT and TRP	Beer	Elimination of natural biogenic amines and pH adjustment	MSPE	LC-HRMS	0.02-0.05	0.05-0.10	[41]
MA , DMA , EA , isoPPA , DEA , isoBA, MBA, PD, isoAA, MF, PP, AA, PHE, DAP, PUT, CAD, HIS and TYR	Beer	pH adjustment, filtration and derivatization (beer)	DLLME	GC-MS	0.3-2.9	1.0-9.5	[42]
TYR, PHE and OCT	Beer	Derivatization	IL-UALLME	HPLC-fluorescence	0.25-0.50	0.83-166.67	[43]
CAD, TYR, TRP, HIS and SPD	Fermented fish, beer and wine	Sonication and filtration (beer and wine)	VSLLME	HPLC-DAD	1.0-2.6	3.3-8.5	[44]
TYR, HIS, PHE, TRP, CAD, PUT, AGM, SPD and SPM	Fermented foods, beer and wine	Sonication and filtration (beer and wine)	DUADLLME	UHPLC-MS	0.3-0.7	2-4	[45]
CAD, HIS, PHE, PUT, SPD, SPM and TYR	Beer	-	Raw filter paper	DI-MS	60-180	200-600	This work

PA: propylamine, DMA: dimethylamine, EA: ethylamine, DEA: diethylamine, MA: methylamine, TRP: tryptamine, BA: butylamine, HEA: hexylamine, isoPA: isopentylamine, AGM: agmatine, RPLC-MS: reversed phase liquid chromatography-mass spectrometry, HILIC: hydrophilic interaction liquid chromatography, MIL-DLLME: magnetic ionic liquid-dispersive liquid-liquid microextraction, PVPP:

polyvinylpolypyrrolidone, ETA: ethanolamine, UHPLC: ultra-high performance liquid chromatography, MSPE: magnetic solid phase extraction, LC: liquid chromatography, isoPPA: isopropylamine, isoBA: isobutylamine, MBA: 2-methybutylamine, PD: pyrrolidine, isoAA: isoamylamine, MF: morfoline, PP: piperidine, AA: amylamine, DAP: 1,3-diaminopropane, GC: gas chromatography, OCT: octopamine, IL-UALLME: ionic liquid-based ultrasound-assisted liquid-liquid microextraction, VSLLME: vortex-assisted surfactant-enhanced emulsification liquid-liquid microextraction, DAD: diode array detector, DUADLLME: derivatization ultrasound-assisted dispersive liquid-liquid microextraction.

4. Conclusions

In the present work, the use of common filter paper for the extraction of seven biogenic amines from beer samples and its subsequent determination via direct infusion mass spectrometry has been described. The use of paper as extracting material has multiple advantages. It is widely available and cost-effective. Its chemical structure enables its interaction with these compounds via hydrogen bonds, not requiring any chemical modification. Thus, it was possible to develop a straightforward and rapid method for the extraction of biogenic amines, a global concern due to their adverse effects on human health. The simplicity of the procedure enables the reduction of the consumption of reagents, solvents, while paper is considered as an environmentally friendly sorbent, which keeps this method in line with the tendency of Green Analytical Chemistry. After their extraction, the analytes are measured by direct infusion mass spectrometry, reducing, even more, the analytical procedure. This strategy significantly reduces the time of analysis and sample throughput while making possible multianalyte analysis.

The use of an external calibration method for the determination of the analytes did not provide acceptable accuracy results. For this reason, the standard addition method is proposed as an alternative. This aspect can be considered as the main limitation of the approach since several standards must be prepared for the analysis of each sample. However, the possibility of the simultaneous extraction of several

standards at the same time in the orbital stirrer and the rapid MS analysis (ca. 2 min) allows compensating this limitation. The applicability of the method was evaluated by analyzing eight commercial beers, in which almost all the analytes were naturally found, at concentrations similar to that obtained in previous works.

The proposed method was compared with other counterparts reported in the literature [17, 19, 39–45]. Our method, together with [19], is the less sensitive one, although it responds to the usual concentrations of the biogenic amines in beer samples. However, our method avoids the analyte derivatization necessary in some methods [19, 39, 40, 43, 45] and simplifies the extraction procedure compared to other approaches [41–44]. Also, the analysis time is reduced compared to those methods based on chromatographic analysis [17, 19, 39–45].

Declaration of Competing Interest

The authors declare that they have no competing interests or personal relationships that could have influenced in any way the work developed in this article.

CRediT authorship contribution statement

M.C. Díaz-Liñán: Investigation, Data curation, Writing - original draft. R. Lucena: Conceptualization, Supervision, Writing - review & editing. S. Cárdenas: Supervision, Funding acquisition, Writing - review & editing. A.I. López-Lorente: Conceptualization, Supervision, Writing - review & editing.

Acknowledgements

Financial support from the Spanish Ministry of Economy and Competitiveness (CTQ2017-83175R) is gratefully acknowledged.

Supplementary materials

Supplementary material associated with this article can be found, in the online version, at doi: 10.1016/j.chroma.2021.462297.

References

[1] G. Spano, P. Russo, A. Lonvaud-Funel, P. Lucas, H. Alexandre, C. Grandvalet, E. Coton, M. Coton, L. Barnavon, B. Bach, F. Rattray, A. Bunte, C. Magni, V. Ladero, M. Alvarez, M. Fernández, P. Lopez, P.F. De Palencia, A. Corbi, H. Trip, J.S. Lolkema, Biogenic amines in fermented foods, Eur. J. Clin. Nutr. 64 (2010) S95–S100, doi: 10.1038/ejcn.2010.218.

[2] D. Doeun, M. Davaatseren, M.S. Chung, Biogenic amines in foods, Food Sci. Biotechnol. 26 (2017) 1463–1474, doi: 10.1007/s10068-017-0239-3.

[3] R. Tofalo, G. Perpetuini, M. Schirone, G. Suzzi, Biogenic amines: toxicology and health effect, in: Encyclopedia Food Health, Elsevier, 2016, pp. 424–429, doi: 10.1016/B978-0-12-384947-2.00071-4.

[4] A. Önal, A review: current analytical methods for the determination of biogenic amines in foods, Food Chem. 103 (2007) 1475–1486, doi: 10.1016/j.foodchem.2006.08.028.

[5] Y. Özogul, F. Özogul, Chapter 1. biogenic amines formation, toxicity, regulations in food, in: 2019: pp. 1–17. doi:10.1039/9781788015813-00001.

[6] European Community, European Commission regulation (EC) no. 2073/2005, 2005.

[7] B. ten Brink, C. Damink, H.M.L.J. Joosten, J.H.J. Huis in't Veld, Occurrence and formation of biologically active amines in foods, Int. J. Food Microbiol. 11 (1990) 73–84, doi: 10.1016/0168-1605(90)90040-C

[8] G. Drabik-Markiewicz, B. Dejaegher, E. De Mey, T. Kowalska, H. Paelinck, Y.V. Heyden, Influence of putrescine, cadaverine, spermidine or spermine on the formation of N -nitrosamine in heated cured pork meat, Food Chem. 126 (2011) 1539–1545, doi: 10.1016/j.foodchem.2010.11.149.

[9] J. Lapa-Guimarães, J. Pickova, New solvent systems for thin-layer chromatographic determination of nine biogenic amines in fish and squid, J. Chromatogr. A 1045 (2004) 223–232, doi: 10.1016/j.chroma.2004.06.014.

[10] H. Yu, D. Zhuang, X. Hu, S. Zhang, Z. He, M. Zeng, X. Fang, J. Chen, X. Chen, Rapid determination of histamine in fish by thin-layer chromatography-image analysis method using diazotized visualization reagent prepared with p-nitroaniline, Anal. Methods 10 (2018) 3386–3392, doi: 10.1039/C8AY00336J.

[11] D. An, Z. Chen, J. Zheng, S. Chen, L. Wang, Z. Huang, L. Weng, Determination of biogenic amines in oysters by capillary electrophoresis coupled with electrochemiluminescence, Food Chem. 168 (2015) 1–6, doi: 10.1016/j.foodchem.2014.07.019.

[12] K. Maráková, J. Piešťanský, Z. Zelinková, P. Mikuš, Simultaneous determination of twelve biogenic amines in human urine as potential biomarkers of inflammatory bowel diseases by capillary electrophoresis–tandem mass spectrometry, J. Pharm. Biomed. Anal. 186 (2020) 113294, doi: 10.1016/j.jpba.2020.113294.

[13] W. Jia, R. Zhang, L. Shi, F. Zhang, J. Chang, X. Chu, Effects of spices on the formation of biogenic amines during the fermentation of dry fermented mutton sausage, Food Chem. 321 (2020) 126723, doi: 10.1016/j.foodchem.2020.126723.

[14] C. Proestos, P. Loukatos, M. Komaitis, Determination of biogenic amines in wines by HPLC with precolumn dansylation and fluorimetric detection, Food Chem. 106 (2008) 1218–1224, doi: 10.1016/j.foodchem.2007.06.048.

[15] M.A. Ali Awan, I. Fleet, C.L. Paul Thomas, Determination of biogenic diamines with a vaporisation derivatisation approach using solid-phase microextraction gas chromatography–mass spectrometry, Food Chem. 111 (2008) 462–468, doi: 10.1016/j.foodchem.2008.03.068.

[16] F. Cecchini, M. Morassut, Effect of grape storage time on biogenic amines content in must, Food Chem. 123 (2010) 263–268, doi: 10.1016/j.foodchem.2010.04.026.

[17] K. Nalazek-Rudnicka, P. Kubica, A. Wasik, Discrepancies in determination of biogenic amines in beer samples by reversed phase and hydrophilic interaction liquid chromatography coupled with tandem mass spectrometry, Microchem. J. 159 (2020) 105574, doi: 10.1016/j.microc.2020.105574.

[18] M.P. Arrieta, M.S. Prats-Moya, Free amino acids and biogenic amines in alicante monastrell wines, Food Chem. 135 (2012) 1511–1519, doi: 10.1016/j.foodchem. 2012.06.008.

[19] M.F. Angulo, M. Flores, M. Aranda, K. Henriquez-Aedo, Fast and selective method for biogenic amines determination in wines and beers by ultra high-performance liquid chromatography, Food Chem. 309 (2020) 125689, doi: 10. 1016/j.foodchem.2019.125689.

[20] V. Sirocchi, G. Caprioli, M. Ricciutelli, S. Vittori, G. Sagratini, Simultaneous determination of ten underivatized biogenic amines in meat by liquid chromatography-tandem mass spectrometry (HPLC-MS/MS), J. Mass Spectrom. 49 (2014) 819–825, doi: 10.1002/jms.3418.

[21] A. Gałuszka, Z. Migaszewski, J. Namieśnik, The 12 principles of green analytical chemistry and the significance mnemonic of green analytical practices, TrAC Trends Anal. Chem. 50 (2013) 78–84, doi: 10.1016/j.trac.2013.04.010.

[22] P.M. Nowak, R. Wietecha-Posłuszny, J. Pawliszyn, White analytical chemistry: an approach to reconcile the principles of green analytical chemistry and functionality, TrAC Trends Anal. Chem. (2021) 116223, doi: 10.1016/j.trac.2021.116223.

[23] G. Mafra, M.T. García-Valverde, J. Millán-Santiago, E. Carasek, R. Lucena, S. Cárdenas, Returning to nature for the design of sorptive phases in solid-phase microextraction, Separations 7 (2020) 2, doi: 10.3390/separations7010002.

[24] N.H. Godage, E. Gionfriddo, Use of natural sorbents as alternative and green extractive materials: a

critical review, Anal. Chim. Acta 1125 (2020) 187–200, doi: 10.1016/j.aca.2020.05.045.

[25] C. Brigham, Biopolymers, Green Chem. (2018) 753–770 Elsevier, doi: 10.1016/B978-0-12-809270-5.00027-3.

[26] M.C. Díaz-Liñán, M.T. García-Valverde, A.I. López-Lorente, S. Cárdenas, R. Lucena, Silver nanoflower-coated paper as dual substrate for surface-enhanced Raman spectroscopy and ambient pressure mass spectrometry analysis, Anal. Bioanal. Chem. 412 (2020) 3547–3557, doi: 10.1007/s00216-020-02603-x.

[27] W. Song, Y. Wang, L. Huang, H. Cheng, J. Wu, Y. Pan, Reactive paper spray mass spectrometry for rapid analysis of formaldehyde in facial masks, Rapid Commun. Mass Spectrom. 33 (2019) 1091–1096, doi: 10.1002/rcm.8445.

[28] W. Jang, H. Byun, J.H. Kim, Rapid preparation of paper-based plasmonic platforms for SERS applications, Mater. Chem. Phys. 240 (2020) 122124, doi: 10.1016/j.matchemphys.2019.122124.

[29] M.C. Díaz-Liñán, A.I. López-Lorente, S. Cárdenas, R. Lucena, Molecularly imprinted paper-based analytical device obtained by a polymerization-free synthesis, Sens. Actuators B Chem. 287 (2019) 138–146, doi: 10.1016/j.snb.2019.02.048.

[30] J. Ríos-Gómez, R. Lucena, S. Cárdenas, Paper supported polystyrene membranes for thin film microextraction, Microchem. J. 133 (2017) 90–95, doi: 10.1016/j.microc.2017.03.026.

[31] M.C. Díaz-Liñán, M.T. García-Valverde, R. Lucena, S. Cárdenas, A.I. López-Lorente, Dual-template molecularly imprinted paper for the determination of drugs of abuse in saliva samples by direct infusion mass spectrometry, Microchem. J. 160 (2021) 105686, doi: 10.1016/j.microc.2020.105686.

[32] F.A. Casado-Carmona, R. Lucena, S. Cárdenas, Magnetic paper-based sorptive phase for enhanced mass transference in stir membrane environmental samplers, Talanta 228 (2021) 122217, doi: 10.1016/j.talanta.2021.122217.

[33] J. Ríos-Gómez, B. Fresco-Cala, M.T. García-Valverde, R. Lucena, S. Cárdenas, Carbon nanohorn suprastructures on a paper support as a sorptive phase, Molecules (2018) 23, doi: 10.3390/molecules23061252.

[34] L.B. Zhao, R. Huang, M.X. Bai, D.Y. Wu, Z.Q. Tian, Effect of aromatic amine–metal interaction on surface vibrational Raman spectroscopy of adsorbed molecules investigated by density functional theory, J. Phys. Chem. C 115 (2011) 4174–4183, doi: 10.1021/jp1117135.

[35] C.M. Altaner, L.H. Thomas, A.N. Fernandes, M.C. Jarvis, How cellulose stretches: synergism between covalent and hydrogen bonding, Biomacromolecules 15 (2014) 791–798, doi: 10.1021/bm401616n.

[36] D. Sawada, Y. Nishiyama, L. Petridis, R. Parthasarathi, S. Gnanakaran, V.T. Forsyth, M. Wada, P. Langan, Structure and dynamics of a complex of cellulose with EDA: insights into the action of amines on

cellulose, Cellulose 20 (2013) 1563–1571, doi: 10.1007/s10570- 013- 9974- 7.

[37] X. Meng, Q. Liu, Y. Ding, Paper-based solid-phase microextraction for analysis of 8-hydroxy-2'-deoxyguanosine in urine sample by CE-LIF, Electrophoresis 38 (2017) 494–500, doi: 10.1002/elps.201600439.

[38] B. Redruello, V. Ladero, B. Del Rio, M. Fernández, M.C. Martin, M.A. Alvarez, A UHPLC method for the simultaneous analysis of biogenic amines, amino acids and ammonium ions in beer, Food Chem. 217 (2017) 117–124, doi: 10.1016/j.foodchem.2016.08.040.

[39] D. Cao, X. Xu, X. Feng, L. Zhang, Designed multifunctional visual observation of magnetic ionic liquid coupling with microwave-assisted derivatization for determination of biogenic amines, Food Chem. 333 (2020) 127518, doi: 10.1016/j.foodchem.2020.127518.

[40] M. Palomino-Vasco, M.I. Acedo-Valenzuela, M.I. Rodríguez-Cáceres, N. Mora-Diez, Automated chromatographic method with fluorescent detection to determine biogenic amines and amino acids. Application to craft beer brewing process, J. Chromatogr. A 1601 (2019) 155–163, doi: 10.1016/j.chroma.2019.04.063.

[41] E. Miao, N. Zhang, S. Lu, Y. Hu, L. Fu, H. Zhou, J. Zhan, M. Wu, Solid phase "*on-situ*" quadraplex isotope dimethyl labeling for the analysis of biogenic amines in beers by liquid chromatography-high resolution mass spectrometry, J. Chromatogr. A 1613 (2020) 460712, doi: 10.1016/j.chroma.2019.460712.

[42] C. Almeida, J.O. Fernandes, S.C. Cunha, A novel dispersive liquid–liquid microextraction (DLLME) gas chromatography-mass spectrometry (GC–MS) method for the determination of eighteen biogenic amines in beer, Food Control 25 (2012) 380–388, doi: 10.1016/j.foodcont.2011.10.052.

[43] K.J. Huang, C.X. Jin, S.L. Song, C.Y. Wei, Y.M. Liu, J. Li, Development of an ionic liquid-based ultrasonic-assisted liquid–liquid microextraction method for sensitive determination of biogenic amines: application to the analysis of octopamine, tyramine and phenethylamine in beer samples, J. Chromatogr. B 879 (2011) 579–584, doi: 10.1016/j.jchromb.2011.01.018.

[44] J. Donthuan, S. Yunchalard, S. Srijaranai, Vortex-assisted surfactant-enhanced-emulsification liquid-liquid microextraction of biogenic amines in fermented foods before their simultaneous analysis by high-performance liquid chromatography, J. Sep. Sci. 37 (2014) 3164–3173, doi: 10.10 02/jssc.20140 0570.

[45] Y. He, X.E. Zhao, R. Wang, N. Wei, J. Sun, J. Dang, G. Chen, Z. Liu, S. Zhu, J. You, Simultaneous determination of food-related biogenic amines and precursor amino acids using *in situ* derivatization ultrasound-assisted dispersive liquid–liquid microextraction by ultra-high-performance liquid chromatography tandem mass spectrometry, J. Agric. Food Chem. 64 (2016) 8225–8234, doi: 10.1021/acs.jafc.6b03536.

SUPPORTING INFORMATION

1. Mass spectrometry parameters

Table S1. SRM parameters of each biogenic amine and the internal standard.

Analyte	Precursor ion ([M+H]+ adduct) (m/z)	Product ions (m/z)	Fragmentor voltage (V)	Collision energy (V)	Collision cell accelerator voltage (CAV) (V)
CAD	103.1	86.2	60	10	7
HIS	112.1	95.1	70	15	7
PHE	122.1	105	60	10	7
PUT	89.1	72.2	120	10	7
SPD	146.2	72.2	80	20	7
SPR	203.1	112	100	20	7
TYR	138.1	121.1	60	10	7
HMDA	117.1	100.1	80	13	7

2. Effect of the extraction time

Fig. S1 shows how the analytical signal varied with the extraction time. An analysis of variance showed that the effect of the extraction time was only statistically significant for SPD. A visual inspection of Fig. S1 may suggest that a marked effect also exist for HIS. However, the high relative standard deviation obtained for this analyte (specially at 15 min) make the variation of the signal with the extraction time non-significant.

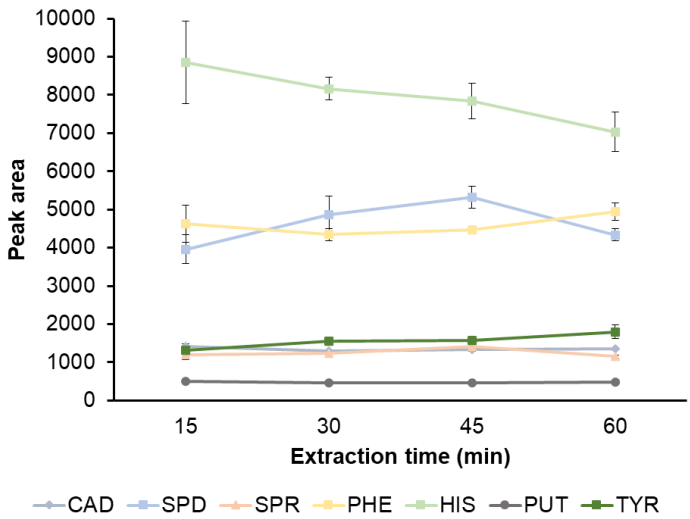

Figure S1. Effect of the extraction time on the peak areas of the analytes after extraction from an aqueous solution with the analytes present at a concentration of 500 $\mu g \cdot L^{-1}$.

3. External calibration models

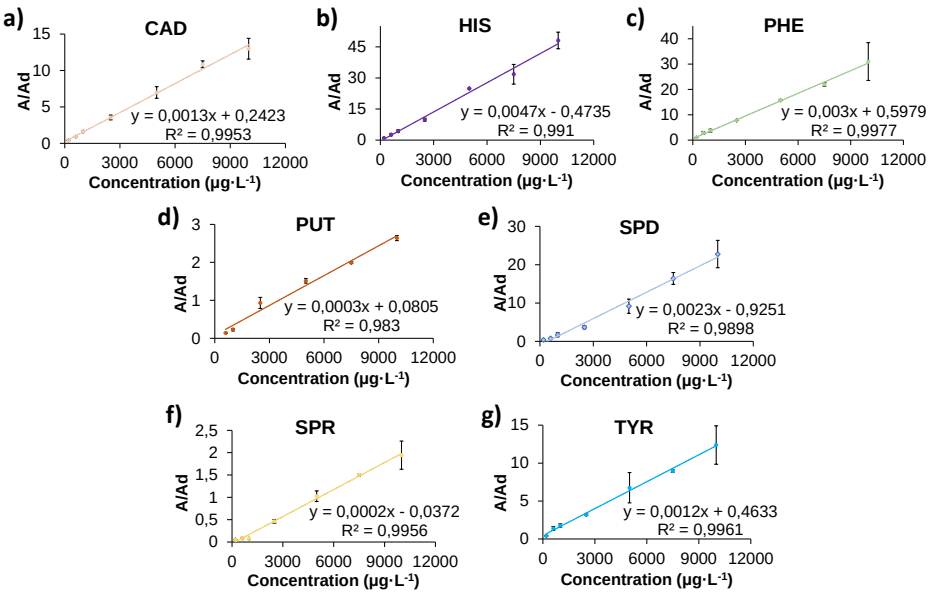

Figure S2. Calibration curves of a) Cadaverine, b) Histamine, c) Phenylethylamine, d) Putrescine, e) Spermidine, f) Spermine and g) Tyramine after extraction from aqueous solutions containing 5% of ethanol, pH 4.34 and 1260 µΩ ionic strength. Results are expressed as the relation of peak areas of each analyte and the internal standard of three independent measurements. The error bars depict the standard deviation of the corresponding mean value.

4. Standard addition calibration models

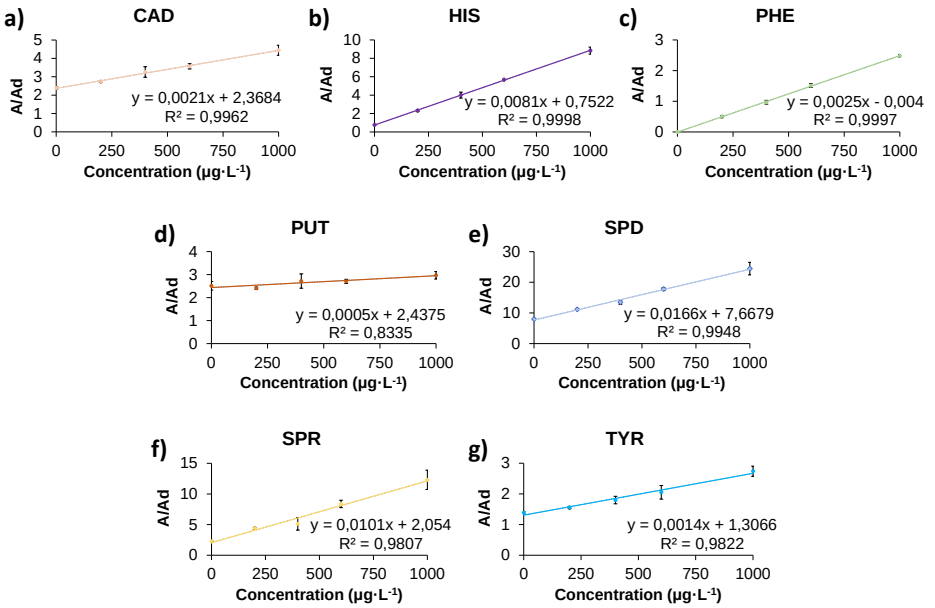

Figure S3. Standard addition calibration curves of a) Cadaverine, b) Histamine, c) Phenylethylamine, d) Putrescine, e) Spermidine, f) Spermine and g) Tyramine after extraction from a degasified dark lager beer. Results are displayed as the ratio of peak areas of the analytes and the internal standard of three independent measurements and error bars illustrate the standard deviation of the corresponding mean value.

BLOQUE III

PAPEL MODIFICADO CON POLÍMEROS DE IMPRESIÓN MOLECULAR

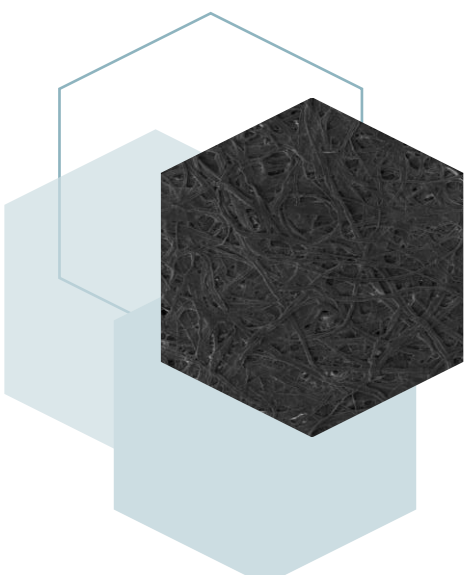

Durante la etapa de tratamiento de muestra es frecuente el uso de técnicas de extracción para aislar y preconcentrar los compuestos de interés. Antes de la aparición de las técnicas de microextracción, la capacidad sorbente de un material era el factor determinante para su elección [1]. Sin embargo, con la miniaturización de estas técnicas, la selectividad pasó a ser una de las características más importantes debido a que, en este caso, la capacidad sorbente se ve limitada [2].

Por este motivo, en los últimos años se ha perseguido el desarrollo de sorbentes con una alta selectividad respecto a los analitos a extraer. De esta manera, se extraen preferentemente los compuestos deseados a la vez que se emplean cantidades reducidas de material, disolventes, reactivos y energía. En definitiva, con la mejora de la selectividad, se consigue mejorar también la sensibilidad, un aspecto muy importante cuando se trabaja con muestras complejas [2].

En este Bloque de la memoria de la Tesis Doctoral, en primer lugar, se presentan los materiales selectivos más utilizados—polímeros de impresión molecular, materiales de acceso restringido, anticuerpos y aptámeros—y las últimas tendencias relacionadas con su uso **(Capítulo 3)**. Además, se ha estudiado una síntesis alternativa de los polímeros de impresión molecular, y su inmovilización en papel de filtro, para la extracción de quinina de muestras de refrescos **(Capítulo 4)** y de dos drogas de abuso de muestras de saliva **(Capítulo 5).**

[1] J. Ríos-Gómez, G. Lasarte-Aragonés, S. Cárdenas, R. Lucena, Selective nanoparticles in microextraction, Encycl. Anal. Chem, John Wiley & Sons, Ltd, Chichester, 2016, pp. 1-13.
[2] R. Lucena, Making biosamples compatible with instrumental analysis, J. Appl. Bioanal. 1 (2015) 72-75.

Capítulo 3

Selectivity-enhanced sorbents

Analytical Sample Preparation with Nano- and other High-Performance Materials, Chapter 10 (2021) 229-252 (Capítulo de libro)

In press

Analytical Sample Preparation with Nano- and other High-Performance Materials
10 (2021)

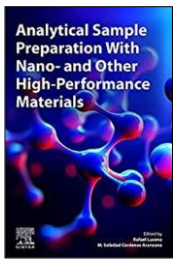

Selectivity-enhanced sorbents

M.C. Díaz-Liñán, G. Lasarte-Aragonés, A.I. López-Lorente, R. Lucena, S. Cárdenas

Departamento de Química Analítica, Instituto Universitario de Investigación en Química Fina y Nanoquímica IUNAN, Universidad de Córdoba, Campus de Rabanales, Edificio Marie Curie (anexo), Córdoba, España

This chapter provides a general overview of the potential of sorbents with enhanced selectivity in solid-phase (micro)extraction techniques. In these techniques, where the sorption capacity is limited by the low amount of sorbent, selectivity becomes a crucial feature. Also, an enhanced selectivity allows to change the traditional paradigms (e.g., sample preparation-chromatography-instrumental technique), opening the door to more straightforward and rapid workflows (e.g., direct combination of sample preparation with the instrumental technique). After an in-depth discussion of the theoretical aspects, the use of synthetic materials (molecularly imprinted polymer and restricted access materials) and natural polymers (antibodies and aptamers) for the selective isolation of target analytes from complex samples will be considered.

Keywords: Molecularly imprinted polymers; restricted access materials; immuno-sorbents; aptarmers.

1. Introduction

Traditionally, the sorbent capacity has been considered the key characteristic in a sorbent, due to a simple consideration: the higher the capacity, the higher the enrichment that can be achieved [1]. The extraction selectivity has been considered a secondary feature, relying the selectivity of the method on a chromatographic separation and/or the use of sophisticated instrumental techniques like mass spectrometry. Although this strategy is applicable in some scenarios (e.g., the use of large sorbent amounts or the treatment of simple matrices), it somewhat limits the potential of sample treatment to design effective and rapid analytical tools. In fact, an effective sample cleanup opens the door to their direct analysis (circumventing the time-consuming chromatographic separation) and has a positive impact on the integrity of the instruments [2].

In microextraction techniques where the sorbent capacity is limited, as its amount is reduced, selectivity appears as a very relevant feature. This aspect is especially significant when complex samples, such as biosamples, are processed since the matrix components can hinder the interaction sorbent-analyte resulting in a poor preconcentration [2]. In this case, the effect of selectivity on sensitivity (also observable when the S/N ratio is used to calculate the limits of detection and quantification) is very clear.

The extraction capacity of conventional sorbents is based on a series of low-selectivity interactions (i.e., hydrophobic/hydrophilic interactions). In the last decades, the interest in the development of sorbents with an enhanced selectivity has experienced a steady increase. The most used selective sorbents can be divided into two main groups, namely, synthetic materials [molecularly imprinted polymers (MIPs) and restricted access materials (RAMs)] and natural polymers (antibodies and aptamers). These materials will be described in-depth in this chapter.

2. Molecularly imprinted polymers

Molecularly imprinting technology has gained great attention in the past years due to the possibility of synthesizing selective materials toward a template molecule. The so-called MIPs are the result of the polymerization of a monomer in the presence of a template molecule and a crosslinker agent. After the removal of the template molecule, very selective recognition sites—which are complementary to the template in size, shape, and position of its functional groups—are available for rebinding of the analyte or a structural-related analog during the extraction process [3]. The recognition activity of the MIPs mimics the antibody-antigen or enzyme-substrate interaction. However, MIPs offer various advantages compared to natural receptors. They present thermal, mechanical, and chemical stability—which makes them potentially reusable—while also being cost-effective and easy to synthesize [4,5].

The use of MIPs as selective sorbents was first described by Sellergren in 1994, when he developed an MIP for the solid-phase extraction (SPE) of pentamidine from urine [6]. Traditionally, only small molecules were employed as template, for example, drugs or pesticides; however, the development and application of MIPs have matured over the past decades, nowadays being possible to recognize large molecules, such as proteins, or even microorganisms [3,7]. Nevertheless, the imprinting of voluminous templates is challenging due to their intrinsic properties, that is, large dimensions, limited solubility and stability, slow mass transfer, and structural flexibility in solution [8,9].

To carry out the synthesis of an MIP, four components are essential: monomer, crosslinker, template, and porogen, as depicted in Fig. 1; furthermore, additional elements can be added, such as an initiator. Since polymerization reaction is a complex process, a variety of factors need to be considered, that is, type and concentration of monomer, crosslinker and initiator, temperature and time of polymerization, and volume of the polymerization mixture [10]. After polymerization, the template molecule is removed by consecutive washing steps,

thereby leaving available the binding sites. Monomers are a source of functional groups that can interact with the template by covalent or noncovalent interactions. The selection of the monomer is vital to ensure high binding capacity of the MIPs, methacrylic acid or acrylic acid being some monomers typically used [10]. On the other hand, the crosslinker agent acts as the glue between the monomers and the template molecule, thus creating a stable and rigid polymer. Commonly used crosslinkers are ethylene glycol dimethacrylate and divinylbenzene. The template molecule is the analyte or a structural-related surrogate to be subsequently determined during the analytical process. Although almost every small molecule can act as a template, it is of high importance that it does not interfere in any way with the polymerization process, for example, by having functional groups that can hinder the process. Furthermore, it should be stable during the polymerization reaction and should possess functional groups that are suitable for interaction with the monomers [10]. Finally, the porogen is employed to generate a pore structure within the polymer to facilitate mass transfer during analyte rebinding.

Molecular imprinting relies on two main interactions, namely, covalent and noncovalent bonds. The first approach was pioneered by Wulff and Sarhan [11], and the latter was introduced by Arshady and Mosbach [12]. Synthesizing an MIP through covalent binding is a tedious process since cleavage of the covalent bonds is necessary to remove the template. Furthermore, the number of compounds available for this approach is limited, and template rebinding is slower [7,10,13]. On the other hand, the noncovalent approach relies on electrostatic forces, hydrogen bonds, van der Waals forces, hydrophobic forces, or a combination thereof [7,10]. During the rebinding process, the target molecule (i.e., template) can form the same interactions, thus the range of compounds available for imprinting is highly expanded, thereby making noncovalent imprinting the most suitable method for molecularly imprinting technology. A third approach was described by Whitcombe *et al.* [14], which involves both covalent and noncovalent bonds, that is, semicovalent approach. Through this method, covalent bonds are formed during the

synthesis process, but rebinding occurs through noncovalent interactions [15].

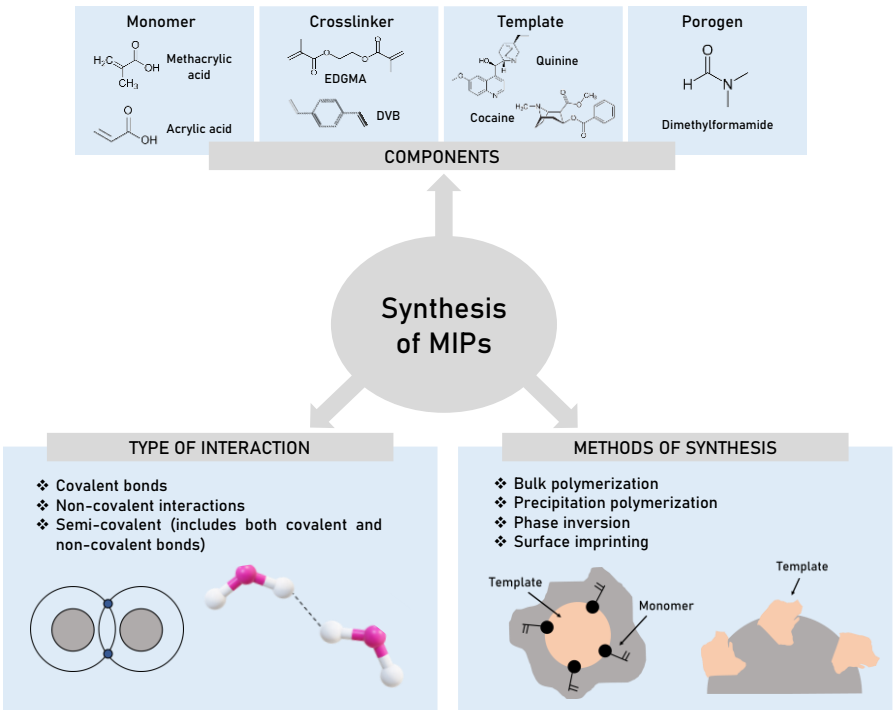

Figure 1. Schematic representation of the synthesis of MIPs where the main components, types of interactions and methods of synthesis are presented.

Within the different methods of synthesis, also summarized in Fig. 1, bulk polymerization is the most popular due to its simplicity [16-18]. In this approach, the template is added into the monomer mixture, which is a homogeneous phase. As a result, the interaction sites are not only located at the surface of the MIP but also within the entire polymeric matrix [19,20]. Without due consideration, this can be an advantage since a large number of interaction sites is achieved, which results in a higher sensitivity in the case of small molecules. However, the majority of those sites are only accessible via diffusion pathways within the polymeric matrix, thus

resulting in slow binding kinetics [19]. Furthermore, bulk polymerization requires the final grinding of the MIP, which is time consuming and entails irregular particles in terms of size and shape, along with the destruction of many binding sites [10]. In order to overcome the drawbacks associated to bulk polymerization, other strategies have been proposed, namely, precipitation polymerization [21-23], phase inversion, and surface imprinting [5,24,25]. These three approaches will be discussed in the following.

In precipitation polymerization, a significantly higher amount of porogen compared to bulk polymerization is used [10]. Furthermore, precipitation polymerization takes place in a heterogeneous phase since the polymer chains precipitate as the polymerization proceeds. Accurate control of the reaction parameters, such as temperature or crosslinkers, results in defined-size MIP spheres [3]. Although this approach has many advantages, for example, surfactant-free, one-step synthesis, or control over particle size; the large volume of porogen needed arises as a drawback since not only increases the cost but also contributes to environmental pollution.

The phase inversion process is also based on the solubility of the polymer in the mixture [26]. Polymer dissolution is a field of great interest, for example, in microlithography, semiconductor industry, or membrane science [27]. Based on the dissolution of the commercial polymer, it is possible to obtain MIPs via polymerization-free synthesis, thus avoiding the strict conditions associated to this process [28,29]. Furthermore, this procedure is not only cost-effective but also speedier and eco-friendlier compared to the previously mentioned approaches, since lower amounts of reagents are used. First, both the polymer and the template are dissolved in an appropriate solvent, allowing their interaction when mixed. Upon the addition of a solvent with different nature, the polymer-template mixture precipitates, thus obtaining the MIP [26]. An alternative to this is the deposition of the mixture in a support and leave the solvent to dry. In this context, an MIP based on the dissolution of nylon-6 in formic acid in the presence of the template molecule was synthesized by Díaz-Liñán *et al.* [30]. The as-synthesized MIP was then

deposited onto a filter paper, which acts as support, and the solvent was left to evaporate. The results showed improved performance compared with the nonimprinted polymer. Furthermore, the MIP deposited onto filter paper was directly coupled to a fluorimetric spectrometer for the quantification of the target analyte quinine.

Surface imprinting can be achieved either by a thin polymer film deposited onto the surface of a substrate or by attaching the template to the surface of a supporting material and subsequent polymerization. Following this approach, binding sites are located at the surface of the material, thus resulting in better template removal and faster binding kinetics due to low mass transfer resistance [10,20], thereby being suitable for (bio)macromolecule imprinting. Soft lithography, emulsion polymerization, and core-shell imprinting are among the surface imprinting strategies [9,20]. Regarding the core-shell approach, inorganic materials, such as quantum dots, silica or magnetic nanoparticles (MNPs), are widely used as cores, the latter being one of the most remarkable ones [9,31]. Once the core is synthesized, a layer-like process is followed: (1) core's surface protection and functionalization, (2) immobilization of the template, (3) polymerization, and (4) template removal [9]. One of the most interesting advantages of these hybrid materials is that they combine the extractant properties of the MIPs along with the properties of the core, for example, the magnetic properties of MNPs. In this context, Wang *et al.* carried out a comparative study of capsaicin MIPs synthesized by bulk and precipitation polymerizations and surface imprinting technology [32]. In the case of surface-imprinted MIPs, MNPs were employed as support. The results showed a better performance of the MIP prepared by surface imprinting compared to the other two in terms of affinity and adsorption capacity. Moreover, the use of MNPs in the case of the surface-imprinted MIP allowed the rapid separation of the composite since it maintained the magnetic properties of the nanoparticles. Furthermore, Wagdy *et al.* synthesized imprinted core-shell silica nanospheres (nanoMIPs) for the selective extraction of asparaginase via copolymerization of asparaginase and 3-

aminophenylboronic acid monohydrated [33]. The molecular recognition properties were characterized in terms of adsorption capacity, binding kinetics and selectivity versus the nonimprinted polymer. Finally, asparaginase was successfully determined in its pure form, as well as in real-world pharmaceutical preparation.

3. Restricted access materials

RAMs are a type of adsorbent that enables the isolation of analytes through a dual surface [34]. When analyzing complex matrices, such as biological fluids, a pretreatment step is required prior to the determination of the target analytes. Since these compounds are usually in a low concentration, simple and reliable pretreatments are preferable not to deplete the amount of analyte present in the sample. In this context, RAMs have been extensively used as sorbents in many analytical methodologies owing to their biocompatibility [35-37]. As already mentioned, these materials possess a dual surface that allows the separation of the analytes from the interferences: the outer surface acts as a barrier that prevents the penetration of macromolecules during the extraction, and the inner surface enables the retention and separation of the low-molecular-weight compounds present in the sample. The mechanism followed to exclude macromolecules can be physical, that is, size exclusion, or chemical, via specific functional groups that interact with the macromolecules [38]. The removal of interferences from the matrix not only helps in the sample cleanup but also results in a better sensitivity, since analytes are preconcentrated.

As aforementioned, RAMs have been employed as sorbents for SPE [39], solid-phase microextraction [40], and stir-bar sorptive extraction [41]; however, most of the analytical methodologies using RAMs are employed in SPE methods. More specifically, automated SPE systems are currently of high interest [13]. On the one side, in the in-line SPE mode, the sample can be directly injected in the column, and the analytes are eluted by applying a gradient elution after removal of the interferences. On the other hand, in on-line SPE mode, the analytes are transferred

to the analytical column, after exclusion of the macromolecules, using a switching valve [13,42].

Considering the advantages of RAMs, many recent studies have been aimed to modify conventional sorbents [e.g., silica-based sorbents, carbon nanotubes (CNTs), polymers] to obtain these hybrid materials, as depicted in Fig. 2. Silica-based RAMs, then known as internal surface reversed phase, were pioneered by Pinkerton *et al.* in 1985 [43], and their subsequent studies led to the consolidation of the RAM concept [34]. Boos and Rudolphi classified RAMs according to their chemical surfaces in two categories, that is, unimodal and bimodal phases [44]. The unimodal-phase RAMs have the same properties in their external and internal surfaces, whereas the bimodal-phase RAMs have a hydrophilic external surface and a hydrophobic internal surface. If this classification is combined with the exclusion mechanism of RAMs, that is, physical or chemical diffusion barriers, four categories are obtained: (1) physical diffusion barriers with unimodal phases, (2) physical diffusion barriers with bimodal phases, (3) chemical diffusion barriers with unimodal phases, and (4) chemical diffusion barriers with bimodal phases.

CNTs are a very versatile material in sorptive processes due to their high surface area and chemical and physical stability. However, the use of CNTs requires a previous pretreatment of the sample to avoid matrix effects related to some biological samples. To solve this problem, CNTs were combined with RAMs to obtain the so-called restricted access carbon nanotubes (RACNTs). This sorbent, firstly introduced by Barbosa *et al.*, was successfully applied for the direct extraction of cadmium from human hair [46]. Recently, Cruz *et al.* employed RACNTs as stationary phase for the determination of antipsychotics in untreated plasma samples from schizophrenic patients [47]. Multiwalled CNTs were functionalized by a coat of bovine serum albumin and subsequently packed in a polyethylene tube. The as-synthesized RACNTs successfully excluded most of the proteins present in the plasma samples, and showed high stability, allowing its re-use for over 120 times.

Although RAMs are highly suitable for the direct coupling of the sample pretreatment with the analytical system, their lack of selectivity toward small molecules present in the sample can potentially affect the efficiency of the analysis. On the other hand, as previously mentioned, MIPs often encounter a problem in complex matrices, since macromolecules (e.g., proteins) can impede the access to the binding sites, thus hindering the extraction efficiency of the MIPs. To overcome these limitations, Haginaka *et al.* combined RAMs and MIPs to obtain the so-called restricted access molecularly imprinted polymers (RAMIPs) [48]. These new hybrid sorbents exploit the positive characteristics of both materials, thus being able to not only extract the target compound but also prevent the attachment of macromolecules on its surface. Since this first approach, several applications of RAMIPs were developed. As an example, Liu *et al.* recently proposed the fabrication of carbon dots coupled with RAMs and MIPs (CDs@RAMIPs) for the determination of metronidazole via fluorescence quenching mechanism [49]. Glycidyl methacrylate was employed as copolymeric monomer to increase the number of hydroxyl groups on the surface, thus avoiding the interference from biological macromolecules. The obtained CDs@RAMIPs were successfully employed for the determination of metronidazole in serum samples, showing high sensitivity and selectivity.

The concept of supramolecular solvents (SUPRASs) refers to water-immiscible liquids made up of supramolecular assemblies dispersed in a continuous phase [50]. Their obtention relies on a two-step process occurring both in molecular and in nanomolecular scale. In the nanomolecular step, a three-dimensional aggregate is formed from amphiphilic molecules. Afterward, in the molecular step, the nanostructure is self-assembled in larger aggregates as a consequence of an external stimulus (e.g., temperature, electrolyte, pH, solvent), these structures being immiscible in water [50]. SUPRAS can be combined with RAMs to obtain a hybrid material that is able to solubilize analytes in a wide polarity range. On the one side, polar analytes are solubilized within the pores due to the interaction between the

acceptor and donor groups of the analytes and the polar groups of the surfactant. On the other hand, nonpolar analytes are solubilized by the van der Waals interactions with the hydrocarbon chains of the oil phase [51]. The exclusion mechanisms of these materials rely on the protein precipitation by the surfactant and size exclusion due to their adjustable cavities.

In a subsequent study carried out by Ballesteros-Gómez and Rubio, the potential of SUPRASs as RAMs was demonstrated, synthesizing a SUPRAS consisting of C7-C14 alkanols in THF/water mixtures [52]. These SUPRASs were employed for the direct isolation of analytes of a wide polarity range from liquid (e.g., sea, river, reservoir water) and solid matrices (e.g., food, sludge) while excluding high-molecular matrix interferences. After its consolidation, various applications of SUPRASs with restricted access properties (SUPRAS-RAMs) were developed. As an example, López-Jiménez *et al.* carried out the extraction of endocrine disruptors from sediments using a SUPRAS-RAM obtained by the dissolution of 1-decanol in a THF/water mixture [53]. The as-prepared SUPRAS-RAM was applied for the extraction of estrone, 17β-estradiol, estriol, 17α-ethynylestradiol, and bisphenol A (BPA) from water samples obtained from three rivers. This method simplified the sample treatment in the analysis of complex matrices since both extraction and cleanup are carried out in a single step, and several samples can be simultaneously processed.

Recently, a SUPRAS-RAM was applied by Martinefski *et al.* for the biomonitoring of monohydroxylated polycyclic aromatic hydrocarbon (OH-PAHs) in urine [45], which are metabolites from polycyclic aromatic hydrocarbons (PAHs). PAHs are associated with lung, colorectal, pancreatic, and prostate cancers. They enter the organism mainly through inhalation, ingestion, and dermal contact. The SUPRASRAM was spontaneously formed *in situ* in the urine by the addition of a colloidal suspension of decanoic acid in THF. The *in situ* production of the SUPRAS-RAM, along with the integration of the analyte extraction and sample cleanup in a single step, considerably simplified the process, enabling the analysis of around 50-

60 samples daily.

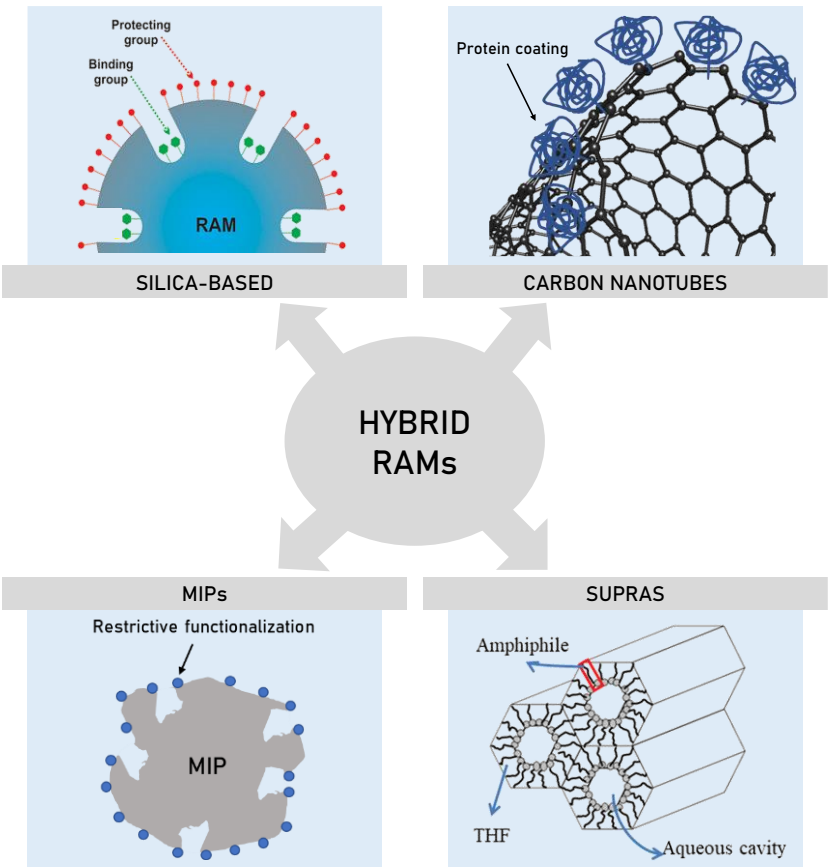

Figure 2. Classification of the different paths for the obtention of hybrid RAMs. Source: Panels of silica- and SUPRAS-based RAMs are adapted from H.D. De Faria, L.C. De C. Abrão, M.G. Santos, A.F. Barbosa, E.C. Figueiredo, New advances in restricted access materials for sample preparation: a review, Anal. Chim. Acta 959 (2017) 43-65. https://doi.org/10.1016/j.ac.2016.12.047 [34]; M. Martinefski, N. Feizi, M.L. Lunar, S. Rubio, Supramolecular solvent-based high-throughput sample treatment platform for the biomonitoring of PAH metabolites in urine by liquid chromatography-tandem mass spectrometry, Chemosphere. 237 (2019) 124525. https://doi.org/10.1016/j.chemosphere.2019.124525. [45] with the permission from Elsevier.

4. Selective biosorbents

Bioconjugation has become a well-established and prolific tool in the context of bio-nanotechnology. In general, it consists of incorporating structural, biorecognition, or catalytic properties of biomolecules to a given nanomaterial. The combination of both materials results in novel biocomposite [54]. Attachment of biomolecules can include virtually any biological molecule from small carbohydrates [55,56] or lipids [57], biopolymers such as nucleic acid [58,50] or peptides [60] to fully functional proteins or enzymes [61]. The combination of nanomaterials properties and biological function generates a large array of applications for biocomposites. In particular, sensing [62], drug delivery [63], bioimaging diagnostic [64], or biocatalysis [65,66].

Immobilization of a biological ligand with biorecognition potential for a given target fills the gap between fast and reliable sample treatment. More importantly, the combination of those with the appropriate solid support and format opens the door for simplification and automation. Strong affinity for a target achieved by bioligands generates cleaner results with fewer steps [67].

4.1. Immunosorbents

An antibody (Ab) can be defined as "a protein (immunoglobulin) produced by the immune system of an organism in response to exposure to a foreign molecule (antigen) and characterized by its specific binding to a site of that molecule" [68]. Its chemical structure is generated from the combination of four polypeptide chains (named as two heavy and two light). This combinatorial space allows immune cells (B-lymphocytes) to develop molecules with extraordinary specificity (in the nM range or better) for its target [69]. However, since ABs are produced by a living organism, the target range is restricted to those that can generate an immune response (immunogenic targets) [70].

Once the immune response is generated in the host (animal), antibodies must be isolated from the blood. Antibodies are classified in Polyclonal (PAb, produced by different cells against different parts or epitopes of the target) and Monoclonal (Mab, produced by a single clone cell against a single epitope of the target). Therefore PAbs are a heterogeneous mixture of Ab that recognize different areas of the target molecules, whereas MAb is a selected Ab from the mixture [71]. This fact has a direct impact on the methods designed using antibodies; PAbs are too heterogeneous to generate reproducible methodologies [72].

Antibodies were crucial in the development of selective sorbents thanks to the specificity of the biorecognition process. They can be attached to a solid support to produce the so-called immunosorbents (IS) that can replace traditional SPE sorbents. Given the fragile nature of the Abs, the logic approach for immobilization is covalent bonding. The free amino groups in the Abs polypeptide chains can react with epoxy or aldehyde group in the solid support. Common supports may include (but not only) agarose, silica, or synthetic polymers [71]. More recently, the use of nanomaterials as support has become a trend in biosensing [73-75].

The application of IS requires the packing of the sorbent in an SPE cartridge or column, which is further used as conventional SPE cartridges. However, to maintain the IS performance, it must be stored on an appropriate buffer (commonly phosphate-buffered saline). One of the most exploited applications of these sorbents is the Immunoaffinity Chromatography (IAC), where the packed sorbent replaces the traditional chromatographic column. In this case, only the target analyte is retained and on-line detected in the eluate. Readers interested in the topic are referred to the specific review of Moser and Hage [76]. This chapter overviews immunoextraction (IE) only. Contrary to IAC, IE follows the same steps as SPE, namely: (1) sorbent conditioning and sample loading, (2) washing the interferents and nonretained molecules; and (3) elution, plus an additional buffer regeneration step.

The use of IE technologies for small detection has rapidly emerged as an efficient and accurate alternative for trace analysis in a variety of environmental and food matrices. Ok *et al.* were able to detect simultaneously two mycotoxins in rice and bran, deoxynivalenol and nivalenol, by combining two antibodies using IE as a cleanup step before HPLCUV analysis [77]. Given the relevance of mycotoxins and aflatoxins analysis in food control, several manufacturers produce commercial disposable columns covering the most relevant and regulated analytes [78,79]. Other food matrices were analyzed by Yao and coworkers in search of BPA using in-house prepared MAbs. The IS was prepared by immobilization of MAb on NHS-activated Sepharose beads. Interestingly, the optimized IS was able to generate cleaner chromatographic results compared to conventional SPE and using a small amount of antibody (0.4 mg) with extended reusability (up to 25 cycles) [80]. Immunosorbent can be employed in dispersive extraction format (dSPE), where the attachment of antibodies to magnetic particles is usually developed to facilitate their recovery step by a simple magnet. Molina-Delgado and coworkers developed a soy protein IE method using gold-coated MNPs as solid support [81]. The key part of the immunomagnetic sorbent is the introduction of cysteamine as a linker between the antisoy protein-Ab and the Au surface. Cysteamine interacts with the gold surface by its thiol group and provides free primary amino group as an anchor point for antibodies immobilization. The optimized immunomagnetic-dSPE protocol was applied to soy milk with similar performance than commercial detection kits. Once eluted, the magnetic-IS can be reused up to 15 times. Other contaminants, such as bacteria, can be detected by means of magnetic-IS. Bakthavathsalam *et al.* used Salmonella MAbs immobilized on MNPs to capture free bacteria from solution [82]. Later, cells are lysed, and bacterial genomic material is detected by Reverse Transcription Polymerase Chain Reaction. The method was tested in food samples (milk and fruit juice), and it was able to detect bacterial contamination as low as 103 CFU (colony forming units) per mL in less than 4 h.

Avoiding coextracted interferents is crucial in the analysis of biological matrices. IS have proven to be an excellent tool for the extraction and concentration of certain analytes in urine samples. Maisonnette and coworkers designed a strategy to detect benzo(a)pyrene and pyrene metabolites as biomarkers for PAHs exposure [83]. Monoclonal antibodies against 3-benzo(a)pyrene-glucuronide (3BPG), 1-pyrene-glucuronide (1PG), and 1-hydroxypyrene (1OHP) were immobilized on cyanogen-bromide-activated sepharose and they were able to recover 80% of the target with a limit of detection (LOD) in the $ng \cdot L^{-1}$ level. When compared with C18 columns, the IS generate much cleaner extracts (Fig. 3). Other examples of urine analysis using IS include the analysis of estrogens [84], recombinant human insulin [85], or doping control in racehorses [86].

Vera-Avila and coworkers prepared an IS by encapsulation of PAb for the extraction of herbicides from water samples [87]. To do so, the authors followed a sol-gel encapsulation protocol, preventing conformational changes on the Abs during the immobilization process. Thanks to the mild procedure, the IS can be reused for 50 extraction cycles. Degelmann compared crushed sol-gel monoliths, and solgel-coated porous silica particle as support for sulfonylureas PAb. Up to 16 analytes can be extracted from environmental water samples with the polyclonal antibodies with both supports, being the crushed monolith the most reusable [88]. Later, Tang *et al.* used a similar protocol to prepare a robust method for Diazinon determination from water and soil samples [89]. Worth to mention that monoclonal antibodies can be combined in a similar fashion for the extraction of different triazines from water samples with no matrix interferences and great sensitivity [90].

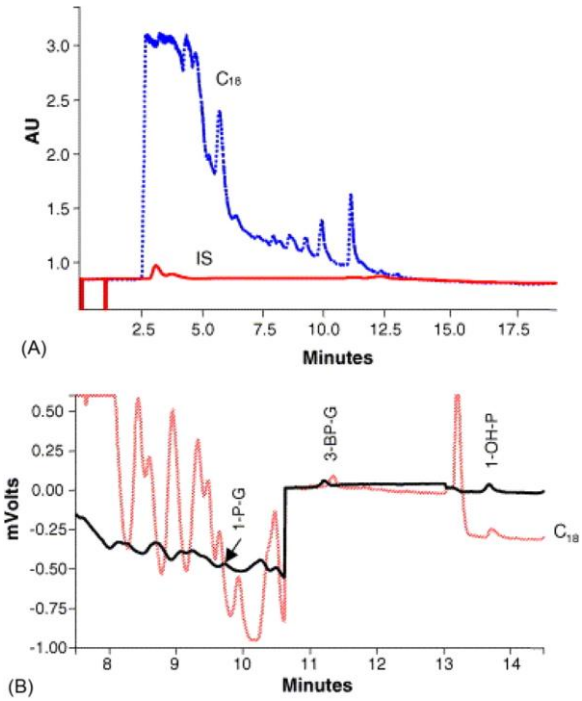

Figure 3 Comparison of chromatograms obtained on C18 silica and on IS after the extraction of 10 mL urine-PBS (1:3, v/v) spiked with 25 pg of each PAH metabolites. (A) UV detection 220 nm and (B) fluorescence detection. Source: Reproduced from C. Maisonnette, P. Simon, M.-C. Hennion, V. Pichon, Selective immunoclean-up followed by liquid chromatography for the monitoring of a biomarker of exposure to polycyclic aromatic hydrocarbons in urine at the ng·L^{-1} level, J. Chromatogr. A. 1120 (2006) 185-193. https://doi.org/10.1016/j.chroma.2005.12.041 [84] with the permission of Elsevier

4.2. Oligosorbents

Aptamers are small synthetic nucleic acids molecules (DNA or RNA) isolated from complex random libraries (10^{13}-10^{16} unique molecules) on an iterative process with high affinity and specificity for a given target molecule [91,92]. Aptamer shape or folding allows target biorecognition by means of different interactive forces (such as hydrogen bond, van der Waals forces, and dipole or stacking interactions) [93].

This conformational flexibility grants aptamers an unlimited range of target analytes, making them of particular interest for enhanced selectivity applications [94-96].

Once the best aptamer is isolated, it can be attached to a solid support (i.e., nanostructure) to generate a novel biocomposite. Although certain immobilization procedures can alter some of the aptamer structural features (affecting its binding capacity) [97], it is necessary to assure reusability and stability [98]. Oligonucleotides are readily available via automated synthesis. During the process, specific functional groups can be incorporated to make conjugation possible in one specific position only. Moreover, when both sorbent and biomolecule possess chemoselectivity, the conjugation is considered biorthogonal [99]. Typical examples of bioconjugation strategies include adsorption [100,101], covalent binding [102], or streptavidinbiotin pairing [103].

Oligonucleotide-modified sorbents (Oligosorbents, OS) can, in practice, replace conventional sorbent in several applications, packed in columns [104], cartridges [105], or dispersed into the sample matrix [106]. The most employed configuration is packing the OS between two frits in cartridges or columns following the steps of conventional SPE: (1) sample loading, (2) washing and (3) elution. The sample loading must be done in similar chemical conditions as the aptamer was selected to achieve the maximum interaction with the target. To do so, the sample may be diluted in buffer with a specific composition (pH, ionic strength) at a certain temperature before getting in touch with the aptamer-modified sorbent [107].

The column/cartridge format has been extensively used for the determination of ochratoxin A (OTA) in beers [108] or ginger powder [109]. In both cases, the authors outperformed immunoaffinity column extraction in terms of reusability and efficiency with an overall cheaper sorbent manufacturing. Other authors use a different coupling gel-based column (diaminodipropylamine) to immobilize the OTA aptamer with similar performance in wheat OTA extraction [110,111]. Prof. Pichon's group biotinylated the OTA aptamer to generate an OS based on the

Streptavidin-biotin pairing. When compared with a covalent attachment for the extraction of OTA from red wine samples, the biotin pairing appears to be less robust due to the presence of ethanol [112]. These results evidence that the immobilization strategy must be carefully selected accordingly to the analytical problem. Another related target, aflatoxin B2, was also extracted from peanuts using an OS-based SPE procedure [113]. According to the authors, the sepharose-based OS was cheaper than the commercial immunoaffinity counterpart but also shows and extended reusability cycle.

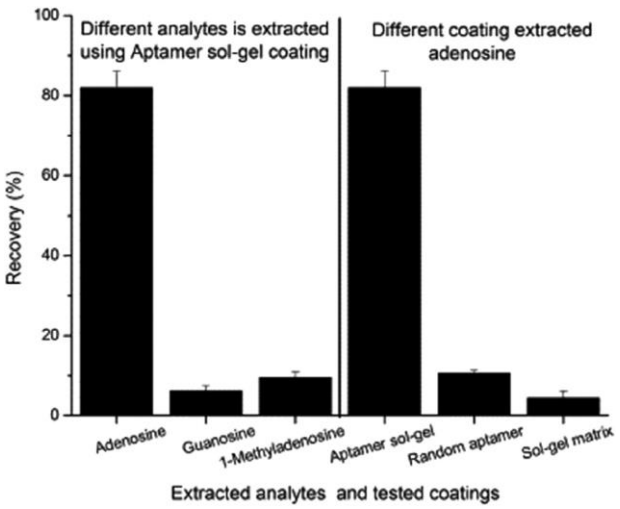

Figure 4. Verification of the sensitivity of the aptamer sol-gel fiber. The spiked concentrations of adenosine, guanosine, and 1-methyladenosine were all 10 $\mu g \cdot L^{-1}$ (n53). Adenosine, guanosine, and 1-methyladenosine were extracted by the adenosine aptamer sol-gel fiber, respectively. Finally, adenosine was extracted by random aptamer sol-gel fiber and bare sol-gel matrix fiber, respectively. Source: Reproduced from L. Mu, X. Hu, J. Wen, Q. Zhou, Robust aptamer sol-gel solid phase microextraction of very polar adenosine from human plasma, J. Chromatogr. A 1279 (2013) 7-12. https://doi.org/10.1016/j.chroma.2013.01.002 [114] with the permission of Elsevier.

The impact of aptamers as selectivity enablers is evident in the determination of small molecules in biological samples. The approach presented by Madru *et al.* is

designed for the extraction of cocaine from human plasma [105]. The complexity of human plasma, containing a large variety of interference molecules, limits the applicability of a single-mechanism strategy (such as C18 cartridge). As a consequence, coextraction of the target analyte and related molecules or metabolites arises as a common problem. However, when the cocaineaptamer is immobilized into sepharose beads and employed in a similar fashion as traditional cartridges, an extraction recovery close to 90% at a concentration level corresponding to a single cocaine dosage is achieved. Also, the same OS can be applied to whole postmortem blood samples with better results than typical protein precipitation. Moreover, when compared with C18-cartridge extraction, OS resulted in better chromatographic behavior with great sensitivity and storage stability [105]. Mu and coworkers followed an aptamer-SPME procedure to extract adenosine from plasma [114]. The aim of this approach is to overcome the limitations of SPME for very polar analytes, such as the target. In this elegant approach, authors immobilized (via sol-gel) the aptamer to the SPME fiber in a covalent attachment. The resulted OS showed enhanced resistance to nucleases (which can degrade the oligonucleotide) and extended reusability when compared with commercial fibers. Also, selectivity was tested using closely related molecules such as 1-methyladenosine and guanosine in the presence of the target analyte. As a result, the recovery of the target analyte was much higher (Fig. 4) and only achieved by the aptamer-modified fiber. As an alternative to the column format, Huy and coworkers anchored anti-Estradiol aptamer to glass microbeads to detect 17β-Estradiol (E2) in environmental water samples [106]. The aptamer was chemically modified during its synthesis to include a reactive amino group that reacts with the modified isothiocyanate glass beads to generate a stable covalent bond. The optimized procedure was used on the extraction of E2 from water samples using HPLC-UV as detection method. Selectivity of the OS was demonstrated since no binding from other estrogens is observed.

To facilitate recovery of the sorbent, when not using a column or cartridge, OS can be combined with magnetic particles [115]. To do so, an OTA aptamer is attached to magnetic nanosphere via carbodiimide crosslinking reaction [116]. The resulting OS was used for the extraction and detection of OTA from three different food samples, namely, coffee, wheat flour, and cereal product. The optimized procedure was applied to certified wheat samples showing good precision. The OS resulted in a better cleanup capacity than commercial C18 cartridge, providing cleaner chromatographic results. An alternative immobilization protocol is possible, taking advantage of the easy link formed between SH groups and Au surfaces [117]. To exploit this additional feature, magnetic gold nanoparticles are synthesized in a core-shell structure. Later, an -SH-modified human α-thrombin aptamer is immobilized via AuS bond. The resulted microspheres are capable of capture the target from serum samples without further processing than simple buffer dilution. The recovered sorbent is later digested with trypsin and subjected to matrix-assisted laser desorption/ionization time of flight mass spectrometry analysis to detect as low as 18 fmol in just 50 μL of the sample. Moreover, in the presence of other proteins 10 times more concentrated, only the target is quantitatively recovered and detected [118].

4.3. Antibodies or aptamers?

The applicability of antibodies as an analysis or diagnostic tool is out of question. They have been employed for trace analysis in food, biological, and environmental matrices. In most cases, they outperform traditional SPE sorbents thanks to their enhanced selectivity. However, there are some limitations; the most important is the dependence of a living organism to produce antibodies. The generation of antibodies against highly toxic targets (they can kill the host before an immune response is developed) is restricted. Furthermore, there is an intrinsic cost associated with antibody production, along with batch-to-batch differences. They are also (naturally) designed to operate under strict conditions that limit its

applicability in terms of thermal or pH stability and restrict the on-demand chemical modification. On the other hand, aptamers are relatively new molecules that can be synthesized on demand at a lower cost after successful identification. Also, the independence of a living organism makes them valid ligand for virtually any analyte. Since their properties (including chemical stability) can be adjusted as required, they can incorporate reporter molecules, fluorescence probes, or even antibodies [119]. In the future, it is expected to see a complementary use of both bioligands, since aptamers can interact with analytes antibodies cannot, but the performance of both can be comparable in terms of specificity and selectivity [120].

5. Conclusions

The extraction of samples with complex matrices is challenging in the microextraction context, where the capacity of the sorptive phases is limited. Selectivity-enhanced materials become the solution as they save this limited capacity for the analytes and some structure-related compounds. Well-established selective materials, like MIPs and IS, have been complemented with novel materials like RAMs and aptamers. Their individual potential and the possibility to be combined in the same extraction protocol [121] makes them very attractive as selectivity enhancers. This chapter has provided a general overview of the chemical characteristics of these materials and their applicability.

The use of selective sorbents opens the door to the simplification of the analytical workflow by the circumvention of the chromatographic separation. In this case, the direct coupling of sample treatment with instrumental techniques (optical or spectrometric ones), a topic that is discussed in Chapter 9, allows increasing the sample throughput, which is essential to answer to the growing information demands in modern societies.

Although it goes beyond the scope of this book, very selective materials are very interesting for the development of sensors.

Acknowledgements

The authors acknowledge the support of the Spanish Ministry of Economy and Competitiveness (Grant CTQ2017-83175R). GLA acknowledges the support of the Spanish Ministry of Science, Innovation and Universities through the Program Juan de la Cierva-Incorporación (Grant IJC 2018-037348-I).

References

[1] J. Ríos-Gómez, G. Lasarte-Aragonés, S. Cárdenas, R. Lucena, Selective nanoparticles in microextraction, Encycl. Anal. Chem, John Wiley & Sons, Ltd, Chichester, 2016, pp. 1-13. Available from: https://doi.org/10.1002/9780470027318.a9529.

[2] R. Lucena, Making biosamples compatible with instrumental analysis, J. Appl. Bioanal. 1 (2015) 72-75. Available from: https://doi.org/10.17145/jab.15.012.

[3] V. Pichon, N. Delaunay, A. Combès, Sample preparation using molecularly imprinted polymers, Anal. Chem. 92 (2020) 16-33. Available from: https://doi.org/10.1021/acs.analchem.9b04816.

[4] J. Guo, Y. Wang, Y. Liu, C. Zhang, Y. Zhou, Magnetic-graphene based molecularly imprinted polymer nanocomposite for the recognition of bovine hemoglobin, Talanta 144 (2015) 411-419. Available from: https://doi.org/10.1016/j.talanta.2015.06.057.

[5] X. Li, B. Zhang, L. Tian, W. Li, H. Zhang, Q. Zhang, Improvement of recognition specificity of surface protein-imprinted magnetic microspheres by reducing nonspecific adsorption of competitors using 2-methacryloyloxyethyl phosphorylcholine, Sens. Actuators B Chem. 208 (2015) 559-568. Available from: https://doi.org/10.1016/j.snb.2014.11.045.

[6] B. Sellergren, Direct drug determination by selective sample enrichment on an imprinted polymer, Anal. Chem. 66 (1994) 1578-1582. Available from: https://doi.org/10.1021/ac00081a036.

[7] P. Zahedi, M. Ziaee, M. Abdouss, A. Farazin, B. Mizaikoff, Biomacromolecule template-based molecularly imprinted polymers with an emphasis on their synthesis strategies: a review, Polym. Adv. Technol. 27 (2016) 1124-1142. Available from: https://doi.org/10.1002/pat.3754.

[8] S. Sykora, A. Cumbo, G. Belliot, P. Pothier, C. Arnal, Y. Dudal, *et al.*, Virus-like particles as virus substitutes to design artificial virus-recognition nanomaterials, Chem. Commun. 51 (2015) 2256-2258. Available from: https://doi.org/10.1039/C4CC08843C.

[9] M. Dinc, C. Esen, B. Mizaikoff, Recent advances on coreshell magnetic molecularly imprinted polymers for biomacromolecules, TrAC. Trends Anal. Chem. 114 (2019) 202-217. Available from: https://doi.org/10.1016/j.trac.2019.03.008.

[10] L. Chen, S. Xu, J. Li, Recent advances in molecular imprinting technology: current status, challenges and highlighted applications, Chem. Soc. Rev. 40 (2011) 2922. Available from: https://doi.org/10.1039/c0cs00084a.

[11] G. Wulff, A. Sarhan, Über die Anwendung von enzymanalog gebauten Polymeren zur Racemattrennung, Angew. Chemie. 84 (1972) 364. Available from: https://doi.org/10.1002/ange.19720840838.

[12] R. Arshady, K. Mosbach, Synthesis of substrate-selective polymers by hostguest polymerization, Die Makromol. Chem. 182 (1981) 687-692. Available from: https://doi.org/10.1002/macp.1981.021820240.

[13] B.H. Fumes, M.R. Silva, F.N. Andrade, C.E.D. Nazario, F.M. Lanças, Recent advances and future trends in new materials for sample preparation, TrAC. Trends Anal. Chem. 71 (2015) 9-25. Available from: https://doi.org/10.1016/j.trac.2015.04.011.

[14] M.J. Whitcombe, M.E. Rodriguez, P. Villar, E.N. Vulfson, A new method for the introduction of recognition site functionality into polymers prepared by molecular imprinting: synthesis and characterization of polymeric receptors for cholesterol, J. Am. Chem. Soc. 117 (1995) 7105-7111. Available from: https://doi.org/10.1021/ja00132a010.

[15] E.V.S. Maciel, A.L. De Toffoli, E.S. Neto, C.E.D. Nazario, F.M. Lanças, New materials in sample preparation: recent advances and future trends, TrAC. Trends Anal. Chem. 119 (2019) 115633. Available from: https://doi.org/10.1016/j.trac.2019.115633.

[16] M. Marć, A. Panuszko, J. Namieśnik, P.P. Wieczorek, Preparation and characterization of dummy-template molecularly imprinted polymers as potential sorbents for the recognition of selected polybrominated diphenyl ethers, Anal. Chim. Acta. 1030 (2018) 77-95. Available from: https://doi.org/10.1016/j.ac.2018.05.022.

[17] A. Sorribes-Soriano, F.A. Esteve-Turrillas, S. Armenta, P. Amorós, J.M. Herrero-Martínez, Amphetamine-type stimulants analysis in oral fluid based on molecularly imprinting extraction, Anal. Chim. Acta. 1052 (2019) 73-83. Available from: https://doi.org/10.1016/j.ac.2018.11.046.

[18] Y. Zhao, C. Simon, M. Daoud Attieh, K. Haupt, A. Falcimaigne-Cordin, Reduction-responsive molecularly imprinted nanogels for drug delivery applications, RSC Adv. 10 (2020) 5978-5987. Available from: https://doi.org/10.1039/C9RA07512G.

[19] G. Mustafa, P.A. Lieberzeit, MIP sensors on the way to real-world applications, Des. Recept. Next Gener. Biosens, Springer Berlin Heidelberg, 2012, pp. 167-187. Available from: https://doi.org/10.1007/5346_2012_21.

[20] M. Gast, H. Sobek, B. Mizaikoff, Advances in imprinting strategies for selective virus recognition a review, TrAC. Trends Anal. Chem. 114 (2019) 218-232. Available from:

https://doi.org/10.1016/j.trac.2019.03.010.

[21] S. Tan, H. Yu, Y. He, M. Wang, G. Liu, S. Hong, *et al.*, A dummy molecularly imprinted solid-phase extraction coupled with liquid chromatography-tandem mass spectrometry for selective determination of four pyridine carboxylic acid herbicides in milk, J. Chromatogr. B 1108 (2019) 65-72. Available from: https://doi.org/10.1016/j.jchromb.2019.01.008.

[22] S. Abbasi, S.A. Haeri, S. Sajjadifar, Bio-dispersive liquid liquid microextraction based on nano rhamnolipid aggregates combined with molecularly imprinted-solid phase extraction for selective determination of paracetamol in human urine samples followed by HPLC, Microchem. J. 146 (2019) 106-114. Available from: https://doi.org/10.1016/j.microc.2018.12.065.

[23] T. Jing, X.-D. Gao, P. Wang, Y. Wang, Y.-F. Lin, X.-Z. Hu, *et al.*, Determination of trace tetracycline antibiotics in foodstuffs by liquid chromatography-tandem mass spectrometry coupled with selective molecular-imprinted solid-phase extraction, Anal. Bioanal. Chem. 393 (2009) 2009-2018. Available from: https://doi.org/10.1007/s00216-009-2641-z.

[24] W. Zhang, D. Li, Y. Xu, Z. Jiang, Y. Chen, P. Wang, Synthesis and application of novel molecularly imprinted solid phase extraction materials based on carbon nanotubes for determination of carbofuran in human serum by high performance liquid chromatography, J. Agric. Food Chem. 67 (2019) 5105-5112. Available from: https://doi.org/10.1021/acs.jafc.9b00967.

[25] M. Arabi, A. Ostovan, A.R. Bagheri, X. Guo, J. Li, J. Ma, *et al.*, Hydrophilic molecularly imprinted nanospheres for the extraction of rhodamine B followed by HPLC analysis: a green approach and hazardous waste elimination, Talanta 215 (2020) 120933. Available from: https://doi.org/10.1016/j.talanta.2020.120933.

[26] J.J. Belbruno, Molecularly imprinted polymers, Chem. Rev. 119 (2019) 94-119. Available from: https://doi.org/10.1021/acs.chemrev.8b00171.

[27] B.A. Miller-Chou, J.L. Koenig, A review of polymer dissolution, Prog. Polym. Sci. 28 (2003) 1223-1270. Available from: https://doi.org/10.1016/S0079-6700(03)00045-5.

[28] E.V. Dmitrienko, R.D. Bulushev, K. Haupt, S.S. Kosolobov, A.V. Latyshev, I.A. Pyshnaya, *et al.*, A simple approach to prepare molecularly imprinted polymers from nylon-6, J. Mol. Recognit. 26 (2013) 368-375. Available from: https://doi.org/10.1002/jmr.2281.

[29] X. Zhu, Q. Zhu, Molecular imprinted Nylon-6 stir bar as a novel extraction technique for enantioseparation of amino acids, J. Appl. Polym. Sci. 109 (2008) 2665-2670. Available from: https://doi.org/10.1002/app.27557.

[30] M.C. Díaz-Liñán, A.I. López-Lorente, S. Cárdenas, R. Lucena, Molecularly imprinted paper-based analytical device obtained by a polymerization-free synthesis, Sens. Actuators B Chem. 287 (2019) 138-

146. Available from: https://doi.org/10.1016/j.snb.2019.02.048.

[31] M. Gast, F. Wondany, B. Raabe, J. Michaelis, H. Sobek, B. Mizaikoff, Use of super-resolution optical microscopy to reveal direct virus binding at hybrid core-shell matrixes, Anal. Chem. 92 (2020) 3050-3057. Available from: https://doi.org/10.1021/acs.analchem.9b04328.

[32] H. Wang, L. Yuan, H. Zhu, R. Jin, J. Xing, Comparative study of capsaicin molecularly imprinted polymers prepared by different polymerization methods, J. Polym. Sci. Part. A Polym. Chem. 57 (2019) 157-164. Available from: https://doi.org/10.1002/pola.29281.

[33] H.A. Wagdy, M. Dinc, B. Mizaikoff, Synthesis of surface imprinted coreshell nanospheres for the selective determination of asparaginase, Anal. Methods 11 (2019) 4034-4043. Available from: https://doi.org/10.1039/C9AY00634F.

[34] H.D. De Faria, L.C. De, C. Abrão, M.G. Santos, A.F. Barbosa, E.C. Figueiredo, New advances in restricted access materials for sample preparation: a review, Anal. Chim. Acta 959 (2017) 43-65. Available from: https://doi.org/10.1016/j.ac.2016.12.047.

[35] V. Neu, N. Delmotte, U. Kobold, T. Dülffer, R. Herrmann, H. Von Der Eltz, *et al.*, Online solid-phase extraction high-performance liquid chromatography-tandem mass spectrometry for the quantitative analysis of tacrolimus in whole blood hemolyzate, Anal. Bioanal. Chem. 404 (2012) 863-874. Available from: https://doi.org/10.1007/s00216-012-6201-6.

[36] T. Schettgen, J. Bertram, T. Kraus, Accurate quantification of the mercapturic acids of acrylonitrile and its genotoxic metabolite cyanoethylene-epoxide in human urine by isotope-dilution LC-ESI/MS/MS, Talanta 98 (2012) 211-219. Available from: https://doi.org/10.1016/j.talanta.2012.06.074.

[37] W. Huang, P. Wang, P. Jiang, X. Dong, S. Lin, Preparation and application of a restricted access material with hybrid poly(glycerol mono-methacrylate) and crosslinked bovine serum albumin as hydrophilic out layers for directly on-line high performance liquid chromatography analysis of enrofloxacin a, J. Chromatogr. A 1573 (2018) 59-65. Available from: https://doi.org/10.1016/j.chroma.2018.08.067.

[38] M. Cruz-Vera, R. Lucena, S. Cárdenas, M. Valcárcel, Highly selective and nonconventional sorbents for the determination of biomarkers in urine by liquid chromatography, Anal. Bioanal. Chem. 397 (2010) 1029-1038. Available from: https://doi.org/10.1007/s00216-010-3476-3.

[39] J. He, J. Yuan, J. Du, X. Chen, X. Zhang, A. Ma, *et al.*, Automated on-line SPE determination of amisulpride in human plasma using LC coupled with restricted-access media column, Microchem. J. 145 (2019) 154-161. Available from: https://doi.org/10.1016/j.microc.2018.10.029.

[40] I.D. Souza, L.P. Melo, I.C.S.F. Jardim, J.C.S. Monteiro, A.M.S. Nakano, M.E.C. Queiroz, Selective molecularly imprinted polymer combined with restricted access material for in-tube SPME/UHPLC-

MS/MS of parabens in breast milk samples, Anal. Chim. Acta 932 (2016) 49-59. Available from: https://doi.org/10.1016/j.ac.2016.05.027.

[41] J.-P. Lambert, W.M. Mullett, E. Kwong, D. Lubda, Stir bar sorptive extraction based on restricted access material for the direct extraction of caffeine and metabolites in biological fluids, J. Chromatogr. A. 1075 (2005) 43-49. Available from: https://doi.org/10.1016/j.chroma.2005.03.119.

[42] N.M. Cassiano, J.C. Barreiro, M.C. Moraes, R.V. Oliveira, Q.B. Cass, Restricted-access media supports for direct high-throughput analysis of biological fluid samples: review of recent applications, Bioanalysis 1 (2009) 577-594. Available from: https://doi.org/10.4155/bio.09.39.

[43] I.H. Hagestam, T.C. Pinkerton, Internal surface reversed-phase silica supports for liquid chromatography, Anal. Chem. 57 (1985) 1757-1763. Available from: https://doi.org/10.1021/ac00285a058.

[44] A. Rudolphi, K.-S. Boos, The use of restricted-access media in HPLC, Part I - classification and review, LC GC 15 (1997) 602-611.

[45] M. Martinefski, N. Feizi, M.L. Lunar, S. Rubio, Supramolecular solvent-based high-throughput sample treatment platform for the biomonitoring of PAH metabolites in urine by liquid chromatography-tandem mass spectrometry, Chemosphere 237 (2019) 124525. Available from: https://doi.org/10.1016/j.chemosphere.2019.124525.

[46] A.F. Barbosa, V.M.P. Barbosa, J. Bettini, P.O. Luccas, E.C. Figueiredo, Restricted access carbon nanotubes for direct extraction of cadmium from human serum samples followed by atomic absorption spectrometry analysis, Talanta 131 (2015) 213-220. Available from: https://doi.org/10.1016/j.talanta.2014.07.051.

[47] J.C. Cruz, H.D. De Faria, E.C. Figueiredo, M.E.C. Queiroz, Restricted access carbon nanotube for microextraction by packed sorbent to determine antipsychotics in plasma samples by high-performance liquid chromatography-tandem mass spectrometry, Anal. Bioanal. Chem. 412 (2020) 2465-2475. Available from: https://doi.org/10.1007/s00216-020-02464-4.

[48] J. Haginaka, H. Takehira, K. Hosoya, N. Tanaka, Uniform-sized molecularly imprinted polymer for (S)-naproxen selectively modified with hydrophilic external layer, J. Chromatogr. A 849 (1999) 331-339. Available from: https://doi.org/10.1016/S0021-9673(99)00570-1.

[49] H. Liu, J. Ding, K. Zhang, L. Ding, Fabrication of carbon dots@restricted access molecularly imprinted polymers for selective detection of metronidazole in serum, Talanta 209 (2020) 120508. Available from: https://doi.org/10.1016/j.talanta.2019.120508.

[50] A. Ballesteros-Gómez, S. Rubio, D. Pérez-Bendito, Potential of supramolecular solvents for the extraction of contaminants in liquid foods, J. Chromatogr. A 1216 (2009) 530-539. Available from:

https://doi.org/10.1016/j.chroma.2008.06.029.

[51] N. Caballero-Casero, H. C¸ abuk, G. Martínez-Sagarra, J.A. Devesa, S. Rubio, Nanostructured alkyl carboxylic acid-based restricted access solvents: application to the combined microextraction and cleanup of polycyclic aromatic hydrocarbons in mosses, Anal. Chim. Acta 890 (2015) 124-133. Available from: https://doi.org/10.1016/j.ac.2015.06.060.

[52] A. Ballesteros-Gómez, S. Rubio, Environment-responsive alkanol-based supramolecular solvents: characterization and potential as restricted access property and mixed-mode extractants, Anal. Chem. 84 (2012) 342-349. Available from: https://doi.org/10.1021/ac2026207.

[53] F.J. López-Jiménez, M. Rosales-Marcano, S. Rubio, Restricted access property supramolecular solvents for combined microextraction of endocrine disruptors in sediment and sample cleanup prior to their quantification by liquid chromatography-tandem mass spectrometry, J. Chromatogr. A 1303 (2013) 1-8. Available from: https://doi.org/10.1016/j.chroma.2013.06.043.

[54] K.E. Sapsford, W.R. Algar, L. Berti, K.B. Gemmill, B.J. Casey, E. Oh, *et al.*, Functionalizing nanoparticles with biological molecules: developing chemistries that facilitate nanotechnology, Chem. Rev. 113 (2013) 1904-2074. Available from: https://doi.org/10.1021/cr300143v.

[55] C. Earhart, N.R. Jana, N. Erathodiyil, J.Y. Ying, Synthesis of carbohydrate-conjugated nanoparticles and quantum dots, Langmuir 24 (2008) 6215-6219. Available from: https://doi.org/10.1021/la800066g.

[56] L.L. Matta, E.C. Alocilja, Carbohydrate ligands on magnetic nanoparticles for centrifuge-free extraction of pathogenic contaminants in pasteurized milk, J. Food Prot. 81 (2018) 1941-1949. Available from: https://doi.org/10.4315/0362-028X.JFP-18-040.

[57] A.J. Mieszawska, Y. Kim, A. Gianella, I. Van Rooy, B. Priem, M.P. Labarre, *et al.*, Synthesis of polymer-lipid nanoparticles for image-guided delivery of dual modality therapy, Bioconjug. Chem. 24 (2013) 1429-1434. Available from: https://doi.org/10.1021/bc400166j.

[58] Q. Wang, B. Zhang, X. Lin, W. Weng, Hybridization biosensor based on the covalent immobilization of probe DNA on chitosan-mutiwalled carbon nanotubes nanocomposite by using glutaraldehyde as an arm linker, Sens. Actuators B Chem. 156 (2011) 599-605. Available from: https://doi.org/10.1016/j.snb.2011.02.004.

[59] P.A. Rasheed, N. Sandhyarani, Carbon nanostructures as immobilization platform for DNA: a review on current progress in electrochemical DNA sensors, Biosens. Bioelectron. 97 (2017) 226-237. Available from: https://doi.org/10.1016/j.bios.2017.06.001.

[60] W.-J. Jeong, J. Bu, L.J. Kubiatowicz, S.S. Chen, Y. Kim, S. Hong, Peptide-nanoparticle conjugates: a next generation of diagnostic and therapeutic platforms? Nano Converg. 5 (2018) 38. Available from: https://doi.org/10.1186/s40580-018-0170-1.

[61] L. Wang, S. Guan, J. Bai, Y. Jiang, Y. Song, X. Zheng, *et al.*, Enzyme immobilized in BioMOFs: facile synthesis and improved catalytic performance, Int. J. Biol. Macromol. 144 (2020) 19-28. Available from: https://doi.org/10.1016/j.ijbiomac.2019.12.054.

[62] I.L. Medintz, H.T. Uyeda, E.R. Goldman, H. Mattoussi, Quantum dot bioconjugates for imaging, labelling and sensing, Nat. Mater. 4 (2005) 435-446. Available from: https://doi.org/10.1038/nmat1390.

[63] A. Sangtani, E. Petryayeva, K. Susumu, E. Oh, A.L. Huston, G. Lasarte-Aragonés, *et al.*, Nanoparticle-peptide-drug bioconjugates for unassisted defeat of multidrug resistance in a model cancer cell line, Bioconjug. Chem. 30 (3) (2019) 525-530. Available from: https://doi.org/10.1021/acs.bioconjchem.8b00755.

[64] L.A. Bentolila, S. Weiss, Single-step multicolor fluorescence *In situ* hybridization using semiconductor quantum dot-DNA conjugates, Cell Biochem. Biophys. 45 (2006) 59-70. Available from: https://doi.org/10.1385/CBB:45:1:59.

[65] L.D. Field, S.A. Walper, K. Susumu, G. Lasarte-Aragonés, E. Oh, I.L. Medintz, *et al.*, A quantum dot-protein bioconjugate that provides for extracellular control of intracellular drug release, Bioconjug. Chem. 29 (2018). Available from: https://doi.org/10.1021/acs.bioconjchem.8b00357.

[66] J.N. Vranish, M.G. Ancona, E. Oh, K. Susumu, G. Lasarte Aragonés, J.C. Breger, *et al.*, Enhancing coupled enzymatic activity by colocalization on nanoparticle surfaces: kinetic evidence for directed channeling of intermediates, ACS Nano 12 (2018). Available from: https://doi.org/10.1021/acsnano.8b02334.

[67] F. Augusto, L.W. Hantao, N.G.S. Mogollón, S.C.G.N. Braga, New materials and trends in sorbents for solid-phase extraction, TrAC. Trends Anal. Chem. 43 (2013) 14-23. Available from: https://doi.org/10.1016/j.trac.2012.08.012.

[68] A.D. Mcnaught, A. Wilkinson, IUPAC. Compendium of Chemical Terminology (the "Gold Book"), second ed., Blackwell Scientific Publications, Oxford, 2019. Available from: https://doi.org/10.1351/goldbook.

[69] A.M. Collins, K.J.L. Jackson, On being the right size: antibody repertoire formation in the mouse and human, Immunogenetics 70 (2018) 143-158. Available from: https://doi.org/10.1007/s00251-017-1049-8.

[70] H.F. Stills, Chapter 11 - Polyclonal antibody production, in: M.A. Suckow, K.A. Stevens, R.P. Wilson (Eds.), The Laboratory Rabbit, Guinea Pig, Hamster, and Other Rodents, Academic Press, 2012, pp. 259-270. Available from: https://doi.org/10.1016/B978-0-12-380920-9.00011-0.

[71] M.-C. Hennion, V. Pichon, Immuno-based sample preparation for trace analysis, J. Chromatogr. A 1000 (2003) 29-52. Available from: https://doi.org/10.1016/S0021-9673(03)00529-6.

[72] N. Delaunay-Bertoncini, V. Pichon, M.-C. Hennion, Comparison of immunoextraction sorbents prepared from monoclonal and polyclonal anti-isoproturon antibodies and optimization of the appropriate monoclonal antibody-based sorbent for environmental and biological applications, Chromatographia 53 (2001) S224-S230. Available from: https://doi.org/10.1007/BF02490332.

[73] L. Gao, Q. Yang, P. Wu, F. Li, Recent advances in nanomaterial-enhanced enzyme-linked immunosorbent assays, Analyst 145 (2020) 4069-4078. Available from: https://doi.org/10.1039/D0AN00597E.

[74] L. Guo, S. Xu, X. Ma, B. Qiu, Z. Lin, G. Chen, Dual-color plasmonic enzyme-linked immunosorbent assay based on enzyme-mediated etching of Au nanoparticles, Sci. Rep. 6 (2016) 32755. Available from: https://doi.org/10.1038/srep32755.

[75] P.R. Aranda, G.A. Messina, F.A. Bertolino, S.V. Pereira, M.A. Fernández Baldo, J. Raba, Nanomaterials in fluorescent laser-based immunosensors: review and applications, Microchem. J. 141 (2018) 308-323. Available from: https://doi.org/10.1016/j.microc.2018.05.024.

[76] A.C. Moser, D.S. Hage, Immunoaffinity chromatography: an introduction to applications and recent developments, Bioanalysis 2 (2010) 769-790. Available from: https://doi.org/10.4155/bio.10.31.

[77] H.E. Ok, S.Y. Lee, H.S. Chun, Occurrence and simultaneous determination of nivalenol and deoxynivalenol in rice and bran by HPLC-UV detection and immunoaffinity cleanup, Food Control. 87 (2018) 53-59. Available from: https://doi.org/10.1016/j.foodcont.2017.12.005.

[78] H.Z. ¸Senyuva, J. Gilbert, Immunoaffinity column clean-up techniques in food analysis: a review, J. Chromatogr. B. 878 (2010) 115-132. Available from: https://doi.org/10.1016/j.jchromb.2009.05.042.

[79] A. Sheibani, M. Tabrizchi, H.S. Ghaziaskar, Determination of aflatoxins B1 and B2 using ion mobility spectrometry, Talanta 75 (2008) 233-238. Available from: https://doi.org/10.1016/j.talanta.2007.11.006.

[80] K. Yao, K. Wen, W. Shan, S. Xie, T. Peng, J. Wang, *et al.*, Development of an immunoaffinity column for the highly sensitive analysis of bisphenol A in 14 kinds of foodstuffs using ultra-high-performance liquid chromatography tandem mass spectrometry, J. Chromatogr. B 1080 (2018) 50-58. Available from: https://doi.org/10.1016/j.jchromb.2018.02.013.

[81] M.Á . Molina-Delgado, M.P. Aguilar-Caballos, A. Gomez-Hens, Determination of soy proteins in food samples by dispersive solid-phase immunoextraction and dynamic long-wavelength fluorometry, Microchim. Acta 180 (2013) 1279-1286. Available from: https://doi.org/10.1007/s00604-013-1056-x.

[82] P. Bakthavathsalam, V.K. Rajendran, U. Saran, S. Chatterjee, B.M. Jaffar Ali, Immunomagnetic nanoparticle based quantitative PCR for rapid detection of Salmonella, Microchim. Acta 180 (2013) 1241-1248. Available from: https://doi.org/10.1007/s00604-013-1052-1.

[83] C. Maisonnette, P. Simon, M.-C. Hennion, V. Pichon, Selective immunoclean-up followed by liquid chromatography for the monitoring of a biomarker of exposure to polycyclic aromatic hydrocarbons in urine at the ngl21 level, J. Chromatogr. A 1120 (2006) 185-193. Available from: https://doi.org/10.1016/j.chroma.2005.12.041.

[84] M. Nakagomi, E. Suzuki, Determination of urinary 15α-hydroxyestrogen levels via immunoaffinity extraction, J. Chromatogr. B 1060 (2017) 336-339. Available from: https://doi.org/10.1016/j.jchromb.2017.06.033.

[85] M. Mazzarino, M. Senofonte, F. Martinelli, X. De La Torre, F. Botrè, Detection of recombinant insulins in human urine by liquid chromatography-electrospray ionization tandem mass spectrometry after immunoaffinity purification based on monolithic microcolumns, Anal. Bioanal. Chem. 411 (2019) 8153-8162. Available from: https://doi.org/10.1007/s00216-019-02203-4.

[86] W.H. Kwok, T.L.S. Choi, G.N.W. Leung, A.S.Y. Wong, S.K. Yue, T.S.M. Wan, *et al.*, Administration study of recombinant human relaxin-2 in horse for doping control purpose, Drug. Test. Anal. 12 (2020) 361-370. Available from: https://doi.org/10.1002/dta.2732.

[87] L.E. Vera-Avila, J.C. Vázquez-Lira, M. García De Llasera, R. Covarrubias, Sol2Gel immunosorbents doped with polyclonal antibodies for the selective extraction of malathion and triazines from aqueous samples, Environ. Sci. Technol. 39 (2005) 5421-5426. Available from: https://doi.org/10.1021/es048000c.

[88] P. Degelmann, S. Egger, H. Jürling, J. Müller, R. Niessner, D. Knopp, Determination of sulfonylurea herbicides in water and food samples using Sol2Gel glass-based immunoaffinity extraction and liquid chromatography2ultraviolet/diode array detection or liquid chromatography-tandem mass spectrometry, J. Agric. Food Chem. 54 (2006) 2003-2011. Available from: https://doi.org/10.1021/jf0527181.

[89] J. Tang, M. Zhang, G. Cheng, Y. Lu, Preparation and evaluation of Sol-Gel glassbased immunoaffinity column and their potential use in determination of diazinon in water and soil samples with high performance liquid chromatography, Anal. Lett. 42 (2009) 243-254. Available from: https://doi.org/10.1080/00032710802585709.

[90] C. Stalikas, D. Knopp, R. Niessner, Sol2Gel glass immunosorbent-based determination of s-triazines in water and soil samples using gas chromatography with a nitrogen phosphorus detection system, Environ. Sci. Technol. 36 (2002) 3372-3377. Available from: https://doi.org/10.1021/es020542b.

[91] A.D. Ellington, J.W. Szostak, In vitro selection of RNA molecules that bind specific ligands, Nature 346 (1990) 818-822. Available from: https://doi.org/10.1038/346818a0.

[92] C. Tuerk, L. Gold, Systematic evolution of ligands by exponential enrichment: RNA ligands to

bacteriophage T4 DNA polymerase, Science 249 (1990). Available from: https://doi.org/10.1126/science.2200121. 505-510.

[93] R. Stoltenburg, C. Reinemann, B. Strehlitz, SELEX—a (r)evolutionary method to generate high-affinity nucleic acid ligands, Biomol. Eng. 24 (2007) 381-403. Available from: https://doi.org/10.1016/j.bioeng.2007.06.001.

[94] Z.-J. Wang, E.-N. Chen, G. Yang, X.-Y. Zhao, F. Qu, Research advances of aptamers selection for small molecule targets, Chin. J. Anal. Chem. 48 (2020) 573-582. Available from: https://doi.org/10.1016/S1872-2040(20)60013-5.

[95] R. Reid, B. Chatterjee, S.J. Das, S. Ghosh, T.K. Sharma, Application of aptamers as molecular recognition elements in lateral flow assays, Anal. Biochem. 593 (2020) 113574. Available from: https://doi.org/10.1016/j.ab.2020.113574.

[96] J. Yan, H. Xiong, S. Cai, N. Wen, Q. He, Y. Liu, *et al.*, Advances in aptamer screening technologies, Talanta 200 (2019) 124-144. Available from: https://doi.org/10.1016/j.talanta.2019.03.015.

[97] A. Sassolas, L.J. Blum, B.D. Leca-Bouvier, Homogeneous assays using aptamers, Analyst 136 (2011) 257-274. Available from: https://doi.org/10.1039/C0AN00281J.

[98] S. Balamurugan, A. Obubuafo, S.A. Soper, D.A. Spivak, Surface immobilization methods for aptamer diagnostic applications, Anal. Bioanal. Chem. 390 (2008) 1009-1021. Available from: https://doi.org/10.1007/s00216-007-1587-2.

[99] J.M. Baskin, C.R. Bertozzi, Bioorthogonal click chemistry: covalent labeling in living systems, QSAR Comb. Sci. 26 (2007) 1211-1219. Available from: https://doi.org/10.1002/qsar.200740086.

[100] V. Singh, M. Zharnikov, A. Gulino, T. Gupta, DNA immobilization, delivery and cleavage on solid supports, J. Mater. Chem. 21 (2011) 10602-10618. Available from: https://doi.org/10.1039/C0JM04359A.

[101] M.I. Pividori, A. Merkoçi, S. Alegret, Electrochemical genosensor design: immobilization of oligonucleotides onto transducer surfaces and detection methods, Biosens. Bioelectron. 15 (2000) 291-303. Available from: https://doi.org/10.1016/S0956-5663(00)00071-3.

[102] J. Escorihuela, M.-J. Banũls, S. Grijalvo, R. Eritja, R. Puchades, Á . Maquieira, Direct covalent attachment of DNA microarrays by rapid thiolene "click" chemistry, Bioconjug. Chem. 25 (2014) 618-627. Available from: https://doi.org/10.1021/bc500033d.

[103] L.Q. Chen, S.J. Xiao, L. Peng, T. Wu, J. Ling, Y.F. Li, *et al.*, Aptamer-based silver nanoparticles used for intracellular protein imaging and single nanoparticle spectral analysis, J. Phys. Chem. B 114 (2010) 3655-3659. Available from: https://doi.org/10.1021/jp9104618.

[104] T.S. Romig, C. Bell, D.W. Drolet, Aptamer affinity chromatography: combinatorial chemistry applied to protein purification, J. Chromatogr. B Biomed. Sci. Appl. 731 (1999) 275-284. Available from: https://doi.org/10.1016/S0378-4347(99)00243-1.

[105] B. Madru, F. Chapuis-Hugon, E. Peyrin, V. Pichon, Determination of cocaine in human plasma by selective solid-phase extraction using an aptamer-based sorbent, Anal. Chem. 81 (2009) 7081-7086. Available from: https://doi.org/10.1021/ac9006667.

[106] G. Dong Huy, N. Jin, B.-C. Yin, B.-C. Ye, A novel separation and enrichment method of 17β-estradiol using aptamer-anchored microbeads, Bioprocess. Biosyst. Eng. 34 (2011) 189-195. Available from: https://doi.org/10.1007/s00449-010-0460-4.

[107] V. Pichon, F. Brothier, A. Combès, Aptamer-based-sorbents for sample treatment—a review, Anal. Bioanal. Chem. 407 (2015) 681-698. Available from: https://doi.org/10.1007/s00216-014-8129-5.

[108] A. Rhouati, N. Paniel, Z. Meraihi, J.-L. Marty, Development of an oligosorbent for detection of ochratoxin A, Food Control. 22 (2011) 1790-1796. Available from: https://doi.org/10.1016/j.foodcont.2011.04.021.

[109] X. Yang, W. Kong, Y. Hu, M. Yang, L. Huang, M. Zhao, *et al.*, Aptamer-affinity column clean-up coupled with ultra high performance liquid chromatography and fluorescence detection for the rapid determination of ochratoxin A in ginger powder, J. Sep. Sci. 37 (2014) 853-860. Available from: https://doi.org/10.1002/jssc.201301136.

[110] J.A. Cruz-Aguado, G. Penner, Determination of ochratoxin A with a DNA aptamer, J. Agric. Food Chem. 56 (2008) 10456-10461. Available from: https://doi.org/10.1021/jf801957h.

[111] A. De Girolamo, M. Mckeague, J.D. Miller, M.C. Derosa, A. Visconti, Determination of ochratoxin A in wheat after clean-up through a DNA aptamer-based solid phase extraction column, Food Chem. 127 (2011) 1378-1384. Available from: https://doi.org/10.1016/j.foodchem.2011.01.107.

[112] F. Chapuis-Hugon, A. Du Boisbaudry, B. Madru, V. Pichon, New extraction sorbent based on aptamers for the determination of ochratoxin A in red wine, Anal. Bioanal. Chem. 400 (2011) 1199-1207. Available from: https://doi.org/10.1007/s00216-010-4574-y.

[113] H. Liu, Y. Luan, A. Lu, B. Li, M. Yang, J. Wang, An oligosorbent-based aptamer affinity column for selective extraction of aflatoxin B2 prior to HPLC with fluorometric detection, Microchim. Acta 185 (2017) 71. Available from: https://doi.org/10.1007/s00604-017-2591-7.

[114] L. Mu, X. Hu, J. Wen, Q. Zhou, Robust aptamer sol-gel solid phase microextraction of very polar adenosine from human plasma, J. Chromatogr. A 1279 (2013) 7-12. Available from: https://doi.org/10.1016/j.chroma.2013.01.002.

[115] X. Wu, J. Hu, B. Zhu, L. Lu, X. Huang, D. Pang, Aptamer-targeted magnetic nanospheres as a solid-phase extraction sorbent for determination of ochratoxin A in food samples, J. Chromatogr. A 1218 (2011) 7341-7346. Available from: https://doi.org/10.1016/j.chroma.2011.08.045.

[116] M. Xie, J. Hu, Y.-M. Long, Z.-L. Zhang, H.-Y. Xie, D.-W. Pang, Lectin-modified trifunctional nanobiosensors for mapping cell surface glycoconjugates, Biosens. Bioelectron. 24 (2009) 1311-1317. Available from: https://doi.org/10.1016/j.bios.2008.07.058.

[117] Y. Wang, H. Wei, B. Li, W. Ren, S. Guo, S. Dong, *et al.*, SERS opens a new way in aptasensor for protein recognition with high sensitivity and selectivity, Chem. Commun. (2007) 5220-5222. Available from: https://doi.org/10.1039/B709492B.

[118] X. Zhang, S. Zhu, C. Deng, X. Zhang, Highly sensitive thrombin detection by matrix assisted laser desorption ionization-time of flight mass spectrometry with aptamer functionalized core-shell Fe3O4@C@Au magnetic microspheres, Talanta 88 (2012) 295-302. Available from: https://doi.org/10.1016/j.talanta.2011.10.044.

[119] S.D. Jayasena, Aptamers: an emerging class of molecules that rival antibodies in diagnostics, Clin. Chem. 45 (1999) 1628-1650. Available from: https://doi.org/10.1093/clinchem/45.9.1628.

[120] V. Pichon, F. Chapuis-Hugon, M.-C. Hennion, 2.19. Bioaffinity sorbents, in: J. Pawliszyn (Ed.), Comprehensive Sampling and Sample Preparation, Academic Press, Oxford, 2012, pp. 359-388. Available from: https://doi.org/10.1016/B978-0-12-381373-2.00045-4.

[121] H.G. Zuo, H. Yang, J.X. Zhu, Y. Ding, Preparation of a novel RAM-MIP for selective solid-phase extraction and gas chromatography determination of heptachlor, endosulfan and their metabolite residues in pork, Anal. Methods 9 (2017) 6009-6018. Available from: https://doi.org/10.1039/C7AY01941F.

Capítulo 4

Molecularly imprinted paper-based analytical device obtained by a polymerization-free synthesis

Sensors and Actuators B: Chemical, 287 (2019) 138-146

Sensors and Actuators B: Chemical
287 (2019) 138–146

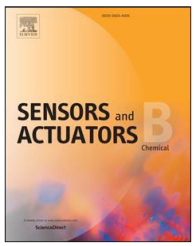

Molecularly imprinted paper-based analytical device obtained by a polymerization-free synthesis

M.C. Díaz-Liñán, A.I. López-Lorente*, S. Cárdenas, R. Lucena

Departamento de Química Analítica, Instituto Universitario de Investigación en Química Fina y Nanoquímica IUNAN, Universidad de Córdoba, Campus de Rabanales, Edificio Marie Curie, E-14071 Córdoba, Spain

In the last years, the imprinting technology has raised attention and different polymers with artificial recognition sites towards a target molecule have been developed. In this article, a polymerization-free method —which only requires the dissolution of nylon-6 polymer and its subsequent incubation with the template molecule— has been employed for the preparation of a molecularly imprinted polymer directly immobilized on filter paper, thus increasing the versatility and manageability of the new material. The molecularly imprinted paper-based analytical device (MIP PAD) has been coupled to a fluorimeter via a custom-built platform, which enables direct measurement of the fluorescence at the surface of the MIP PAD. Extraction efficiency of the MIP PAD was evaluated using quinine as model analyte, measuring the fluorescence directly at the MIP PAD surface after incubation on aqueous standards of quinine and soda drink, showing that the performance of the imprinted material was superior to that of the non-imprinted polymer. In addition, the selectivity of the MIP PAD versus analogous organic fluorescent molecules has been further evaluated using norfloxacin, observing that the molecular imprinting results in selective extraction of quinine. The performance

of the method has been evaluated for quantitative analysis, achieving limits of detection (LOD) and quantification (LOQ) for aqueous standards of 0.37 and 1.24 $mg \cdot L^{-1}$, respectively, while in the case of spiked soda drink the LOD and LOQ were 0.63 and 2.11 $mg \cdot L^{-1}$, respectively. The reproducibility of the measurements was also evaluated, observing values within range 2.30 and 9.07% measured as relative standard deviation.

Keywords: Molecularly imprinted polymer, Nylon-6, Microextraction, Cellulose paper, Quinine, Fluorescence, Paper-based analytical device.

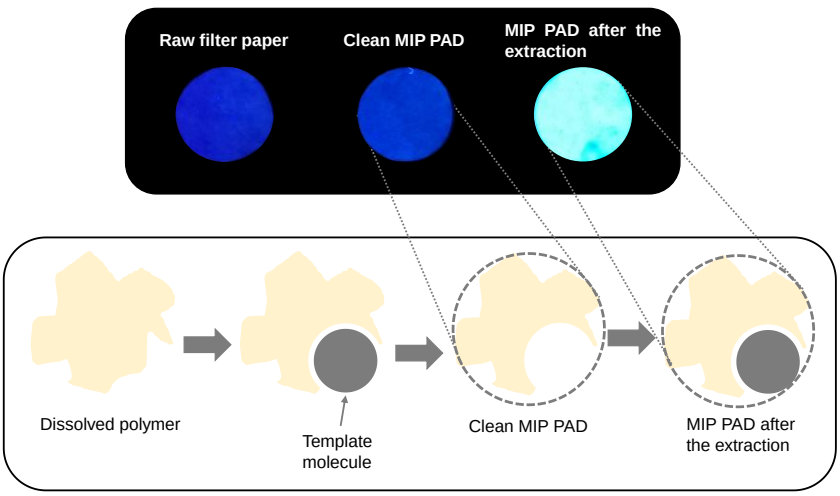

1. Introduction

In the last years, the development of sensors for the rapid detection of target analytes has raised great attention. The direct determination of these analytes is difficult because of the large number of compounds present in the matrix, therefore, a sample pre-treatment and/or extraction technique is usually required prior to the final detection [1–4]. During the past decades, researchers have been searching for the perfect selective sorbent to isolate the target analytes. Among all of the methods developed, molecular imprinting technology is, nowadays, a consolidated one [5].

Molecularly imprinted polymers (MIPs) are selective materials with artificially generated recognition sites towards a control molecule or structural-related analogue [6,7]. Traditionally, MIPs have been synthesized via two different methods, namely bulk polymerization [8] and precipitation [9]. In bulk polymerization, the process takes place in a homogeneous phase [10]. Along the process, small amounts of initiator, catalysts, stabilizers, etc., are added and solubilized in the reaction medium. It is of high importance to control the viscosity and to manage the energetics of the polymerization in order to control the process. On the other hand, precipitation polymerization starts as a homogeneous phase; nevertheless, the polymer finally precipitates as a completely separate phase, the addition of a stabilizer being not necessary [10]. Despite their widespread use, these methods are relatively intricated since a stringent control of the experimental conditions —namely, temperature, pH, time, among others— is required along with a high volume of porogen [11]. Polymer dissolution is a field of great interest, for example in microlithography, semiconductor industry or membrane science [12]. Based on the dissolution of commercial polymer [13,14], a simple approach for the synthesis of MIPs has been used in this work, avoiding the strict conditions of the polymerization process. This procedure for the preparation of MIPs is not only cost-effective, but also speedier and eco-friendlier as compared those previously described, since lower amounts of reagents are used.

Nylon-6 is a widely used synthetic polyamide thanks to its excellent properties, including strength, flexibility, abrasion resistance and toughness [15]. However, modification of the surface of the polymer, e.g., by introducing functional groups, is mandatory in order to broaden its applications scope [15]. For example, amide groups can be functionalized via hydrolysis [16] or N-alkylation [17]. Thanks to its biocompatibility, nylon-6 has been widely used in the biomedical field [18], while the combination of its mechanical strength, heat resistance and chemical stability properties when synthesized by anionic polymerization [19] has enabled its application in engineering fields. On the other hand, in the food industry, it is used as a food-packaging material due to its resistance to different microorganisms, e.g., fungi [20]. Regarding the structure, it is worth to highlight the inter- and intramolecular hydrogen bond-ability through its amide groups, which makes it suitable for the imprinting technology [13].

The use of paper-based materials has been increasing in the past decades. One of the main advantages of solid materials is the easy handling and incorporation into other devices [21,22], such as a fluorimeter cell. Furthermore, commercial filter paper is widely available and cost-effective and can be easily modified via wet chemistry. Sorbents based on paper coated by a polymer, namely polystyrene [23], poly-(3,4-ethylenedioxythiophene) [24] or polyborneolacrylate [25] have been described. Also, filter paper modified by immobilizing different nanostructures on them, such as carbon nanohorns [21], Pd nanoparticles [26], Au nanoparticles [27] or TiO_2 nanoparticles [28] has been reported. They combine the properties of the immobilized material with the easy use, portability and disposability of the paper [29–31]. Among other applications, they have been used in the determination of metals [32], bacteria [33] or hydrogen sulfide [34].

In this work, an approach for the preparation of molecularly imprinted polymer based on the dissolution of nylon-6 in formic acid in the presence of the template molecule, avoiding the polymerization process, has been used for the preparation of a MIP paper-based analytical device (MIP PAD). The polymer solution with the

template is deposited onto a filter paper, which acts as support, and the solvent left to evaporate. This MIP PAD can be directly coupled to a fluorimetric spectrometer for subsequent quantification of the target analyte —quinine. The extraction ability of the MIP has been compared with the non-imprinted polymer (NIP), showing improved performance. The selectivity of the MIP PAD has been further evaluated observing that norfloxacin is not extracted neither interferes on the determination of quinine.

2. Materials and methods

2.1. Reagents

All reagents were of analytical grade or better. Unless otherwise specified, they were purchased from Sigma-Aldrich (Madrid, Spain). A standard solution of the analyte (quinine) was prepared in milli-Q water (Millipore Corp., Madrid, Spain) at a concentration of 1000 $mg \cdot L^{-1}$ and stored in the dark at 4 °C. Working solutions were prepared by the appropriate dilution of the stock solution in milli-Q water. Methanol:acetic acid (90:10) was used for the cleaning of the MIP PADs after the synthesis. Selectivity studies were carried out with sodium chloride and norfloxacin. The ionic strength was evaluated using sodium sulphate. For the final evaluation of the applicability of the MIP PADs, a soda drink was also employed. This drink is mainly composed of carbonated water, additives and sweeteners, such as acesulfame K.

The filter paper employed to make the PADs is a Filter-Lab ream (42×52, density: 73 $g \cdot m^{-2}$).

2.2. Synthesis of the MIP PADs

MIPs were synthesized through a simple procedure summarized in Scheme 1 and detailed as follows. First of all, 70 mg of nylon-6 pellets were dissolved in 10 mL of formic acid under vigorous stirring with a magnetic stirrer. Next, 20 mg of the

template molecule (quinine), along with 374 µL of the porogen, i.e., dimethylformamide (DMFA), were added to the solution and stirred for 5 min to assess the distribution of all the components. Finally, 20 µL of the solution were added to circular filter PADs (1.26 cm of diameter). This last step was repeated three times, allowing the PADs to dry between additions. The obtained MIP PADs were stirred in 10 mL of methanol-acetic acid mixture (90:10) until all the quinine template was quantitatively eliminated, as fluorometrically proven. After this, MIP PADs were rinsed with milli-Q water and dried in the laboratory fume hood.

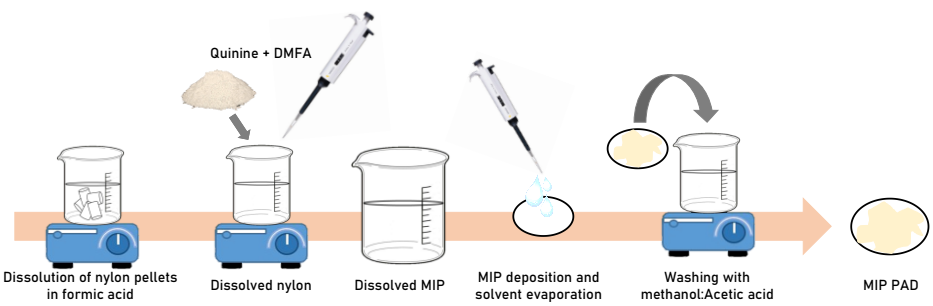

Scheme 1. Diagram of the different steps of the synthesis of molecularly imprinted polymer PADs, namely: dissolution of nylon pellets in formic acid, addition of quinine and DMFA, MIP deposition and solvent evaporation and washing with methanol-acetic acid solution and water prior drying. For further details see text.

2.3. Characterization of the MIP PADs

Three different PADs were characterized, namely raw filter paper, a MIP PAD prepared at the selected conditions and a MIP PAD with a higher amount of polymer. Pure nylon-6 was also studied for comparative purposes.

PADs were characterized using different techniques including scanning electron microscopy (SEM), infrared spectroscopy and Raman spectroscopy. SEM

micrographs were acquired at the central Service for Research Support (SCAI) of the University of Córdoba using a JEOL JSM 7800 F microscope (JEOL, Tokyo, Japan) and were used to characterize the pore structure of the polymer.

Raman measurements were performed with a confocal Raman spectrometer (alpha500, manufactured by WITec GmbH, Ulm, Germany). For excitation, a frequency doubled Nd:YAG laser at 532 nm (second harmonic generation) was employed, using a laser power of 4mW (measured prior the objective lens). The laser beam was focused on the sample using a 20x/0.4 Zeiss objective.

Attenuated total reflection infrared (ATR-IR) spectra were acquired in a Bruker Tensor 37 FT-IR spectrometer (Bruker Optik, GmbH, Ettlingen, Germany) equipped with a three internal reflections diamond ATR cell (Platinum ATR accessory, Bruker). A room temperature operating deuterated triglycine sulphate (DTGS) detector was employed for signal recording. Measurements were performed in the spectral window of 4000-400 cm^{-1} at a 4 cm^{-1} spectral resolution by averaging 64 scans each spectrum. Data collection and processing was done using OPUS software package (Bruker, Ettligen, Germany).

2.4. Adsorption procedure and fluorimetric measurements

The adsorption procedure was carried out by immersing the MIP PAD in a beaker with 2 mL of an aqueous solution of quinine and stirring in a magnetic stirrer for 5 min. The same procedure was used for the extraction in a soda drink after degasification.

Fluorescence measurements were performed with a PTI QuantaMaster Spectrofluorometer (Horiba, Horiba Jobin Yvon) at an excitation wavelength of 270 nm. Fig. 1 depicts a scheme of the measurement process. After being synthesized, the MIP PAD was introduced in a custom-built magnetic piece that holds the PAD. After this, the piece was placed in the fluorimeter cell with an angle of 45°. Data were acquired and analysed with the PTI software.

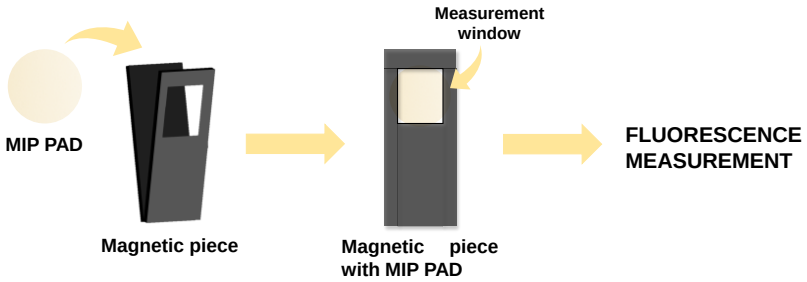

Figure 1. Scheme of the custom-built magnetic piece that holds the MIP PAD for fluorometric measurements.

3. Results and discussion

3.1. Synthesis of the MIP PADs

The process of dissolution of a polymer into an appropriate solvent usually takes place through a two-step procedure, which involves solvent diffusion and the disentanglement of the polymer chain [12]. Acids, such as formic, acetic or hydrochloric acids, have been reported [35,36] to dissolve polyamides together with solvents such as 2,2,2- trifluoroethanol [14]. Herein the solubility of nylon-6 on formic acid has been exploited for the preparation of a molecularly imprinted polymer. Once the nylon-6 polymer is dissolved in formic acid, the chains remain solvated in solution and are able to interact with the target molecule via different interactions typical from polyamine chains. On the one hand, nylon-6 possesses an amide group, which provides the ability of interact with the template via inter- and intramolecular hydrogen bonds, which can lead to a specific recognition of the target analyte. Also, the carboxylic residues and protonated amino groups can form ionic interactions with the template [14]. In addition, non-polar hydrophobic interactions with the aliphatic region are also possible.

In this approach, instead of carrying out the polymerization process from monomers, formation of the MIPs is based on the dissolution of nylon-6 in the presence of the template and the subsequent casting of the solution on a filter paper and evaporation of the solvent. Filter paper provides the three-dimensional support for the deposition of the MIP. After removal of the template with the appropriate solution (methanol-acetic acid mixture), a MIP PAD with active sites towards the target analyte is obtained.

3.2. Characterization of the MIP PADs

The surface of three different MIP PADs was characterized by SEM. Fig. 2a shows the surface structure of raw filter paper, where the cellulose fibres forming a non-uniform three-dimensional network can be observed. Fig. 2b and c depict the surface of the PADs modified with the MIP at different polymer concentrations. Hydroxyl groups of paper may interact with the amide groups of the polymer; however, the interaction between paper and nylon-6 is expected to be physical, as the polymer dries once it is deposited on the paper. The most significant difference is observed between raw filter paper (Fig. 2a) and the PAD with excess amount of polymer (Fig. 2c). At the selected conditions (Fig. 2b) the MIP layer covers the filter paper, while the irregular surface provided by the different fibres within the paper are maintained, which helps to the extraction of analytes. When the amount of polymer is increased, the surface of the MIP PAD becomes flatter, which will affect, as explained in more detail later on, to the extraction process. A PAD modified with the NIP at the selected amount of nylon-6 was also characterized, nevertheless, no significant differences in comparison with Fig. 2b were found. Furthermore, a PAD modified with both the NIP and the MIP at the selected conditions before template extraction were also characterized (Fig. S1, Supplementary Information), nevertheless, no significant differences were observed when compared to Fig. 2b.

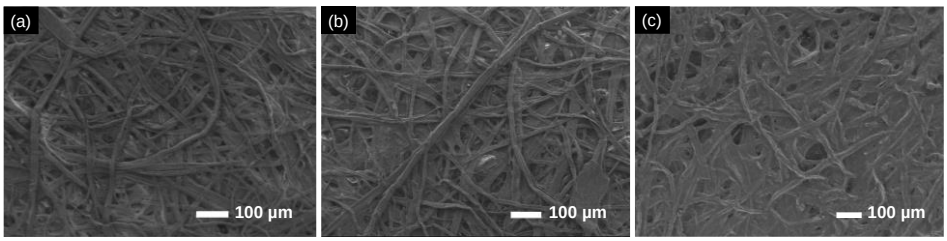

Figure 2. SEM micrographs of (a) raw filter paper, (b) MIP PAD with selected amount of nylon-6 and (c) MIP PAD with a higher amount of polymer.

In addition, the MIP PADs were also characterized by infrared spectroscopy. Fig. 3 depicts IR spectra of raw filter paper (a), pure nylon-6 (g), NIP (b) as well as MIP PADs at different steps of the process, namely MIP PAD with the quinine template before removal (c), MIP PAD after removal of the template (d), MIP PAD after incubation in aqueous standard solution of quinine (5 mg·L^{-1}) (e) and, finally, a clean MIP PAD prepared with higher amount of polymer (f). Typical bands of paper are observed at 3334, 2897, 1161 and 1033 cm^{-1}, which are related to the OH stretching, CH symmetrical stretching, asymmetrical C–O–C stretching and C–O stretching, respectively [37,28]. The latter is the most intense band among the four mentioned and is present in all the MIP PADs (spectra a–f). On the other hand, two characteristics bands of nylon-6 are observed at 1546 and 1642 cm^{-1}, corresponding to the C=O stretching of the amide group and the N–H deformation band of the amide, respectively [37,28]. The intensity of these bands is proportional to the content of nylon-6, as shown in spectra (b–e) as compared spectrum (f), the latter corresponding to the MIP PAD with a higher amount of polymer. This band can be also clearly observed in the IR spectrum of pure nylon-6 (g). However, in spectra (b–e) these two bands have a very low intensity, probably because of the thin layer of nylon-6 formed on the surface of the paper. This fact also affects to the intensity of other typical bands of nylon-6, being not possible to distinguish them from the background signal of paper. It should be pointed out that IR spectroscopy

did not enable monitoring of the adsorption process of quinine after incubation of the MIP PAD on standard solution. Nevertheless, the IR spectrum of the MIP PAD before removal of the template did not also provide bands due to the contribution of quinine in spite of the fact that the amount of quinine as template was higher. Thus, owing to the fluorescence properties of the target analyte, fluorimetry was selected as the analytical technique for the quantification of quinine, as it provided better sensitivity.

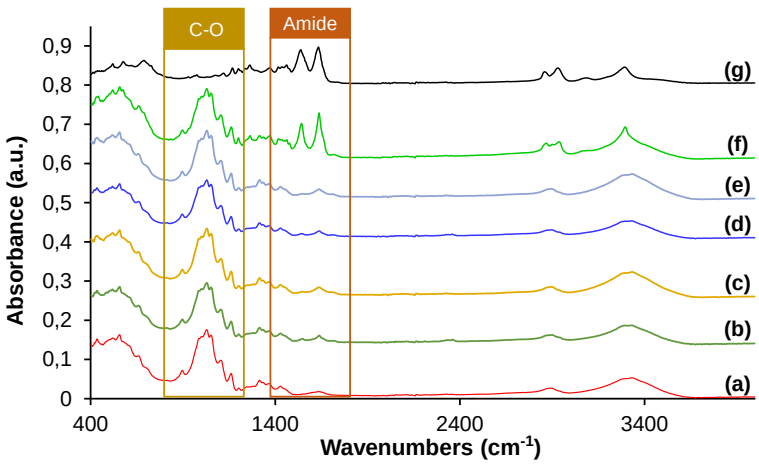

Figure 3. ATR-IR spectra of (a) raw filter paper; (b) non-imprinted polymer; MIP PAD with selected amount of nylon-6 at different steps: (c) containing the quinine template before removal, (d) after removal of the template, (e) MIP PAD after incubation in aqueous standard solution of quinine (5 $mg \cdot L^{-1}$); (f) MIP PAD with higher amount of nylon-6 and (g) pure nylon-6.

As observed in the IR spectra, the characteristics bands of nylon-6 are barely seen in the MIP PADs with selected amount of polymer (Fig. 3b), thus, Raman spectroscopy was also employed for MIP PADs characterization. Raman spectrum of the MIP PAD at selected conditions showed the characteristics bands of nylon-6, thus confirming the modification of the paper surface. As shown in Fig. 4a, the Raman spectrum of raw filter paper is dominated by cellulose bands [28], such as

the vibrations of C_6 glucose rings, namely CCC vibration observed at 380 and 435 cm^{-1} and CCO vibrations at about 435 and 458 cm^{-1}. In addition, the band at 520 cm^{-1} can be ascribed to the CCC vibration of ring and glycoside bond. The asymmetric and symmetric vibration of such bonds also lead to the appearance of two bands at ca. 1096 and 1120 cm^{-1}, respectively. CH_2 bending together with skeletal vibrations are observed at about 1380 cm^{-1}. CH_2 vibrations are also observed in the high Raman shift part of the spectrum at ca. 2890 cm^{-1}.

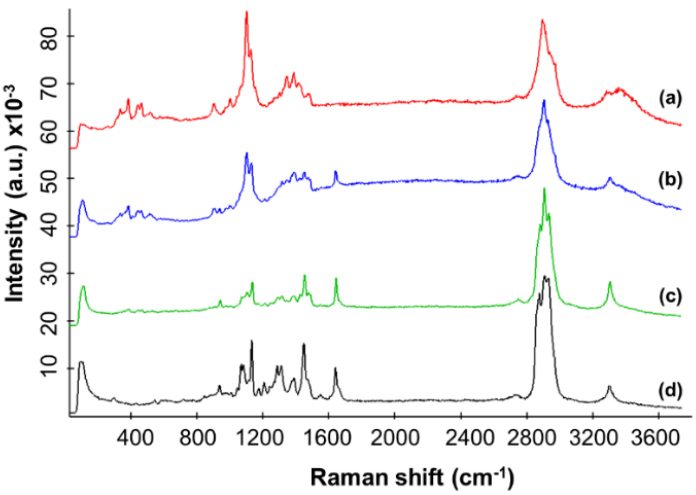

Figure 4. Raman spectra of (a) raw filter paper, (b) MIP PAD with selected concentration of nylon-6, (c) MIP PAD with higher amount of nylon-6 and (d) pure nylon-6.

On the other hand, the main bands in the Raman spectrum of pure nylon-6 (Fig. 4d) are that at 2859-2936 cm^{-1} corresponding to the asymmetric and symmetric CH_2 stretching. Other CH_2 vibrations are also shown, such as the CH_2 bending (1448 cm^{-1}), CH_2 wagging (1375 cm^{-1}) and CH_2 twisting (1308 cm^{-1}) [38]. The amide I band, corresponding to the C=O vibrations, can be observed at 1638 cm^{-1}, while the amide III band (C-N stretch and N-H bend) appears at ca. 1283 cm^{-1}. The band at ca.

3300 cm^{-1} is ascribed to the N–H stretching. In addition, the C–C skeletal backbone bands appear in the range 1071–1133 cm^{-1}, while the C–C–O stretching is observed at 932 cm^{-1} [39]. Upon modification of the cellulose paper with the MIP based on nylon-6, the characteristic amide I band of the nylon-6 at 1638 cm^{-1} can be distinguished within the bands of cellulose (Fig. 4b). In those PADs with low concentration of nylon-6 forming the MIP, the Raman spectrum is still dominated by the Raman features of cellulose; however, as the amount of nylon-6 was increased, the bands of cellulose were barely observed while those corresponding to nylon-6 increased in intensity (e.g., those at 1638, 3300, 1448 and 1133 cm^{-1}), which confirms the immobilization of the MIPs at the PADs.

3.3. Adsorption capacity and selectivity of the MIP PADs

To assess the adsorption capacity of the MIP PADs, quinine was chosen as the model analyte, due to its fluorescent properties, which enable a straightforward evaluation of the extraction of the analyte. Fig. 5a depicts photographs under ultraviolet lamp of raw filter paper, MIP PAD before template removal, MIP PAD after removal of the template (clean MIP PAD) as well as both NIP and MIP PAD after incubation with the target analyte solution. As can be observed, raw filter paper does not show fluorescence at the measurement conditions, which is confirmed by the fluorescence spectrum (Fig. 5b). As previously described, the dissolved nylon-6 in the presence of the template were casted on the PAD and left to dry. The MIP PAD shows fluorescence emission due to the presence of quinine as template (Fig. 5a). However, the clean MIP PAD after removal of the template does not provide fluorescence under ultraviolet lamp (Fig. 5a), neither in the fluorescence spectrum shown in Fig. 5b. On the other hand, after incubation of the MIP PAD with the target analyte, fluorescence arising from the quinine adsorbed at the PAD is observed (Fig. 5a and b), demonstrating the adsorption capacity of the prepared MIP PADs. However, the fluorescence intensity of the MIP PAD after the extraction of the analyte compared to that of the MIP PAD before template removal is lower, as

observed in Fig. 5a, since the amount of quinine is lower as well. In comparison, after incubation of the NIP PAD with the target analyte, fluorescence is observed under ultraviolet lamp and in the fluorescence spectrum as shown in Fig. 5a and b, nevertheless, the intensity is much lower.

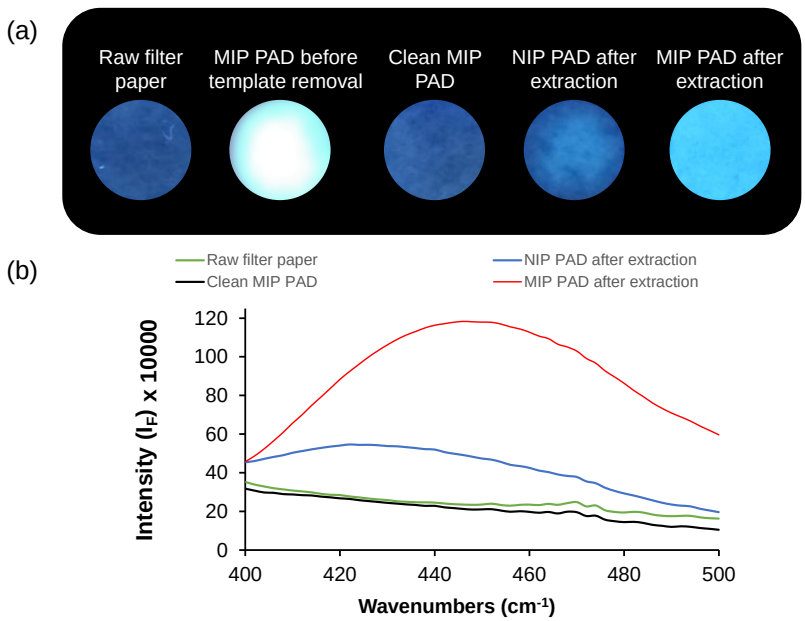

Figure 5. (a) Photographs under ultraviolet lamp of raw filter paper, MIP PAD before template removal, MIP PAD after removal of the template and NIP and MIP PADs after extraction of the target analyte from aqueous solutions at a concentration of 5 $mg \cdot L^{-1}$. (b) Fluorescence emission spectra of raw filter paper, MIP PAD after removal of the template and NIP and MIP PADs after extraction of the target analyte.

Moreover, in addition to the adsorption capacity of the MIP PADs, selectivity is also an important factor of MIPs. The extraction capacity of the MIP PAD was compared with that of the NIP PAD, the MIP PAD showing a higher adsorption capacity (Fig. 6) as compared the polymer without the imprinted cavities for selective molecular recognition.

For further demonstration of the selectivity of the MIP PADs, the effect of NaCl was evaluated, as chloride anions are able of quenching the fluorescence of quinine. The study was carried out by varying the concentration of NaCl in the range of 1–5 $mg \cdot L^{-1}$ at a fixed concentration of quinine, i.e., 5 $mg \cdot L^{-1}$. As can be seen in Fig. 7, there are no significant differences in the range of concentrations studied, so it can be concluded that the retention of quinine molecules at the MIP PADs avoids the quenching effect of the chloride ions, which is otherwise observed in aqueous solution. Nevertheless, much higher concentrations of NaCl (> 50 $mg \cdot L^{-1}$) results in a decrease of the fluorescence signal, since, as discussed later, an increase in the ionic strength does not favour the extraction process.

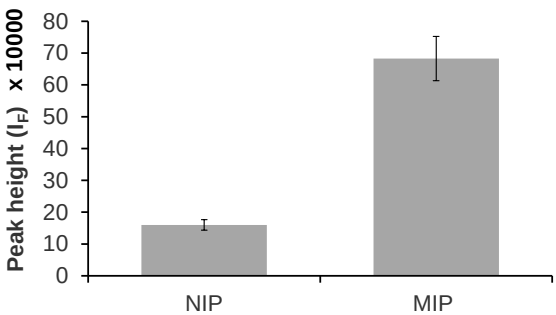

Figure 6. Comparison of the extraction capacity of quinine of MIP and NIP PADs from a 10 $mg \cdot L^{-1}$ solution.

Finally, a further study of selectivity was carried out by using another organic fluorescent molecule, i.e., norfloxacin. Norfloxacin is a synthetic quinolone antibiotic used to treat bacterial infections. The structure of this quinolone is similar to that of quinine, so this study is interesting in order to demonstrate the selectivity of the MIP PAD towards quinine. Fig. S2 (see Supporting Information) depicts images under ultraviolet lamp of MIP PAD after extraction of a 5 $mg \cdot L^{-1}$ solution of quinine, MIP PAD used for extraction of a solution of norfloxacin (5 $mg \cdot L^{-1}$) and a MIP PAD employed for the extraction of a solution containing both quinine and norfloxacin at

the same concentration of 5 mg·L^{-1}. As can be observed, fluorescence only arises when quinine is present, thus demonstrating the selectivity of the MIP PADs. Moreover, the presence of norfloxacin within the quinine solution does not interfere with the extraction process neither the fluorescent properties of the target analyte.

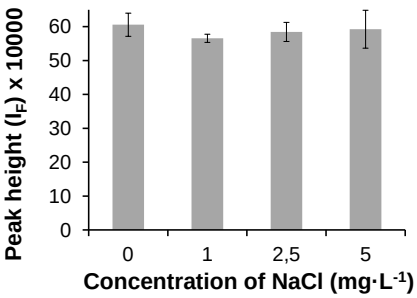

Figure 7. Effect of chloride ions on the fluorescence signal after the extraction of aqueous solutions of quinine at 5 mg·L^{-1} on the MIP PADs.

3.4. Evaluation of variables affecting the extraction capacity of MIP PAD

Firstly, variables related to the synthesis of the MIP PADs were studied by evaluating the fluorescence signal of quinine after incubation of the MIP PADs prepared at the different conditions in 2 mL of an aqueous solution of the target molecule at 5 mg·L^{-1}. There are different variables that play an important role in the formation of the MIP, namely the amount of both polymer and template molecule. In addition, the role of the porogen is very important, as it influences the bonding strength between the polymer and the template and also the morphology of the final imprinted polymer, which affects to the analyte diffusion [40]. Therefore, the effect of these three variables was evaluated following a univariate approach.

The amount of nylon-6 polymer was evaluated in the range of 0–125 mg. As can be observed in Fig. 8a, the signal increased up to 14 mg of nylon-6. However, a decrease of the signal was observed over this value due to the excess polymer in the structure of the MIP, which causes the saturation of the formed pores. This behaviour suggests

that the increase of the thickness of coating affects to the extraction kinetics, and thus the analyte cannot diffuse correctly. In addition, as previously advanced, an increase in polymer coverage on the paper results in a flattering of the three-dimensional network formed by cellulose fibres, and, thus, in less extraction capacity of quinine of the MIP PAD. No significant differences are observed within 1.5 and 14 mg of nylon-6, so 14 mg was selected due to the better precision obtained.

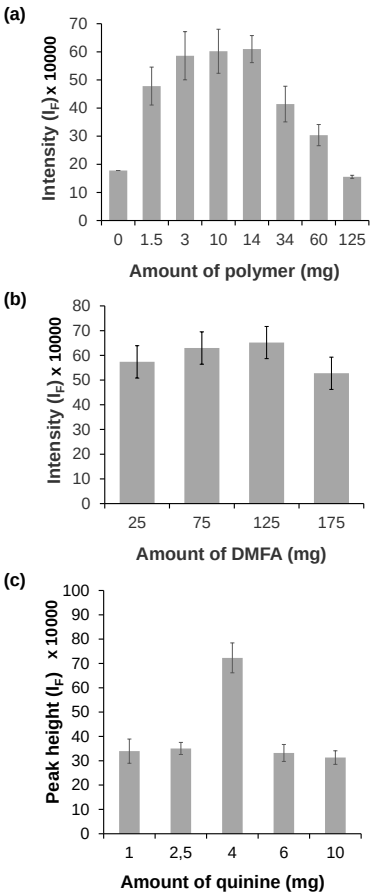

Figure 8. Effect of (a) amount of polymer, (b) amount of porogen and (c) amount of quinine on the fluorescence signal recorded after extraction.

The presence of a porogen, i.e., DMFA, favours the formation of cavities in the MIP. The amount of DMFA was evaluated by adding different volumes of the porogen to the polymer solution in the range of 0 to 175 µL. As observed in Fig. 8b, the signal increased up to 125 µL, from which it decreased. This fact suggests that an excess amount of cavities is formed and therefore the structure of the MIP is not consistent. However, the signal increase is not significant between 25 and 125 µL, and therefore 75 µL was the selected value in order to use the lowest volume of DMFA providing a good signal.

As previously described, quinine acts as the template molecule, leaving the cavities in the MIP once it is eliminated of the structure. Therefore, the study of this variable is of high importance in order to create the appropriate number of cavities in the MIP. This variable was evaluated by adding different amounts of quinine to the polymer solution in the range of 0–10 mg. As observed in Fig. 8c, the best signal was obtained when 4 mg of quinine were added. This behaviour suggests that when an excess or lack of quinine is added, the structure of the polymer does not form well and, consequently, neither do the cavities, resulting in a non-effective imprinting.

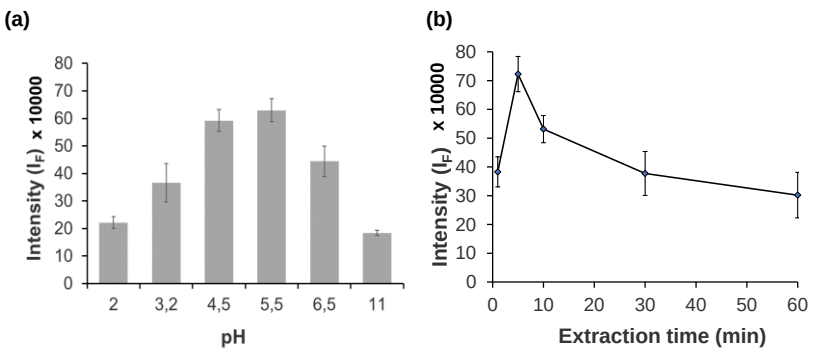

Figure 9. Results of the studies of the effect of (a) pH and (b) extraction time on the fluorescence signal.

Moreover, the effect of several variables —namely pH, ionic strength and time—, on the extraction of the analyte were also evaluated. pH commonly affects the process

of extraction if the target molecule contains acid and/or basic functional sites. In this study, pH range from 2 to 11 was studied. The results show an increase of the signal up to pH 5.5, which is the initial pH of the solution (Fig. 9a). This was expected, due to the pK_a values of the template molecule and the polymer (4.1 and 8.5 for quinine, and 5 and 9 for nylon-6). At pH 5.5 the functional groups of the quinine and the nylon-6 are deprotonated and therefore are able to interact with each other. However, nylon-6 could be considered almost as a neutral molecule, since the ionisable groups available are those located at the end of each polymer chain. An increase on the extraction time allows the MIP PAD to extract a higher amount of analyte. This study was carried out at different times in the range of 1–60 minutes. As can be observed in Fig. 9b, the signal increased up to 5 min. This suggest that quinine may be re-dissolved when the MIP PAD is stirred for too long in the solution [41], as a consequence of the increase of the temperature.

On the other hand, ionic strength affects the solubility of the compounds in solution and, therefore, its retention on the MIP. This effect was indirectly studied with NaCl previously; however, sodium sulphate was selected for further studies due to the fact that it provides higher ionic strength thanks to the charge of the anion as well as to discard any possible quenching effect of chloride ions. The study of this variable was evaluated by adding different concentrations of sodium sulphate to the extraction solution in the range 0–100 $mg \cdot L^{-1}$. The results show that the highest signal was obtained when no salt was added (figure not shown). This behaviour suggests that an excessive increase of the ionic strength results in a diffusion problem of the target molecule.

3.5. Application of the MIP PAD as fluorescent sensor

The applicability of the developed MIP PAD for quinine determination was evaluated both with standard aqueous solutions as well as with spiked soda drinks. The optimized procedure was characterized in terms of sensitivity and precision. A calibration graph was built by extracting in triplicate eight aqueous solutions of

quinine in the range from 1 to 10 mg·L^{-1} and plotting the peak height in the fluorescence spectra versus concentration (Fig. 10a). Each point corresponds to the average of the three independent extractions, and error bars illustrate the standard deviation of the mean value. As can be observed, the calibration curve can be fitted to a Langmuir isotherm function (R^2=0.991), which depicts the adsorption process of quinine on the MIP PAD. The corresponding Langmuir equation was y = (a·b·x^(1-c))/ (1 + b·x^(1-c)) fitted by the following parameters: a=2,034,371.3, b=0.0922, c=0.1967. This plot displays a linear variation at low concentrations of quinine (R^2=0.993), as shown in the inset of Fig. 10a. The limit of detection (LOD) and limit of quantification (LOQ) were calculated from the linear fit as (3Sa)/b and (10Sa)/b, respectively, for y=b·[quinine] + a, obtaining values of concentrations of 0.37 and 1.24 mg·L^{-1}, respectively. The precision of the measurements was evaluated at a concentration level of 5 mg·L^{-1} obtaining a relative standard deviation (n=3) of 2.30%.

Furthermore, a calibration graph was also built for a soda drink with low sugar content (7up free) by extracting in triplicate nine solutions spiked with quinine in the range from 2 to 40 mg·L^{-1} (Fig. 10b). The soda drink without spiking was also analysed and no quinine was found, as expected considering the composition of the drink. The differences observed in the signal intensity at the same concentration of quinine for soda drink samples as compared aqueous standards may be related to the higher ionic strength within the drink. As previously discussed, an increase in the ionic strength of the medium did not favour the extraction and subsequent detection of the analyte. Nevertheless, as observed in Fig. 9b, the plot of the peak height in the fluorescence spectra versus concentration was fitted to a Langmuir isotherm (R^2=0.996), similar to that for aqueous samples. The Langmuir equation was y = (a·b·x^(1-c))/ (1 + b·x^(1-c)) fitted by the following parameters: a=1,219,187.4, b=0.0281, c=0.1251. Again, data at low concentrations of quinine were linearly fitted (R^2=0.998), which enabled the calculation of the LOD and LOQ, as previously described, as 0.63 and 2.11 mg·L^{-1}, respectively. The relative standard

deviation obtained after three measurements at a concentration of 5 mg·L^{-1} was 9.07%. This deviation is inter-PAD in both of the calibration curves, as different MIP PADs are used for each measurement.

In addition, the reusability of the MIP PADs was evaluated. The study was carried out by extracting six aqueous solutions of the analyte at 5 mg·L^{-1} and cleaning the MIP PADs with methanol-acetic acid between measurements. The fluorimetric signal did not decrease significantly with any extraction (figure not shown), meaning that the MIP PADs can be used at least six times. The intra-PAD relative standard deviation obtained was 8.31%.

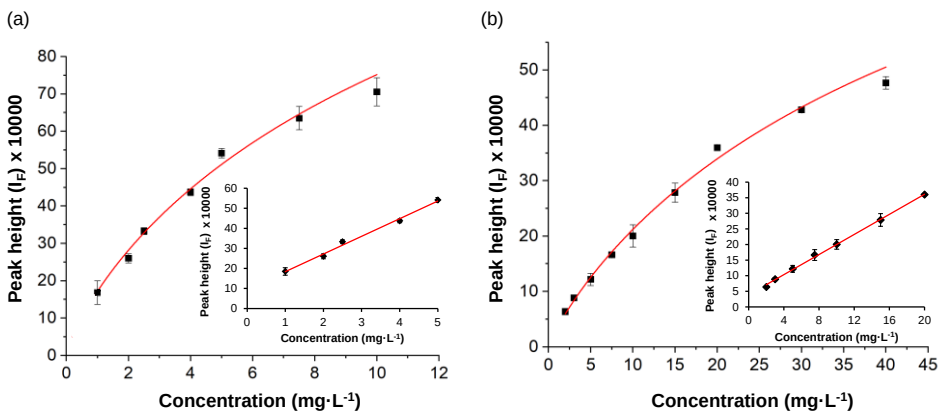

Figure 10. (a) Peak height in the fluorescence spectrum of quinine after extraction vs. concentration of quinine in the aqueous solutions. (b) Peak height in the fluorescence spectrum of quinine after extraction vs. concentration of quinine in soda drink samples. Each point represents the average of three independent measurements; error bars relate to the standard deviation of the corresponding mean value. Curves were fitted to a Langmuir isotherm. The inset of both graphs depicts linear range of each curve at low concentrations.

4. Conclusions

In this article, a MIP PAD has been developed following a methodology which avoids polymerization, facilitating the entire synthetic process. The synthesis of the MIP

PAD, as abovementioned, is simple, as it only requires the dissolution of the polymer in the appropriate solvent, and the later addition of the porogen and template molecule. Related to this, the volume of solvent used is very low and the entire process of synthesis is rapid (< 15 min). The detection method, i.e., fluorescence, of the MIP PAD is immediate. A custom-built magnetic piece that holds the MIP PAD in the measurement window is introduced in the fluorimeter cell in a 45° angle. After this, spectra are obtained in less than 40 s.

This method of MIP PAD synthesis opens a wide range of opportunities in further investigations in this field, as it is an easy and rapid way to prepare these useful materials. Also, since the MIP is immobilized in common filter paper, not only the cost is lower but also the versatility increases, as PADs can be coupled to different techniques and can be modified with a wide range of compounds. Furthermore, the porosity of the paper itself is exploited, since the MIP is both immobilized inside the structure and in the surface, increasing the amount of material available in a single PAD.

Compliance with ethical standards

The authors declare that they have no competing interests.

Acknowledgements

The authors wish to thank Spanish Ministry of Economy, Industry and Competitiveness for funding project CTQ2017-83175-R. The authors also thank the Central Service for Research Support (SCAI) of the University of Córdoba for the service provided to obtain the SEM images.

Appendix A. Supplementary data

Supplementary material related to this article can be found, in the online version, at doi: https://doi.org/10.1016/j.snb.2019.02.048.

References

[1] Q. Han, Z. Wang, J. Xia, X. Zhang, H. Wang, M. Ding, Application of graphene for the SPE clean-up of organophosphorus pesticides residues from apple juices, J. Sep. Sci. 37 (1-2) (2014) 99–105.

[2] G. Mohammed, A. Bashammakh, A. Alsibaai, H. Alwael, M. El-Shahawi, A critical overview on the chemistry, clean-up and recent advances in analysis of biogenic amines in foodstuffs, Trac Trends Anal. Chem. 78 (2016) 84–94.

[3] A. Speltini, A. Scalabrini, F. Maraschi, M. Sturini, A. Profumo, Newest applications of molecularly imprinted polymers for extraction of contaminants from environmental and food matrices: a review, Anal. Chimita Acta 974 (2017) 1–26.

[4] S. Boulanouar, S. Mezzache, A. Combès, V. Pichon, Molecularly imprinted polymers for the determination of organophosphorus pesticides in complex samples, Talanta 176 (2018) 465–478.

[5] M. Marć, T. Kupka, P.P. Wieczorek, J. Namieśnik, Computational modeling of molecularly imprinted polymers as a green approach to the development of novel analytical sorbents, Trac Trends Anal. Chem. 98 (2018) 64–78.

[6] S. Zink, F. Moura, P.A. da Silva Autreto, D. Galvão, B. Mizaikoff, Virtually imprinted polymers (VIPs): understanding molecularly templated materials via molecular dynamics simulations, J. Chem. Soc. Faraday Trans. 20 (19) (2018) 13145–13152.

[7] N.A. Samah, M.-J. Sánchez-Martín, R.M. Sebastián, M. Valiente, M. López-Mesas, Molecularly imprinted polymer for the removal of diclofenac from water: synthesis and characterization, Sci. Total Environ. 631 (2018) 1534–1543.

[8] M. Marć, A. Panuszko, J. Namieśnik, P.P. Wieczorek, Preparation and characterization of dummy-template molecularly imprinted polymers as potential sorbents for the recognition of selected polybrominated diphenyl ethers, Anal. Chim. Acta (2018).

[9] M.C. Alcudia-León, R. Lucena, S. Cárdenas, M. Valcárcel, Selective extraction of Bactrocera oleae sexual pheromone from olive oil by dispersive magnetic microsolid phase extraction using a molecularly imprinted nanocomposite, J. Chromatogr. A 1455 (2016) 57–64.

[10] M.A. Villalobos, J. Debling, E. Saldivar-Guerra, E. Vivaldo-Lima (Eds.), Bulk and Solution Processes. In: Handbook of Polymer Synthesis, Characterization, and Processing, John Wiley & Sons., 2013, pp. 273–294.

[11] P.A. Cormack, A.Z. Elorza, Molecularly imprinted polymers: synthesis and characterisation, J. Chromatogr. B 804 (1) (2004) 173–182.

[12] B.A. Miller-Chou, J.L. Koenig, A review of polymer dissolution, Prog. Polym. Sci. 28 (8) (2003) 1223–

1270.

[13] X. Zhu, Q. Zhu, Molecular imprinted Nylon-6 stir bar as a novel extraction technique for enantioseparation of amino acids, J. Appl. Polym. Sci. 109 (4) (2008) 2665–2670.

[14] E. Dmitrienko, R. Bulushev, K. Haupt, S. Kosolobov, A. Latyshev, I. Pyshnaya, D. Pyshnyi, A simple approach to prepare molecularly imprinted polymers from nylon-6, J. Mol. Recognit. 26 (8) (2013) 368–375.

[15] X. Jia, M. Herrera-Alonso, T.J. McCarthy, Nylon surface modification. Part 1. Targeting the amide groups for selective introduction of reactive functionalities, Polymer 47 (14) (2006) 4916–4924.

[16] G.F. Bickerstaff, Immobilization of enzymes and cells, Immobilization of Enzymes and Cells, Springer, 1997, pp. 1–11.

[17] T. Beeskow, K.H. Kroner, F.B. Anspach, Nylon-based affinity membranes: impacts of surface modification on protein adsorption, J. Colloid Interface Sci. 196 (2) (1997) 278–291.

[18] S. Swar, V. Zajícová, J. Müllerová, P. Šubrtová, J. Horáková, B. Dolenský, M. Řezanka, I. Stibor, Effective poly (ethylene glycol) methyl ether grafting technique onto Nylon 6 surface to achieve resistance against pathogenic bacteria Staphylococcus aureus and Pseudomonas aeruginosa, J. Mater. Sci. 53 (20) (2018) 14104–14120.

[19] S. Aslanzadeh, H. Saghlatoon, M.M. Honari, R. Mirzavand, C. Montemagno, P. Mousavi, Investigation on electrical and mechanical properties of 3D printed nylon 6 for RF/microwave electronics applications, Addit. Manuf. 21 (2018) 69-75.

[20] A.E. Shearer, J.S. Paik, D.G. Hoover, S.L. Haynie, M.J. Kelley, Potential of an antibacterial ultraviolet-irradiated nylon film, Biotechnol. Bioeng. 67 (2) (2000) 141–146.

[21] J. Ríos-Gómez, B. Fresco-Cala, M.T. García-Valverde, R. Lucena, S. Cárdenas, Carbon Nanohorn Suprastructures on a Paper Support as a Sorptive Phase, Molecules 23 (6) (2018) 1252.

[22] J.F. da Silveira Petruci, A.A. Cardoso, Sensitive luminescent paper-based sensor for the determination of gaseous hydrogen sulfide, Anal. Methods 7 (6) (2015) 2687–2692.

[23] J. Ríos-Gómez, R. Lucena, S. Cárdenas, Paper supported polystyrene membranes for thin film microextraction, Microchem. J. 133 (2017) 90–95.

[24] R. Trouillon, M.A. Gijs, Paper-based polymer electrodes for bioanalysis and electrochemistry of neurotransmitters, ChemPhysChem 19 (10) (2018) 1164–1172.

[25] J. Xu, Y. Bai, M. Wan, Y. Liu, L. Tao, X. Wang, Antifungal Paper Based on a Polyborneolacrylate coating, Polymers 10 (4) (2018) 448.

[26] W. Zhang, X. Niu, X. Li, Y. He, H. Song, Y. Peng, J. Pan, F. Qiu, H. Zhao, M. Lan, A smartphone-integrated ready-to-use paper-based sensor with mesoporous carbon dispersed Pd nanoparticles as a highly active peroxidase mimic for H2O2 detection, Sens. Actuators B Chem. 265 (2018) 412–420.

[27] T.-T. Tsai, C.-Y. Huang, C.-A. Chen, S.-W. Shen, M.-C. Wang, C.-M. Cheng, C.- F. Chen, Diagnosis of tuberculosis using colorimetric gold nanoparticles on a paper-based analytical device, ACS Sens. 2 (9) (2017) 1345–1354.

[28] J. Ríos-Gómez, B. Ferrer-Monteagudo, ÁI. López-Lorente, R. Lucena, R. Luque, S. Cárdenas, Efficient combined sorption/photobleaching of dyes promoted by cellulose/titania-based nanocomposite films, J. Clean. Prod. 194 (2018) 167–173.

[29] Y. Zhang, L. Zhang, K. Cui, S. Ge, X. Cheng, M. Yan, J. Yu, H. Liu, Flexible electronics based on micro/nanostructured paper, Adv. Mater. 30 (1801588) (2018).

[30] Y. Yang, E. Noviana, M.P. Nguyen, B.J. Geiss, D.S. Dandy, C.S. Henry, Paper-based microfluidic devices: emerging themes and applications, Anal. Chem. 89 (2017) 71–91.

[31] B. Yao, J. Zhang, T. Kou, Y. Song, T. Liu, Y. Li, Paper-based electrodes for flexible energy storage devices, Adv. Sci. 4 (1700107) (2017).

[32] Y. Kim, G. Jang, T.S. Lee, New fluorescent metal-ion detection using a paper-based sensor strip containing tethered rhodamine carbon nanodots, ACS Appl. Mater. Interfaces 7 (28) (2015) 15649–15657.

[33] M.M. Ali, C.L. Brown, S. Jahanshahi-Anbuhi, B. Kannan, Y. Li, C.D. Filipe, J.D. Brennan, A printed multicomponent paper sensor for bacterial detection, Sci. Rep. 7 (1) (2017) 12335.

[34] J.F. da Silveira Petruci, A.A. Cardoso, Portable and disposable paper-based fluorescent sensor for *in situ* gaseous hydrogen sulfide determination in near real-time, Anal. Chem. 88 (23) (2016) 11714–11719.

[35] M. Zeni, R. Riveros, J.F. de Souza, K. Mello, C. Meireles, G. Rodrigues Filho, Morphologic analysis of porous polyamide 6, 6 membranes prepared by phase inversion, Desalination 221 (1-3) (2008) 294–297.

[36] X. Zhu, J. Cai, J. Yang, Q. Su, Y. Gao, Films coated with molecular imprinted polymers for the selective stir bar sorption extraction of monocrotophos, J. Chromatogr. A 1131 (1-2) (2006) 37–44.

[37] E. Reyes-Gallardo, R. Lucena, S. Cárdenas, Silica nanoparticles–nylon 6 composites: synthesis, characterization and potential use as sorbent, RSC Adv. 7 (4) (2017) 2308–2314.

[38] L.-L. Cho, Identification of textile fiber by Raman microspectroscopy, Forensic Sci. J. 6 (1) (2007) 55–62.

[39] J.V. Miller, E.G. Bartick, Forensic analysis of single fibers by Raman spectroscopy, Appl. Spectrosc. 55 (12) (2001) 1729–1732.

[40] L. Chen, S. Xu, J. Li, Recent advances in molecular imprinting technology: current status, challenges and highlighted applications, Chem. Soc. Rev. 40 (5) (2011) 2922–2942.

[41] M. Roldán-Pijuán, R. Lucena, M.C. Alcudia-León, S. Cárdenas, M. Valcárcel, Stir octadecyl-modified borosilicate disk for the liquid phase microextraction of triazine herbicides from environmental waters, J. Chromatogr. A 1307 (2013) 58.

SUPPORTING INFORMATION

SEM characterization of the MIP PADs

The surface of different MIP PADs was characterized by SEM. Fig. S1 depicts a PAD modified with both the NIP and the MIP at the selected conditions before template extraction. Nevertheless, no significant differences were observed when compared to Fig. 2b, showing the MIP PAD with selected amount of nylon-6 after removal of quinine template.

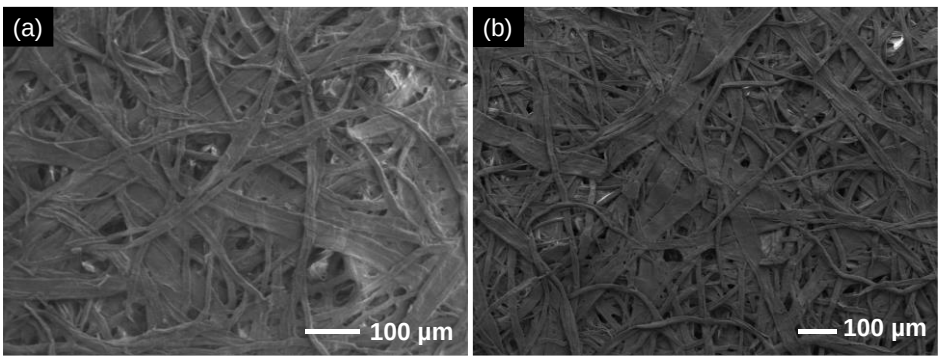

Figure S1. SEM micrographs of (a) NIP PAD before template removal and (b) MIP PAD before template removal.

Selectivity study of MIP PAD

A further study of selectivity was carried out by using another organic fluorescent molecule, i.e., norfloxacin. Norfloxacin is a synthetic quinolone antibiotic used to treat bacterial infections. The structure of this quinolone is similar to that of quinine, so this study is interesting in order to demonstrate the selectivity of the MIP PAD towards quinine. Fig. S2 depicts images under ultraviolet lamp of MIP PAD after extraction of a 5 $mg \cdot L^{-1}$ solution of quinine, MIP PAD used for extraction of a solution of norfloxacin (5 $mg \cdot L^{-1}$) and a MIP PAD employed for the extraction of a solution

containing both quinine and norfloxacin at the same concentration of 5 mg·L^{-1}. As can be observed, fluorescence only arises when quinine is present, thus demonstrating the selectivity of the MIP PADs. Moreover, the presence of norfloxacin within the quinine solution does not interfere with the extraction process neither the fluorescent properties of the target analyte.

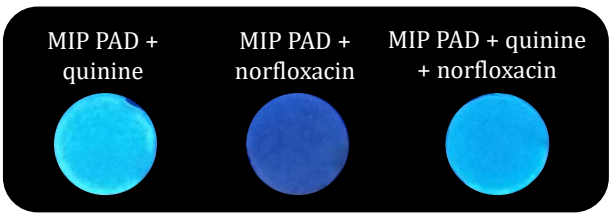

Figure S2. Photographs under ultraviolet lamp of a MIP PAD after extraction of the target analyte (quinine) from an aqueous solution at a concentration of 5 mg·L^{-1}; MIP PAD after extraction of norfloxacin from a 5 mg·L^{-1} aqueous solution and MIP PAD after extraction of a solution containing both quinine and norfloxacin at the same concentration of 5 mg·L^{-1}.

Capítulo 5

Dual-template molecularly imprinted paper for the determination of drugs of abuse in saliva samples by direct infusion mass spectrometry

Microchemical Journal, 160 (2021) 105686

Microchemical Journal
160 (2021) 105686

Dual-template molecularly imprinted paper for the determination of drugs of abuse in saliva samples by direct infusion mass spectrometry

M.C. Díaz-Liñán, M.T. García-Valverde, R. Lucena*, S. Cárdenas, A.I. López-Lorente

Departamento de Química Analítica, Instituto Universitario de Investigación en Química Fina y Nanoquímica IUNAN, Universidad de Córdoba, Campus de Rabanales, Edificio Marie Curie, E-14071 Córdoba, Spain

Chromatographic separation improves method selectivity at the expense of analysis time. In this article, the use of a molecularly imprinted polymer (MIP) paper combined with direct infusion electrospray ionization tandem mass spectrometry (DI-ESI-MS/MS) in the selected reaction monitoring (SRM) mode is presented as an alternative to the classical workflow for the determination of cocaine and methamphetamine in saliva samples. The MIP paper is synthesized by dip-coating, just immersing the paper substrate into a polymeric solution (nylon-6 in formic acid) containing cocaine and methamphetamine as templates. The evaporation of the solvent induces the rearrangement of the polymeric chains around the template, creating selective cavities that are released when the MIP paper is washed. The MIP paper presents a better affinity for the analytes than for 6-acetylmorphine, which was selected as model interfering compound. Also, the MIP paper showed a better performance than the non-imprinted (NIP) one. The extraction can be easily performed in an Eppendorf tube, enabling the simultaneous extraction of several

samples, which increases the sample throughput. Working at the optimum conditions, a matrix-matched calibration model was built for both analytes using deuterated analogs as internal standards. The limits of quantification and detection were 10 $\mu g \cdot L^{-1}$ and 3 $\mu g \cdot L^{-1}$, respectively, for both analytes. The precision, expressed as relative standard deviation, was better than 5.9%, and the recovery values were found in the interval 84.3–98.0%.

Keywords: Paper-based sorptive phase, Molecularly imprinted polymer, Direct infusion mass spectrometry, Cocaine, Methamphetamine, Saliva.

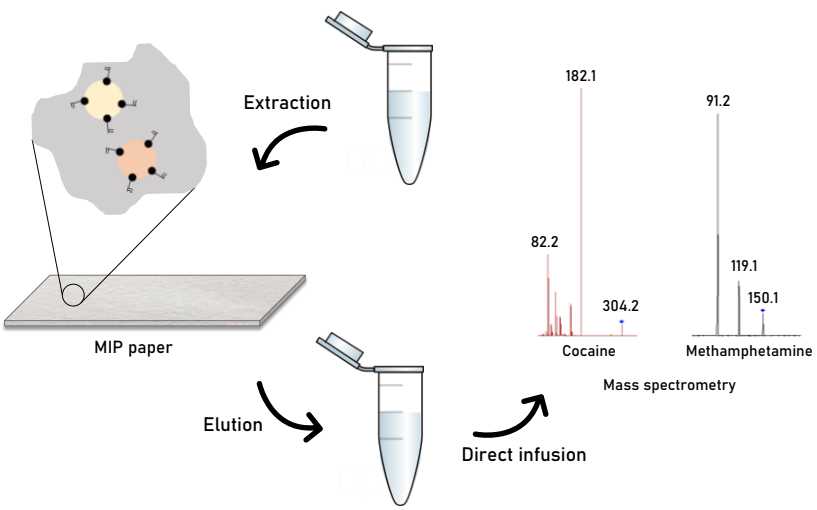

1. Introduction

Cocaine and methamphetamine are among the most widely used illicit substances in the world. Both are stimulant drugs that affect the central nervous system, causing hyperactivity and restlessness, while also suppressing hunger and thirst [1,2]. Furthermore, the reiterated use of these substances can cause long-term health effects, namely hypertension, arrhythmia, or even acceleration of certain diseases such as atherosclerosis [3]. A wide variety of analytical techniques have been reported for the determination of drugs throughout the years, including gas chromatography-mass spectrometry [4,5], capillary electrophoresis [6,7] and liquid chromatography-mass spectrometry [1,8], the latter being one of the most employed. In addition, the determination of drugs in different biological samples has been described, namely blood [9,10], hair [1] or urine [11], but they require an invasive collection procedure or even specialized personnel. However, the collection of saliva is an easy, painless, non-invasive procedure that can be closely supervised to avoid adulteration or substitution of the sample, which can happen with urine samples [12,13]. Furthermore, saliva is stable for several hours at room temperature and up to a week in the refrigerator [14]. Nevertheless, pretreatment is mandatory prior to mass spectrometry measurements to suppress the matrix effect derived from complex samples.

Sample pretreatment is usually the most time-consuming step in the analytical process, hence the urge to develop new strategies that allow rapid and reliable procedures. In this sense, paper has emerged as a relevant material in the production of sorbents for the isolation and preconcentration of analytes from complex matrices. Paper-based materials have unique advantages over other traditional materials, including fluid transport based on its own capillary action or the ability to retain compounds on its cellulose fibers, while still being cost-effective [15]. Furthermore, paper-based analytical devices (PADs) are flexible and portable, which facilitate its coupling to other instrumental devices [16,17]. The high porosity of PADs increases the surface area to volume ratio, providing a higher extraction

ability when compared to less porous materials. Additionally, it is environmentally-friendly, since it is biodegradable and non-toxic [15]. Paper can be easily modified via wet chemistry, which increases the versatility of the material. PADs modifications via polymer coating [18–20] or the immobilization of different nanostructures [16,21–23] have been also described.

Selectivity is one of the greatest challenges when designing a sorbent. Throughout the decades, a wide variety of methods have been proposed, but in the last years, the molecularly imprinting technology has been consolidated. Molecularly imprinted polymers (MIPs) are selective materials with artificially generated recognition sites towards a target molecule, known as template, or a structural-related analogue [24,25]. Traditionally, MIPs have been synthesized following different approaches, namely bulk polymerization or precipitation. Despite their widespread use, these methods require a stringent control of the experimental conditions, such as pH, temperature or time, and high amounts of reagents are employed during the synthesis. Although the synthesis of MIP papers following those approaches has been successfully reported [26–28], our group proposed a simple method based on the dissolution and subsequent rearrangement of the polymer around the templates [29]. This procedure was not only cost-effective, but also fast and eco-friendly. The former approaches involving MIPs employed a single molecule as template, thus having a specific MIP for a sole molecule [24,30]. Nevertheless, in many cases, various compounds are required to be extracted, hence synthesizing a MIP for each one would be time-consuming and an unnecessary waste of reagents. Instead, the addition of multiple templates in the reaction mixture is preferable to obtain a single MIP able to recognize multiple analytes [31,32]. This strategy is of high importance in water treatment, where compounds are usually isolated and determined by groups [33,34], and in those cases in which the amount of sample is limited [35].

Selectivity is also important when mass spectrometry is involved to avoid the effects derived from complex matrices, as already mentioned. This aspect is one of the

reasons why chromatography is necessary prior to mass spectrometry. However, the use of sorbents for the previous isolation of the analytes avoids this step. In a previous work proposed by our group, cotton fibers functionalized with β-cyclodextrins were employed for the extraction of cocaine and methamphetamine from saliva samples [36]. This step allowed the direct infusion of the analytes, thus saving time and solvents. Also, since the interferents are previously eliminated, ion suppression is avoided and, therefore, a higher sensitivity is obtained [37]. In the present work, direct infusion was also possible since MIPs isolate the analytes from all the interferent compounds.

Herein, a dual-template molecularly imprinted polymer based on the dissolution of nylon-6 in formic acid in the presence of the template molecules, namely cocaine and methamphetamine, has been developed. The polymer solution is incorporated into filter paper via dip-coating to provide a solid support. The procedure of both MIP formation and immobilization onto the filter paper is very simple and fast, providing improved selectivity towards the target analytes. The MIP paper can be directly coupled to mass spectrometry via direct infusion, which enabled the subsequent quantification of the drugs with high sensitivity.

2. Materials and methods

2.1. Reagents

Unless otherwise specified, all reagents were of analytical grade or better and purchased from Sigma-Aldrich (Madrid, Spain). Stock solutions of the template molecules, namely cocaine (CO) and methamphetamine (MTA), were prepared in methanol at a concentration of 10 $mg \cdot L^{-1}$ and stored in the dark at -18 ºC. Working solutions were prepared by dilution of the stock in Milli-Q water (Millipore Corp., Madrid, Spain) or in saliva sample. Cocaine-d3 (CO-d_3) and methamphetamined5 (MTA-d_5) were employed as internal standards (IS) and are added to the elution media prior ESI-MS/MS analysis.

For the study of selectivity of the MIP paper, 6-acetylmorphine (6-AM) was employed. Milli-Q water and ammonium formate were employed as the mobile phase during the mass spectrometry measurements.

For the synthesis of the MIP papers, standard filter paper (Filter-Lab ream 42x52 cm, density: 73 $g \cdot m^{-2}$), nylon-6, formic acid, and dimethylformamide (DMF) were employed.

2.2. Saliva sampling and storage

Saliva samples were collected using the Salivette® system (SciMart, Saint Louis, MO), consisting of a roll-shaped cotton collector which is introduced in the volunteer's mouth for a while. The cotton is then introduced in a plastic tube and centrifuged for 5 min at 2500 rpm, thus recovering around 3 mL of saliva. Then, the sample is transferred to a glass vial and stored at 4 °C. Before the extraction procedure, the samples were diluted with MilliQ water at 1:1 ratio and pH was adjusted to 10 with NaOH.

Due to the current situation, blank saliva samples were kindly donated by only one healthy volunteer (the first author of this article) for the development and characterization of this method.

2.3. Synthesis and characterization of the MIP papers

MIPs were synthesized following a similar procedure to that described in our previous research [29]. Initially, a solution of nylon-6 in formic acid (8.3 $mg \cdot mL^{-1}$) was prepared. Next, 20 µL of 10 $mg \cdot L^{-1}$ solutions of the template molecules, along with 75 µL of porogen, i.e., DMF, were added to the solution and stirred for 5 min. Finally, the filter paper was dipped once in the solution and dried naturally. The obtained MIP paper was stirred in a methanol-acetic acid mixture (90:10) for 10 min and then rinsed in methanol for 5 min until the template molecules were quantitatively eliminated. In order to verify the removal of the template molecules,

mass spectrometry measurements of the eluents of the cleaned MIP papers were carried out. The same procedure, except the addition of the templates, was employed for the synthesis of the nonimprinted polymers paper (NIPs).

Three MIP papers at different conditions, in terms of the amount of nylon-6 and number of dips, were characterized via Raman spectroscopy. Raw filter paper and pure nylon-6 were also studied for comparative purposes. Spectra were acquired with a confocal Raman spectrometer (alpha500, manufactured by WITec GmbH, Ulm, Germany). For excitation, a frequency-doubled Nd:YAG laser at 532 nm (second harmonic generation) was employed, using a laser power of 0.362 mW (measured prior to the objective lens). The laser beam was focused on the sample using a 20x/0.4 Zeiss objective. The integration time was 0.5 s, and a total of 50 accumulations were acquired for each spectrum.

2.4. Extraction procedure

The extraction procedure was carried out by immersing the MIP paper in an Eppendorf tube with 1 mL of an aqueous solution at pH 10 containing both cocaine and methamphetamine at the appropriate concentration and stirring in an orbital stirrer for 45 min. Next, the MIP paper was rinsed with Milli-Q water for 5 min to remove the non-attached analytes and left to dry. Finally, the MIP papers were eluted with 500 μL of methanol for 5 min. The same procedure was used for the extraction in saliva after 1:1 dilution in Milli-Q water and pH adjustment. The IS were added in the eluent prior mass spectrometry measurements.

2.5. Optimization of the extraction procedure

The different variables that could potentially affect the final adsorption ability of the MIP papers were evaluated. Initially, the effect of pH in the sample, along with the ionic strength and the dilution factor of the sample, were evaluated following a univariate approach.

Additionally, a multivariate 3^3 Box-Behnken design (BDD) was carried out to evaluate the second order interactions among variables having a significant effect on the adsorption ability. In this sense, the amount of nylon-6 (X_1), number of dips (X_2) and extraction time (X_3) were studied by response surface methodology (RSM). The differences in the extraction efficiency were evaluated by analysis of variance (ANOVA) using the Statgraphics Centurion XVI software. The total number of tests of the BDD was calculated through the following equation:

$$N = 2k \cdot (k - 1) + C_p \qquad (1)$$

where N is the number of experiments, k is the number of factors, and C_p is the number of central points [38], thus resulting in 15 experiments including 3 replicates of the central point for the assessment of the test error. The experiments were carried out by duplicate to increase the accuracy of the obtained results, resulting in a total of 30 experiments. Each experimental factor was defined between a minimum and a maximum value. The analytical responses of the design were the relations of peak areas of CO (A_{CO}) and MTA (A_{MTA}) and the peak area of the isotope-labelled IS, A_{d3} and A_{d5}, respectively. The multiple linear regression for each response is composed of three main elements, namely linear, quadratic, and terms related to the interactions between the different experimental variables; all of them correlated through the following quadratic polynomial equation:

$$Y = \beta_0 + \sum \beta_i x_i + \sum \beta_{ii} x_i^2 + \sum \beta_{ij} x_i x_j + \varepsilon \qquad (2)$$

where Y refers to A_{CO}/A_{d3} or A_{MTA}/A_{d5}; β_0 is the constant term; β_i, β_{ii} and β_{ij} are the regression coefficients of the design; x_i and x_j represent the variables, and ε is the residual error associated to the experiments [38,39].

The Derringer function or desirability function is a multicriteria methodology that evaluates the different responses of a multivariate design to find optimal

compromises between them. In this case, the desirability function was used to obtain the optimal extraction conditions to maximize the analytical signals of CO and MTA, which represent their retention in the MIP papers. Thereby, the overall desirability (D) of the experiment is defined through the following equation:

$$D = \sqrt[m]{d_1(Y_1)d_2(Y_2)\dots d_m(Y_m)} \qquad (3)$$

where m is the number of responses studied in each experiment, and $d_i(Y_i)$ is the individual desirability of each response studied in each experiment, calculated as follows:

$$d_i = \frac{Y_i - Y_{min}}{Y_{max} - Y_{min}} \qquad (4)$$

The individual desirability function scale ranges between 0, for a completely undesirable response, and 1, which represents a fully desirable response [38].

2.6. Mass spectrometry measurements

Analyses were performed by direct infusion mass spectrometry (DIMS) using an Agilent 1260 Infinity HPLC system (Agilent, Palo Alto, CA, USA) equipped with a binary high-pressure pump and an autosampler. The injection volume was 10 μL, which were driven by the carrier phase (0.1% ammonium formate aqueous solution) directly to the mass spectrometer at a flow rate of 0.3 $mL \cdot min^{-1}$. Each analysis took about 2 min.

An Agilent 6420 triple quadrupole MS with an electrospray source was used for analytes detection and quantification. Mass spectrometer settings were fixed to improve the selected reaction monitoring (SRM) signal. Flow and temperature of the drying gas (N_2 with a purity of 99.9%) were 10 $L \cdot min^{-1}$ and 300 °C, respectively. Nebulizer pressure was 18 psi, and the capillary voltage was 2000 V in positive

mode. Full-scan and MS/MS spectra of CO, CO-d_3, MTA, and MTA-d_5 were obtained by direct infusion of 1 mg·L^{-1} of standards in methanol. The SRM parameters for the target analytes and their isotopologues, as well as the ones for 6-AM, are specified in Table S1. Agilent MassHunter Software (version B.06.00) was employed for data analyses.

3. Results and discussion

3.1. Synthesis of the MIP papers

MIPs were synthesized following a similar procedure to that described in our previous work, which is based on the solubility of nylon-6 in formic acid [29]. During the process of dissolution of a polymer, the solvent causes the disentanglement of the polymer chains, which remain solvated in solution and can interact with the template via different bonds typical from polyamine chains. Inter- and intramolecular hydrogen bonds can be formed through the amide group, providing a specific recognition of the target analyte. On the other hand, non-polar hydrophobic interactions with the aliphatic region are also possible. In this approach, the formation of the MIPs was carried out by dissolution of nylon-6 in the presence of the template molecules, namely CO and MTA, and the subsequent dip coating of filter paper and evaporation of the solvent, paper acting as a solid and three-dimensional support for the deposition of the MIP. The evaporation of the solvent results in the rearrangement of the polymer chains around the templates, thus creating the cavities once the template molecules are eliminated.

Three MIP paper synthesized at different conditions, in terms of the amount of nylon-6 and dips, were characterized via Raman spectroscopy, along with raw filter paper and pure nylon-6. Fig. S1 (supplementary material) depicts the different Raman spectra of (a) raw filter paper, (b) a MIP paper with 8.3 mg·mL^{-1} of nylon-6 and 3 dips, (c) a MIP paper with 15 mg·mL^{-1} of nylon-6 and 1 dip, (d) a MIP paper with 15 mg·mL^{-1} of nylon-6 and 3 dips, and (e) pure nylon-6. The characteristic bands of cellulose can be observed in the Raman spectra of raw filter paper (Fig.

S1a). In the region between 380 and 520 cm^{-1} appear the vibrations of C_6 glucose rings along with the CCC vibration of ring and glycoside bond. The bands appearing at ca. 1096 and 1120 cm^{-1} can be ascribed to the asymmetric and symmetric vibrations of the mentioned bonds, respectively. The skeletal vibrations and CH_2 bending appear together at around 1280 cm^{-1}, the latter also observed in the high Raman shift part of the spectrum at ca. 2890 cm^{-1}.

Regarding nylon-6, the main bands are observed in Fig. S1e. On the one hand, in the region between 932 and 1133 cm^{-1} appear the skeletal backbone bands alongside the C-C-O stretching. The amide I and III bands can be observed at 1638 and 1283 cm^{-1}, respectively. These bands can be ascribed to the C=O vibrations and the C-N stretch and N–H bend, respectively, while the band at ca. 3300 cm^{-1} is related to the N–H stretching. On the other hand, the CH_2 vibrations are shown in different parts of the Raman spectrum, such as the asymmetric and symmetric stretching, at 2859–2936 cm^{-1}, and the twisting (1308 cm^{-1}), wagging (1375 cm^{-1}) and bending (1448 cm^{-1}) vibrations. Upon modification of the cellulose paper with the MIP, the amide I band of nylon-6 can be distinguished within the bands of cellulose (Fig. S1b, c and d). Moreover, the intensity of the band increased with the amount of nylon-6 and the number of dips, while the intensity of the cellulose bands decreased, thus confirming the functionalization of the papers with the MIPs. The MIP paper with 8.3 $mg \cdot mL^{-1}$ of nylon-6 and 1 dip was also characterized, however, the characteristic bands of the polymer were not distinguishable from the background signal of paper. This can be ascribed to the thin layer of polymer deposited, which was covering the internal pores of the paper and, therefore, was not available in the surface.

3.2. Evaluation of the selectivity of MIP papers

In order to evaluate the initial selectivity of the MIP papers, a comparative study vs. the NIP papers was carried out. 6-acetylmorphine (6-AM), which is the primary metabolite of heroin, one of the most addictive illicit drugs [40], was used. Fig. 1 depicts the comparison of the MIP papers and the NIP papers after extraction of

standard solutions of CO, MTA and 6-AM. The signal obtained in the case of 6-AM was so low that it was not distinguishable when compared to the signal of CO and MTA and, therefore, the Y axis had to be changed to a logarithmic scale. With this study, the selectivity of the MIP papers towards the template molecules was evaluated. However, further selectivity studies were carried out, as discussed below.

After the optimization, two comparative studies vs. the NIP papers were carried out in order to evaluate the final extraction ability and selectivity of the MIP papers. First, the extraction ability of the MIP paper was compared with that of the NIP paper in standard solutions of CO and MTA. As can be observed in Fig. 2a, the MIP paper possesses a higher adsorption ability due to the previous imprinting with the template molecules.

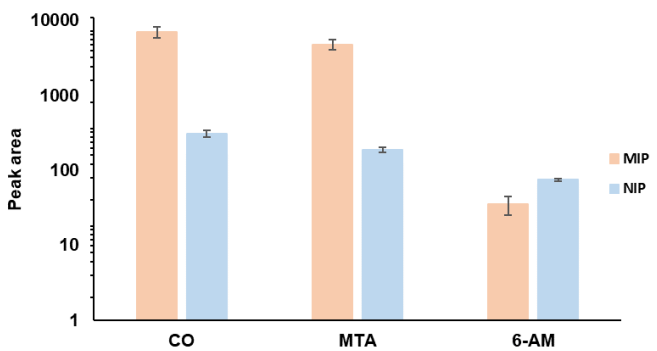

Figure 1. Preliminary evaluation of the selectivity of the MIP papers vs the NIP papers in a 25 $\mu g \cdot L^{-1}$ of cocaine, methamphetamine and 6-acetylmorphine. Results are expressed in a logarithmic scale since the signal of 6-AM was very low.

The adsorption ability of the MIP papers was also compared with that of the NIP papers in the sample matrix, diluted saliva. As can be observed in Fig. 2b, the adsorption ability of the MIP papers was higher than that of the NIP papers, however, when compared with standards, the signal of the MIP papers decreased significantly. This can be ascribed to the proteins present in the sample, which obstruct the

cavities and thereby hinder the extraction ability of the material.

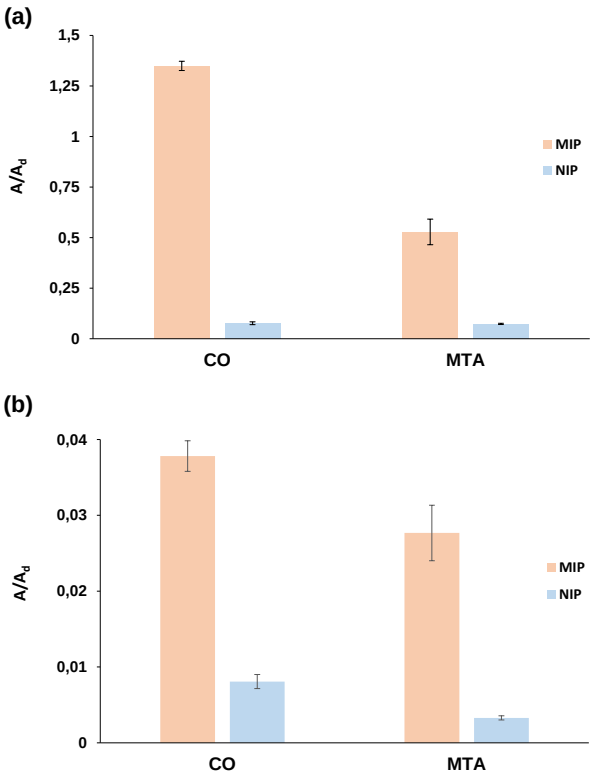

Figure 2. Studies of adsorption ability and selectivity of the MIP papers vs. NIP papers in (a) 100 μg·L^{-1} standard solutions of CO and MTA and (b) saliva samples spiked with 100 μg·L^{-1} of CO and MTA. Results are expressed as the relation between the areas of CO and MTA and their respective isotope-labelled IS of three independent measurements, and error bars illustrate the standard deviation of the corresponding mean value.

3.3. Effect of pH, dilution of the sample and ionic strength

The variables that could affect the final extraction ability of the MIP papers were evaluated following a univariate approach, namely pH, ionic strength and the dilution factor of the sample.

pH commonly affects those analytes with acid or basic functional sites modifying their form in solution and, therefore, affecting the interaction between the polymer chain and the analytes. For this reason, pH values between 3 and 12 were studied, showing an increasing signal up to pH 10, from which it decreased, as observed in Fig. S2a. These results were expected due to the alkaline character of both CO and MTA (pKa = 8.61 and 9.87, respectively). Furthermore, at this pH value, the functional groups of nylon-6 are also deprotonated (pKa = 5 and 9), thus allowing the interaction between the polymer and the analytes during the extraction process.

Saliva samples contain compounds, e.g., proteins, that can obstruct the cavities present in the MIP papers, and thus hinder their extraction ability. In order to avoid this problem, the dilution factor of the sample was evaluated by dilution of the sample in Milli-Q water up to 4 times, as can be observed in Fig. S2b. Although there is not a dramatic difference between the various dilution factors, the best results were obtained when the sample was diluted with the same amount of Milli-Q water (1:1).

The study of ionic strength is of high importance, since it affects the solubility of the analytes in solution and, therefore, their retention on the MIP papers. This variable was studied in the range from 0 to 100 $mg \cdot mL^{-1}$, however, the signal was dramatically affected by the presence of salts, and the best results were obtained when no salt was added (figure not shown). This can be ascribed to a diffusion problem of the molecules towards the cavities in the MIP papers. This effect was also observed in the case of saliva samples, since this media has a higher ionic strength than aqueous standards, along with other compounds that also hinder the extraction ability of the MIP papers, e.g., proteins.

3.4. Optimization of the extraction procedure

As previously mentioned, the different variables that could affect the final extraction ability of the MIP papers were studied. However, among all of them, the amount of nylon-6, number of dips and extraction time are intimately related, therefore it was

interesting the study of their interaction through a multivariate approach. Both the amount of nylon-6 and the number of dips affect the thickness of the coating, and thereby to the kinetics of the extraction. An excessively thick coating would difficult the diffusion of the analytes towards the cavities, and consequently, higher extraction times would be necessary.

The statistical significance of the effect of the main factors and their second-order interactions upon the adsorption ability for CO and MTA were evaluated by analysis of variance (ANOVA), reported in Tables S2 and S3. Considering the p-values of each model term, only the extraction time (X_3) and the quadratic (X_1^2 and X_3^2 for CO, and X_1^2 for MTA) terms significantly affect the analytical signal of CO and MTA and, therefore, their retention in the MIP papers. The analysis of the regression indicated the adequacy of the model since the p-values were equal to or greater than 0.05. Moreover, the p-value of the lack-of-fit test reveals the adequacy of the model as well.

Regarding the relation between the factors, the surface response plots for each response were built as a way to evaluate the interaction of the extraction time with the amount of nylon-6 and the number of dips. As can be observed in Figs. S3a and b, and Figs. S4a and b, at low extraction times, the adsorption ability was depleted compared to higher extraction times. This was expected since an increase in the extraction time allows the MIP papers to extract a higher amount of analyte. The interaction between the amount of nylon-6 and the number of dips was also evaluated, as depicted in Figs. S3c and S4c, however, it was not that significant since the number of dips was not particularly relevant, and can even affect negatively to the adsorption ability, as also observed in the main effects plot (Figs. S3d and S4d). This can be ascribed to the fact that is a layering process and, as each layer is deposited, the previous one is coated and the cavities are blocked, therefore leaving available only the cavities on the upper layer.

In addition, in Figs. S3d and S4d the effect of the different variables can be observed. The amount of nylon-6 (X_1) and the extraction time (X_3) affected positively to the

retention of the analytes in the MIP papers, being the extraction time the most significant, as already seen in the surface response plots. However, an excessive amount of nylon-6 affected negatively to the extraction of the analytes due to the increase of the thickness of the coating, which affects to the extraction kinetics, and thus the analytes cannot diffuse correctly. Furthermore, the effect of the number of dips (X_2) was not particularly relevant, as previously mentioned.

The desirability function approach provided the optimal conditions for the proposed model, being 8.3 $mg \cdot mL^{-1}$ of nylon-6 (X_1), 1 dip (X_2) and 45 min of extraction (X_3).

3.5. Application of the MIP papers for the determination of illicit drugs

The applicability of the MIP papers for CO and MTA determination was evaluated both with standards solutions and saliva samples. The optimized procedure was characterized in terms of sensitivity and precision. A calibration graph was built at seven concentration levels by extraction of CO and MTA from aqueous solutions in the range of 1 to 100 $\mu g \cdot L^{-1}$, the IS being at 20 $\mu g \cdot L^{-1}$, and plotting the relation between the areas of the analytes and the isotope-labelled IS versus the concentration (Fig. 3a). The straight fit functions enabled a R^2 of 0.9974 and 0.9953 for CO and MTA, respectively. The limits of quantification (LOQ), which were calculated using a signal to noise ratio (S/N) of 10, resulted to be 1 $\mu g \cdot L^{-1}$ for both analytes. The precision of the measurements was evaluated at a concentration level of 15 $\mu g \cdot L^{-1}$, obtaining a relative standard deviation (n = 3) of 5.6 and 4.9% for CO and MTA, respectively.

Furthermore, as previously mentioned, the MIP papers were also evaluated for the extraction of CO and MTA in saliva samples. Similarly to the previous one, a matrix matched calibration was built at six concentration levels by extraction of the analytes from diluted saliva samples spiked with the analytes in the range of 10 to 150 $\mu g \cdot L^{-1}$, containing the IS at 20 $\mu g \cdot L^{-1}$, and plotting the ratio of areas of CO and MTA and the isotope-labelled IS versus the concentration (Fig. 3b). Again, the

straight fit function enabled a R^2 of 0.9938 and 0.9931 for CO and MTA, respectively. The LODs and LOQs were obtained from a signal to noise ratio (S/N) of 3 and 10, respectively, affording values of 3 and 10 $\mu g \cdot L^{-1}$, in order, for both analytes. The relative standard deviation obtained from three replicates at a concentration of 50 $\mu g \cdot L^{-1}$ was 5.9 and 2.5% for CO and MTA, respectively.

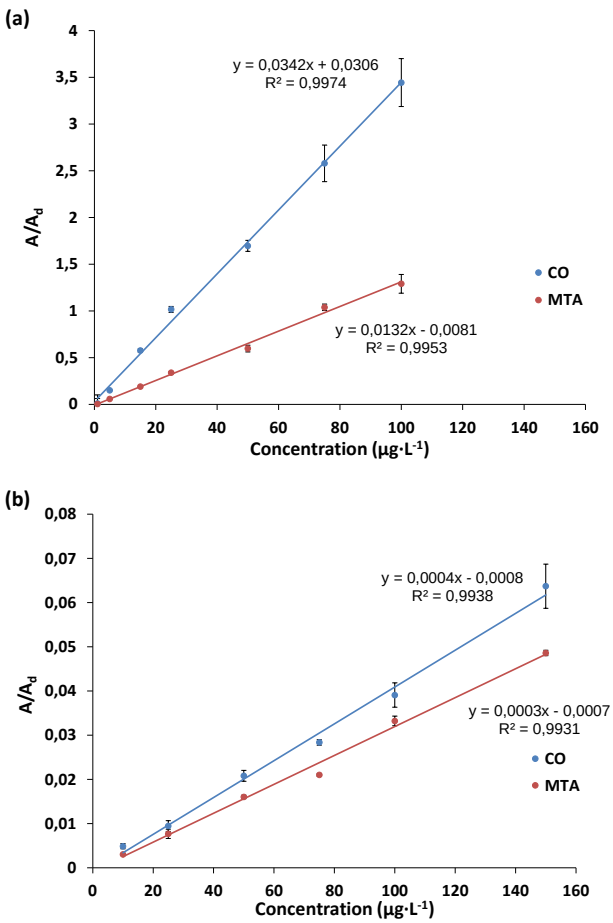

Figure 3. Relation of areas of CO and MTA and the isotope-labelled IS vs. concentration after extraction of the analytes from (a) aqueous standards and (b) diluted saliva samples. Each point represents the average of three independent measurements and error bars illustrate the standard deviation of the corresponding mean value.

If the slopes of the calibration graphs obtained for aqueous standards and spiked samples are compared, a matrix effect is easily observed. The accuracy of the matrix-matched calibration model was evaluated using an independent sample pool (different to that used for the calibration). Table 1 represents the recovery values calculated at three concentration levels employing the straight fit function of the matrix matched calibration graph, obtaining values between 84 and 98%. These results demonstrate that the matrix-matched calibration model can be used for the quantification of the drugs in real samples.

Table 1. Recovery values of diluted saliva samples

Spiked concentration ($\mu g \cdot L^{-1}$)	Recovery (%)	
	CO	MTA
25	91.2 ± 12.0	98.0 ± 12.5
75	94.7 ± 9.6	84.3 ± 3.6
150	96.2 ± 3.3	89.2 ± 3.3

4. Conclusions

This article describes the synthesis of a molecularly imprinted paper-based analytical device for the detection of cocaine and methamphetamine in saliva samples via mass spectrometry detection. The synthesis of the MIP was carried out following a procedure which avoids the polymerization process, thus facilitating the entire synthesis.

The potential of the MIP papers was compared to that of the nonimprinted ones, showing a better adsorption ability of the MIP papers in both aqueous standards and saliva samples. However, in the case of saliva, a decrease of the signal was observed due to the proteins present in the sample, which block the cavities of the MIP papers, thus hindering their extraction ability. Furthermore, the selectivity of the MIP papers was evaluated employing a different analyte, i.e., 6-acetylmorphine, resulting in a poor extraction, thus demonstrating the selectivity of the MIP papers

towards cocaine and methamphetamine.

The MIP papers were successfully employed for the detection of cocaine and methamphetamine in both aqueous standards and saliva samples, thereby demonstrating the suitability of MIP papers towards the templates. In addition, since the MIP is immobilized in common filter paper, the versatility of the material increases, considering that paper can be chemically modified and easily coupled to different techniques, while still being cost-effective.

The development of new strategies that allow rapid and reliable analysis is of high importance nowadays. The MIP papers synthesized in this work enable the determination of cocaine and methamphetamine in saliva samples in a relatively short time, taking into account that multiple extractions can be performed simultaneously. As previously mentioned, the determination of these drugs has been commonly carried out in different biological samples, namely blood [9,10], hair [1] or urine [11], thus requiring invasive collection or specialized personnel. However, the collection of saliva is an easy, painless and non-invasive procedure. Also, no sample pretreatment besides dilution and pH adjustment was needed in this work, unlike other methods already described [41], in which the sample is treated to remove interferents such as proteins. Furthermore, MIPs can be synthesized in the presence of multiple template molecules, thus resulting in a final material that can selectively extract more than one analyte, avoiding intricated modifications of the sorbents or special ones, such as packed sorbents [42], which are more expensive.

On the other hand, regarding other methods employing MIPs [11,43–45], this procedure avoids the polymerization reaction and its inherent rigorous experimental conditions, thus significantly simplifying the entire synthesis process, while still being comparable to these methods in terms of precision and limits of quantification.

Concerning reusability, the MIP papers employed in this work were not used more

than once. Since the synthesis method is cheap and simple, we preferred to obtain new MIP papers instead of cleaning and reusing the previous ones. This approach avoids cross-contamination and excessive handling of materials that have been in contact with biosamples. However, a study on the durability of the MIP papers would be very interesting to be able to obtain big batches of the material.

CRediT authorship contribution statement

M.C. Díaz-Liñán: Investigation, Writing - original draft. M.T. García-Valverde: Writing - original draft. R. Lucena: Conceptualization, Funding acquisition, Writing - review & editing. S. Cárdenas: Supervision, Funding acquisition, Writing - review & editing. A.I. López-Lorente: Conceptualization, Writing - review & editing.

Declaration of Competing Interest

The authors declare that they have no known competing financial interests or personal relationships that could have appeared to influence the work reported in this paper.

Acknowledgements

Financial support from the Spanish Ministry of Economy and Competitiveness (CTQ2017-83175R) is gratefully acknowledged.

Appendix A. Supplementary data

Supplementary data to this article can be found online at https://doi.org/10.1016/j.microc.2020.105686.

References

[1] V. Thibert, P. Legeay, F. Chapuis-Hugon, V. Pichon, Synthesis and characterization of molecularly imprinted polymers for the selective extraction of cocaine and its metabolite benzoylecgonine from hair extract before LC–MS analysis, Talanta. 88 (2012) 412–419, https://doi.org/10.1016/j.talanta.2011.11.009.

[2] E. Pimentel, K. Sivalingam, M. Doke, T. Samikkannu, Effects of Drugs of Abuse on the Blood-Brain Barrier: A Brief Overview, Front. Neurosci. 14 (2020), https://doi.org/10.3389/fnins.2020.00513.

[3] B.G. Schwartz, S. Rezkalla, R.A. Kloner, Cardiovascular Effects of Cocaine, Circulation. 122 (2010) 2558–2569, https://doi.org/10.1161/CIRCULATIONAHA.110.940569.

[4] F.S. Pelição, M.D. Peres, J.F. Pissinate, B.S. De Martinis, A One-Step Extraction Procedure for the Screening of Cocaine, Amphetamines and Cannabinoids in Postmortem Blood Samples, J. Anal. Toxicol. 38 (2014) 341–348, https://doi.org/10.1093/jat/bku039.

[5] T.R. Fiorentin, B.K. Logan, D.M. Martin, T. Browne, E.F. Rieders, Assessment of a portable quadrupole-based gas chromatography mass spectrometry for seized drug analysis, Forensic Sci. Int. 313 (2020), 110342, https://doi.org/10.1016/j.forsciint.2020.110342.

[6] I. Kohler, J. Schappler, S. Rudaz, Highly sensitive capillary electrophoresis-mass spectrometry for rapid screening and accurate quantitation of drugs of abuse in urine, Anal. Chim. Acta. 780 (2013) 101–109, https://doi.org/10.1016/j.aca.2013.03.065.

[7] D.N. Barreto, M.M.A.C. Ribeiro, J.T.C. Sudo, E.M. Richter, R.A.A. Muñoz, S. G. Silva, High-throughput screening of cocaine, adulterants, and diluents in seized samples using capillary electrophoresis with capacitively coupled contactless conductivity detection, Talanta. 217 (2020), 120987, https://doi.org/10.1016/j.talanta.2020.120987.

[8] A. Orfanidis, H. Gika, G. Theodoridis, O. Mastrogianni, N. Raikos, Development of a UHPLC-MS/MS method for the determination of 84 pharmaceuticals and drugs of abuse in human liver, J. Chromatogr. B. 1151 (2020), 122192, https://doi.org/10.1016/j.jchromb.2020.122192.

[9] S.U. Mokhtar, C. Kulsing, J.T. Althakafy, A. Kotsos, O.H. Drummer, P.J. Marriott, Simultaneous Analysis of Drugs in Forensic Cases by Liquid Chromatography–High-Resolution Orbitrap Mass Spectrometry, Chromatographia. 83 (2020) 53–64, https://doi.org/10.1007/s10337-019-03814-w.

[10] L. de, L.F. Lizot, A.C.C. da Silva, M.F. Bastiani, T.F. Maurer, R.Z. Hahn, M.S. Perassolo, M.V. Antunes, R. Linden, Simultaneous Determination of Cocaine and Metabolites in Human Plasma Using Solid Phase Micro-Extraction Fiber Tips C18 and UPLC–MS/MS, J. Anal. Toxicol. (2019), https://doi.org/10.1093/jat/bkz042.

[11] J. Sánchez-González, M.J. Tabernero, A.M. Bermejo, P. Bermejo-Barrera, A. Moreda-Piñeiro, Porous membrane-protected molecularly imprinted polymer micro-solid-phase extraction for analysis of urinary cocaine and its metabolites using liquid chromatography – Tandem mass spectrometry, Anal. Chim. Acta. 898 (2015) 50–59, https://doi.org/10.1016/j.aca.2015.10.002.

[12] L.F. Hofman, Human Saliva as a Diagnostic Specimen, J. Nutr. 131 (2001) 1621S–1625S, https://doi.org/10.1093/jn/131.5.1621S.

[13] S. Chojnowska, T. Baran, I. Wilińska, P. Sienicka, I. Cabaj-Wiater, M. Knaś, Human saliva as a diagnostic material, Adv. Med. Sci. 63 (2018) 185–191, https://doi.org/10.1016/j.advms.2017.11.002.

[14] F.T.S.M. Ferreira, R.B.R. Mesquita, A.O.S.S. Rangel, Novel microfluidic paper-based analytical devices (μPADs) for the determination of nitrate and nitrite in human saliva, Talanta. 219 (2020), 121183, https://doi.org/10.1016/j.talanta.2020.121183.

[15] T. Ozer, C. McMahon, C.S. Henry, Advances in Paper-Based Analytical Devices, Annu. Rev. Anal. Chem. 13 (2020) 85–109, https://doi.org/10.1146/annurevanchem-061318-114845.

[16] J. Ríos-Gómez, B. Fresco-Cala, M. García-Valverde, R. Lucena, S. Cárdenas, Carbon Nanohorn Suprastructures on a Paper Support as a Sorptive Phase, Molecules 23 (2018) 1252, https://doi.org/10.3390/molecules23061252.

[17] J.F. da, S. Petruci, A.A. Cardoso, Sensitive luminescent paper-based sensor for the determination of gaseous hydrogen sulfide, Anal. Methods 7 (2015) 2687–2692, https://doi.org/10.1039/C4AY02952F.

[18] J. Ríos-Gómez, R. Lucena, S. Cárdenas, Paper supported polystyrene membranas for thin film microextraction, Microchem. J. 133 (2017) 90–95, https://doi.org/10.1016/j.microc.2017.03.026.

[19] J. Li, Y. Zheng, W. Mi, T. Muyizere, Z. Zhang, Polystyrene-impregnated paper substrates for direct mass spectrometric analysis of proteins and peptides in complex matrices, Anal. Methods. 10 (2018) 2803–2811, https://doi.org/10.1039/C8AY01081A.

[20] R. Trouillon, M.A.M. Gijs, Paper-Based Polymer Electrodes for Bioanalysis and Electrochemistry of Neurotransmitters, ChemPhysChem. 19 (2018) 1164–1172, https://doi.org/10.1002/cphc.201701124.

[21] M.C. Díaz-Liñán, M.T. García-Valverde, A.I. López-Lorente, S. Cárdenas, R. Lucena, Silver nanoflower-coated paper as dual substrate for surface-enhanced Raman spectroscopy and ambient pressure mass spectrometry analysis, Anal. Bioanal. Chem. 412 (2020) 3547–3557, https://doi.org/10.1007/s00216-020-02603-x.

[22] M. Saraji, N. Mehrafza, Phenyl carbamate functionalized zinc oxide nanorods for paper-based thin film microextraction, RSC Adv. 7 (2017) 50210–50215, https://doi.org/10.1039/C7RA06061K.

[23] T.-T. Tsai, C.-Y. Huang, C.-A. Chen, S.-W. Shen, M.-C. Wang, C.-M. Cheng, C.-F. Chen, Diagnosis of Tuberculosis Using Colorimetric Gold Nanoparticles on a Paper-Based Analytical Device, ACS Sensors. 2 (2017) 1345–1354, https://doi.org/10.1021/acssensors.7b00450.

[24] N.A. Samah, M.-J. Sánchez-Martín, R.M. Sebastián, M. Valiente, M. López-Mesas, Molecularly imprinted polymer for the removal of diclofenac from water: Synthesis and characterization, Sci. Total Environ. 631–632 (2018) 1534–1543, https://doi.org/10.1016/j.scitotenv.2018.03.087.

[25] S. Zink, F.A. Moura, P.A. da, S. Autreto, D.S. Galvão, B. Mizaikoff, Virtually imprinted polymers (VIPs): understanding molecularly templated materials via molecular dynamics simulations, Phys. Chem. Chem. Phys. 20 (2018) 13145–13152, https://doi.org/10.1039/C7CP08284C.

[26] T.P.P. Mendes, I. Pereira, M.R. Ferreira, A.R. Chaves, B.G. Vaz, Molecularly imprinted polymer-coated paper as a substrate for highly sensitive analysis using paper spray mass spectrometry: quantification of metabolites in urine, Anal. Methods. 9 (2017) 6117–6123, https://doi.org/10.1039/C7AY01648D.

[27] N. Nuchtavorn, M. Dvořák, P. Kubáň, Paper-based molecularly imprinted interpenetrating polymer network for on-spot collection and microextraction of dried blood spots for capillary electrophoresis determination of carbamazepine, Anal. Bioanal. Chem. 412 (2020) 2721–2730, https://doi.org/10.1007/s00216-020-02523-w.

[28] Y. Akbulut, A. Zengin, A molecularly imprinted whatman paper for clinical detection of propranolol, Sensors Actuators B Chem. 304 (2020), 127276, https://doi.org/10.1016/j.snb.2019.127276.

[29] M.C. Díaz-Liñán, A.I. López-Lorente, S. Cárdenas, R. Lucena, Molecularly imprinted paper-based analytical device obtained by a polymerization-free synthesis, Sensors Actuators B Chem. 287 (2019) 138–146, https://doi.org/10.1016/j.snb.2019.02.048.

[30] Y. Geng, M. Guo, J. Tan, S. Huang, Y. Tang, L. Tan, Y. Liang, A fluorescent molecularly imprinted polymer using aptamer as a functional monomer for sensing of kanamycin, Sensors Actuators B Chem. 268 (2018) 47–54, https://doi.org/10.1016/j.snb.2018.04.065.

[31] W. Lu, J. Liu, J. Li, X. Wang, M. Lv, R. Cui, L. Chen, Dual-template molecularly imprinted polymers for dispersive solid-phase extraction of fluoroquinolones in water samples coupled with high performance liquid chromatography, Analyst. 144 (2019) 1292–1302, https://doi.org/10.1039/C8AN02133C.

[32] Y.-P. Duan, C.-M. Dai, Y.-L. Zhang, Ling-Chen, Selective trace enrichment of acidic pharmaceuticals in real water and sediment samples based on solid-phase extraction using multi-templates molecularly imprinted polymers, Anal. Chim. Acta. 758 (2013) 93–100, https://doi.org/10.1016/j.aca.2012.11.010.

[33] Y. Fan, G. Zeng, X. Ma, Multi-templates surface molecularly imprinted polymer for rapid separation and analysis of quinolones in water, Environ. Sci. Pollut. Res. 27 (2020) 7177–7187, https://doi.org/10.1007/s11356-019-07437-4.

[34] L.M. Madikizela, P.S. Mdluli, L. Chimuka, Experimental and theoretical study of molecular interactions between 2-vinyl pyridine and acidic pharmaceuticals used as multi-template molecules in molecularly imprinted polymer, React. Funct. Polym. 103 (2016) 33–43, https://doi.org/10.1016/j.reactfunctpolym.2016.03.017.

[35] C. Sun, J. Wang, J. Huang, D. Yao, C.-Z. Wang, L. Zhang, S. Hou, L. Chen, C.-S. Yuan, The Multi-Template Molecularly Imprinted Polymer Based on SBA-15 for Selective Separation and Determination of Panax notoginseng Saponins Simultaneously in Biological Samples, Polymers (Basel). 9 (2017) 653, https://doi.org/10.3390/polym9120653.

[36] M.T. García-Valverde, M.L. Soriano, R. Lucena, S. Cárdenas, Cotton fibers functionalized with β-

cyclodextrins as selectivity enhancer for the direct infusion mass spectrometric determination of cocaine and methamphetamine in saliva samples, Anal. Chim. Acta. 1126 (2020) 133–143, https://doi.org/10.1016/j.aca.2020.05.070.

[37] T.M. Annesley, Ion Suppression in Mass Spectrometry, Clin. Chem. 49 (2003) 1041–1044, https://doi.org/10.1373/49.7.1041.

[38] M.A. Bezerra, R.E. Santelli, E.P. Oliveira, L.S. Villar, L.A. Escaleira, Response surface methodology (RSM) as a tool for optimization in analytical chemistry, Talanta. 76 (2008) 965–977, https://doi.org/10.1016/j.talanta.2008.05.019.

[39] L. Vera Candioti, M.M. De Zan, M.S. Cámara, H.C. Goicoechea, Experimental design and multiple response optimization. Using the desirability function in analytical methods development, Talanta. 124 (2014) 123–138, https://doi.org/10.1016/j.talanta.2014.01.034.

[40] A.M.S. Kvello, J.M. Andersen, F. Boix, J. Mørland, I.L. Bogen, The role of 6-acetylmorphine in heroin-induced reward and locomotor sensitization in mice, Addict. Biol. 25 (2020), https://doi.org/10.1111/adb.12727.

[41] A.M. Ares, P. Fernández, M. Regenjo, A.M. Fernández, A.M. Carro, R.A. Lorenzo, A fast bioanalytical method based on microextraction by packed sorbent and UPLC–MS/MS for determining new psychoactive substances in oral fluid, Talanta. 174 (2017) 454–461, https://doi.org/10.1016/j.talanta.2017.06.022.

[42] A. Sorribes-Soriano, A. Monedero, F.A. Esteve-Turrillas, S. Armenta, Determination of the new psychoactive substance dichloropane in saliva by microextraction by packed sorbent – Ion mobility spectrometry, J. Chromatogr. A. 1603 (2019) 61–66, https://doi.org/10.1016/j.chroma.2019.06.054.

[43] M.P. Chantada-Vázquez, C. De–Becerra–Sánchez, A. Fernández–del–Río, J. Sánchez-González, A.M. Bermejo, P. Bermejo-Barrera, A. Moreda-Piñeiro, Development and application of molecularly imprinted polymer – Mn-doped ZnS quantum dot fluorescent optosensing for cocaine screening in oral fluid and serum, Talanta. 181 (2018) 232–238, https://doi.org/10.1016/j.talanta.2018.01.017.

[44] R.A. Bernardo, L.C. da Silva, M.E.C. Queiroz, B.G. Vaz, A.R. Chaves, Lab-made solid phase microextraction phases for offline extraction and direct mass spectrometry analysis: Evaluating the extraction parameters, J. Chromatogr. A. 1603 (2019) 23–32, https://doi.org/10.1016/j.chroma.2019.06.038.

[45] T. Bouvarel, N. Delaunay, V. Pichon, Selective extraction of cocaine from biological samples with a miniaturized monolithic molecularly imprinted polymer and online analysis in nano-liquid chromatography, Anal. Chim. Acta. 1096 (2020) 89–99, https://doi.org/10.1016/j.aca.2019.10.046.

SUPPORTING INFORMATION

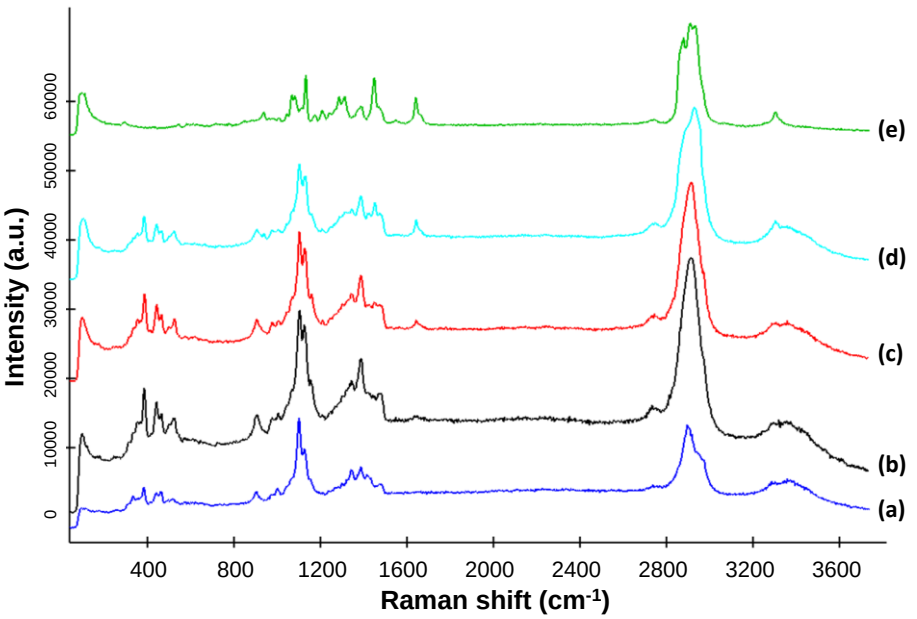

Figure S1. Raman spectra of (a) raw filter paper, (b) MIP paper with 8.3 mg·mL^{-1} of nylon-6 and 3 dips, (c) MIP paper with 15 mg·mL^{-1} of nylon-6 and 1 dip, (d) MIP paper with 15 mg·mL^{-1} of nylon-6 and 3 dips and (e) pure nylon-6.

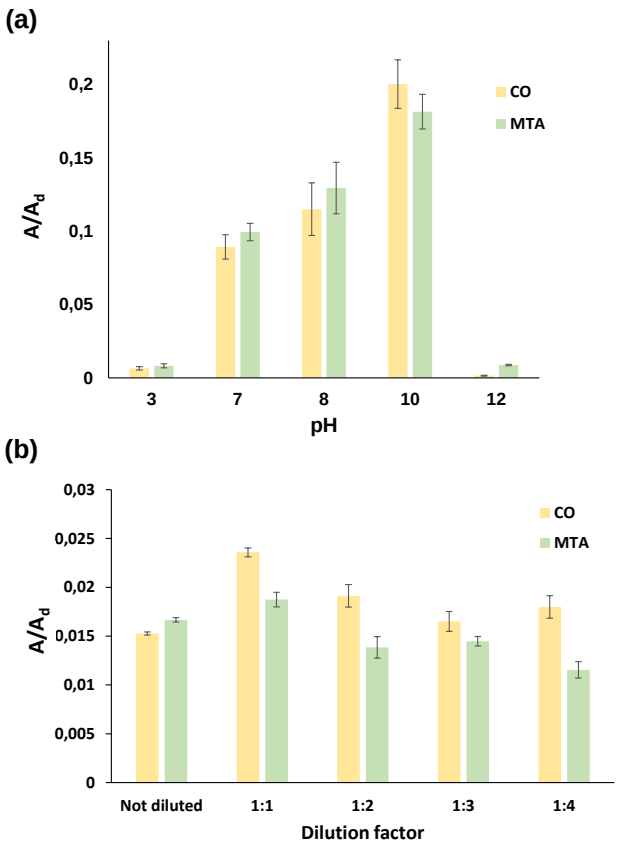

Figure S2. Study of the influence of (a) pH and (b) dilution factor after extraction from 25 and 50 µg·L^{-1} standard solutions, respectively. Results are expressed as the relation of peak areas of CO and MTA and their respective isotope-labelled IS of three independent measurements, and error bars illustrate the standard deviation of the corresponding mean value.

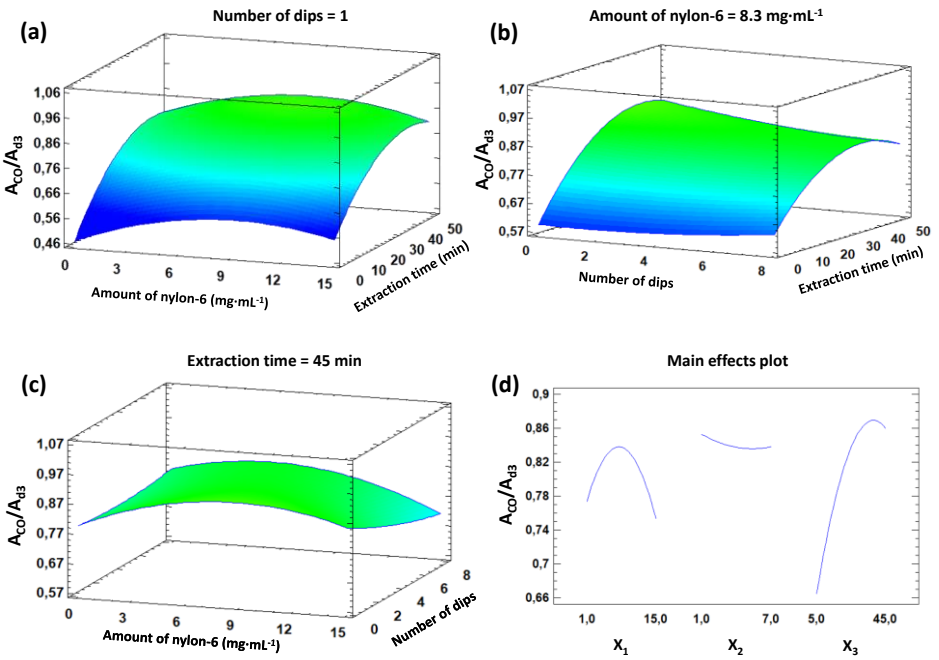

Figure S3. Response surface plots of the extraction of CO depending on the interaction of the variables (a) extraction time and amount of nylon-6 and (b) extraction time and the number of dips, (c) amount of nylon-6 and number of dips, and (d) main effects plot for each variable.

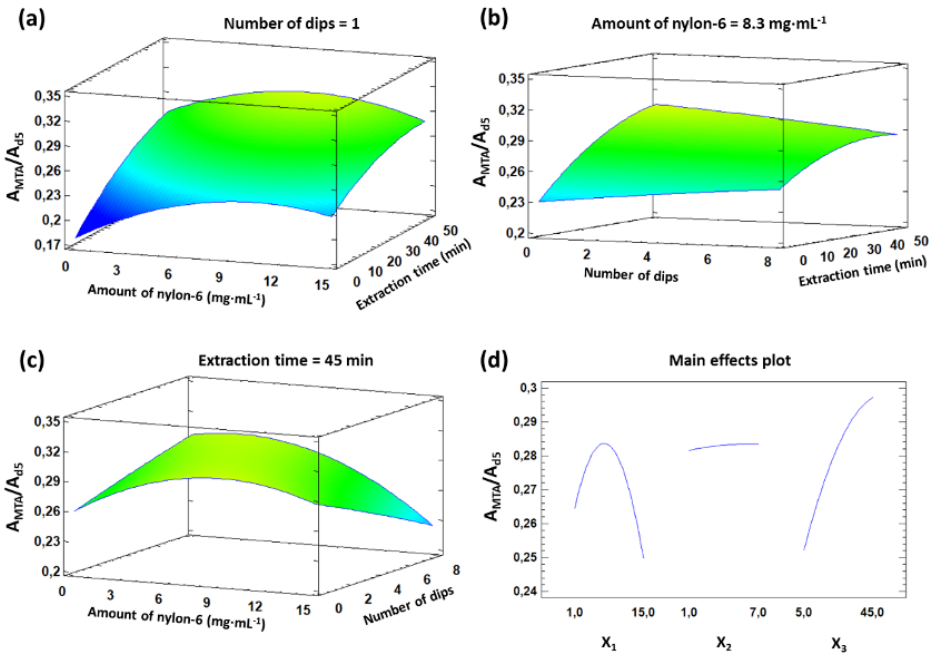

Figure S4. Response surface plots of the extraction of MTA depending on the interaction of the variables (a) extraction time and amount of nylon-6 and (b) extraction time and number of dips, (c) amount of nylon-6 and number of dips, and (d) main effects plot for each variable.

Table S1. SRM parameters of each analyte and the internal standards.

Analyte	Precursor ion ($[M+H]^+$ adduct) (m/z)	Product ions (m/z)	Fragmentor voltage (V)	Collision energy (V)	Collision cell accelerator voltage (CAV) (V)
CO	304.1	182.1	125	20	7
CO-d_3	307.1	85.2	140	34	7
MTA	150.2	91.2	80	20	7
MTA-d_5	155.1	92.1	100	18	7
6-AM	328.1	165.1	155	40	7

Table S2. Analysis of variance of the RSM of cocaine.

Source	Coefficients	Sum of squares	Df	Mean square	F-value	p-value
X_1	0.0288825	0.00159454	1	0.00159454	0.32	0.6030
X_2	0.0074447	0.000848748	1	0.000848748	0.17	0.7019
X_3	0.0159393	0.152018	1	0.152018	30.30	0.0053
X_1^2	-0.00150028	0.0399082	1	0.0399082	7.95	0.0478
X_1X_2	-0.00118448	0.00494973	1	0.00494973	0.99	0.3768
X_1X_3	-0.0000626508	0.00061546	1	0.00061546	0.12	0.7438
X_2^2	0.00087203	0.000454858	1	0.000454858	0.09	0.7783
X_2X_3	-0.000294916	0.00250489	1	0.00250489	0.50	0.5188
X_3^2	-0.000187695	0.041625	1	0.041625	8.30	0.0450
Lack-of-fit		0.109643	15	0.00060927	1.46	**0.3876**

X_1, X_2 and X_3 refer to amount of nylon-6 ($mg \cdot mL^{-1}$), number of dips and extraction time (min), respectively.

Table S3. Analysis of variance of the RSM of methamphetamine.

Source	Coefficients	Sum of squares	Df	Mean square	F-value	p-value
X_1	0.0119498	0.000853494	1	0.000853494	1.93	0.2370
X_2	0.00997942	0.000012779	1	0.000012779	0.03	0.8732
X_3	0.00298963	0.00804242	1	0.00804242	18.19	0.0130
X_1^2	-0.000528888	0.00495961	1	0.00495961	11.22	0.0286
X_1X_2	-0.000816545	0.00235228	1	0.00235228	5.32	0.0823
X_1X_3	-0.0000505921	0.000401339	1	0.000401339	0.91	0.3946
X_2^2	0.0000702752	0.000002954	1	0.000002954	0.01	0.9388
X_2X_3	-0.000103478	0.000308383	1	0.000308383	0.70	0.4506
X_3^2	-0.0000209998	0.000521049	1	0.000521049	1.18	0.3387
Lack-of-fit		0.00913905	15	0.00060927	1.38	**0.4119**

X_1, X_2 and X_3 refer to amount of nylon-6 ($mg \cdot mL^{-1}$), number of dips and extraction time (min), respectively.

BLOQUE IV

PAPEL MODIFICADO CON NANOPARTÍCULAS

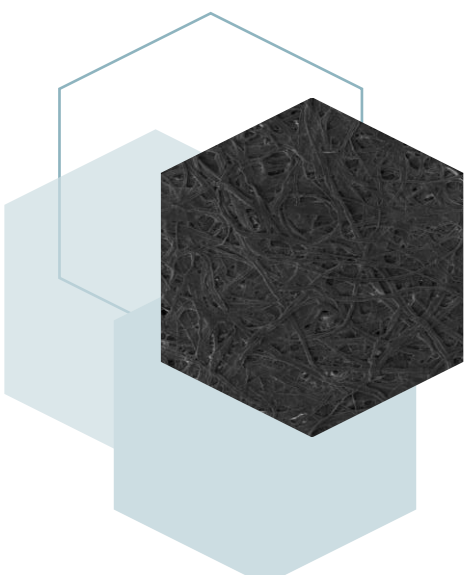

El empleo de nanomateriales como sorbentes, o componentes de fases sorbentes, ha supuesto una revolución en la etapa de tratamiento de muestra. Los nanomateriales presentan una serie de ventajas con respecto a algunos sorbentes tradicionales que los hacen muy útiles en esta etapa. Su elevada área superficial, la variedad de nanomateriales diferentes (en forma y composición) y la posibilidad de su modificación superficial con diferentes grupos son las ventajas más destacadas.

Las nanopartículas de metales nobles, como las nanopartículas de oro o de plata, han despertado gran interés en los últimos años debido a sus múltiples ventajas. Por un lado, cabe destacar su gran área superficial, facilidad de obtención, así como su estabilidad prolongada y biocompatibilidad. Además, debido a sus características ópticas, como la resonancia del plasmón superficial, estas nanopartículas han sido muy utilizadas en técnicas espectroscópicas como la espectroscopia Raman amplificada en superficie, donde son capaces de aumentar la señal Raman en varios órdenes de magnitud, mejorando así la sensibilidad de la técnica [1].

El empleo de estos nanomateriales inmovilizados en sustratos supone una ventaja, debido a que aumentan su estabilidad al evitar que se agreguen y pierdan su tamaño nanométrico y, por tanto, las propiedades que los caracterizan. Por tanto, en este Bloque de la memoria de la Tesis Doctoral, se hace una introducción previa sobre el uso de membranas modificadas con nanopartículas, desde los distintos formatos de membranas hasta las diferentes formas de modificación con nanomateriales que se han utilizado en los últimos años **(Capítulo 6).** Por otro lado, se describe la síntesis de un papel de filtro modificado con nanoflores de plata como sustrato para la determinación de ketoprofeno en muestras de saliva mediante espectroscopia Raman y espectrometría de masas en la modalidad de *paper-spray* **(Capítulo 7)**, donde las nanoflores de plata jugaron un papel esencial en la mejora de la sensibilidad de ambas técnicas.

[1] A.I. López-Lorente, Recent developments on gold nanostructures for surface enhanced Raman spectroscopy: particle shape, substrates and analytical applications. A review, Anal. Chim. Acta 1168 (2021) pp. 338474.

Capítulo 6

Particle loaded membranes

Solid-Phase Extraction, Chapter 12 (2020) 341-354
(Capítulo de libro)

Solid-Phase Extraction
Handbooks in Separation Science
(2020) 341-354

Particle loaded membranes

M. C. Díaz-Liñán, A. I. López-Lorente, R. Lucena, S. Cárdenas

Departamento de Química Analítica, Instituto Universitario de Investigación en Química Fina y Nanoquímica IUNAN, Universidad de Córdoba, Campus de Rabanales, Edificio Marie Curie, E-14071 Córdoba, Spain

1. Introduction

Membranes have been extensively used at the industrial scale as, in general, they act as physical barriers which, based on permeability or size cut-off criteria allow the transfer of gas, liquid, or particulate material between two, usually miscible, phases. Therefore, the membrane can participate as an active or passive element with a common role in facilitating the contact of both phases at the membrane interface.

Membranes are employed in sample treatment, either for analyte preconcentration or sample cleanup. Moreover, they can be used in the microextraction context to prevent damage or blockage of the sorbent phase when dirty samples are processed. A paradigmatic example is hollow fiber protected liquid phase microextraction [1]. No doubt, the most interesting application is the use of membranes for analyte enrichment. In this case, target compounds migrate from the sample matrix to the membrane by a chemical, pressure, or electrical field gradient [2]. The so-called hollow fiber liquid phase microextraction (HF-LPME) is identified as a reference technique in microextraction [3]. It can be used in the two-phase (2D) or three-phase (3D) modes. 2DHF-LPME uses two immiscible phases, with the extractant

located in the lumen of the fiber. In 3D-HF-LPME the sample and the extractant are miscible (generally aqueous) while the pores of the HF are filled with an organic solvent or solution. The analytes are first extracted into the organic phase, and then transferred to the aqueous solution inside the HF. A chemical mechanism, usually a pH gradient, is used to avoid the reextraction of the analytes to the external aqueous matrix.

However, the advantages of using planar formats, mainly related to the higher surface area that can be exposed to the sample, have gained recognition in recent years. Therefore, to increase both the variety of chemistries available for extraction and the membrane capacity and selectivity, there is great interest in developing membranes incorporating nanoparticles and nanostructures. The potential of these materials in solid-phase microextraction is well-known [4]. These outstanding properties, however, are dramatically decreased if the nanoscale is lost. This is common for hydrophobic nanoparticles, especially carbon-based nanoparticles.

To avoid this inconvenience, carbon nanoparticles are either dispersed in a micellar media or immobilized on a solid surface. The addition of nanoparticles into a membrane is a synergic combination as, on the one hand aggregation is avoided and, on the other, new capabilities including higher surface area are conferred to the membrane. A clear precursor of this concept is disks-based solid-phase extraction, where the sorbent phase is placed in a planar element to minimize channeling during sample processing steps. In addition, higher flow rates can be used, thus allowing the preconcentration of large sample volumes in a reasonable time. If a low eluent volume is used, the enrichment factor that can be achieved leads to improved method sensitivity. There are many membrane formats which can be loaded with (nano)particles, namely planar and hollow fiber membranes, and membranes fabricated via electrospinning and thin films, among others.

This chapter provides an overview of the use of particle-loaded membranes in sample treatment. The first section describes the classical approach using membrane formats with a hollow fiber or planar geometry. In the second part, the

potential of thin film microextraction as an extension of the particle-loaded membrane concept is described.

2 Membranes modified with nanoparticles

2.1 Hollow fiber membranes

Polypropylene hollow fibers (HF) provide an excellent support for the confinement of the extraction solvent in either 2D or 3D formats. However, considering the small dimensions of HF microextraction units, and thus the small volume of extraction solvents, in the low microliter range, the efficiency of the process can be jeopardized. If an HF is intended to be used in micro solid phase extraction, a similar limitation would appear unless highly efficient sorbents, such as nanostructured solids, are used.

Carbon nanoparticles in general, and carbon nanotubes (CNTs) in particular, are by far the preferred nanomaterials for the construction of so-called reinforced HF on account of their outstanding sorbent capacity. These nanoparticles can be held in the lumen or immobilized into the pores of the HF, which eliminates the aggregation typically observed in other micro solid phase extraction formats, such as dispersive extraction techniques. The location of the CNTs inside the HF usually requires the preparation of a composite material using sol-gel technology. Eshaghy *et al.* prepared an organic/inorganic polymer containing oxidized multiwalled carbon nanotubes (o-MWNTs) in which orthosilicate was used as precursor and HCl as catalyst, for the *in situ* gelation inside the HF [5]. The reinforced-HF was immersed directly into the sample solution for the extraction, and the porosity of the HF allows fast resorption of the analytes. The fiber also prevents large molecules from reaching and diminishing the adsorption capacity of the extraction phase for the analytes. The fiber was discarded after each extraction. A simplification of this procedure was proposed by Song *et al.* by replacing the sol-gel approach with a surfactant hexadecyltrimethylammonium bromide (CTAB) [6]. No interference was observed for the extraction of carbamate pesticides from fruits [6] or strychnine and

brucine in clinical samples [7].

If CNTs are dispersed in a liquid phase, the sealing of the fiber end is required to avoid material losses [8]. As an alternative, the dispersion of the CNTs either in 1-octanol [9] or water [10] can be added to HF, and external energy (ultrasounds or pressure) used to force the nanomaterial into the wall pores of the HF. In this case, a sort of CNTs-supported liquid membrane is obtained. The role of the CNTs is to increase the surface area of the extraction phase and also to increase the partition constant, especially if a 3D configuration is used.

Concerning other carbon nanoparticles, Jiménez-Soto *et al.* evaluated the use of oxidized single-walled carbon nanohorns (o-SWNHs) as the sorbent phase for 2D reinforced HF microextraction [11]. SWNHs are conical-ended carbon nanoparticles of smaller dimensions than CNTs capable of generating stable aggregates with a dahlia shape. These aggregates are still in the nanometric range (less than 100 nm diameter) and therefore maintain the extraction capacity associated with the nanoworld. The o-SWNHs were immobilized on the pores of the HF. An inserted stainless steel wire maintains the rigidity of the fiber allowing its direct immersion in the sample. Triazine herbicides were determined in waters with a sensitivity comparable to, or better than, other microextraction approaches designed for the same analytical problem. It was possible to reuse the fiber up to 30 times. Graphene (G), or its oxidized form (GO), exhibits an enhanced adsorption capacity for many compounds. Graphene was used as a dispersion in 1-octanol in the lumen of an HF membrane for the extraction of carbamate pesticides with better detection limits than those provided when CNTs were used [12]. GO is more suitable for the extraction of inorganic ions and was used for the extraction of heavy metals from waters by a hollow fiber membrane containing a composite adsorbent prepared from GO nanoparticles and silica. The hydrophilic interactions (electrostatic and coordination) that can be established between the oxygenated groups and the metals were identified as the driving force of the extraction [13].

2.2 Planar membranes

This section is focused on planar membranes modified with (nano)particles. Most of the functionalized membranes described within this section are commercially available and based on different polymers (e.g., nylon, poly(ethylene terephthalate) (PET), poly(vinylidene fluoride) (PVDF), among others), in which the particles have been incorporated via different routes, for example, dip coating, drop-casting directly on the membrane or after a membrane functionalization, that is, amino, carboxylic, etc. Different types of (nano)particles can be loaded onto the membranes, such as metal nanoparticles (Au, Ag, Pd, etc.) as well as some semiconductor nanoparticles (SiO_2, Al_2O_3, etc.) In addition, carbon nanomaterials have also been used as membrane coatings.

The incorporation of (nano)particles into membranes can respond to two general needs: (i) improvement of the adsorption/filtration process; and (ii) assist in the subsequent elution and/or detection procedure. For example, nanoparticles can provide interaction sites due to their affinity toward the analyte. In this regard, nylon membranes impregnated with metallic nanoparticles, namely Au and Ag, have been used for the solid phase extraction of Hg by filtration of the water through the membrane [14]. The large surface area of the nanoparticles is responsible for the high efficiency adsorption of Hg into the membrane. Also, Pd nanoparticles have been deposited by dip coating on pore walls of carboxylic and amino group functionalized poly(ethylene terephthalate) membranes [15]. The functionalization was critical for the subsequent immobilization of the Pd nanoparticles (Fig. 1). These membranes were used in hydrogen separation and sensing. Furthermore, nanosilica extracted from rice straw was combined with a polyether-polyamide block copolymer (PEBA) to form a nanocomposite polymeric membrane for the separation of CO_2 in gas streams [16]. Huang *et al.* prepared PVDF/SiO_2 hybrid membranes by a sol-gel process for the preconcentration of fennel oil from herbal water extracts [17]. The presence of SiO_2 nanoparticles combined with PVDF resulted in an improvement of the thermal and mechanical properties of the

membrane. Zhang *et al.* [18] developed a micro-solid phase extraction method for food colorants based on the impregnation of a nylon filter membrane with Al_2O_3 NPs. The performance of the Al_2O_3 NPs was compared with SiO_2 and TiO_2 NPs and conventional sorbents such as octadecylsiloxane-bonded silica for the extraction of tartrazine and Sunset yellow in food. The membrane impregnated with Al_2O_3 NPs exhibited the best extraction efficiency. In addition, solid phase micromembrane tip extraction using 1-butyl-3-methylimidazole iron nanoparticles enclosed within a membrane followed by chiral liquid chromatography was used to evaluate the stereoselective interactions of profens with proteins [19], as well as for the analysis of vitamin B in human plasma [20].

Wang *et al.* prepared a "pH-paper-like" chip for the enrichment and detection of organic pollutants[21]. The chip was composed of a PVDF membrane with a polydopamine (PDA) film and AuNPs. Each component of the chip membranes has a specific role, the PVDF membrane and PDA facilitating the adsorption of organic analytes via hydrophobic interactions and π- π stacking, while AuNPs facilitated the subsequent quantification of the analytes via surface-assisted laser desorption/ionization time-of-flight mass spectrometry.

Metallic NPs are used extensively as a substrate in surface enhanced Raman spectroscopy (SERS) due to their capability to enhance the Raman signal. Typical substrates are based on rigid solid materials such as silicon, glass, etc.; however, recently SERS active membranes based on flexible materials have also been described. For example, liquid-crystal polymer (LCP) textile fibers decorated with AgNPs supported by a polyamide filter were used for the extraction and detection of the pesticide thiram [22]. This is an example of the role of metal nanoparticles on the subsequent detection step. Nevertheless, the NPs can play a dual role by supplying additional interaction sites for adsorption of the analytes, for example, via the binding affinity of gold toward sulfur or silver toward amine groups. Granger *et al.* developed a SERS-based point-of-need diagnostic test for alphafetoprotein (AFP) screening using solid phase microextraction membranes with functionalized AuNPs

as Raman enhancer and selective tag for capturing AFP [23]. This field is very extensive and a more detailed description would go beyond the scope of this chapter [24]. However, particle-loaded membranes are expected to have a significant impact on the coupling of extraction with Raman and related detection methods. As well as optical sensors, metallic NPs loaded membranes are used in electrochemical devices, for example, AuNPs formed *in situ* in a polymer inclusion membrane were used for the electrode immobilization of anti-Salmonella antibodies [25].

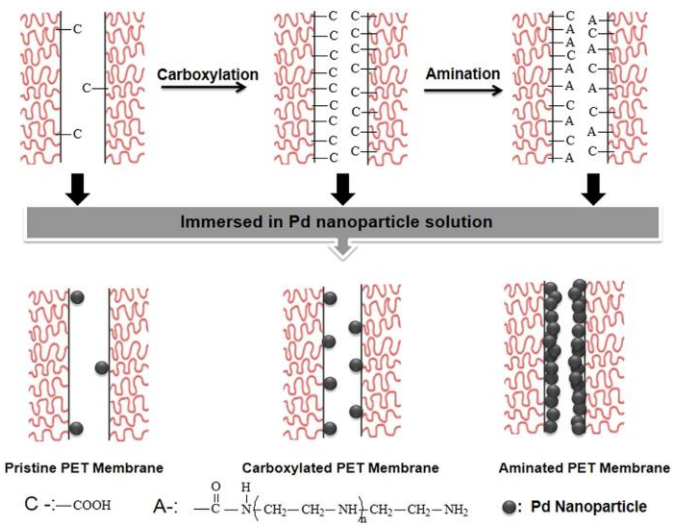

Figure 1. Scheme of the functionalization process of the poly(ethylene terephthalate) membrane with carboxylic and amino groups and their effect on the immobilization of Pd NPs. Reproduced from Awasthi K, Choudhury S, Komber H, Simon F, Formanek P, Sharma A, *et al.* Functionalization of track-etched poly (ethylene terephthalate) membranes as a selective filter for hydrogen purification. Int J Hydrogen Energy 2014;39:9356e9365 with permission from Elsevier.

Dispersions of MWCNTs and single layer graphene (SLG) nanoparticles have been incorporated into cellulose triacetate polymer matrix membranes [26]. The membranes are prepared via drop-casting of a cellulose triacetate (CTA) polymer matrix and carbon nanomaterials dispersed in dichloromethane on a flat glass

surface. Carbon nanomaterials enable the extraction of aromatic compounds, for example, polycyclic aromatic hydrocarbons in sewage pond water samples.

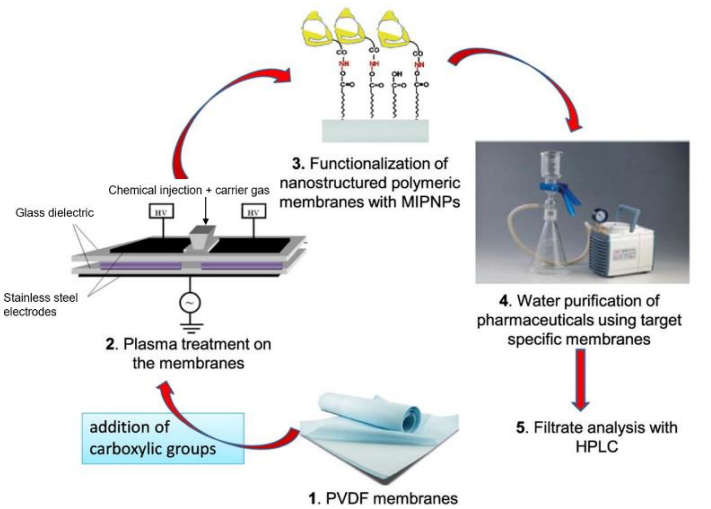

Figure 2. Development of functionalized nanostructured polymeric membranes with MIPNPs from PVDF membranes for water purification of pharmaceuticals and subsequent HPLC analysis. Reproduced from Altintas Z, Chianella I, Ponte GD, Paulussen S, Gaeta S, Tothill IE. Development of functionalized nanostructured polymeric membranes for water purification. Chem Eng J 2016;300:358e366 with permission from Elsevier.

One of the challenges to overcome in membrane-based extraction is the specific recognition properties of the membranes as well as their permeation performance. This led to the development of molecularly imprinted membranes (MIMs), which combine molecularly imprinted polymers with membrane separation techniques. Altintas *et al.* reported the fabrication of MIMs as filters coupled to SPE for the evaluation of water purification processes [27]. MIMs were formed by molecularly imprinted polymer nanoparticles (MIPNPs) toward pharmaceuticals, which were applied onto plasma-treated PVDF membranes (see Fig. 2). In addition, the synthesis of molecularly imprinted nanocomposite membranes (MINCMs) has also

been described [28]. Nanocomposite membranes were prepared by infiltrating the functional monomer modified with the NPs onto a polydopamine-modified regenerated cellulose membrane, followed by an imprinting procedure. Imprinted PDA@SiO_2 MINCMs for the selective extraction of m-cresol was reported in which the high surface-to-volume ratio and, thus, the large surface area of the SiO_2 nanoparticles played an important role in the extraction of the target analyte [29].

3 Particle-loaded membranes in a thin film microextraction format

Thin film microextraction (TFME) is a miniaturized sample preparation technique where a flat film of a high surface area-to-volume ratio is used as the extraction phase [30]. Originally proposed in 2001 [31], as an alternative approach to in-fiber SPME, it has continued to evolve with an expanding number of applications. Among the proposed formats, this chapter is focused only on thin films modified with nanoparticles in a membrane configuration generally prepared by dip coating and electrospinning techniques. Readers interested in different coating technologies, theoretical aspects, and applications are referred to more detailed reviews [30,32].

3.1 Nanoparticle-loaded membranes synthesized via electrospinning

Electrospinning is a simple, versatile, and widely used technique to synthesize fibrous materials with a variety of diameters, morphologies, and compositions. Briefly, the electrospinning technique consists of a viscous polymeric solution to which a high voltage is applied, after which the charged polymer ejects from the solution toward the collector wire as a fibrous filament [33]. This phenomenon is based on the repulsive electrostatic force that overcomes the surface tension of the polymer when the high voltage is applied. Different electrospinning procedures, for example, magnetic field-assisted electrospinning, melt electrospinning, or bilayer electrospinning, have been described for the synthesis of nanofibers [34].

An advantage of electrospinning is that the resulting material can be deposited uniformly on a flat surface, thus forming a thin film suitable as an extraction material

for TFME or SPME, among others. Moreover, the resulting fibers possess a high surface area, porous structure, and flexibility, desirable for extraction techniques [35]. Sometimes, the electrospinning process is followed by secondary steps, such as reactions for surface modification and other procedures.

The incorporation of nanomaterials into electrospun fibers affords different characteristic properties compared with the starting materials; in particular, the surface area-to-volume ratio related to the adsorption capacity and in specific cases the adsorption selectivity. For instance, among magnetic nanoparticles, Fe_3O_4 nanoparticles have acquired special attention in the electrochemical field due to their unique properties, such as excellent conformation stability, better contact between a biocatalyst and its substrate, ease of preparation, and large surface area, among others [36].

The incorporation of nanoparticles into the fiber structure can be carried out by different procedures. Fig. 3 illustrates two methods employed to immobilize nanoparticles in electrospun nanofibers, that is, dispersing the nanoparticles into the precursor solution of the polymer or through a chemical procedure in which the fibers are modified to immobilize the nanoparticles into its structure. Both approaches will be discussed in this section.

3.1.1 One pot synthesis of electrospun fibers with embedded nanoparticles

This approach is the fastest and easiest way to incorporate nanomaterials into electrospun fibers. It consists of the addition of the nanoparticles into the solution of monomers, prior to polymerization. When the nanoparticles are dispersed in the precursor solution of the polymer, they are easily incorporated to the fibers compared to the chemical modification of the fibers with the nanoparticles after electrospinning [34]. Bagheri *et al.* synthesized electrospun poly(butylene terephthalate) (PBT) nanofibers with embedded magnetic nanoparticles for the isolation of triazines [37]. The inorganic nanoparticles increased the surface area and porosity of the sorbent, thus leading to higher extraction efficiency.

Furthermore, since these nanoparticles have magnetic properties, the nanofibers could be easily isolated from solution by an external magnet once the microextraction is complete.

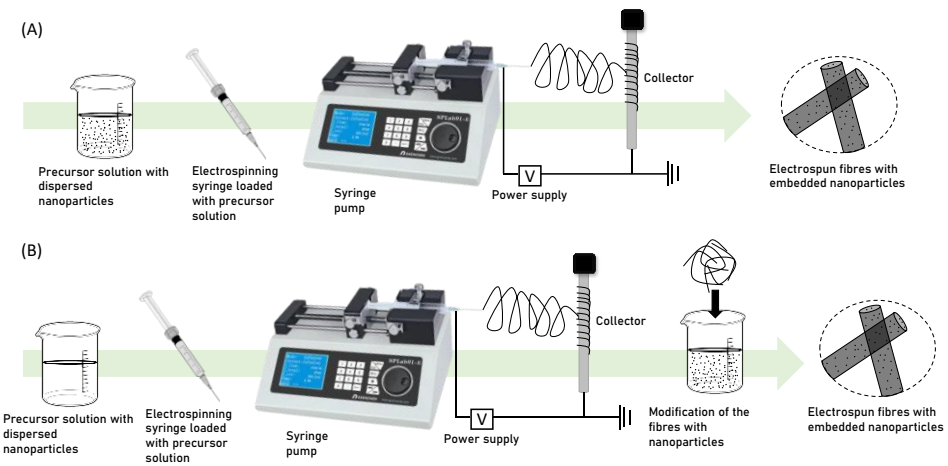

Figure 3. Scheme of the alternatives employed to synthesize electrospun fibers with embedded nanoparticles (A) by dispersing the nanoparticles into the precursor solution and (B) by chemical modification of the electrospun fibers and immobilization of nanoparticles.

Although electrospinning provides long synthetic fibers, these can be organized into a membrane format, especially useful for TFME. Liu and Xu obtained electrospun polystyrene/metal-organic frameworks-199 (PS/MOF-199) nanofiber film for TFME of aldehydes in human urine [38]. For the collection of the nanofiber, aluminum foil was employed. MOFs properties, such as tunable pore size, high surface area, and good thermal stability, enhanced the extraction efficiency of the PS/MOF-199 nanofiber film, compared with poly(styrene) films and an MOF-199 coated mesh. Furthermore, no loss of MOF-199 nanoparticles was found during the microextraction procedure, which demonstrates the enhanced mechanical stability of the material. Aldehydes were selected as model analytes, since they are

considered to be potential biomarkers of lung cancer. Thus, this method was successfully applied for the determination of aldehydes in urine samples of eight healthy subjects and seven lung cancer patients. Wu *et al.* synthesized nanofibrous membranes with multianalyte selectivity by encapsulating two types of molecularly imprinted polymer nanoparticles (MIPNPs) into electrospun poly(vinyl alcohol) nanofibers for the simultaneous extraction of bisphenol A and tebuconazole in vegetable and juice samples [39]. Nanofibrous molecularly imprinted membranes (nano-MIMs) retain the advantages of MIP-NPs, such as high molecular selectivity, high binding capacity, and fast binding kinetics, attributed to the large surface-to-volume ratio and the high number of recognition sites at the surface of the core-shell material. In addition, due to their geometric features MIP-NPs provide better accessibility to recognition sites for the analyte as well as lower mass-transfer resistance [40]. The combination of different MIP-NPs resulted in the selective extraction of both analytes from complex food samples.

3.1.2 Chemical modification to immobilize nanoparticles in electrospun fibers

He *et al.* prepared polyaniline coated silica nanofibers (PANI/SiO_2) by combining electrospinning with *in situ* polymerization for the extraction of fluoroquinolones from honey [41]. After electrospinning of the silica nanofibers, aniline monomers were polymerized on the surface of the electrospun fibers. The extraction procedure was carried out by packing PANI/SiO_2 nanofibers in a syringe. When combining silica nanofibers with PANI nanoparticles, the aggregation problems of PANI particles are eliminated, thus obtaining a uniform coating of PANI nanoparticles on the surface of the silica fibers. Morillo *et al.* developed PAN nanofibers to which superparamagnetic iron oxide nanoparticles (SPION) were fixed after hydrolysis of the electrospun fibers [42]. Nonhydrolyzed PAN fibers resulted in a low fixation of nanoparticles compared with the hydrolyzed fibers. The PAN-modified fibers were used for the removal of As(V) from wastewater. Liu *et al.* prepared a composite membrane from poly(vinyl alcohol)/poly(acrylic acid)/carboxyl-functionalized

graphene oxide (GO) modified with silver nanoparticles (PVA/PAA/GO-COOH@AgNPs) for the catalytic degradation of the dye methylene blue [43]. Electrospun fibers containing graphene oxide were impregnated with silver nanoparticles by treatment with a silver nitrate solution containing ascorbic acid. The PVA/PAA/GO-COOH@AgNPs nanocomposite showed a significantly enhanced performance for the elimination of model dyes.

3.1.2.1 Nanoparticles in paper-based coated sorptive phases

The use of paper, a cellulose-based support, to fabricate thin film microextraction units is a low-cost and reliable alternative. Due to its porosity, it is typically employed for filtration purposes. The raw paper is, in general, incompatible with its immersion in liquid phases. However, if it is covered by a polymeric layer, a flexible and resistant device is obtained. As a general procedure, a piece of paper is immersed in a solution of the extraction phase (polymer), and after a number of dipping cycles, the polymeric layer is generated after solvent evaporation. Ríos-Gómez *et al.* demonstrated that changing the dipping direction ensures a homogeneous distribution of the polymer (in this case polystyrene) which resulted in improved reproducibility for microextraction [44]. In this case, the polystyrene film was placed in a 100 mL pipette tip for the extraction of methadone from water. Zinc oxide nanorods have been synthesized onto paper by repeated immersion into a precursor solution. The functionalized extractant phase was used for the isolation of phenylurea herbicides from water [45].

The mechanical stability of the coating is the main challenge to overcome when NPs are used in the fabrication of paper-based sorptive phases. The nanomaterial must remain in the coating during the whole extraction process to obtain reproducible extractions. The inclusion of NPs in a polymeric network can be obtained by a simple solvent exchange [46,47]. Ríos-Gómez *et al.* synthesized a paper-based phase with photocatalytic activity by this approach [48]. A segment of paper is immersed in a dispersion consisting of a polyamide dissolved in formic acid to which TiO_2 NPs are

subsequently added. Evaporation of the solvent induces the precipitation of the polyamide embedding the NPs in the polymeric network. The polymer entraps the NPs increasing their mechanical stability and enhances the sorption capacity of the paper-based membrane toward the target contaminants which are subsequently degraded by the photocatalytic action of the TiO_2 nanoparticles.

The use of a protective polymeric network is an efficient strategy to synthesize NPs-based coatings. However, Ríos-Gomez *et al.* also investigated the synthesis of coatings consisting only of NPs [49]. The capacity of SWNHs to form stable and ordered aggregates (dahlia) paved the way to this development. For this purpose, the paper is immersed in a dispersion of SWNHs in chloroform. When the solvent evaporates, a mechanically stable coating of SWNHs is obtained.

4 Conclusions

Membranes have been used extensively in the analytical chemistry for the extraction and preconcentration of target compounds from different samples. Membrane modification by loading (nano)particles on commercial membranes (both hollow-fiber or planar formats), paper, or electrospun supports, effectively expands their range of applications. In fact, the use of planar configurations increases the surface available for interaction with the analytes which clearly enhances the efficiency of the (micro) extraction step. Nanoparticles can be used for the extraction as well as for environmental remediation if nanoparticles with catalytic activity are embedded in the polymeric network. Electrospun membranes are easily doped with NPs and the appearance of new fabrication approaches (like paper-based sorptive phases) will increase interest and drive further applications of particle-loaded membranes in coming years.

Acknowledgements

Financial support for the Spanish Ministry of Economy and Competitiveness (MINECO) is gratefully acknowledged (Grant number CTQ2017-83175R).

References

[1] Pedersen-Bjergaard S, Rasmussen KE. Liquid-liquid-liquid microextraction for sample preparation of biological fluids prior to capillary electrophoresis. Anal Chem 1999;71:2650e6.

[2] Patnaik P. Handbook of environmental analysis. CRC Press; 2010. https://doi.org/10.1201/b10505. Epub ahead of print 21 May 2010.

[3] Gjelstad A. Three-phase hollow fiber liquid-phase microextraction and parallel artificial liquid membrane extraction. TrAC Trends Anal Chem 2019;113:25e31.

[4] Lucena R, Simonet BM, Cárdenas S, Valcárcel M. Potential of nanoparticles in sample preparation. J Chromatogr A 2011;1218:620e37.

[5] Es'haghi Z, Rezaeifar Z, Rounaghi G-H, Nezhadi ZA, Golsefidi MA. Synthesis and application of a novel solid-phase microextraction adsorbent: hollow fiber supported carbon nanotube reinforced sol-gel for determination of phenobarbital. Anal Chim Acta 2011;689:122e8.

[6] Song X-Y, Shi Y-P, Chen J. Carbon nanotubes-reinforced hollow fibre solid-phase microextraction coupled with high performance liquid chromatography for the determination of carbamate pesticides in apples. Food Chem 2013;139:246e52.

[7] Song X-Y, Shi Y-P, Chen J. Carbon nanotubes reinforced hollow fiber solid phase microextraction for the determination of strychnine and brucine in urine. Talanta 2013;116:188e94.

[8] Zhao G, Wang C, Wu Q, Wang Z. Determination of carbamate pesticides in water and fruit samples using carbon nanotube reinforced hollow fiber liquid-phase microextraction followed by high performance liquid chromatography. Anal Methods 2011;3:1410.

[9] Wu C, Liu Y, Wu Q, Wang C, Wang Z. Combined use of liquid-liquid microextraction and carbon nanotube reinforced hollow fiber microporous membrane solid-phase microextraction for the determination of triazine herbicides in water and milk samples by high-performance liquid chromatography. Food Anal Methods 2012;5:540e50.

[10] Hylton K, Chen Y, Mitra S. Carbon nanotube mediated microscale membrane extraction. J Chromatogr A 2008;1211:43e8.

[11] Jiménez-Soto JM, Cárdenas S, Valcárcel M. Oxidized single-walled carbon nanohorns as sorbent for porous hollow fiber direct immersion solid-phase microextraction for the determination of triazines in waters. Anal Bioanal Chem 2013;405:2661e9.

[12] Ma X, Wang J, Wu Q, Wang C, Wang Z. Extraction of carbamate pesticides in fruit samples by graphene reinforced hollow fibre liquid microextraction followed by high performance liquid chromatographic detection. Food Chem 2014;157:119e24.

[13] Su S, Chen B, He M, Hu B. Graphene oxide-silica composite coating hollow fiber solid phase microextraction online coupled with inductively coupled plasma mass spectrometry for the determination of trace heavy metals in environmental water samples. Talanta 2014;123:1e9.

[14] Panichev N, Kalumba MM, Mandiwana KL. Solid phase extraction of trace amount of mercury from natural waters on silver and gold nanoparticles. Anal Chim Acta 2014;813:56e62.

[15] Awasthi K, Choudhury S, Komber H, Simon F, Formanek P, Sharma A, *et al.* Functionalization of track-etched poly (ethylene terephthalate) membranes as a selective filter for hydrogen purification. Int J Hydrogen Energy 2014;39:9356e65.

[16] Bhattacharya M, Mandal MK. Synthesis of rice straw extracted nano-silica-composite membrane for CO_2 separation. J Clean Prod 2018;186:241e52.

[17] Huang X, Zhang J, Wang W, Liu Y, Zhang Z, Li L, *et al.* Effects of PVDF/SiO_2 hybrid ultrafiltration membranes by sol-gel method for the concentration of fennel oil in herbal water extract. RSC Adv 2015;5:18258e66.

[18] Zhang Z, Wang L, Liu X, Zhang D, Zhang L, Li Q. Nano-Al_2O_3 -based micro solid-phase filter membrane extraction for simultaneous determination of tartrazine and sunset yellow in food. RSC Adv 2015;5:86445e52.

[19] Ali I, Suhail M, Alothman ZA, Badjah AY. Stereoselective interactions of profen stereomers with human plasma proteins using nano solid phase micro membrane tip extraction and chiral liquid chromatography. Separ Purif Technol 2018;197:336e44.

[20] Ali I, Kulsum U, AL-Othman ZA, Alwarthan A, Saleem K. Functionalized nanoparticles based solid-phase membrane micro-tip extraction and high-performance liquid chromatography analyses of vitamin B complex in human plasma. J Sep Sci 2016;39:2678e88.

[21] Wang S, Niu H, Cai Y, Cao D. Multifunctional Au NPs-polydopamine-polyvinylidene fluoride membrane chips as probe for enrichment and rapid detection of organic contaminants. Talanta 2018;181:340e5.

[22] Fateixa S, Raposo M, Nogueira HIS, Trindade T. A general strategy to prepare SERS active filter membranes for extraction and detection of pesticides in water. Talanta 2018;182:558e66.

[23] Granger JH, Skuratovsky A, Porter MD, Scaife CL, Shea JE, Li Q, *et al.* Coupling solid phase microextractions and surface-enhanced Raman scattering: towards a point-of-need tool for hepatic cancer screening. Anal Methods 2017;9:4641e6.

[24] Fedick PW, Bills BJ, Manicke NE, Cooks RG. Forensic sampling and analysis from a single substrate: surface-enhanced Raman spectroscopy followed by paper spray mass spectrometry. Anal Chem

2017;89:10973e9.

[25] Silva NFD, Magalhães JMCS, Barroso MF, Oliva-Teles T, Freire C, Delerue-Matos C. *In situ* formation of gold nanoparticles in polymer inclusion membrane: application as platform in a label-free potentiometric immunosensor for Salmonella typhimurium detection. Talanta 2019;194:134e42.

[26] Mukhtar NH, See HH. Carbonaceous nanomaterials immobilised mixed matrix membrane microextraction for the determination of polycyclic aromatic hydrocarbons in sewage pond water samples. Anal Chim Acta 2016;931:57e63.

[27] Altintas Z, Chianella I, Ponte GD, Paulussen S, Gaeta S, Tothill IE. Development of functionalized nanostructured polymeric membranes for water purification. Chem Eng J 2016;300:358e66.

[28] Wu Y, Liu X, Meng M, Lv P, Yan M, Wei X, *et al.* Bio-inspired adhesion: fabrication of molecularly imprinted nanocomposite membranes by developing a hybrid organic-inorganic nanoparticles composite structure. J Membr Sci 2015;490:169e78.

[29] Wu Y, Cui J, Meng M, Yan M, Yan Y, Li C. Bio-inspired adhesion: fabrication and evaluation of molecularly imprinted nanocomposite membranes by developing a "bioglue" imprinted methodology. RSC Adv 2015;5:46146e57.

[30] Jiang R, Pawliszyn J. Thin-film microextraction offers another geometry for solid-phase microextraction. TrAC Trends Anal Chem 2012;39:245e53.

[31] Wilcockson JB, Gobas FAPC. Thin-film solid-phase extraction to measure fugacities of organic chemicals with low volatility in biological samples. Environ Sci Technol 2001;35:1425e31.

[32] Olcer YA, Tascon M, Eroglu AE, Boyacı E. Thin film microextraction: towards faster and more sensitive microextraction. TrAC Trends Anal Chem 2019;113:93e101.

[33] Bagheri H, Roostaie A. Electrospun modified silica-polyamide nanocomposite as a novel fiber coating. J Chromatogr A 2014;1324:11e20.

[34] Reyes-Gallardo EM, Lucena R, Cárdenas S. Electrospun nanofibers as sorptive phases in microextraction. TrAC Trends Anal Chem 2016;84:3e11.

[35] Huang J, Deng H, Song D, Xu H. Electrospun polystyrene/graphene nanofiber film as a novel adsorbent of thin film microextraction for extraction of aldehydes in human exhaled breath condensates. Anal Chim Acta 2015;878:102e8.

[36] Bagheri H, Roostaie A. Roles of inorganic oxide nanoparticles on extraction efficiency of electrospun polyethylene terephthalate nanocomposite as an unbreakable fiber coating. J Chromatogr A 2015;1375:8e16.

[37] Bagheri H, Najafi Mobara M, Roostaie A, Baktash MY. Electrospun magnetic polybutylene

terephthalate nanofibers for thin film microextraction. J Sep Sci 2017;40:3857e65.

[38] Liu F, Xu H. Development of a novel polystyrene/metal-organic framework-199 electrospun nanofiber adsorbent for thin film microextraction of aldehydes in human urine. Talanta 2017;162:261e7.

[39] Wu Y, Zhang Y, Zhang M, Liu F, Wan Y, Huang Z, *et al.* Selective and simultaneous determination of trace bisphenol A and tebuconazole in vegetable and juice samples by membrane-based molecularly imprinted solid-phase extraction and HPLC. Food Chem 2014;164:527e35.

[40] Wackerlig J, Lieberzeit PA. Molecularly imprinted polymer nanoparticles in chemical sensing e synthesis, characterisation and application. Sensor Actuator B Chem 2015;207:144e57.

[41] He X-M, Zhu G-T, Zheng H-B, Xu S-N, Yuan B-F, Feng Y-Q. Facile synthesis of polyaniline-coated SiO_2 nanofiber and its application in enrichment of fluoroquinolones from honey samples. Talanta 2015;140:29e35.

[42] Morillo D, Faccini M, Amantia D, Pérez G, García MA, Valiente M, *et al.* Superparamagnetic iron oxide nanoparticle-loaded polyacrylonitrile nanofibers with enhanced arsenate removal performance. Environ Sci Nano 2016;3:1165e73.

[43] Liu Y, Hou C, Jiao T, Song J, Zhang X, Xing R, *et al.* Self-assembled AgNP-containing nanocomposites constructed by electrospinning as efficient dye photocatalyst materials for wastewater treatment. Nanomaterials 2018;8:35.

[44] Ríos-Gómez J, Lucena R, Cárdenas S. Paper supported polystyrene membranes for thin film microextraction. Microchem J 2017;133:90e5.

[45] Saraji M, Mehrafza N. Phenyl carbamate functionalized zinc oxide nanorods for paperbased thin film microextraction. RSC Adv 2017;7:50210e5.

[46] Reyes-Gallardo EM, Lucena R, Cárdenas S, Valcárcel M. Magnetic nanoparticles-nylon 6 composite for the dispersive micro solid phase extraction of selected polycyclic aromatic hydrocarbons from water samples. J Chromatogr A 2014;1345:43e9.

[47] Reyes-Gallardo EM, Lucena R, Cárdenas S. Silica nanoparticles-nylon 6 composites: synthesis, characterization and potential use as sorbent. RSC Adv 2017;7:2308e14.

[48] Ríos-Gómez J, Ferrer-Monteagudo B, López-Lorente AI, Lucena R, Luque R, Cárdenas S. Efficient combined sorption/photobleaching of dyes promoted by cellulose/titania-based nanocomposite films. J Clean Prod 2018;194:167e73.

[49] Ríos-Gómez J, Fresco-Cala B, García-Valverde M, Lucena R, Cárdenas S. Carbon nanohorn suprastructures on a paper support as a sorptive phase. Molecules 2018;23:1252.

Capítulo 7

Silver nanoflower-coated paper as dual substrate for surface-enhanced Raman spectroscopy and ambient pressure mass spectrometry analysis

Analytical and Bioanalytical Chemistry, 412 (2020) 3547-3557

Springer Link **Analytical and Bioanalytical Chemistry**
412 (2020) 3547-3557

Silver nanoflower-coated paper as dual substrate for surface-enhanced Raman spectroscopy and ambient pressure mass spectrometry analysis

M.C. Díaz-Liñán, M.T. García-Valverde, A.I. López-Lorente*, S. Cárdenas, R. Lucena

Departamento de Química Analítica, Instituto Universitario de Investigación en Química Fina y Nanoquímica IUNAN, Universidad de Córdoba, Campus de Rabanales, Edificio Marie Curie, E-14071 Córdoba, Spain

Paper-based analytical devices (PADs) have encountered a wealth of applications in recent years thanks to the numerous advantages of paper as a support. A silver nanoflower (AgNF) modified paper-based dual substrate for both surface-enhanced Raman spectroscopy (SERS) and ambient pressure paper spray mass spectrometry (PS-MS) was developed. AgNFs were immobilized on nylon-coated paper modified with silver and ethylenediamine. The developed substrate was characterized via scanning electron microscopy and infrared spectroscopy. The densely packed nanoscale petals of the AgNFs lead to a large number of so-called hot spots at their overlapping points, which result in an enhancement of the Raman signal. In addition, the presence of the AgNFs produces an increase in the sensitivity of the mass spectrometric analysis as compared with bare paper and nylon/Ag-coated paper. The dual substrate was evaluated for the identification and quantification of ketoprofen in aqueous standards as well as human saliva from healthy volunteers. The method enables the determination of ketoprofen with a limit of detection and

limit of quantification via PS-MS of 0.023 and 0.076 mg L^{-1}, respectively, with a relative standard deviation (RSD) of 3.4% at a concentration of 0.1 mg L^{-1}. This dual substrate enables the simple and fast detection of ketoprofen with minimal sample preparation, providing complementary Raman and mass spectrometric information.

Keywords: Silver nanoflowers, Surface-enhanced Raman spectroscopy, Paper spray mass spectrometry, Paper-based analytical device, Ketoprofen

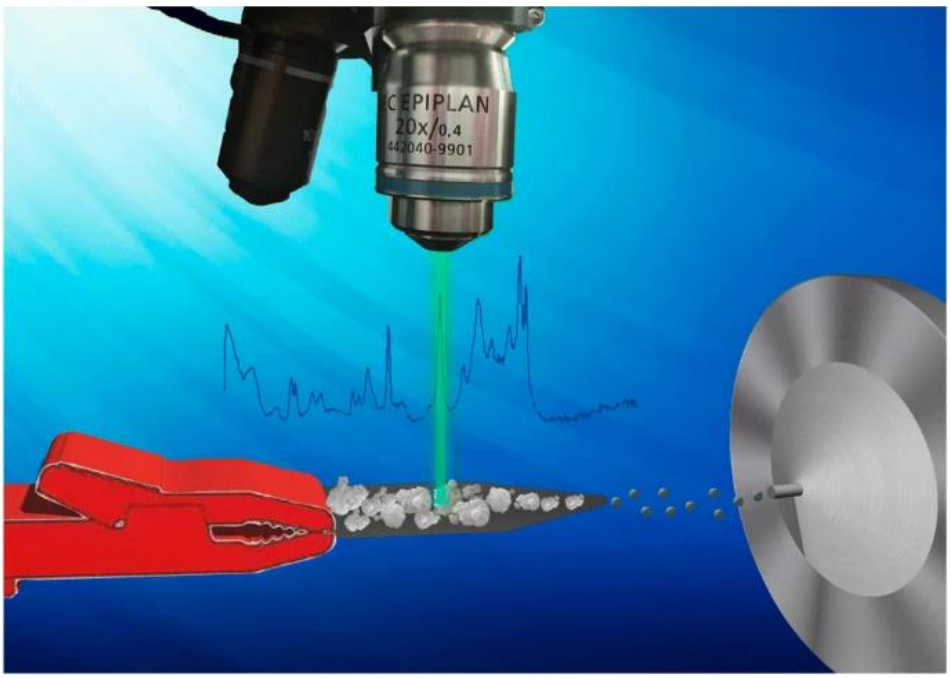

1. Introduction

With the steady increase of attention on the development of rapid and reliable sensors throughout the past decades, paper has emerged as a relevant support owing to the numerous benefits associated with its use (e.g., low price, versatility and availability) [1]. One of the main advantages of solid materials is their easy handling, which facilitates their coupling with instrumental techniques, such as fluorimetry [2], electrochemistry [3], mass spectrometry (MS) [4] and surface-enhanced Raman spectroscopy (SERS) [5]. In addition, paper-based supports reduce both sample and reagent consumption since the structure and physical characteristics of cellulose enable the natural and spontaneous fluidic transport of compounds. Furthermore, common filter paper is widely available and cost-effective, while its easy modification via wet chemistry allows the fabrication of hybrid materials that synergistically combine the properties of both paper and the immobilized coating. For example, paper-based supports modified with a polymer coating [6, 7] or by incorporation of different nanostructures [8–10] have been described.

Regarding the latter, metallic nanoparticles, especially gold and silver nanoparticles, have raised great attention in the past decades in spectroscopic techniques, e.g., SERS, owing to their unique localized surface plasmon resonance (LSPR) [11] properties. Two mechanisms are thought to be responsible for the SERS effect, namely electromagnetic, due to the high electric field strength surrounding the nanoparticles, and chemical enhancement given by the chemical interactions between the analytes and the nanoparticles [12]. The electromagnetic enhancement is based on the increase of the Raman signal as a consequence of the ability of plasmon-resonant nanoparticles to confine light in nanoscopic regions, so-called hot spots. Within these regions, strong electromagnetic field confinement is achieved as a result of the high induced electric field intensities, thus resulting in an enhancement of the Raman intensity [12, 13]. The SERS intensity relies on various factors related to the nanoparticles, i.e., size, shape, metal type and aggregation rate

[14]. Among others, spherical [15, 16], flower-shaped [14] and star-shaped [17] nanoparticles have been evaluated as SERS substrates, showing that the electromagnetic field surrounding nanoparticles with sharp edges or tips is significantly higher compared to those with planar surfaces due to the larger number of hot spots generated [18]. Silver nanoflowers (AgNFs) prepared through different methods, such as electrodeposition [19] or biosynthetic procedures [20], have been used for sensitive SERS detection [14]. Nevertheless, a bottleneck hindering their broadband application is the low-cost and simple fabrication of reproducible SERS-active substrates in large quantities, which has been overcome e.g., by growing AgNFs on reduced graphene oxide fibres [21] or in this work by immobilizing the nanomaterial on the cellulose fibres of paper.

Furthermore, paper-based substrates can be coupled to MS for the direct analysis of samples via ambient pressure paper spray mass spectrometry (PS-MS). This technique significantly simplifies the analytical process [8], as it avoids sample pretreatment, i.e., extraction or clean-up [22], as well as complex separations by chromatographic techniques prior to MS analysis, thus reasonably reducing the time of analysis. Briefly, the basic principle of this technique consists in loading the sample onto a triangular-shaped piece of paper, and the application of a high voltage after the addition of a small volume of solvent acting as the mobile phase in chromatography. The accumulation of charge at the tip of the triangle causes the formation of droplets, which later undergo solvent evaporation, leaving an ionic spray, similar to what occurs in electrospray [23, 24]. In PS-MS, the position of the paper relative to the inlet of the mass spectrometer, as well as the applied voltage, is crucial to obtain reproducible analyses, since ionization efficiency is directly influenced by these variables [25]. Although PS-MS is a relatively new technique, it has been already applied in many different fields such as food chemistry, clinical or biomedical analysis of complex samples, e.g., blood [26–28], tissue [29, 30] or illegal additives [31]. Nevertheless, the modification of the paper substrate in PS-MS with nanomaterials has been scarcely investigated, e.g., as a chemical reactor for studying

heterogeneous catalysis mediated by Pd, Ag or Au NPs [32] and by using a commercial SERS substrate [33]. Notwithstanding, as far as we are concerned, improvement of sensitivity in PS-MS analysis as a consequence of the modification of the paper substrate with nanoparticles has not been described until now.

Herein, a dual SERS and PS-MS substrate based on the immobilization of AgNFs in a chemically modified paper-based analytical device (PAD) was developed. AgNFs were obtained via a wet chemistry reaction involving boric acid and L-ascorbic acid solutions. The raw paper was modified with nylon, silver and ethylenediamine in order to anchor the AgNFs and form the modified paper-based analytical device (ny-AgNF PAD). The enhancement features of the ny-AgNF PAD were evaluated with crystal violet (CV) as a SERS reporter. The dual detection ability of the developed substrate was evaluated by using ketoprofen as a model drug, which was determined through both SERS and PS-MS, the substrate providing enhanced sensitivity not only in SERS but also in mass spectrometric analysis. Ketoprofen, or 2-(3-benzoylphenyl)propionic acid, is a nonsteroidal anti-inflammatory drug widely used in many formulations for the treatment of inflammatory diseases. AgNFs have been employed for the first time in PS-MS, improving the detection of ketoprofen. The developed method enables fast and straightforward analysis with minimal sample preparation, providing complementary fingerprinting Raman spectroscopic information with m/z identification and quantification by mass spectrometry. The substrate was applied to the determination of ketoprofen in dried saliva spots (DSS) via swabbing and PS-MS analysis. DSS is a convenient sampling technique for bioanalysis, facilitating the transport of saliva samples as compared to saliva poured into a tube at the same time that is suitable for forensic analysis.

2. Materials and methods

2.1. Reagents

All reagents were of analytical grade or better. Unless otherwise specified, they were

purchased from Sigma-Aldrich (Madrid, Spain). Standard solutions of crystal violet and ketoprofen were prepared at a concentration of 10,000 mg·L^{-1} in milli-Q water (Millipore Corp., Madrid, Spain) and 1000 mg·L^{-1} in methanol (Panreac, Barcelona, Spain), respectively. Working solutions were prepared by appropriate dilution of the stock solutions in milli-Q water or methanol. Ketoprofen-d3 was selected as internal standard (IS) in PS-MS analysis. The stock standard solution was prepared in methanol at a concentration of 25 mg·L^{-1} and stored at −20 °C. Solutions of nylon-6, ethylenediamine, silver nitrate, sodium citrate dibasic, boric acid, L-ascorbic acid and ammonia were employed for the synthesis of ny-AgNF PADs. LC-MS-quality methanol (Panreac, Barcelona, Spain) and formic acid (Scharlab, Barcelona, Spain) were employed as eluent in PS-MS.

2.2. Synthesis of ny-AgNF PADs

2.2.1 Synthesis of AgNFs

Silver nanoflowers were synthesized following a slightly modified version of a procedure described elsewhere [34], replacing ammonium citrate by sodium citrate tribasic. To begin with, 25 mL of 0.3 mol·L^{-1} silver nitrate was mixed with 25 mL of 0.15 mol·L^{-1} sodium citrate tribasic for 2 min at 50 °C to afford a white precipitate. Then, ammonia was added dropwise until the solution became transparent, and 25 mL of 0.5 mol·L^{-1} boric acid was immediately added. Finally, 25 mL of 0.5 mol·L^{-1} L-ascorbic acid was added, turning the solution into a blackish colour, confirming the formation of silver nanoflowers.

2.2.2 Modification of PADs

The preparation of the PADs consists of a first coating of the paper with nylon-6 in order to overcome limitations in SERS detection of ketoprofen due to the highly porous structure of the paper. The coating was obtained by immersion of the paper twice in a 3% (w/v) solution of nylon-6 in formic acid and drying. Afterwards, 10 µL of 0.3 mol·L^{-1} silver nitrate was drop-casted onto the surface of the filter paper with

the shape and dimensions shown in Electronic Supplementary Material (ESM) Fig. S1. PADs were then irradiated with 254 nm UV light at 1 J·cm^{-2} (UV lamp Bio link crosslinker from Labolan S.L., Spain) for 15 min, which turned the paper dark grey as a result of the formation of metallic silver. Next, to functionalize the silver surface of the paper, it was incubated in 1 mL of 2 mmol·L^{-1} of ethylenediamine overnight. Finally, the PAD was immersed in the AgNFs solution for 6 h and rinsed with milli-Q water to remove the unattached AgNFs, thus affording the final nylon-AgNF PAD (ny-AgNF PAD).

In order to evaluate the role of the nylon coating prior to subsequent functionalization with the AgNFs, PADs without nylon (AgNF PADs) were prepared following the procedure described above, but omitting the first step (nylon-6 coating).

2.3. Characterization of PADs

Four types of PADs, namely raw filter paper, filter paper with nylon-6, AgNF PAD and ny-AgNF PAD were characterized by two different techniques, i.e., scanning electron microscopy (SEM) and attenuated total reflection infrared spectroscopy (ATR-IR). SEM micrographs were performed at the central Service for Research Support (SCAI) of the University of Córdoba using a JEOL JSM 7800F microscope (JEOL, Tokyo, Japan) and were used to characterize the structure of the PADs at different stages of the synthesis.

ATR-IR spectra (see ESM) were acquired with a Bruker Tensor 37 FT-IR spectrometer (Bruker Optik, GmbH, Ettlingen, Germany) equipped with a three internal reflections diamond ATR cell (Platinum ATR accessory, Bruker). A room temperature operating deuterated triglycine sulfate (DTGS) detector was employed for signal recording. Measurements were performed in the spectral window of 4000-400 cm^{-1} at a 4 cm^{-1} spectral resolution by averaging 64 scans each spectrum. Data collection and processing were done using the OPUS software package (Bruker, Ettligen, Germany).

2.4. SERS measurements

Raman measurements were performed with a confocal Raman spectrometer (alpha500, manufactured by WITec GmbH, Ulm, Germany). For excitation, a frequency-doubled Nd:YAG laser at 532 nm (second harmonic generation) was employed, using a laser power of 0.362 mW for crystal violet and 1.202 mW for ketoprofen (measured prior to the objective lens). The laser beam was focused on the sample using a 20x/0.4 Zeiss objective. Measurements were performed in five different points of each replica, thus obtaining 15 points for each concentration.

2.5. Paper spray measurements

MS experiments were performed in a Thermo LTQ Orbitrap XL hybrid mass spectrometer (Thermo Fisher Scientific, San José, CA, USA). The instrument was set to collect spectra in automatic gain control mode with a maximum ion injection time of 100 ms and three microscans per spectrum. The optimized ionization parameters were as follows: spray and capillary voltages were 4 kV and 35.0 V, respectively; the capillary temperature was 250 °C and the tube lens was 130 V. The data-dependent MS/MS events were always performed on the most intense ions detected in positive mode full scan MS. The MS/MS isolation width was 1 amu and the normalized collision energy was 20% and 40% for ketoprofen and the IS, respectively. Tandem mass spectrometry (MS/MS) experiments were carried out by collision-induced dissociation (CID) using helium as the collision gas. MS spectra were recorded in full scan mode (m/z range 199.1–219.1 and 202.0–222.0 for ketoprofen and IS, respectively). Data was collected and analysed with Xcalibur 2.1.0 software (Thermo Fisher Scientific).

Sample introduction was carried out with the paper spray technique. The PAD was placed in an electric clamp, keeping 16 mm of the paper tip visible and located in front of the MS, with a separation of 4–7 mm between the tip and the MS inlet [35]. An aliquot of 3 μL of the standard was loaded onto the area closest to the PAD tip and allowed to dry. Then, spray voltage was set to 4 kV and applied to the PAD

through the clamp. Finally, analytes were eluted with 20 µL of methanol containing 0.1% (v/v) formic acid, loading the eluent in the paper section between sample location and the electric clamp. Samples obtained by the surface swabbing technique were analysed by PS-MS under the same experimental conditions.

3. Results and discussion

3.1. Preparation of ny-AgNF PADs

As previously mentioned, the synthesis of AgNFs was carried out using silver nitrate as silver precursor; a whitish precipitate was formed corresponding to a silver citrate complex controlled by sodium citrate [34]. The dropwise addition of ammonia results in the formation of an ionic complex between silver and ammonia, while boric acid is used to keep the pH of the mixture neutral (ca. 7). Finally, anisotropic growth of AgNFs is mediated by ascorbic acid, the solution acquiring a blackish colour [34].

The fibrous structure of paper is one of the advantages of this material when used as a sorbent, as it provides a high surface area. Nevertheless, for ketoprofen determination it was a drawback, as the analyte penetrates the fibres of the filter paper and is thereby not available at the surface for SERS detection. To overcome this problem, PADs were firstly coated with nylon by immersion in a 3% (w/v) solution of nylon-6 in formic acid, thus filling the gaps throughout the entire fibrous net. Once the PADs were coated, silver nitrate was drop-casted onto the surface and reduced with UV light, providing a homogeneous silver surface for the interaction with the amino groups of ethylenediamine by overnight incubation of the PADs in a 2 $mmol \cdot L^{-1}$ solution of ethylenediamine. Finally, the PADs were immersed in the AgNFs solution for 6 h, which resulted in the attachment of the AgNFs to ethylenediamine through interaction with amino groups. Although the preparation of the PADs is time-consuming, it should be mentioned that several ny-AgNF PADs can be prepared at once, which can be later used for the rapid dual detection of the analytes via SERS and PS-MS.

3.2. Characterization of PADs

The surfaces of four different PADs were characterized by SEM. Fig. 1a shows the surface structure of filter paper, where the non-uniform three-dimensional cellulosic network can be observed. Fig. 1b depicts the surface of a filter paper coated with nylon-6, while Fig. 1c shows a AgNF PAD, and Fig. 1d depicts a ny-AgNF PAD. Regarding the nylon-coated filter paper, no significant differences were observed when compared with raw filter paper. However, in the presence of silver nanoflowers, a uniform coating of these nanostructures can be observed throughout the entire PAD, thus having an appropriate environment for the interaction with the analytes. This is very important, since homogeneity can affect the SERS effect. Furthermore, the presence of the well-distributed nanoflowers throughout the surface of the PAD also led to an improved ionization of the analytes in the case of PS-MS. Moreover, the flower-like shape of the nanoparticles and its petals can be observed in the inset of Fig. 1d. The petal-like structure in the nanoparticles is vital in SERS, since it is within the regions close to them that hot spots are created, which will lead to a proper increase of the signal. Nonhomogeneous distribution of the nanoflowers on the surface of the PADs could result in coverage of the hot spots and, thus, in a poor SERS effect.

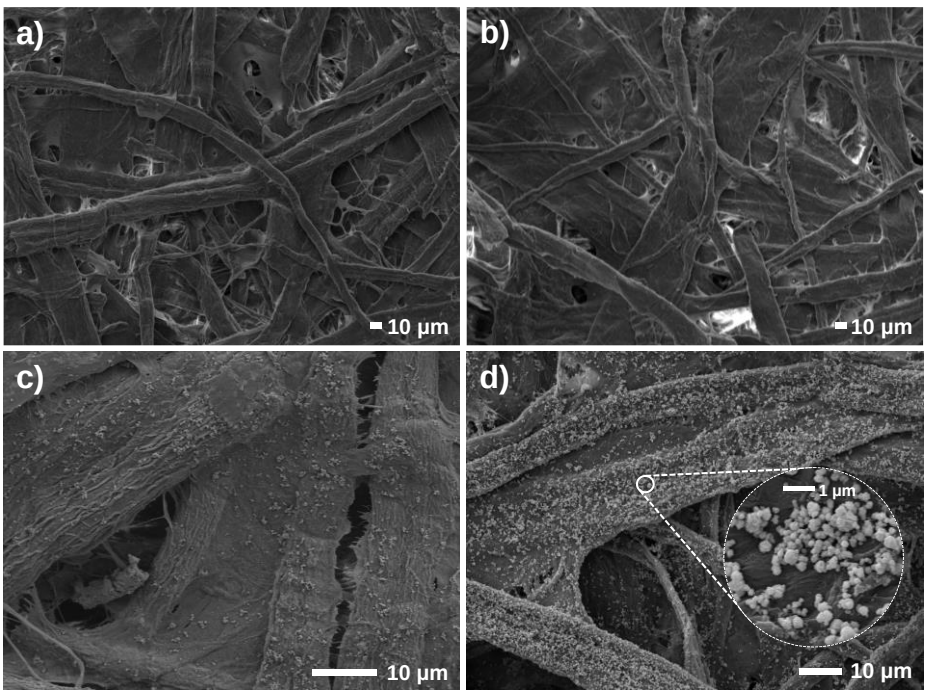

Figure 1. Scanning electron microscopy micrographs of (a) raw filter paper, (b) filter paper coated with nylon-6, (c) AgNF PAD and (d) ny-AgNF PAD.

3.3. SERS measurements

3.3.1 SERS enhancement

The enhancing properties of AgNFs immobilized at the functionalized PADs were evaluated via SERS studies using crystal violet (CV) as a model analyte. Crystal violet is a minimally fluorescent dye commonly applied in SERS studies as SERS reporter in order to evaluate the enhancement produced on the Raman signal due to the presence of the SERS substrate. Each measurement was performed after two consecutive depositions of 3 µL into each PAD and drying. Fig. 2a shows the vibrational bands observed in the Raman and SERS spectra of CV in (a) raw filter

paper at 5000 mg·L^{-1}, (b) Ag PAD at 10,000 mg·L^{-1}, (c) AgNF PAD at 10 mg·L^{-1} and (d) ny-AgNF PAD at 10 mg·L^{-1}. The Raman bands of crystal violet can be ascribed to the out-of-plane bending mode of C–C_{centre}–C (416 cm^{-1}), bending mode of C–N–C, out-of-plane aromatic C–C deformation (bands around 517 and 554 cm^{-1}, respectively) and C–H in-plane bending vibrations, according to the literature [36, 37]. As seen in Fig. 2a, the main differences are observed between the filter papers and the PADs containing AgNFs, making it possible to distinguish the characteristic bands of CV in the latter. Furthermore, no significant differences between the AgNF PAD and the ny-AgNF PAD were observed; thus, we conclude that nylon-6 does not interfere with the SERS measurements of CV.

The enhancement factor (EF) was obtained by comparing the Raman signal of 5000 mg·L^{-1} crystal violet solution deposited on raw filter paper and the enhanced signal obtained with 0.5 mg·L^{-1} crystal violet solution deposited on ny-AgNF PAD. It was calculated following $EF = (I_{SERS}/I_{Raman}) \times (N_{Raman}/N_{SERS})$, where I is the intensity of the band at 1181 cm^{-1}, and N represents the total number of molecules deposited on the substrate, thus affording an EF of $1.97 \cdot 10^4$.

For further evaluation, a calibration graph was built by deposition in triplicate on the ny-AgNF PAD of seven aqueous standards of CV in the range of 0.5 to 10 mg·L^{-1} and plotting the SERS intensity of the CV band at 1181 cm^{-1} vs. the concentration (Fig. 2b). Each point corresponds to the average of three independent replicas, each of them measured at five different positions throughout the entire piece of ny-AgNF PAD, and error bars illustrate the standard deviation of the mean value. As can be observed in Fig. 2b, a straight fit function enabled an R^2 value of 0.9955. The limit of detection (LOD) and limit of quantification (LOQ) were calculated from the linear fit as $(3S_a)/b$ and $(10S_a)/b$, respectively, affording values of concentration of 0.5 and 1.6 mg·L^{-1}, respectively. The reproducibility expressed as the relative standard deviation (n = 3) was 8% for a CV concentration of 3 mg·L^{-1}.

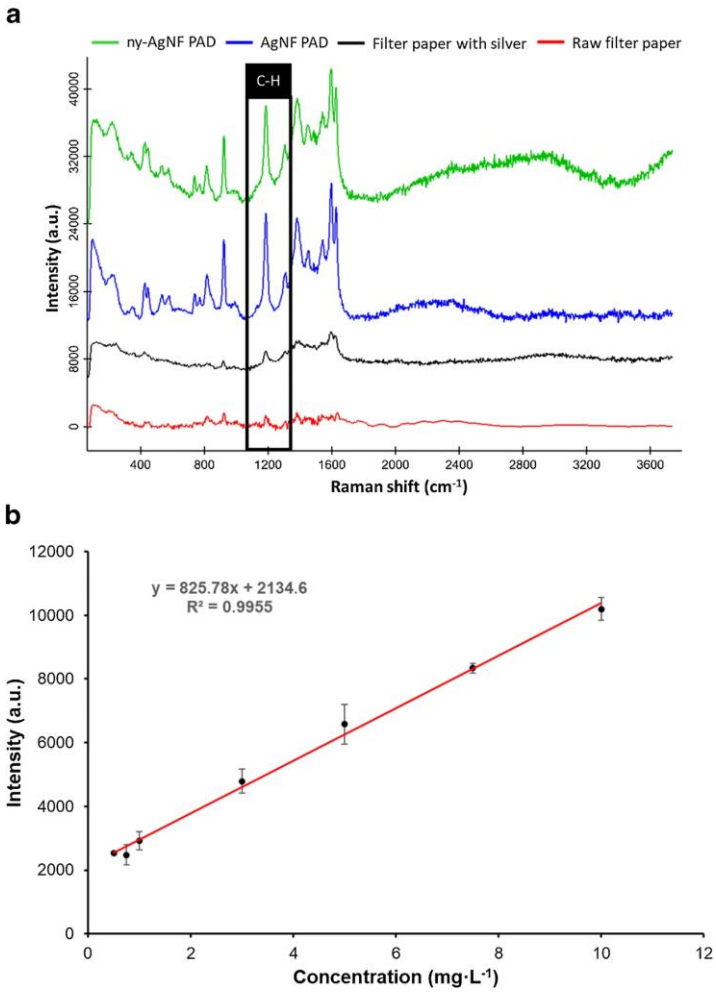

Figure 2. (a) Raman and SERS spectra of crystal violet on raw filter paper at 5000 mg·L^{-1}, Ag PAD at 10,000 mg·L^{-1}, AgNF PAD at 10 mg·L^{-1} and ny-AgNF PAD at 10 mg·L^{-1}. (b) Intensity of the crystal violet SERS band at 1181 cm^{-1} vs. concentration of CV in the aqueous solutions. Each point represents the average of three independents measurements and error bars relate to the standard deviation of the corresponding mean value.

3.3.2 SERS determination of ketoprofen

The suitability of the ny-AgNF PADs for quantitative measurements was also evaluated using ketoprofen as analyte. Fig. 3 shows the vibrational bands observed for solid ketoprofen and ketoprofen at a concentration of 10 mg·L^{-1} deposited on AgNF PAD and ny-AgNF PAD. As can be observed, at the same level of concentration, it was difficult to detect ketoprofen in bare AgNF PAD. For this reason, it was necessary to coat the paper with nylon-6 in order to favour the availability of the analyte at the surface of the substrate and, thus, its interaction with the AgNFs. In the presence of nylon-6 a good signal-to-noise ratio was obtained for the reference peak of ketoprofen (ca. 1000 cm^{-1}), which can be ascribed to the benzene ring deformation [38]. Furthermore, upon modification of the cellulose paper with nylon-6, the characteristics bands of the polymer were not observed in the spectra and thus did not interfere with the measurements of the analyte. Fig. 3 depicts the positive effect of nylon on the SERS detection of ketoprofen.

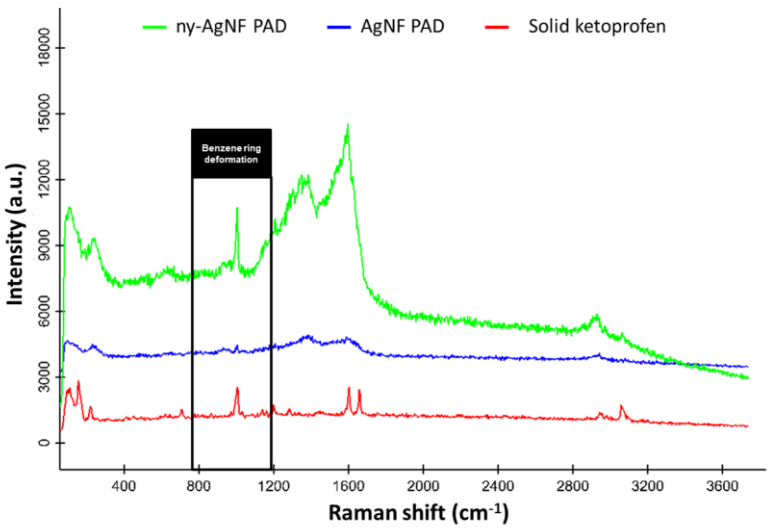

Figure 3. Raman spectra of solid ketoprofen, 10 mg·L^{-1} ketoprofen solution on an AgNF PAD and 10 mg·L^{-1} ketoprofen solution on a ny-AgNF PAD.

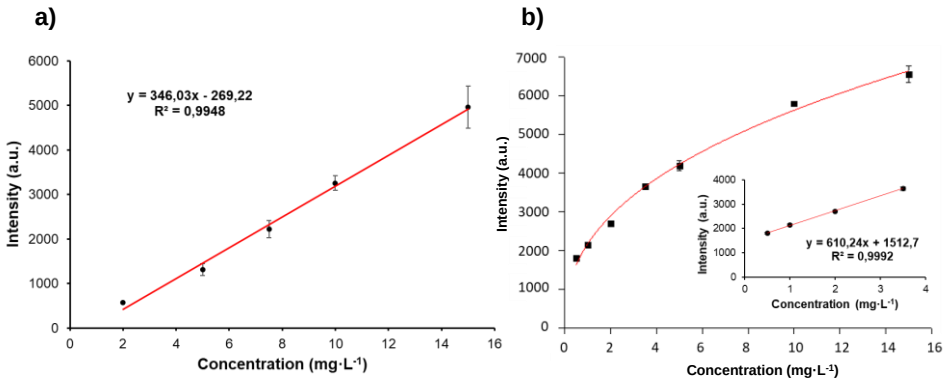

Figure 4. (a) Plot of the intensity of the band at 1000 cm^{-1} in the SERS spectrum of ketoprofen obtained by deposition vs. concentration of aqueous standards of ketoprofen. (b) Plot of the intensity of the band at 1000 cm^{-1} in the SERS spectrum of ketoprofen after swabbing vs. concentration of aqueous standards of ketoprofen. The inset depicts the linear range of the curve at low concentrations. Each point represents the average of three independents measurements and error bars relate to the standard deviation of the corresponding mean value.

Finally, a calibration graph was built by depositing five aqueous standards of ketoprofen in the range of 2 to 15 $mg{\cdot}L^{-1}$ and plotting the SERS intensity of the band at around 1000 cm^{-1} vs. concentration (Fig. 4a). Each point corresponds to the average of three independent replicas, each of them measured at five different points throughout the entire piece of ny-AgNF PAD, and error bars illustrate the standard deviation of the mean value. As can be observed in Fig. 4a, a straight fit function enabled an R^2 value of 0.995. The LOD and LOQ, calculated from the linear fit as $(3S_a)/b$ and $(10S_a)/b$, respectively, were 1.1 and 3.8 $mg{\cdot}L^{-1}$, respectively. The reproducibility expressed as the relative standard deviation (n = 3) was 8.8% for a ketoprofen concentration of 7.5 $mg{\cdot}L^{-1}$. Similarly, a calibration graph was built by swabbing of seven aqueous standards of ketoprofen in the range of 0.5 to 15 $mg{\cdot}L^{-1}$ and plotting the SERS intensity vs. concentration. As can be observed in Fig. 4b, the calibration curve can be fitted to a Langmuir isotherm function (R^2 = 0.9920), which

depicts the adsorption process of ketoprofen on the ny-AgNF PADs. The corresponding Langmuir equation was $y = (abx^{1-c})/(1 + bx^{1-c})$, fitted by the following parameters: a = 296,111.78, b = 0.00739, c = 0.58183. This plot displays a linear variation at low concentrations of ketoprofen ($R^2 = 0.9992$), as shown in the inset of Fig. 4b. The LOD and LOQ were calculated from the linear fit as $(3S_a)/b$ and $(10S_a)/b$, respectively, affording values of concentrations of 0.1 and 0.4 $mg \cdot L^{-1}$, respectively. The precision of the measurements was evaluated at a concentration level of 3.5 $mg \cdot L^{-1}$, affording a relative standard deviation (n = 3) of 2.1%.

3.4. PS-MS determination of ketoprofen

The performance of ny-AgNF PADs at different stages of the synthesis was evaluated via direct analysis with PS-MS. First of all, a calibration graph was built at five concentration levels by deposition of ketoprofen standard onto raw filter paper in the range of 0.25 to 2 $mg \cdot L^{-1}$ in methanol, containing the IS at 0.25 $mg \cdot L^{-1}$, and plotting the ratio between the areas of the target analyte and the isotope-labelled IS versus concentration. A straight fit function enabled an R^2 value of 0.994. The corresponding equation was y = bx + a, where the slope was 2.56. The LOD and LOQ were calculated as $(3S_a)/b$ and $(10S_a)/b$, affording values of concentrations of 0.139 and 0.465 $mg \cdot L^{-1}$, respectively. The RSD at a concentration of 0.25 $mg \cdot L^{-1}$ was 4.2%. As expected, paper spray mass spectrometry enabled the detection of ketoprofen. In order to further lower the limit of detection of the method, the developed AgNFs PADs were also investigated as substrates for PS-MS.

An enhancement of the sensitivity was observed using the developed ny-AgNF PADs owing to the presence of the metallic nanostructures. Similarly to raw filter paper, a calibration graph was built at five concentration levels by deposition of ketoprofen standards in methanol on ny-AgNF PADs in the range of 0.025 to 0.5 $mg \cdot L^{-1}$, the IS being at 0.050 $mg \cdot L^{-1}$, and plotting the relation between the areas of the target analyte and the IS vs. concentration. As can be observed in Fig. 5c, the straight fit function enabled an R^2 value of 0.997 and the slope of the calibration equation was

22.5. The LOD and LOQ were calculated from the straight fit as ($3S_a$)/b and ($10S_a$)/b, respectively, affording values of concentrations of 0.023 and 0.076 mg·L^{-1}, respectively. The RSD for a concentration of 0.1 mg·L^{-1} was 3.46%. Comparing the sensitivity values of LOD and LOQ obtained for ny-AgNF PAD with the ones using raw filter paper, one can elucidate the improvement in the spray generation due to the presence of the silver nanostructures at the surface of the paper substrate. The analytical signal intensity increases when ny-AgNF PAD is used as substrate, being able to reduce the analyte concentration almost ten times the latter. By way of example, a complete chronogram at the lowest level of the calibration curve is included in ESM, Fig. S3. Additionally, the mass spectrum was monitored at different times (0.20, 0.75 and 2.50 min) to evaluate the chemical noise surrounding the relevant m/z signals.

To ascertain that the improvement of the sensitivity was given by the AgNFs and not by the metallic silver surface of the PADs, a calibration graph was built by deposition on ny/Ag-paper of ketoprofen standard at five concentration levels in the range of 0.25 to 2 mg·L^{-1} in methanol, containing the IS at 0.25 mg·L^{-1}. Nevertheless, the LOD obtained under these conditions was 0.45 mg·L^{-1}, indicating a decline in the sensitivity in comparison with that of ny-AgNF PAD, and even with that obtained using raw filter paper. The result was unexpected since metallic silver should enhance the formation of the spray. However, this behaviour can be ascribed to the presence of nylon-6, which may hinder the formation of the spray as a result of the flattening of the surface of the PADs. Additionally, as can be observed in Fig. 1d, the micrograph of ny-AgNF PADs shows an increase in the surface roughness of the substrate. AgNFs remain on the surface coating fostering the ionization of the target analyte.

In the light of the results obtained, a study of the background noise using the different PADs was carried out. As it is observed in ESM, Fig. S4a–c, the chemical noise surrounding the relevant m/z signals is much higher in the raw filter paper and ny/Ag-paper. The use of ny-AgNF also increase the relevant m/z signals, thus

providing a better sensitivity and allowing the detection of the analyte at a lower concentration (ESM, Fig. S4d).

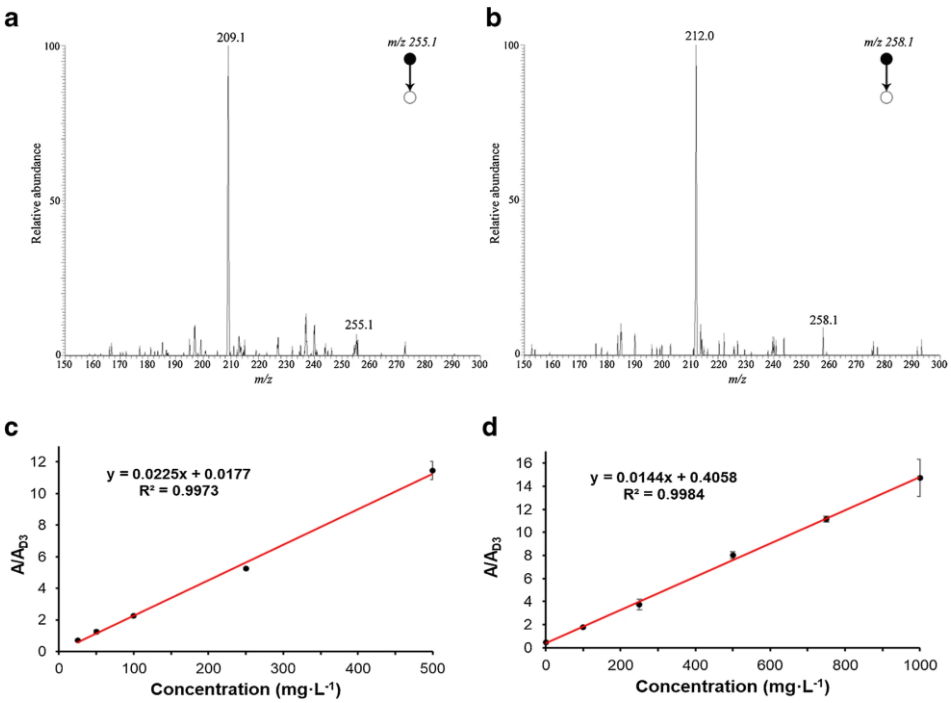

Figure 5. PS-MS spectra of (a) ketoprofen and (b) ketoprofen-d3 in methanol. Relation of areas of ketoprofen standard and the isotope-labelled IS vs. concentration in (c) methanol and (d) saliva samples. Each point represents the average of three independents measurements and error bars relate to the standard deviation of the corresponding mean value.

For further evaluation of the performance of ny-AgNF PADs in PS-MS, direct analysis of saliva was carried out. First of all, a calibration graph was built by deposition of saliva spiked at six concentration levels from 0 to 1 mg·L^{-1}, containing the IS at 0.05 mg·L^{-1}. Calibration graphs of the ratio of the areas of the target analyte and its corresponding IS vs. concentration are depicted in Fig. 5d. The straight fit function provided an R^2 value of 0.998 and a slope value of 14.4. The LOD and LOQ were

obtained from the linear fit as described before, affording values of 0.034 and 0.114 mg·L^{-1}, respectively. The RSD at a concentration of 0.1 mg·L^{-1} was 5.7%. Thus, the ny-AgNF PADs provide better detection limits not only with standards but also when samples with complex matrices such as saliva are measured. The mass spectra (ESM, Fig. S5) do not show a relevant chemical noise around the characteristic m/z of the analyte. The signal reduction, observed for the analysis of saliva samples, was therefore ascribed to the ion-suppression effect during the spray formation. The use of IS, however, allows the correction of this effect when such samples are processed. Table 1 summarizes the analytical features of merit obtained with the different substrates for the determination of ketoprofen both via SERS and PS-MS.

Table 1. Analytical figures of merit of the developed method for the determination of ketoprofen via SERS and PS-MS analysis.

Analytical technique	Substrate	Sample/methodology	LOD (mg·L^{-1})	LOQ (mg·L^{-1})	Linear range (mg·L^{-1})	R^2	RSD (%)
SERS	ny-AgNF PADs	Ketoprofen standard/deposition	1.1	3.8	LOQ-15	0.995	8.8
SERS	ny-AgNF PADs	Ketoprofen standard/swabbing	0.1	0.4	LOQ-3.5	0.999	2.1
PS-MS	Raw filter paper	Ketoprofen standard/deposition	0.139	0.465	LOQ-2	0.994	4.2
PS-MS	ny/Ag-paper	Ketoprofen standard/deposition	0.45	1.501	LOQ-2	0.945	9.5
PS-MS	ny-AgNF PADs	Ketoprofen standard/deposition	0.023	0.076	LOQ-0.5	0.997	3.46
PS-MS	ny-AgNF PADs	Ketoprofen spiked saliva/deposition	0.034	0.114	LOQ-1	0.998	5.7

Finally, ny-AgNF PADs were employed for the analysis of dried saliva spots spiked with ketoprofen via swabbing. Dried saliva spot samples can be used as an alternative sampling technique to saliva poured into a tube. DSS using filter paper has been used as a reliable sampling method for bioanalysis [39]. First, 10 μL of saliva spiked with ketoprofen was deposited onto a glass slide and left to dry. Next, swabbing was performed by the addition of 3 μL of milli-Q water onto the dried

saliva and gently sweeping with the triangular tip of the ny-AgNF PADs. The analysis was carried out by PS-MS with the same procedure described in "Paper spray measurements". Table 2 depicts the recovery values calculated employing the straight fit equation of the calibration graph built by deposition of saliva on the ny-AgNF PADs (Fig. 5b).

Table 2. Recovery values of swabbing of dried saliva spot samples.

Spiked concentration ($mg \cdot L^{-1}$)	Recovery (%)
0.1	119 ± 22
0.5	97 ± 14
1	107 ± 7

4. *Conclusions*

This article describes the synthesis of silver nanoflower-coated paper, which was successfully applied as a substrate for both SERS and PS-MS. The paper substrate is consecutively coated with three different layers, namely nylon 6, metallic silver and silver nanoflowers.

The potential of the material as a SERS substrate was initially evaluated using crystal violet, a well-reported molecule in this type of application. The results showed an enhancement factor of $1.97 \cdot 10^4$ compared with the bare paper, thus indicating the dramatic SERS effect of the nanoflowers. Once the potential was explored, the SERS effect was studied for a different target analyte, ketoprofen. In the context of this study, the role of the nylon-6 coating was demonstrated as the presence of the polymer increases the SERS signal. This fact was ascribed to the partial filling of the paper pores with the polymer, thus promoting the surface availability of the analyte and an improved effect of the AgNFs. Finally, the SERS substrate was evaluated for swab sampling using dried standards over a glass slide

as proof of concept.

The synthesized silver nanoflower-coated paper also showed potential in PS-MS by providing better sensitivity than that obtained with bare paper. This aspect is extremely important since MS can extend the applicability of the substrate to more complex samples where the SERS technique has problems due to selectivity issues. The silver nanoflower-coated paper was successfully used to the analysis of dried saliva spot samples which are new and relevant samples in bioanalysis and forensic science.

The preparation of the substrates is simple, although it requires some consecutive non-automated steps. The mechanical stability of the nanostructures is achieved thanks to the previous metallic silver coating and the use of ethylenediamine as the chemical bridge. The polymer plays a relevant role, and it also provides the material with enough stiffness to maintain the paper stable and close to the MS inlet, thus improving the spray stability.

Further investigations will be driven in different directions. On the one hand, the practical application of the silver nanoflower-coated paper under the swabbing mode to solve problems in food analysis (e.g., contaminated fruits) or forensics (e.g., surfaces contaminated with drugs of abuse) will be faced. On the other hand, the substrates will be evaluated as sorptive phases to isolate target analytes from liquid samples and enrich them over the active surface for their final analysis.

Acknowledgements

Financial support from the Spanish Ministry of Economy and Competitiveness (CTQ2017-83175R) is gratefully acknowledged. The authors would like to thank Prof. A. Molina, Prof. J.F. García-Reyes and Dr. M. Beneito-Cambra (all of them from the University of Jaen, Spain) for their help with PS-MS technique. Additionally, the authors would like to thank the Central Service for Research Support (SCAI) of the University of Córdoba for the service provided to obtain the micrographs and especially to Carlos Fuentes Almagro, from the Proteomics Units, for all the help

with Xcalibur software. This article is based upon work from the Sample Preparation Task Force and Network, supported by the Division of Analytical Chemistry of the European Chemical Society.

Compliance with ethical standards

Informed consent was obtained for saliva samples from all individual participants (healthy volunteers) involved in the study. The study was approved by the appropriate ethics committee ("Comité Ético de Investigación con humanos") as part of the "Comité de Bioética y Bioseguridad de la Universidad de Córdoba" and was performed in accordance with the ethical standards.

Conflict of interest

The authors declare that they have no competing interests.

Appendix A. Supplementary data

Supplementary data to this article can be found online at https://doi.org/10.1016/j.microc.2020.105686.

References

[1] Nery EW, Kubota LT. Sensing approaches on paper-based devices: a review. Anal Bioanal Chem. 2013;405(24):7673–595.

[2] Díaz-Liñán MC, López-Lorente AI, Cárdenas S, Lucena R. Molecularly imprinted paper-based analytical device obtained by a polymerization-free synthesis. Sens Actuators B Chem. 2019;287:138–46.

[3] Channon RB, Yang Y, Feibelman KM, Geiss BJ, Dandy DS, Henry CS. Development of an electrochemical paper-based analytical device for trace detection of virus particles. Anal Chem. 2018;90(12):7777–83.

[4] SongW,Wang Y, Huang L, Cheng H,Wu J, Pan Y. Reactive paper spray mass spectrometry for rapid analysis of fomaldehyde in facial masks. Rapid Commun Mass Spectrom. 2019;33(12):1091–6.

[5] Jang W, Byun H, Kim JH. Rapid preparation of paper-based plasmonic platforms for SERS applications. Mater Chem Phys. 2020;240:122124.

[6] Ríos-Gómez J, Lucena R, Cárdenas S. Paper supported polystyrene membranes for thin film microextraction. Microchem J. 2017;133:90–5.

[7] Hashemian Z, Khayamian T, Saraji M. Anticodeine aptamer immobilized on a Whatman cellulose paper for thin-film microextraction of codeine from urine followed by electrospray ionization ion mobility spectrometry. Anal Bioanal Chem. 2015;407:1615–23.

[8] Ríos-Gómez J, Fresco-Cala B, García-Valverde MT, Lucena R, Cárdenas S. Carbon nanohorn suprastructures on a paper support as a sorptive phase. Molecules. 2018;23(6):E1252.

[9] Tsai TT, Huang CY, Chen CA, Shen SW, Wang MC, Cheng CM, *et al.* Diagnosis of tuberculosis using colorimetric gold nanoparticles on a paper-based analytical device. ACS Sensors. 2017;2(9):1345–54.

[10] Saraji M, Mehrafza N. Phenyl carbamate functionalized zinc oxide nanorods for paper-based thin film microextraction. RSC Adv. 2017;7:50210–5.

[11] Zhang MR, Jiang QM, Wang ZG, Zhang SH, Hou F, Pan GB. Three-dimensional gallium nitride nanoflowers supports decorated by gold or silver nanoparticles to fabricate surface-enhanced Raman scattering substrates. Sens Actuators B Chem. 2017;253:652–9.

[12] Bibikova O, Haas J, López-Lorente AI, Popov A, Kinnunen M, Meglinski I, *et al.* Towards enhanced optical sensor performance: SEIRA and SERS with plasmonic nanostars. Analyst. 2017;142:951–8.

[13] Fikiet MA, Khandasammy SR,Mistek E, Ahmed Y, Halámková L, Bueno J, *et al.* Surface enhanced Raman spectroscopy: a review of recent applications in forensic science. Spectrochim Acta A Mol Biomol Spectrosc. 2018;197:255–60.

[14] Roy S, Ajmal CM, Baik S, Kim J. Silver nanoflowers for singleparticle SERS with 10 pM sensitivity. Nanotechnol. 2017;28:465705.

[15] López-Lorente AI, Simonet BM, Valcárcel M, Mizaikoff B. Bare gold nanoparticles mediated surface-enhanced Raman spectroscopic determination and quantification of carboxylated single-walled carbon nanotubes. Anal Chim Acta. 2013;788:122–8.

[16] Al-ShalalfehMM, Onawole AT, Saleh TA, Al-Saadi AA. Spherical silver nanoparticles as substrates in surface-enhanced Raman spectroscopy for enhanced characterization of ketoconazole. Mater Sci Eng C Mater Biol Appl. 2017;76:356–64.

[17] Bibikova O, Haas J, López-Lorente AI, Popov A, Kinnunen M, Ryabchikov Y, *et al.* Surface enhanced infrared absorption spectroscopy based on gold nanostars and spherical nanoparticles. Anal Chim Acta. 2017;990:141–9.

[18] Aroca RF. Plasmon enhanced spectroscopy. Phys Chem Chem Phys. 2013;15:5355–63.

[19] Bi J. Electrodeposited silver nanoflowers as sensitive surface-enhanced Raman scattering sensing substrates. Mater Lett. 2019;236:398–402.

[20] Wu L, Wu W, Jing X, Huang J, Sun D, Odoom-Wubah T, *et al.* Trisodium citrate-assisted biosynthesis

of silver nanoflowers by Canarium album foliar broths as a platform for SERS detection. Ind Eng Chem Res. 2013;52(14):5085–94.

[21] Tong J, Xu Z, Bian Y, Niu Y, Zhang Y,Wang Z. Flexible and smart fibers decorated with ag nanoflowers for highly active surface-enhanced Raman scattering detection. J Raman Spectrosc. 2019;50(10):1468–76.

[22] Assis C, Pereira HV, Amador VS, Augusti R, de Oliveira LS, Sena MM. Combining mid infrared spectroscopy and paper spray mass spectrometry in a data fusion model to predict the composition of coffee blends. Food Chem. 2019;281:71–7.[23] da Silva Ferreira P, Fernandes de Abreu e Silva D, Augusti R, Piccin E. Forensic analysis of ballpoint pen inks using paper spray mass spectrometry. Analyst. 2015;140:811–19.

[24] Bartella L, Di Donna L, Napoli A, Sindona G, Mazzotti F. Highthroughput determination of vitamin E in extra virgin olive oil by paper spray tandem mass spectrometry. Anal Bioanal Chem. 2019;411(13):2885–90.

[25] Bartella L, Di Donna L, Napoli A, Siciliano C, Sindona G,Mazzotti F. A rapid method for the assay of methylxanthines alkaloids: theobromine, theophylline and caffeine, in cocoa products and drugs by paper spray tandem mass spectrometry. Food Chem. 2019;278:261–6.

[26] Liu J, Wang H, Manicke NE, Lin JM, Cooks RG, Ouyang Z. Development, characterization, and application of paper spray ionization. Anal Chem. 2010;82(6):2463–71.

[27] Yang Q, Manicke NE, Wang H, Petucci C, Cooks G, Ouyang Z. Direct and quantitative analysis of underivatized acylcarnitines in serum and whole blood using paper spray mass spectrometry. Anal Bioanal Chem. 2012;404(5):1389–97.

[28] Suraritdechachai S, Charoenpakdee C, Young I, Maher S, Vilaivan T, Praneenararat T. Rapid detection of the antibiotic sulfamethazine in pig body fluids by paper spray mass spectrometry. J Agric Food Chem. 2019;67(10):3055–61.

[29] Liu J, Wang H, Cooks RG, Ouyang Z. Leaf spray: direct chemical analysis of plant material and living plants by mass spectrometry. Anal Chem. 2011;83(20):7608–13.

[30] Wang H, Manicke NE, Yang Q, Zheng L, Shi R, Cooks RG, *et al.* Direct analysis of biological tissue by paper spray mass spectrometry. Anal Chem. 2011;83(4):1197–201.

[31] Yu M, Wen R, Jiang L, Huang S, Fang Z, Chen B, *et al.* Rapid analysis of benzoic acid and vitamin C in beverages by paper spray mass spectrometry. Food Chem. 2018;268:411–5.

[32] Banerjee S, Basheer C, Zare RN. A study of heterogeneous catalysis by nanoparticle-embedded paper-spray ionization mass spectrometry. Angew Chem Int Ed. 2016;55(41):12807–11.

[33] Fedick PW, Bills BJ, Manicke NE, Cooks RG. Forensic sampling and analysis from a single substrate: surface-enhanced Raman spectroscopy followed by paper spray mass spectrometry. Anal Chem. 2017;89(20):10973–9.

[34] Muhammed Ajmal C, Faseela KP, Swati S, Seunghyun B. Hierarchically-structured silver nanoflowers for highly conductive metallic inks with dramatically reduced filler concentration. Sci Rep. 2016;6:34894.

[35] Lara-Ortega FJ, Beneito-Cambra M, Robles-Molina J, García- Reyes JF, Gilbert-López B,Molina-Díaz A. Direct olive oil analysis by mass spectrometry: a comparison of different ambient ionization methods. Talanta. 2018;180:168–75.

[36] Lai K, Zhang Y, Du R, Zhai F, Rasco BA, Huang Y. Determination of chloramphenicol and crystal violetwith surface enhanced Raman spectroscopy. Sens Instrum Food Quality Safety. 2011;5:19–24.

[37] Mao A, Jin X, Gu X, Wei X, Yang G. Rapid, green synthesis and surface-enhanced Raman scattering effect of single-crystal silver nanocubes. J Mol Struct. 2012;1021:158–61.

[38] Atassi F, Mao C, Masadeh AS, Byrn SR. Solid-state characterization of amorphous and mesomorphous calcium ketoprofen. J Pharm Sci. 2010;99(9):3684–597.

[39] Numako M, Takayama T, Noge I, Kitgawa Y, Todoroki K, Mizuno H, *et al.* Dried saliva spot (DSS) as a convenient and reliable sampling for bioanalysis: an application for the diagnosis of diabetes mellitus. Anal Chem. 2016;88:635–9.

SUPPORTING INFORMATION

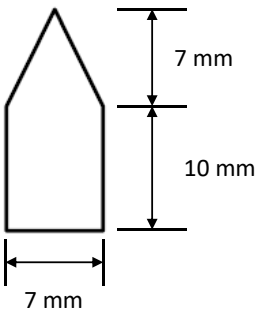

Figure S1. Shape and dimensions of filter paper used as substrate for immobilization of the AgNFs.

Attenuated total reflection infrared spectroscopy characterization of the PADs

The different PADs were also characterized by infrared spectroscopy. The ATR-IR spectra of raw filter paper, filter paper coated with 3% nylon-6 in formic acid (ny-paper), filter paper coated with 3% nylon-6 in formic acid and reduced silver on its surface (ny/Ag-paper), the final ny-AgNF PAD and pure nylon-6 are shown in Fig. S2. The spectrum of bare paper shows bands at 3334, 2897, 1161 and 1033 cm^{-1}, which are related to the OH stretching, CH symmetrical stretching, asymmetrical C-O-C stretching, and C-O stretching, respectively [1, 2]. The latter is the most intense band among the four mentioned and it is present in the four PADs. On the other hand, two characteristic amide bands of nylon-6 are observed at 1546 and 1642 cm^{-1} (Fig. S2e), corresponding to the C=O stretching of the amide group and the N-H deformation band of the amide, respectively [1, 2]. However, these bands are not visible in the spectra of the PADs as the content of nylon-6 is very low. It should be pointed out that in the case of the ny/Ag-paper (Fig. S2c), the amide bands are barely observed. This could be as a consequence of the silver layer directly in the contact with the nylon coating, which could lead to an enhancement of the infrared absorption. Nevertheless, after further coating with ethylendiamine and AgNFs, the

effect on the signal of nylon is negligible. In general, the main difference observed between the four PADs is related to the OH stretching band at 3334 cm^{-1}, which decreases when AgNFs are present, as shown in Fig. S2d.

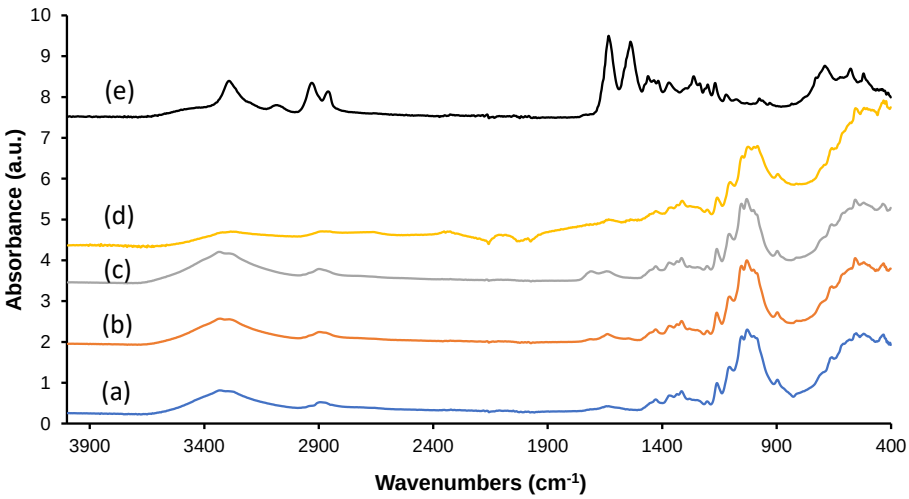

Figure S2. ATR-IR spectra of (a) raw filter paper, (b) filter paper with nylon-6, (c) filter paper with nylon-6 and silver, (d) ny-AgNF PAD and (e) pure nylon-6.

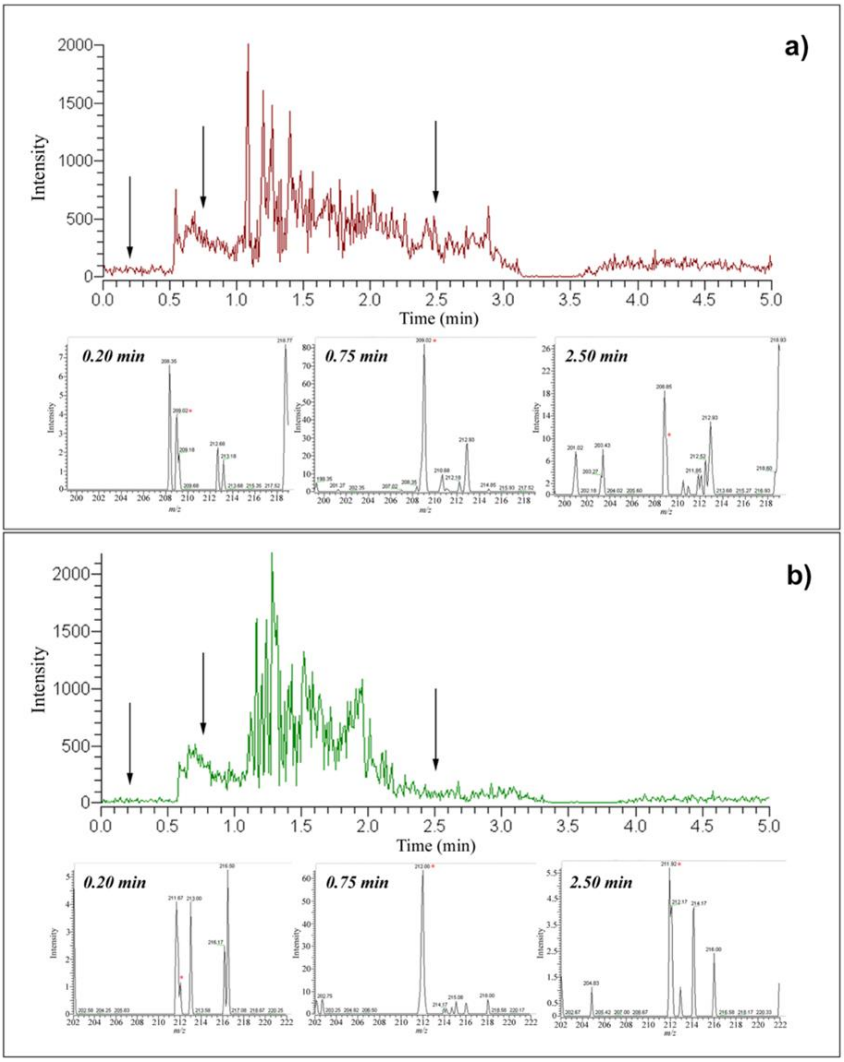

Figure S3. Chronogram by deposition of (a) ketoprofen and (b) the IS on ny-AgNF PADs at 0.025 mg·L^{-1} in methanol. In the lower section of each panel, the total ion mass spectra at different times (0.20, 0.75 and 2.50 min) are shown. The characteristic m/z signals marked with an asterisk.

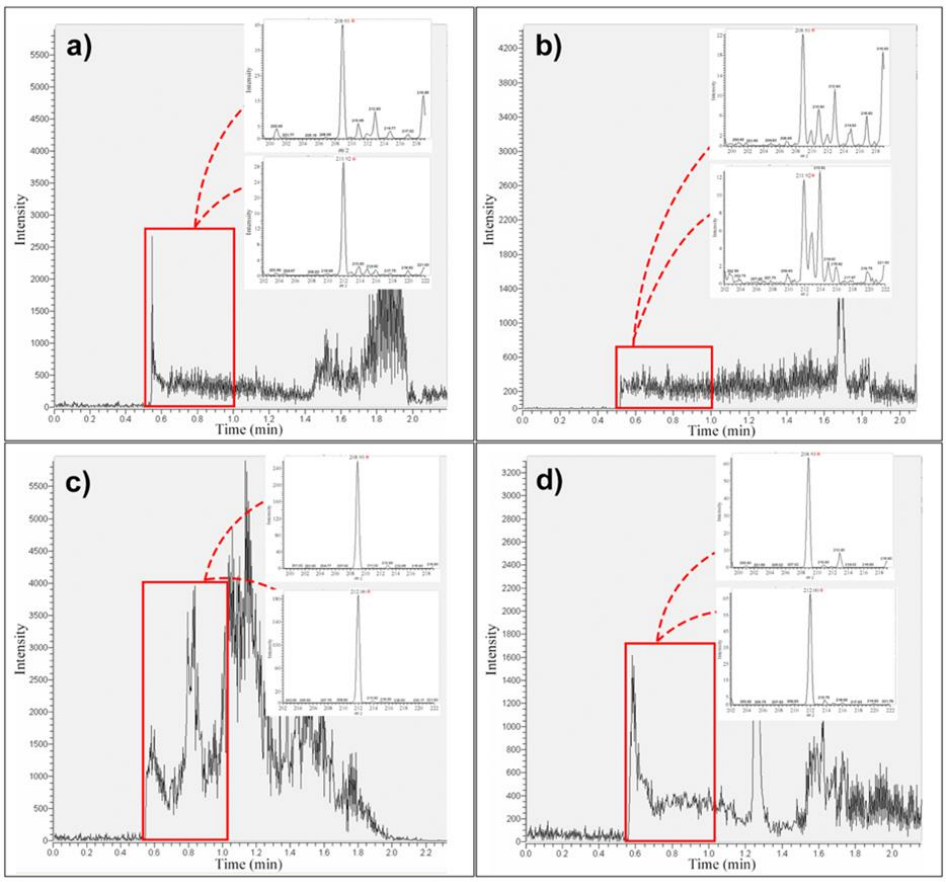

Figure S4. Chronograms of the PS-MS analysis using (a) raw filter paper, (b) ny/Ag-paper and (c) ny-AgNF PADs at 0.25 mg·L^{-1} in methanol. Additionally, the response of ny-AgNF PADs at a lower concentration (0.025 mg·L^{-1}) is represented (d).

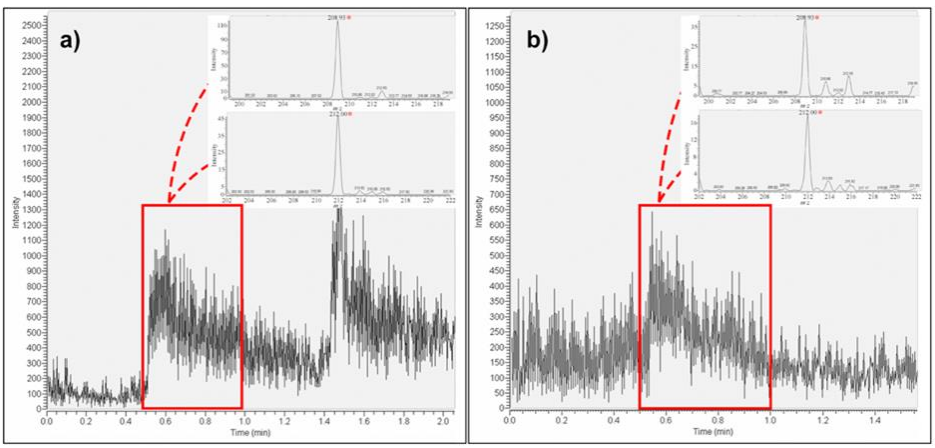

Figure S5. Chronograms and mass spectra of the PS-MS analysis using ny-AgNF PADs at 0.25 mg·L^{-1} in (a) methanol and (b) saliva.

References

[1] Ríos-Gómez J, Ferrer-Monteagudo B, López-Lorente AI, Lucena R, Luque R, Cárdenas S. Efficient combined sorption/ photobleaching of dyes promoted by cellulose/titania-based nanocomposite films. J Clean Prod. 2018;194:167–73.

[2] Reyes-Gallardo EM, Lucena R, Cárdenas S. Silica nanoparticles-nylon 6 composites: synthesis, characterization and potential use as sorbent. RSC Adv. 2017;7:2308–14.

BLOQUE V

RESULTADOS Y DISCUSIÓN

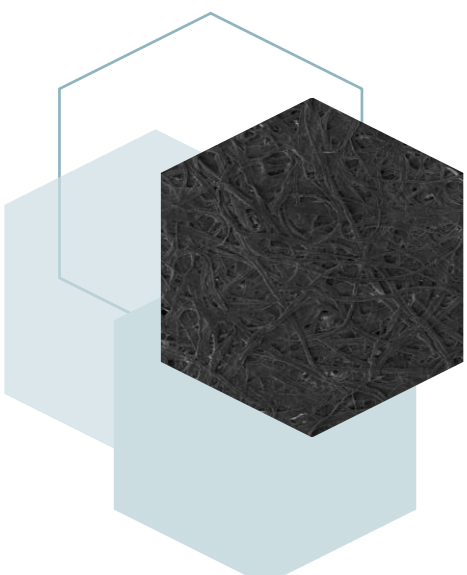

En este apartado se recogen los resultados más relevantes obtenidos a lo largo del desarrollo de la presente Tesis Doctoral. Teniendo en cuenta que los resultados específicos de cada trabajo han sido previamente discutidos en profundidad en los respectivos capítulos, en este apartado se expondrán los aspectos más importantes del trabajo experimental llevado a cabo, destacando las ventajas e inconvenientes de los métodos desarrollados.

De manera general, el trabajo experimental llevado a cabo en esta Memoria ha consistido en la síntesis de soportes planos basados en papel modificados con polímeros o nanopartículas para su empleo como sistemas analíticos de respuesta rápida acoplados con distintas técnicas instrumentales. Este bloque se divide en tres secciones, según el grado de complejidad de la modificación del soporte plano basado en papel empleado:

- **Papel de filtro sin modificar como alternativa sostenible y asequible.** En este apartado se discutirán las ventajas del empleo del papel de filtro sin modificar como material sorbente.
- **Soportes planos basados en papel modificados con polímeros de impresión molecular.** En este apartado se describirá la síntesis y caracterización de los polímeros de impresión molecular (MIPs) desarrollados y su aplicación como recubrimiento de papel de filtro para el desarrollo de materiales selectivos.
- **Soportes planos basados en papel modificados con nanopartículas.** En este apartado se abordará la síntesis y caracterización de nanopartículas de plata con geometrías no convencionales y su empleo en la modificación de papel de filtro para el desarrollo de soportes planos duales compatibles con distintas técnicas instrumentales.

1. Papel de filtro sin modificar como alternativa sostenible y asequible.

Uno de los principios de la Química Analítica Verde sugiere el análisis directo de las muestras, evitando el tratamiento de estas, para minimizar el impacto ambiental de

los procedimientos analíticos. Sin embargo, hay matrices de muestra que son extremadamente complejas y, por tanto, el tratamiento de muestra se vuelve imprescindible en su análisis. En estos casos, la solución consiste en desarrollar procedimientos de tratamiento de muestra que tengan un impacto medioambiental bajo y que a su vez sean eficientes.

El uso de materiales naturales, como por ejemplo el papel, ha aumentado en los últimos años como alternativa a los procedimientos de extracción tradicionales. En este caso, se estudió su potencial como material sorbente sin modificar, aprovechando la interacción que se produce entre los grupos funcionales de la celulosa y las aminas, las cuales son capaces de introducirse entre las fibras de celulosa y formar puentes de hidrógeno con estas **(Capítulo 2)**.

Las aminas biogénicas son moléculas de bajo peso molecular relacionadas con distintos procesos metabólicos de las células y que se pueden encontrar en algunos alimentos y bebidas. La ingesta de una gran cantidad de estos compuestos puede derivar en serios problemas de salud, como arritmias o dolor de cabeza, entre otros, por lo que el control de la cantidad de aminas biogénicas en matrices alimenticias es de gran importancia. El procedimiento desarrollado en este trabajo permitió la determinación rápida y directa de cadaverina, histamina, feniletilamina, putrescina, espermidina, espermina y tiramina en ocho cervezas de distintas características.

1.1. Optimización del proceso de extracción

Se estudiaron tres variables que podían afectar al proceso de extracción, como son el contenido de etanol, el pH y la fuerza iónica. Los resultados obtenidos en el caso del contenido de etanol y la fuerza iónica no presentaron diferencias significativas en el intervalo estudiado, 0-20 % y 18-3.5·10^{-4} μΩ·cm, respectivamente, por lo que se decidió trabajar con los valores observados en las muestras reales para simular la matriz de la muestra. En el caso del pH, la extracción de la espermidina y la histamina se vio favorecida a pH básico, sin embargo, se decidió trabajar a pH ácido debido a que se obtuvieron mejores resultados de reproducibilidad, y la señal de

todos los compuestos era buena. Además, las muestras tenían valores similares de pH, por lo que se evitó tener que ajustar este parámetro, simplificando así el procedimiento.

También se estudió el tiempo de extracción en el intervalo de 15 a 60 min, aunque no hubo diferencias significativas entre los resultados obtenidos, lo cual se comprobó mediante análisis de varianza (ANOVA). Por este motivo, se seleccionó un tiempo intermedio de 45 min para asegurar que todos los compuestos se extrajeran adecuadamente.

Tras este estudio, se concluyó que las muestras podrían ser analizadas directamente, sin necesidad de un tratamiento complejo de muestra, siendo únicamente necesaria su desgasificación previa a la extracción, lo que aceleró considerablemente el proceso analítico.

1.2. Determinación de aminas biogénicas en muestras de cerveza mediante espectrometría de masas.

Para la validación analítica del método, fue necesario llevar a cabo dos modelos de calibración diferentes. Inicialmente, se construyó una recta de calibrado para cada uno de los analitos con estándares acuosos ajustados con valores de pH, fuerza iónica y contenido de etanol similares a los de las muestras reales. Sin embargo, no se pudo aplicar este modelo de calibración para el análisis de las muestras reales debido a que las pendientes de las rectas fueron estadísticamente diferentes. Por lo tanto, se procedió al análisis de las muestras mediante el método de adición estándar. Todas las aminas se detectaron en las ocho muestras, excepto la histamina y la feniletilamina, cuyos valores de concentración estuvieron por debajo del límite de detección en algunas de ellas.

Los valores de LODs y LOQs obtenidos estuvieron por encima a los obtenidos en otros trabajos anteriormente publicados. Sin embargo, en estos casos se introduce una separación cromatográfica previa, lo que requiere un tiempo de análisis superior. Teniendo en cuenta que normalmente las aminas biogénicas se

encuentran a una concentración relativamente alta, no se vio necesario incluir una etapa de separación cromatográfica. En su lugar, se procedió a la infusión directa de los eluidos, y los valores de concentración de aminas biogénicas obtenidos se ajustaron a los que normalmente se encuentran en cervezas.

Este trabajo presenta numerosas ventajas. En primer lugar, se aprovecharon las ventajas del papel de filtro como material sorbente, destacando la posibilidad de interacción con las aminas biogénicas sin necesidad de ser modificado, además de ser barato y de fácil disponibilidad. La simplicidad del proceso permitió reducir el consumo de reactivos y disolventes, así como del tiempo del proceso analítico. Por otro lado, el empleo de infusión directa en el espectrómetro de masas también reduce el tiempo de análisis, ya que se evita la etapa previa de separación cromatográfica, obteniéndose así resultados en menos de 2 minutos. Además, debido a que la extracción se lleva a cabo en tubos Eppendorf, es posible realizar varias extracciones simultáneas, lo que aumenta la frecuencia de análisis de manera considerable.

Esta primera evaluación del potencial del papel de filtro sin modificar para la extracción de aminas biogénicas de muestras alimenticias abre la puerta para otras futuras aplicaciones con muestras de alimentos más complejas, como por ejemplo pescados o quesos.

2. Soportes planos basados en papel modificados con polímeros de impresión molecular.

Como se ha descrito anteriormente en el **Capítulo 3**, la capacidad sorbente de un material ha sido tradicionalmente el factor más importante para su elección, dejando en segundo plano la selectividad que proporciona. Por este motivo, se hace necesario introducir una etapa de separación cromatográfica y/o técnicas instrumentales sofisticadas, como la espectrometría de masas, para conseguir la selectividad que no proporciona el material sorbente. Sin embargo, en la actualidad existe una tendencia hacia el desarrollo de procedimientos más simples y rápidos

que a su vez proporcionen resultados fiables. Por este motivo, la selectividad de los sorbentes empleados en el tratamiento de la muestra ha adquirido mayor protagonismo. Además, el hecho de poder eliminar las interferencias de la matriz en etapas previas permite el análisis directo del extracto, simplificando y acelerando los procesos de medida.

Por otro lado, en las técnicas de microextracción, la cantidad de material sorbente empleada es menor debido a la miniaturización de la técnica, por lo que es muy importante tener en cuenta la selectividad de dicho material, sobre todo cuando se trabaja con muestras especialmente complejas, donde los componentes de la matriz dificultan la interacción de los analitos diana con el sorbente. En este contexto, el empleo de la tecnología de impresión molecular ha experimentado un gran crecimiento debido a las múltiples ventajas de estos materiales.

En este escenario se enmarca el segundo bloque de la Memoria, en el que se describe el empleo de polímeros de impresión molecular como recubrimiento de papel de filtro. Estos soportes planos basados en papel se emplean como sorbentes en la etapa de tratamiento de la muestra. En el **Capítulo 3** se recogen las propiedades de los polímeros de impresión molecular que los convierten en un gran aliado en los procesos de extracción, siendo la principal ventaja la capacidad de reconocer selectivamente a la molécula empleada como molde durante el proceso de síntesis. Los MIPs poseen estabilidad química y mecánica, entre otras, lo que los convierte en una alternativa idónea a las biomoléculas de reconocimiento selectivo. En cuanto a su obtención, tradicionalmente se han sintetizado llevando a cabo una polimerización en presencia de la molécula molde. No obstante, las condiciones experimentales asociadas a este tipo de reacción son muy estrictas. Por este motivo, en los **Capítulos 4 y 5** se aborda una síntesis alternativa basada en la disolución del polímero comercial.

2.1 Síntesis, caracterización y aplicación de los MIPs como material sorbente.

El objetivo de los **Capítulos 4 y 5** fue la síntesis de polímeros impresos

molecularmente y su posterior deposición en papel de filtro para su empleo como material sorbente en microextracción.

Como se ha mencionado, la síntesis tradicional de estos materiales lleva asociada una polimerización, por lo que es necesario llevar un control exhaustivo de las condiciones experimentales. Sin embargo, en el caso de los MIPs empleados en esta Tesis Doctoral, se utilizó un procedimiento alternativo. La obtención de los MIPs se desarrolló aprovechando la solubilidad del nylon-6 en ácido fórmico. Durante este proceso, las cadenas del polímero se separan y permanecen solvatadas en la disolución, pudiendo así interaccionar con la molécula molde a través de interacciones típicas de las poliamidas. Por un lado, se pueden formar puentes de hidrógeno inter- e intramoleculares gracias al grupo amida del nylon-6. Además, las interacciones iónicas también son posibles debido a los residuos carboxílicos y los grupos amino protonados. Por otro lado, debido a la naturaleza alifática de las cadenas poliméricas, también se pueden formar interacciones hidrofóbicas. Todos estos tipos de interacción posibilitan el reconocimiento selectivo de los analitos.

Una vez preparada la disolución precursora de polímero del MIP, el recubrimiento del papel se lleva a cabo mediante simple deposición **(Capítulo 4)** o mediante inmersión de una tira de papel de filtro en la disolución **(Capítulo 5)**. Tras la evaporación del disolvente, se forma el MIP, que queda físicamente inmovilizado en la superficie del papel. Gracias a esta síntesis alternativa, la cantidad de disolvente empleado se reduce, lo que va en sintonía con las tendencias de la Química Verde. Este procedimiento rápido y simple de síntesis supone una gran ventaja en la obtención de estos materiales.

Una vez sintetizado el papel modificado con el MIP, el material se caracterizó mediante tres técnicas: microscopía electrónica de barrido (*scanning electron microscopy*, SEM), espectroscopia Raman y espectroscopia infrarroja en la modalidad de reflectancia total atenuada (*attenuated total reflection Infrared spectroscopy*, ATR-IR). De este modo, se pudo verificar la modificación del papel con el MIP no solo visualmente mediante SEM, sino también gracias a las bandas

características del nylon-6 observadas en los espectros Raman e IR.

- *Microscopía electrónica de barrido*: mediante el empleo de esta técnica, se pudo estudiar la morfología de la superficie del material sintetizado, observándose un mayor recubrimiento de la estructura del papel a medida que aumentaba la concentración de polímero. En la Figura 1a se muestran imágenes SEM del papel de filtro sin recubrir y recubierto por el MIP, respectivamente. Como se puede observar, el papel pierde parte de la porosidad de su estructura como consecuencia de la modificación con el MIP.
- *Espectroscopia Raman*: el análisis de la superficie del papel modificado con MIPs reveló bandas características tanto del papel como del nylon-6, cuya intensidad aumentó a medida que lo hacía la concentración de polímero. Al mismo tiempo, las bandas del papel desaparecieron progresivamente debido al recubrimiento polimérico, como se puede observar en la Figura 1b.
- *Espectroscopia infrarroja*: al igual que la espectroscopia Raman, la espectroscopia infrarroja reveló las bandas características del papel y del nylon-6. Asimismo, en la Figura 1c se observa que la intensidad de las bandas correspondientes al grupo amida del nylon-6 fue aumentando a medida que lo hizo la concentración de polímero. Sin embargo, en este caso, las bandas características del papel no desaparecieron.

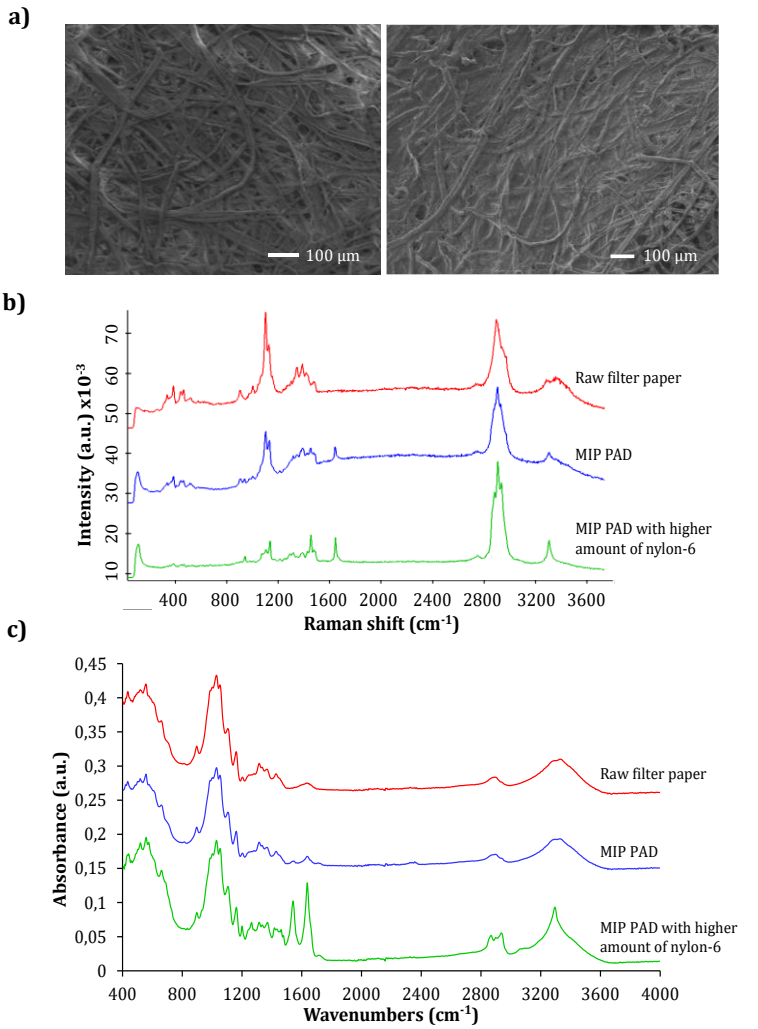

Figura 1. a) Imágenes SEM de papel de filtro sin modificar (izquierda) y papel de filtro modificado con MIP (derecha), b) espectros Raman de papel de filtro sin modificar, MIP PAD y MIP PAD con una mayor cantidad de nylon-6 (de arriba hacia abajo, respectivamente) y c) espectros IR de papel de filtro sin modificar, MIP PAD y MIP PAD con una mayor cantidad de nylon-6 (de arriba hacia abajo, respectivamente).

Por otro lado, también se evaluó la capacidad sorbente del material y se llevaron a cabo estudios de selectividad para comprobar que el MIP mejora la extracción del analito diana. Para ello, en el **Capítulo 4** se empleó la quinina como analito modelo debido a la fluorescencia intrínseca de esta molécula. En primer lugar, se comparó la capacidad de adsorción de un papel modificado con el MIP (MIP PAD), un papel sin modificar y un papel modificado con un polímero no impreso molecularmente (NIP PAD) para demostrar la extracción preferente del analito diana del MIP. Además, se llevaron a cabo estudios de selectividad en los que se evaluaron tanto el efecto del NaCl como la presencia de otra molécula orgánica fluorescente, como es la norfloxacina. Con los resultados obtenidos se pudo demostrar que:

- Los MIP PADs poseen una mayor capacidad de adsorción. En la Figura 2a se muestran imágenes bajo la lámpara ultravioleta (UV) del papel sin modificar y un MIP PAD y un NIP PAD tras la extracción de disoluciones acuosas de quinina. Como se puede observar, la intensidad de fluorescencia es mayor cuando se emplea el MIP PAD. Esta diferencia también se comprobó de manera cuantitativa (Figura 2b), demostrándose así la mayor capacidad de extracción de los MIP PADs.
- La inmovilización de las moléculas de quinina en los MIP PADs minimizan el conocido efecto *quenching* de fluorescencia provocado por los iones cloruro del NaCl en disolución. No obstante, una elevada concentración de NaCl provocó una disminución de la señal de fluorescencia como consecuencia del aumento de la fuerza iónica.
- La presencia de otra molécula orgánica fluorescente no interfiere con el proceso de extracción de la quinina o en sus propiedades fluorescentes. En la Figura 2c se muestran imágenes bajo la lámpara UV del MIP PADs tras la extracción de una disolución de quinina, una disolución de norfloxacina y una disolución conteniendo ambos analitos, respectivamente. Como se puede observar, únicamente hay intensidad de fluorescencia en presencia de quinina, demostrándose así la selectividad en la extracción de los MIP PADs.

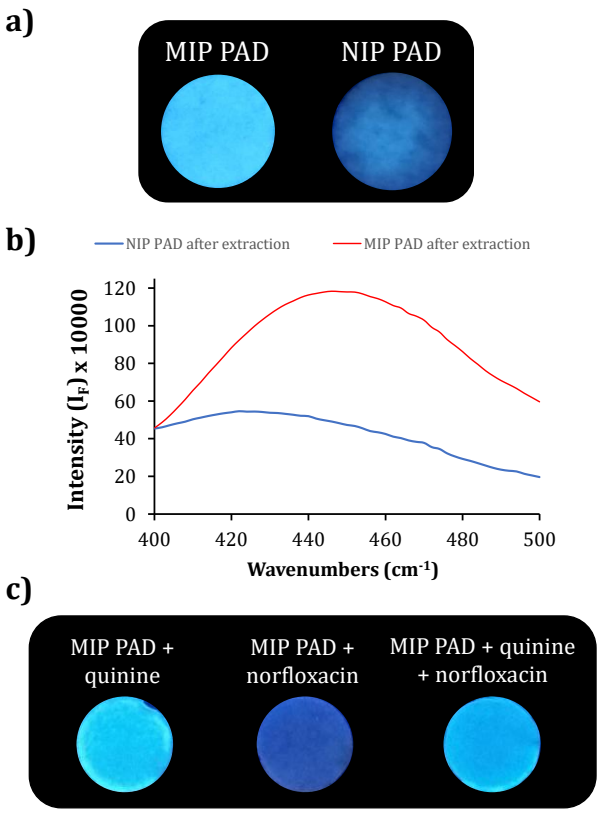

Figura 2. a) Imágenes bajo la lámpara UV de un MIP PAD (izquierda) y un NIP PAD (derecha) tras la extracción de una disolución de quinina a 5 mg·L^{-1}, b) espectros de fluorescencia de un MIP PAD y un NIP PAD tras la extracción del analito y c) imágenes bajo la lámpara UV del estudio de selectividad de un MIP PAD tras la extracción de una disolución de quinina de 5 mg·L^{-1}, un MIP PAD tras la extracción de una disolución de norfloxacina a 5 mg·L^{-1} y un MIP PAD tras la extracción de una disolución conteniendo ambos analitos a 5 mg·L^{-1}.

En el **Capítulo 5** la síntesis del MIP se llevó a cabo del mismo modo que en el caso anterior, aunque, en este caso, se emplearon dos moléculas molde: cocaína (CO) y metanfetamina (MTA). El empleo de un doble *imprinting* permite simplificar el proceso analítico debido a que no es necesario sintetizar un material para cada uno

de los analitos, sino que con el mismo es posible extraer ambos compuestos. Además, se reduce el consumo de reactivos y disolventes. Debido a la similitud de este papel con MIP y el MIP PAD descrito en el **Capítulo 4,** en este caso no se llevó a cabo una caracterización exhaustiva del material. En cuanto a la evaluación de la selectividad del papel MIP, se realizó a dos niveles: antes y después de la optimización de variables. Antes de la optimización se estudió la selectividad inicial del material en comparación con la de un papel modificado con el NIP empleando 6-acetilmorfina (6-AM) como interferente. La señal obtenida en el caso de la 6-AM fue despreciable frente a la de la CO y MTA. Además, el papel MIP proporcionó una señal mayor para el CO y MTA, demostrándose así no solo la selectividad del material frente a los analitos diana, sino también su mayor capacidad de extracción.

Tras la optimización de las distintas variables que podían afectar a la capacidad sorbente de los MIPs (pH, fuerza iónica, dilución de la muestra, cantidad de nylon-6, número de *dips* y tiempo de extracción), se llevaron a cabo dos estudios comparativos de los papeles MIP frente al papel modificado con el NIP. En primer lugar, se comparó la capacidad de extracción de ambos tras la extracción de disoluciones acuosas de CO y MTA, y en segundo lugar se llevó a cabo este mismo procedimiento, pero en la matriz de la muestra, saliva diluida. En ambos casos la señal del papel MIP fue considerablemente superior a la del papel modificado con el NIP, sin embargo, cuando se comparó la señal de las muestras de saliva con la proporcionada por los estándares, se observó una disminución. Esto se puede atribuir a la presencia de proteínas en la muestra, las cuales obstruyen las cavidades y, por tanto, disminuyen la capacidad de extracción del material. No obstante, este problema puede solventarse mediante una dilución mayor de la muestra.

2.2. Determinación de quinina en bebidas carbonatadas.

En el **Capítulo 4** se empleó un MIP PAD para la determinación de quinina en bebidas carbonatadas mediante espectrofluorimetría. La quinina es un alcaloide que se emplea como aromatizante en bebidas como la tónica, proporcionándole su

característico sabor amargo. Se seleccionó esta molécula como analito debido a su fluorescencia intrínseca, la cual permitió la evaluación rápida y simple del material desarrollado.

Debido a que la síntesis de los MIPs se realizó mediante un proceso alternativo al tradicional, se estudiaron diversas variables que podían afectar a la capacidad final de extracción de los MIP PADs. En primer lugar, se evaluaron tres variables relacionadas con la síntesis del MIP, como son la cantidad de nylon-6, la cantidad de porógeno (dimetilformamida, DMFA) y la cantidad de molécula molde (quinina), ya que estas pueden influir tanto en el espesor del MIP en el papel como en la morfología final del MIP, así como en la formación de las cavidades y puntos de reconocimiento de los analitos diana. Por otro lado, se estudiaron las variables relacionadas con el proceso de extracción que podían afectar a la interacción del analito con el MIP, es decir, el pH, el tiempo de extracción y la fuerza iónica. De todos los estudios, se puede destacar la importancia de la optimización del pH, pues este parámetro afecta a la forma en la que se encuentran los analitos y el polímero y, por tanto, puede afectar considerablemente a la interacción entre ambos.

También se estudió la reusabilidad de los MIP PADs extrayendo disoluciones acuosas de quinina y limpiando el material con una mezcla de metanol y ácido acético entre medidas. De esta manera, se comprobó que los MIP PADs se pueden reutilizar al menos seis veces.

Un aspecto a destacar de este trabajo es la síntesis simple y rápida llevada a cabo para la obtención de los MIPs, así como su inmovilización en papel de filtro, lo cual aumentó la versatilidad del material. De esta manera, se disminuyó el volumen de disolvente empleado en comparación con la síntesis convencional de los MIPs, y además el tiempo de obtención fue inferior a 15 min. Por otro lado, al emplear fluorimetría, la obtención de resultados es casi inmediata (< 40 s). Teniendo en cuenta que las medidas se realizan directamente sobre el papel y se evita la etapa de elución, el tiempo y el consumo de disolventes se ve reducido aún más.

Otra ventaja de la síntesis llevada a cabo en este trabajo es que es posible emplear

el polímero comercial, evitando así la reacción de polimerización y el control de las condiciones experimentales que conlleva. Además, se podría evaluar la posibilidad de reciclar polímeros para la síntesis de los MIPs, lo que disminuiría aún más el coste del procedimiento, así como el impacto medioambiental.

2.3. Determinación de cocaína y metanfetamina en muestras de saliva.

En el **Capítulo 5** se llevó a cabo la determinación de CO y MTA en muestras de saliva mediante el empleo de un papel MIP y espectrometría de masas. Estas dos drogas son estimulantes y pueden afectar al sistema nervioso, causando hiperactividad y disipando la sensación de cansancio, hambre y sed. Además, el abuso en su consumo puede derivar en problemas cardíacos o incluso acelerar el proceso degenerativo de algunas enfermedades como la arterosclerosis. Por lo tanto, la determinación de estos compuestos es de vital importancia. Tradicionalmente, la determinación de drogas de abuso se ha llevado a cabo en diversas muestras biológicas, como la sangre, el pelo o la orina, pero la toma de estas muestras es invasiva y, además, requiere la presencia de personal especializado. Sin embargo, la recolección de saliva en un proceso fácil, indoloro y no invasivo, que no requiere de personal especializado. Por otro lado, se puede monitorizar el proceso de recolección, evitando así la alteración de la muestra.

Como se ha mencionado anteriormente, la síntesis empleada en la obtención de este papel modificado con MIP es la misma que la llevada a cabo en el **Capítulo 4**, excepto porque en este caso se utilizan dos moléculas molde, CO y MTA. De igual forma se sintetizaron los NIPs, pero sin adicionar las moléculas molde.

El proceso de extracción también es distinto al llevado a cabo en el **Capítulo 4**, ya que en este caso se realiza en tubos Eppendorf colocados en un agitador orbital. De este modo, es posible llevar a cabo múltiples extracciones de manera simultánea (Figura 3), lo que aumenta el rendimiento del proceso analítico y disminuye el tiempo global de análisis. Por otro lado, el empleo de la espectrometría de masas permite detectar concentraciones muy bajas en comparación con la

espectrofluorimetría.

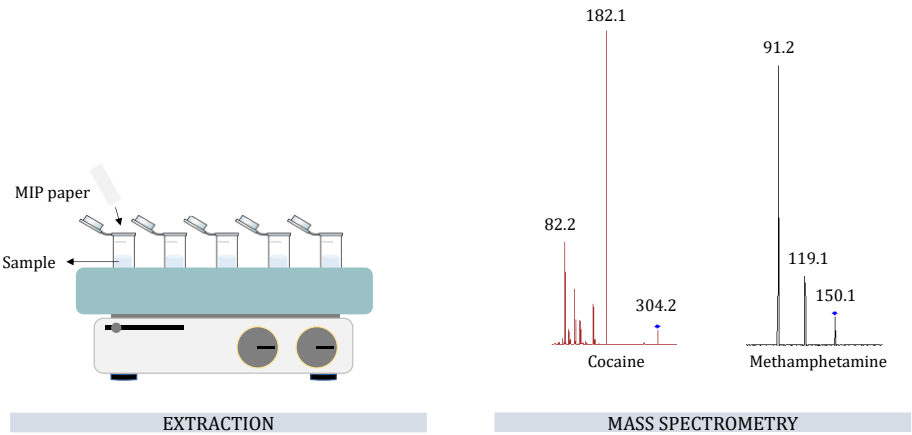

Figura 3. Esquema representativo del proceso de extracción (izquierda) y de los espectros de masas de la cocaína y la metanfetamina, con sus respectivos iones precursores e iones producto (derecha).

Para la optimización de variables se realizó un diseño factorial completo de tres niveles y tres factores (3^3 + 3 puntos centrales). Los factores seleccionados fueron la cantidad de nylon-6, el número de inmersiones del papel en la disolución del MIP y el tiempo de extracción. El efecto de estos factores y su interacción en función de la eficacia de la extracción se llevó a cabo mediante análisis de varianza (ANOVA). Tras este estudio, se seleccionó 8.3 $mg \cdot mL^{-1}$ como concentración óptima de polímero, con una única inmersión del papel en la disolución del MIP y 45 min de tiempo de extracción. Por otro lado, la dilución de la muestra, el pH y la fuerza iónica se evaluaron de manera independiente. El valor de pH seleccionado como óptimo fue de 10, y, en el caso de la fuerza iónica, los mejores resultados se obtuvieron sin ajustarla. Además, como ya se ha mencionado, la matriz de la muestra posee proteínas que pueden obstruir las cavidades del MIP y, por tanto, disminuir su capacidad de extracción, por lo que finalmente la muestra se diluyó 1:1 en agua milliQ.

Finalmente, el papel MIP se utilizó para la determinación de CO y MTA en saliva diluida mediante infusión directa en el espectrómetro de masas. La caracterización analítica del proceso se llevó a cabo mediante la construcción de dos rectas de calibrado, una en estándares acuosos y otra *in-matrix*. Los límites de detección obtenidos estuvieron en el orden de los $\mu g \cdot L^{-1}$, con buenos valores de reproducibilidad (desviación estándar relativa, DER, < 5.9%) y una recuperación el 84 y el 98%, demostrándose así la aplicabilidad del papel MIP sintetizado.

3. Soportes planos basados en papel modificados con nanopartículas.

El papel de filtro posee múltiples ventajas como sorbente, siendo una de ellas la posibilidad de modificarlo químicamente. Estas modificaciones aumentan la versatilidad del material desarrollado, proporcionándole nuevas vías de interacción con los analitos, o incluso estabilidad mecánica y química extra. Al igual que en el caso de los MIPs, la modificación del papel con nanopartículas aumenta el área superficial de este, así como su selectividad. En el **Capítulo 6** de la Memoria se muestra una visión general del uso de membranas modificadas con nanopartículas en la etapa de tratamiento de muestra.

La incorporación de nanopartículas en soportes planos no solo puede ser favorable en los procesos de adsorción y posterior elución, sino que también pueden ser un aliado en técnicas como la espectrometría de masas en la modalidad de *paper-spray*. Esta técnica simplifica considerablemente el proceso analítico, evitando la etapa de tratamiento de muestra. El principio de esta técnica se basa en la creación de un aerosol de la muestra como consecuencia de la diferencia de potencial que se produce entre la entrada del espectrómetro de masas y la punta del soporte. Debido a esto, el empleo de nanopartículas metálicas puede influir positivamente en la creación de este aerosol, ya que aumentan la conductividad del soporte empleado.

Por otro lado, el empleo de nanopartículas metálicas, especialmente de oro y de plata, han sido objeto de estudio en las últimas décadas en técnicas espectroscópicas como la espectroscopia Raman amplificada en superficie (*surface-enhanced Raman*

spectroscopy, SERS) debido a las propiedades del plasmón superficial que poseen. Gracias a esto, se consigue un aumento de la señal Raman y, por lo tanto, la sensibilidad de la técnica también aumenta. Este efecto se puede explicar teniendo en cuenta dos mecanismos, el electromagnético (*electromagnetic mechanism,* EM*)* y el químico (*chemical mechanism,* CM*)*. En el caso del EM, se produce un incremento del campo electromagnético en la superficie del nanomaterial debido a la excitación del plasmón superficial, de modo que la luz se confina en ciertas regiones conocidas como *hot spots*, las cuales son responsables del efecto SERS. En cuanto al CM, el incremento de la señal Raman viene dado por interacciones químicas entre el analito diana y el sustrato. Por otro lado, la geometría de la nanopartícula también afecta al efecto SERS observado, obteniéndose una mejora de la señal cuando se emplean geometrías con bordes afilados, puntas, aristas, etc., debido al aumento del número de *hot spots.* Entre ellas, se pueden encontrar nanoestrellas, nanotriángulos, nanocubos o, en el caso de este trabajo, nanoflores de plata (AgNFs). Sin embargo, la síntesis de sustratos SERS que sean reproducibles no es simple ni asequible, aunque, en el trabajo desarrollado en el **Capítulo 7** ha sido posible superar esta limitación gracias a la inmovilización de las AgNFs en las fibras del papel de filtro.

3.1. Síntesis, caracterización y aplicación de los AgNF PADs como material sorbente.

El objetivo del trabajo que se describe en el **Capítulo 7** de la Memoria fue la síntesis de un papel de filtro modificado con nanoflores de plata para su uso como sorbente, soporte conductor y sustrato SERS que amplifique la señal en espectroscopia Raman amplificada en superficie y espectrometría de masas de alta resolución en la modalidad de *paper-spray* (*paper-spray mass spectrometry,* PS-MS).

La síntesis de las AgNFs se llevó a cabo empleando un procedimiento anteriormente descrito que emplea nitrato de plata como precursor de plata. La adición de citrato de sodio en el medio deriva en la formación de un complejo entre la plata y el citrato, observándose un precipitado de color blanco. Por otro lado, la adición de amoniaco

provoca que el precipitado se disuelva como consecuencia de la formación de un complejo iónico entre la plata y el amoniaco. Finalmente, la adición de ácido ascórbico provoca el crecimiento de las AgNFs, lo cual se puede comprobar con el cambio de color de la disolución de transparente a negro.

Anteriormente se ha discutido la utilidad de la estructura fibrilar del papel, la cual proporciona una gran área superficial. Sin embargo, en SERS es necesario que el analito esté disponible en la superficie del soporte, por lo que la porosidad del papel es una desventaja en este caso, ya que el analito se introduce entre los huecos de las fibras y, por tanto, no está disponible en la superficie. Para evitar esto, el papel de filtro se recubrió previamente con nylon-6 para rellenar los huecos entre las fibras del papel. A continuación, se creó una capa de plata metálica añadiendo nitrato de plata, el cual fue reducido a plata metálica empleando luz ultravioleta. Por último, se creó el anclaje para las AgNFs mediante la incubación del papel de filtro en etilendiamina. Tras la inmersión del papel en la disolución de AgNFs, estas quedaron unidas a la etilendiamina mediante interacción con los grupos amino, obteniéndose así los AgNF PADs.

La caracterización del papel de filtro sin modificar, papel de filtro con nylon-6, un AgNF PAD sin nylon-6 y un AgNF PAD con nylon-6 (ny-AgNF PAD) se llevó a cabo mediante SEM y ATR-FTIR. De este modo se pudo observar la morfología de las AgNFs y su distribución por la superficie del papel, así como las bandas correspondientes a los distintos materiales presentes en el sustrato.

Las imágenes SEM no revelaron diferencias significativas en la estructura del papel en cuanto a la presencia de nylon-6. Sin embargo, sí es posible observar diferencias cuando las AgNFs están presentes, ya que se encuentran recubriendo la superficie del papel, como se muestra en la Figura 4a. La homogeneidad del recubrimiento es un factor muy importante, ya que puede afectar al efecto SERS. Además, en el detalle de la Figura 4a, se puede observar la estructura amorfa de las AgNFs, la cual contribuye positivamente al efecto SERS debido al aumento del número de *hot spots* mencionado anteriormente. El recubrimiento de AgNFs también derivó en una

mejora en la ionización de los analitos en el caso de PS-MS.

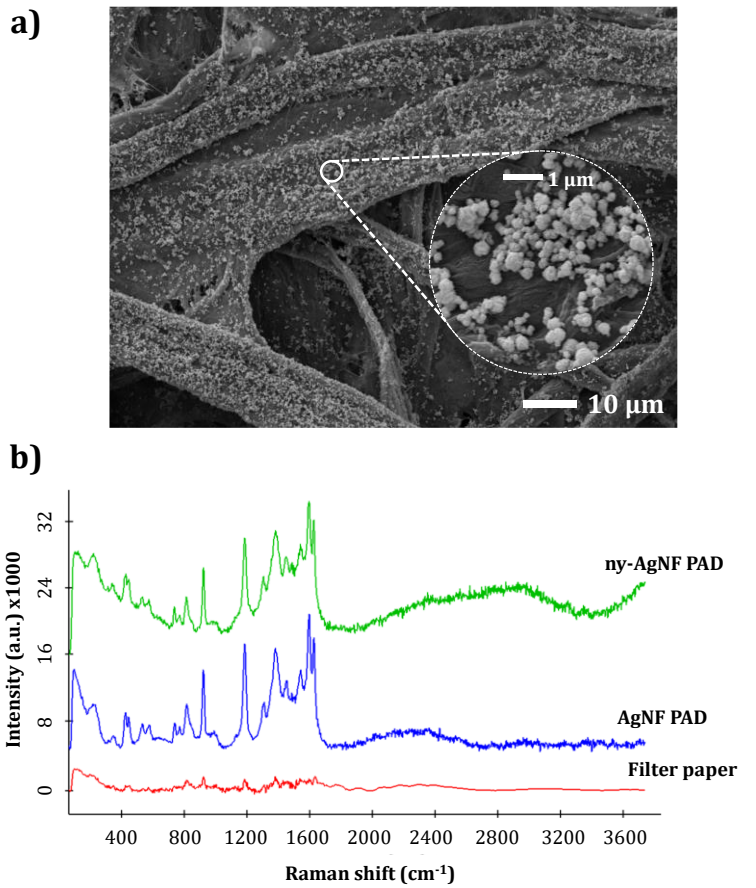

Figura 4. a) Imagen SEM de la distribución homogénea de AgNFs en el papel de filtro y b) espectros Raman de papel de filtro tras la deposición de CV a 5000 mg·L^{-1} y SERS de AgNF PAD y ny-AgNF PAD tras la deposición de CV a 10 mg·L^{-1}.

Una vez sintetizados y caracterizados, se evaluó el efecto SERS de los ny-AgNF PADs. Para ello, en primer lugar, se realizaron estudios con violeta cristal (CV, *crystal violet*, en inglés) como analito modelo. Este compuesto se utiliza con frecuencia en estudios

SERS para evaluar el efecto SERS de los sustratos, dada su baja fluorescencia y buena respuesta de amplificación de la señal. En la Figura 4b se muestran los espectros Raman del papel de filtro, y SERS de un AgNF PAD y un ny-AgNF PAD, respectivamente, tras depositar CV a 5000 $mg \cdot L^{-1}$ en el caso del papel de filtro sin modificar, y 10 $mg \cdot L^{-1}$ en el caso de los PADs. También se analizó un papel de filtro únicamente con plata metálica y el analito depositado en su superficie para comprobar que el aumento de la señal se debía a la presencia de las AgNFs y no a la capa de plata depositada previamente. Las principales diferencias se observaron entre los espectros de los sustratos con AgNFs y el papel de filtro, pudiéndose observar claramente las bandas características del CV. Por otro lado, la presencia del nylon-6 en la estructura del papel no interfiere con las medidas SERS del CV, pues no se observan diferencias significativas entre el AgNF PAD y el ny-AgNF PAD. El factor de aumento de la señal (*enhancement factor,* EF) se calculó a partir de las señales del CV en papel de filtro y en el ny-AgNF PAD, siendo este de $1.97 \cdot 10^4$.

3.2. Determinación de ketoprofeno mediante SERS.

Se evaluó la aplicabilidad de los ny-AgNF PADs para la determinación cuantitativa de ketoprofeno es estándares acuosos mediante deposición directa del analito en la superficie del material y mediante swabbing.

Al contrario que ocurre con el CV, en las medidas SERS del ketoprofeno sí se observan diferencias significativas con la presencia del nylon-6. Al mismo nivel de concentración, la determinación de ketoprofeno con AgNF PADs sin nylon-6 fue complicada, justificándose así el recubrimiento previo del papel con este polímero. Además, también se puede observar que las bandas características del nylon-6 no aparecen en el espectro, por lo que se concluye que la presencia de este no afecta en la determinación del analito.

Se construyeron dos rectas de calibrados, una mediante deposición directa del analito en la superficie del ny-AgNF PAD y otra mediante *swabbing* del ketoprofeno de la superficie de un portaobjetos. En ambos casos, los límites de detección (LOD)

y cuantificación (LOQ) estuvieron en el nivel de $mg \cdot L^{-1}$, pero en el caso del calibrado mediante *swabbing* los límites fueron menores. Además, la precisión de las medidas fue buena (DER < 8.8%).

3.3. Determinación de ketoprofeno en muestras de saliva mediante PS-MS.

Se evaluó la aplicabilidad de los ny-AgNF PADs en distintas etapas de la síntesis para la determinación de ketoprofeno mediante PS-MS. Para ello, se construyeron rectas de calibrado con papel de filtro, con papel de filtro modificado con nylon-6 y plata metálica (ny/Ag-papel), así como con ny-AgNF PADs utilizando estándares acuosos y con muestras de saliva. Los resultados mostraron un aumento de la sensibilidad en el caso de los ny-AgNF PADs como consecuencia de la presencia de las AgNFs. Sin embargo, para comprobar que esta mejora era consecuencia de la presencia de las AgNFs y no debido a la superficie de plata metálica depositada previamente, se construyó la recta de la calibrado con el ny/Ag-papel, demostrándose que la mejora de la sensibilidad se produjo gracias a las AgNFs.

Finalmente, se evaluaron los ny-AgNF PADs en la determinación de ketoprofeno en muestras de saliva mediante deposición y mediante *swabbing* de la muestra fortificada de la superficie de un portaobjetos. Así, se consiguieron LODs y LOQs del orden de pocos $mg \cdot L^{-1}$ en ambos casos, con buena reproducibilidad (DER < 5.7%) y una recuperación del ketoprofeno entre el 97 y el 119%.

Los aspectos a destacar de este trabajo son varios. En primer lugar, la síntesis del sustrato se realiza mediante un procedimiento simple. La capa inicial de plata metálica y la incubación en etilendiamina proporcionan estabilidad mecánica a las AgNFs, de manera que no se desprenden durante el proceso de extracción ni durante las medidas PS-MS. Además, la presencia de nylon-6 confiere al papel de una rigidez superior, lo que resulta útil para mantener una posición estable durante las medidas PS-MS. Por otro lado, al rellenar parcialmente los huecos del papel, asegura que el analito esté disponible superficialmente y se pueda medir correctamente mediante SERS.

Por otro lado, la presencia de nanoestructuras metálicas, como son las AgNFs, permitieron el aumento de la señal del CV y el ketoprofeno en SERS en comparación con el papel de filtro sin modificar. De igual manera, las AgNFs permitieron una mejora de la sensibilidad en las medidas PS-MS en comparación con los sustratos en distintas etapas de la síntesis de los ny-AgNF PADs.

En la Tabla 1 se muestra un resumen general de las características de los trabajos presentados en la Memoria de esta Tesis Doctoral, resaltando las ventajas de cada uno de ellos, así como la función que ha desempeñado el papel y la modificación llevada a cabo para mejorar la extracción de los analitos diana. Además, también se incluye la técnica a la que se acopla el soporte plano basado en papel desarrollado en los trabajos presentados.

Tabla 1. Características de los trabajos desarrollados en la presente Tesis Doctoral.

Rol del papel	Modificación	Analito diana	Técnica	Ventaja
Soporte	MIP	Quinina	Fluorimetría	Síntesis rápida y sencilla
Soporte	MIP	CO y MTA	MS (infusión directa)	Es posible determinar dos analitos con un único soporte plano
Soporte	AgNFs	Ketoprofeno	SERS y PS-MS	El soporte se puede acoplar a dos técnicas y mejora la sensibilidad de ambas
Fase extractante	-	Aminas biogénicas	MS (infusión directa)	Se explota la reactividad intrínseca de la celulosa con los analitos diana, sin modificación química

MIP: Polímero de impresión molecular, CO: Cocaína, MTA: Metanfetamina, MS: Espectrometría de masas, AgNFs: Nanoflores de plata, SERS: Espectroscopia Raman amplificada en superficie, PS-MS: Espectrometría de masas en la modalidad de *paper-spray*.

CONCLUSIONES

CONCLUSIONS

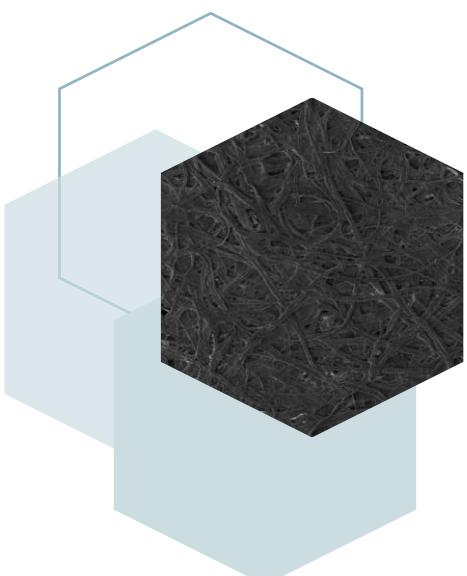

La investigación realizada en la presente Tesis Doctoral se ha centrado en el desarrollo de sistemas analíticos de respuesta rápida a través de la síntesis de soportes planos basados en papel que actúen como alternativa a las unidades de microextracción convencionales.

Como se ha discutido a lo largo de la Memoria, el tratamiento de muestra es una de las etapas más importantes del proceso analítico que, a su vez, conlleva mucho tiempo. Por este motivo, la tendencia de la Química Analítica en las últimas décadas se ha dirigido hacia la simplificación de esta etapa mediante el desarrollo de metodologías sencillas y rápidas que a la vez proporcionen resultados fiables. Esta simplificación lleva asociada la disminución de reactivos y disolventes, así como del volumen de muestra empleado, por lo que está en sintonía con los principios de la Química Verde.

El trabajo experimental se ha dividido en tres bloques en función de la modificación del papel llevada a cabo, y en ellos se ha descrito la síntesis, caracterización y evaluación analítica de los diferentes soportes planos basados en papel propuestos. En este bloque se resumen las conclusiones de los resultados obtenidos.

En cuanto a la **síntesis**, se han evaluado tres alternativas diferentes cuyo punto común es el uso del papel de filtro como soporte. En este sentido, los soportes planos basados en papel descritos en esta Memoria se han clasificado en base a que sea necesaria (con polímeros de impresión molecular o con nanopartículas) o no (papel sin tratar) la modificación del papel para favorecer la interacción con los analitos. Además, estos se han acoplado con técnicas instrumentales capaces de ofrecer resultados fiables y muy rápidos.

En el caso del **papel modificado con polímeros de impresión molecular (MIP)**, la síntesis utilizada se basó en la disolución de nylon-6 en ácido fórmico, de manera que las cadenas del polímero se separasen y quedasen solvatadas en disolución, pudiendo interaccionar con la molécula molde. De este modo, se evitó la reacción de polimerización normalmente empleada en la síntesis de estos materiales, la cual

requiere un control estricto de las condiciones experimentales y, además, un consumo mayor de reactivos, disolventes y energía. Además, la inmovilización del MIP en el papel de filtro aumentó la versatilidad de este soporte, pudiéndose acoplar fácilmente a la celda de un fluorímetro a través de una pieza magnética diseñada en el laboratorio.

Por otro lado, la síntesis del **papel modificado con nanopartículas** es un proceso sencillo compuesto por diversos pasos que dan lugar a la obtención de nanopartículas amorfas de plata. La inmovilización de las **nanoflores de plata (AgNFs)** en papel de filtro se consiguió a través de la funcionalización previa de la superficie del papel con plata metálica y etilendiamina, la cual sirvió como enlace para el anclaje de las AgNFs. Además, también fue necesario realizar un recubrimiento previo del papel con nylon-6 para asegurar la disponibilidad superficial del analito y, por tanto, su correcta determinación.

Finalmente, se evaluó el potencial del **papel de filtro sin modificar** como sorbente. Gracias a la estructura química de la celulosa, fue posible aprovechar su interacción con los analitos para aislarlos de la matriz de la muestra de manera eficiente. Esta aproximación permite una síntesis completamente respetuosa con el medio ambiente y, por tanto, en línea con los principios de la Química Verde, pues no se necesitan ni reactivos ni disolventes para su desarrollo.

La **caracterización** de los distintos soportes planos basados en papel obtenidos durante el desarrollo de esta Tesis Doctoral se ha llevado a cabo mediante diversas técnicas instrumentales con el objetivo de obtener información sobre su morfología y composición. De este modo, ha sido posible dilucidar la manera en la que se ha producido la interacción soporte-analito. Para ello se han empleado las siguientes técnicas: microscopía electrónica de barrido (SEM), espectroscopia Raman y espectroscopia de infrarrojo (ATR-FTIR).

- Mediante SEM fue posible comprobar cómo se iba recubriendo la superficie del papel con el aumento de la concentración de MIP. Además, también

permitió observar la morfología de las AgNFs.

- La espectroscopia Raman reveló la necesidad de realizar un recubrimiento inicial de nylon-6 en el caso del papel modificado con AgNFs para la correcta determinación del analito, y permitió evaluar cualitativa y cuantitativamente la aplicabilidad de este sustrato. Además, también proporcionó información sobre la composición de los distintos soportes planos basados en papel sintetizados.
- En cuanto a la ATR-FTIR, sirvió para estudiar las bandas características del papel y del MIP, observándose un aumento de la intensidad de las bandas del polímero a medida que aumentaba su concentración.

En cuanto al proceso de **extracción**, se ha perseguido su simplificación, consiguiendo en algunos casos un elevado rendimiento gracias a la realización de extracciones simultáneas mediante el uso de tubos Eppendorf y un agitador orbital. Además, también ha sido posible su miniaturización, empleando una cantidad reducida de muestra. Sin embargo, no se ha automatizado completamente este proceso, lo cual sería conveniente para evitar el error humano asociado a la etapa de tratamiento de muestra.

Las metodologías anteriormente descritas y discutidas en profundidad a lo largo de la Memoria se han evaluado mediante su aplicación en **muestras biológicas** (saliva) y **alimentos** (bebidas carbonatadas y cerveza), alcanzándose en todos los casos valores coherentes de sensibilidad y precisión con respecto a la técnica instrumental empleada.

El uso de saliva como matriz para la determinación de compuestos es una alternativa ideal al resto de muestras biológicas, ya que no requieren personal especializado para su obtención. Además, este procedimiento es no invasivo, como ocurre con las muestras de pelo o sangre, y permite un seguimiento controlado de la recolección, evitándose así la potencial alteración de la muestra. Por otro lado, el almacenamiento de saliva no requiere de medidas especiales, lo cual facilita su análisis. También es de especial interés para la demostración de la aplicabilidad de

los soportes planos basados en papel sintetizados, pues posee suficientes interferentes que sirven de desafío al proceso de extracción. Teniendo esta muestra como matriz, se determinaron un antiinflamatorio no esteroideo (ketoprofeno) y dos drogas de abuso (cocaína y metanfetamina). En el primer caso, la extracción se llevó a cabo mediante el empleo de un papel de filtro modificado con nanoflores de plata, y su determinación se realizó mediante espectroscopia Raman amplificada en superficie (SERS) y espectrometría de masas en la modalidad de *paper-spray (*PS-MS). En el segundo caso, la extracción de cocaína y metanfetamina se realizó a través de un papel modificado con un MIP y se determinaron mediante infusión directa en MS.

En cuanto a las muestras de alimentos se aprovechó la fluorescencia intrínseca de la quinina para su determinación en bebidas carbonatadas mediante espectrofluorimetría empleando un MIP PAD como sorbente. Por otro lado, se evaluó el potencial del papel de filtro sin modificar como sorbente para la extracción de aminas biogénicas de muestras de cerveza mediante infusión directa en MS.

Las técnicas instrumentales empleadas en los distintos trabajos llevados a cabo en la Tesis Doctoral han permitido la obtención simple y rápida de los resultados. El empleo de la espectrofluorimetría permite obtener espectros en un tiempo inferior a 40 s, pudiéndose así analizar una gran cantidad de muestras. Por otro lado, la infusión directa en espectrometría de masas evita la separación cromatográfica, por lo que el proceso de medida se acorta considerablemente, a la vez que mantiene su gran selectividad característica. En cuanto a SERS, es una alternativa a la espectroscopia Raman tradicional que se basa en el aumento de la señal gracias a confinamiento del campo electromagnético en regiones localizadas del sustrato—modificado con nanopartículas metálicas—conocidas como *hot spots*. De este modo, soslaya las desventajas de la espectroscopia Raman y se convierte en un aliado en el desarrollo de metodologías rápidas, simples y altamente sensibles. Por último, el empleo de la espectrometría de masas en la modalidad de *paper-spray* permite la determinación de los analitos de manera directa, es decir con una mínima o

inexistente preparación de la muestra, lo que simplifica considerablemente el proceso analítico de medida.

The research performed in this Doctoral Thesis is focused on the development of rapid response analytical methodologies via the synthesis of paper-based flat supports as an alternative to the conventional microextraction units.

As previously mentioned throughout this Doctoral Thesis, sample treatment is one of the most important steps of the analytical process, but it also requires a considerable amount of time. For this reason, Analytical Chemistry has aimed for the simplification of this step in the last decades through the development of simple and rapid procedures that provide reliable results. This simplification also implies the reagents and solvents used, as well as the sample volume, thus being in line with the principles of Green Chemistry.

The experimental work has been divided into three blocks according to the modification of the paper carried out, in which the synthesis, characterization and analytical evaluation of the paper-based flat supports synthesized have been discussed. In this block the conclusions from the obtained results are summarized.

Regarding the **synthesis**, three different alternatives having filter paper in common have been evaluated. Therefore, the paper-based flat supports described in this Thesis can be classified according to the modification performed on the filter paper to improve the interaction with the analytes, namely molecularly imprinted polymers, nanoparticles or no modification at all. Furthermore, these materials have been coupled to different instrumental techniques that have provided reliable results in a reduced amount of time.

On the topic of **filter paper modified with molecularly imprinted polymers (MIP)**, the synthesis was based on the dissolution of nylon-6 on formic acid, thus inducing the detachment of the polymer chains, which remained solvated in the solution, being able to interact with the template molecule. As a result, the strict control of the experimental conditions of the polymerization reaction usually carried out in the synthesis of these materials was avoided, and the volume of reagents, solvents and energy was reduced. Furthermore, the immobilization of the

MIP on the surface of filter paper increased the versatility of this support, allowing its coupling to different techniques, such as a fluorimeter cell via a custom-built magnetic piece.

On the other hand, the synthesis of **filter paper modified with nanoparticles** is a multiple-step simple procedure that leads to the obtention of silver nanoflowers. The immobilization of silver nanoflowers (AgNFs) on filter paper was carried out via the previous functionalization of the surface of paper with metallic silver and ethylenediamine, which acted as a bridge for the anchorage of AgNFs. In addition, a previous coating of nylon-6 was also necessary to assure the surface availability of the analyte and hence its appropriate determination.

Finally, the potential of **non-modified filter paper** as a sorbent was evaluated. Owing to the chemical structure of cellulose, its interaction with the analytes was possible, thus allowing the efficient isolation of the analytes from the sample matrix. This approach enables a completely environmentally friendly synthesis, thus being in line with the principles of Green Chemistry, since no reagents or solvents are needed.

The **characterization** of the different paper-based flat supports obtained in this Doctoral Thesis was accomplished employing various instrumental techniques that provided information on their morphology and composition. Consequently, it was possible to explain the interactions between the support and the analyte. The employed techniques were scanning electron microscopy (SEM), Raman spectroscopy and infrared spectroscopy (ATR-FTIR).

- SEM micrographs revealed the coverage of the surface of the paper with the MIP and how the structure of cellulose was flattened as the amount of MIP increased. Furthermore, it allowed to elucidate the morphology of AgNFs.
- Raman spectroscopy demonstrated the need of a previous coating with nylon-6 of the paper modified with AgNFs to assure the appropriate determination of the analyte, and also allowed the qualitative and quantitative evaluation of the

applicability of this substrate. On the other hand, it also provided information on the composition of the obtained paper-based flat supports.

- Regarding ATR-FTIR, this technique enabled the evaluation of the characteristic bands of filter paper and the MIP, observing an increase of the intensity of the bands as the concentration of the polymer increased.

As for the **extraction** process, the objective was to simplify it, and in some cases a high throughput has been achieved, since multiple extractions were performed simultaneously using Eppendorf tubes and an orbital stirrer. Furthermore, the extraction was also miniaturized, as a low amount of sample were employed. However, full automation of the process was not possible, which would be convenient to avoid the human error associated to the sample treatment step.

The methodologies already deeply discussed throughout this Doctoral Thesis have been applied for the determination of analytes in **biological samples** (saliva) and **food products** (soft drinks and beer), achieving appropriate values of sensitivity and precision according to the instrumental technique employed in each case.

The use of saliva as matrix for the determination of compounds is a good alternative compared to the other biological samples, since no specialized personnel is required for its collection. Moreover, the collection procedure is non-invasive—compared to hair, or blood—and can be closely supervised to avoid the potential adulteration of the sample. On the other hand, the storage of saliva does not require special measures, which facilitated its analysis. It is also appropriate for the demonstration of the applicability of the obtained paper-based flat supports, since it contains enough interferents to challenge the performance of the extraction procedure. One non-steroidal antiinflamatory drug (ketoprofen) and two drugs of abuse (cocaine and methamphetamine) were determined in this matrix. Regarding ketoprofen, the extraction was carried out employing a filter paper modified with AgNFs, and the determination was performed via Surface Enhanced Raman Spectroscopy (SERS) and paper-spray mass spectrometry (PS-MS). As for cocaine and methamphetamine, a MIP paper was employed for the isolation of the analytes, which were

subsequently determined via direct infusion MS.

In the case of food products, the intrinsic fluorescence of quinine was exploited for its determination in soft drinks via fluorimetry by means of a MIP PAD as sorbent. On the other hand, the potential of non-modified cellulose was evaluated for the extraction of biogenic amines from beer samples via direct infusion MS.

The instrumental techniques employed on the different investigations carried out in this Doctoral Thesis enabled the simple and rapid obtention of results. Fluorimetry provided results within 40 s, which allowed the determination of multiple samples in a reduced amount of time. On the other hand, direct infusion MS avoids chromatographic separations, thus simplifying the entire analytical process while maintaining its high selectivity. Regarding SERS, this technique is an alternative to traditional Raman spectroscopy based on the increase of the Raman signal as a consequence of the confinement of the electromagnetic field in certain regions of the substrate modified with metallic nanoparticles known as hot spots. Therefore, SERS eludes the disadvantages of Raman spectroscopy and emerges as a ideal choice for the development of rapid, simple and highly sensitive methodologies. Finally, PS-MS enables the direct determination of the analytes, avoiding further sample preparation, which simplifies considerably the analytical process.

ANEXOS

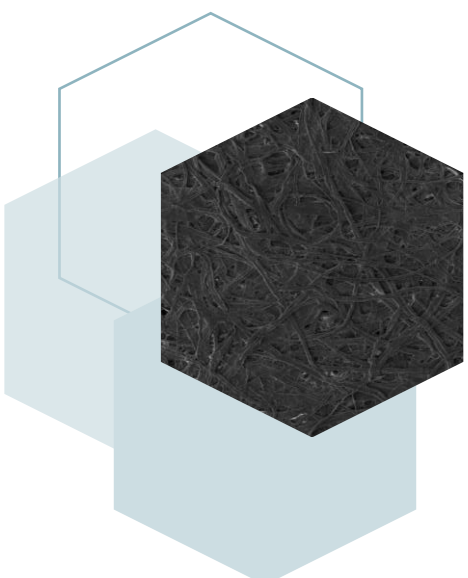

Anexo A

Publicaciones científicas de la Tesis Doctoral

1. Molecularly imprinted paper-based analytical device obtained by a polymerization-free synthesis

M. C. Díaz-Liñán, A. I. López-Lorente, S. Cárdenas, R. Lucena

Sensors and Actuators B: Chemical, 2019, *287, 138-146*

https://doi.org/10.1016/j.snb.2019.02.048

2. Particle loaded membranes

M. C. Díaz-Liñán, A. I. López-Lorente, R. Lucena, S. Cárdenas

Solid-Phase Extraction, 2020, *341-354 (Capítulo de libro)*

https://doi.org/10.1016/B978-0-12-816906-3.00012-1

3. Silver nanoflower-coated paper as a dual substrate for surface-enhanced Raman spectroscopy and ambient pressure mass spectrometry analysis

M. C. Díaz-Liñán, M. T. García-Valverde, A. I. López-Lorente, S. Cárdenas, R. Lucena

Analytical and Bioanalytical Chemistry, 2020, *412 (15), 3547-3557*

https://doi.org/10.1007/s00216-020-02603-x

4. Paper-based sorptive phases for microextraction and sensing

M. C. Díaz-Liñán, M. T. García-Valverde, R. Lucena, S. Cárdenas, A. I. López-Lorente

Analytical Methods, 2020, *12 (24), 3074-3091*

https://doi.org/10.1039/D0AY00702A

5. Dual-template molecularly imprinted paper for the determination of drugs of abuse in saliva samples by direct infusion mass spectrometry

M. C. Díaz-Liñán, M. T. García-Valverde, R. Lucena, S. Cárdenas, A. I. López-Lorente

Microchemical Journal, 2021, *160, 105686*

https://doi.org/10.1016/j.microc.2020.105686

6. Unmodified cellulose filter paper, a sustainable and affordable sorbent for the isolation of biogenic amines from beer samples

M. C. Díaz-Liñán, R. Lucena, S. Cárdenas, A. I. López-Lorente

Journal of Chromatography A, 2021, *1651, 462297*

DOI: https://doi.org/10.1016/j.chroma.2021.462297

7. Selectivity-enhanced sorbents

M. C. Díaz-Liñán, G. Lasarte-Aragonés, A. I. López-Lorente, R. Lucena, S. Cárdenas

Analytical Sample Preparation with Nano- and other High-Performance Materials, 2021, *229-252 (Capítulo de libro)*

In press.

Anexo B

Actividades de divulgación científica

1. Participación en el "Paseo por la Ciencia" en las ediciones de 2014, 2017, 2018 y 2019.

2. Participación en la "Noche Europea de los Investigadores" en la edición de 2018.

3. Participación en el "II Campus de Investigación de la Universidad de Córdoba" como profesora del proyecto "¿Cuánta cafeína consumimos? Determinación de cafeína y alcaloides en bebidas" en la edición de 2018.

4. Participación en las "XII Jornadas de Introducción al Laboratorio Experimental de Química" del 5º Plan Anual de Captación de Estudiantes (PACE) dirigido a Institutos de Educación Secundaria y Centros Docentes Privados en la edición de 2019.

5. Publicación de una entrada en el blog *Microextraction Tech.* Disponible en: https://microextraction.blogspot.com/2020/04/silver-nanoflower-coated-paper-as-dual.html

Anexo C

Comunicaciones a congresos

1. Comunicación flash y póster

M. C. Díaz-Liñán, A. I. López-Lorente, S. Cárdenas, R. Lucena

Silver-nanoflower paper-based analytical device for Surface Enhanced Raman Spectroscopy

VII Encuentro sobre Nanociencia y Nanotecnología (NanoUCO), Córdoba, enero de 2019

2. Póster

M. C. Díaz-Liñán, A. I. López-Lorente, S. Cárdenas, R. Lucena

Silver-nanoflower paper-based analytical device for Surface Enhanced Raman Spectroscopy

IX International Congress on Analytical Nanoscience and Nanotechnology (NyNA), Zaragoza, julio de 2019

3. Oral

M. C. Díaz-Liñán, M. T. García-Valverde, A. I. López-Lorente, S. Cárdenas, R. Lucena

Soporte modificado con nanoflores de plata para la determinación de ketoprofeno mediante espectrocopia Raman amplificada en superficie y espectrometría de masas con paper-spray

VIII Congreso Científico de Investigadores en Formación, Córdoba, febrero de 2020

4. Póster

M. C. Díaz-Liñán, M. T. García-Valverde, A. I. López-Lorente, S. Cárdenas, R. Lucena

Silver nanoflower-coated paper for the determination of ketoprofen via Surface Enhanced Raman Spectroscopy and ambient pressure paper spray mass spectrometry

Virtual Raman Imaging Poster Summit, International Conference for Chemical Characterization & Imaging, Córdoba, octubre de 2020

5. Comunicación flash y póster

M. C. Díaz-Liñán, M. T. García-Valverde, R. Lucena, S. Cárdenas, A. I. López-Lorente

Determination of drugs of abuse in saliva samples via dual-template molecularly imprinted paper and direct infusion mass spectrometry

1st European Sample Preparation e-Conference, Córdoba, marzo de 2021

Silver-Nanoflower Paper-based Analytical Device for Surface Enhanced Raman Spectroscopy

María del Carmen Díaz-Liñán, Ángela I. López-Lorente, Soledad Cárdenas, Rafael Lucena

Departamento de Química Analítica, Instituto Universitario de Nanoquímica (IUNAN), Universidad de Córdoba, Campus de Rabanales, Edificio Marie Curie Anexo, E-14071 Córdoba, España
q32dilim@uco.es

Introduction

Recently, plasmonic nanoparticles of different nature, e.g. gold and silver, have attracted substantial interest in plasmonics, photonics, biomedical field as well as optical sensing and surface enhanced vibrational spectroscopies, owing to their exceptional properties. Metal nanoparticles with sharped edges show the so called "hot spots" which lead to strong electromagnetic field confinement, thus significantly increasing the low interaction cross sections observed in vibrational spectroscopies such as Raman spectroscopy. Nanoparticles of different nature and geometries have been used in surface enhanced Raman spectroscopy (SERS) including spherical nanoparticles, nanorods, nanostars, among others.
On the other hand, the development of paper-based analytical devices (PADs) has increased in the last years thanks to the advantages of cellulose paper as substrate, such as its availability, versatility, easy handling and cost effectiveness.

Synthesis of AgNFs PADs

Modification of the paper strip to **obtain the PADs** was carried out as follows:

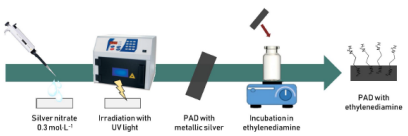

Figure 1. Paper strips modification process

The synthesis of the **AgNFs and their attachment on the PADs** was carried out as follows:

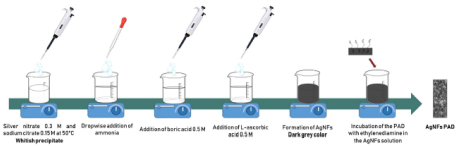

Figure 2. AgNFs synthesis and attachment processes

SEM characterization

The **surface of the Ag-NFs PADs** were characterized by SEM.
As can be seen in Figure 3(c), **the nanoparticles present multiple petals**, which increase the intensity of the peaks by acting as "**hot spots**".

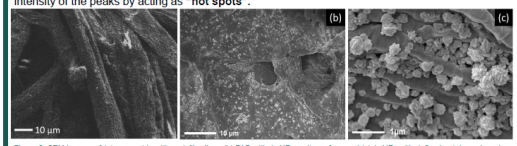

Figure 3. SEM images of (a) paper strip with metallic silver, (b) PAD with AgNFs on its surface and (c) AgNFs with defined petals anchored on PAD surface

Irradiation time

The **irradiation time** was optimized by irradiating with UV light different paper strips with the same amount of silver nitrate 0.1 mol·L⁻¹ at different periods of time.

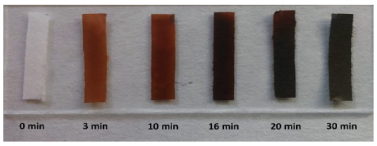

Figure 4. Paper strips after irradiation with UV light at different times

Optimization of experimental conditions

In order to obtain the highest peak intensity, the Raman **integration time** was evaluated.

❖ **Range: 1 to 180 seconds**

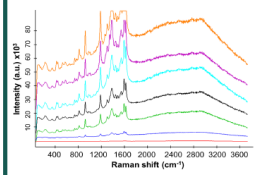

Figure 5. Raman spectra of crystal violet (CV) obtained at different integration times (CV concentration: 10 mol·L⁻¹).

Ethylenediamine is employed to bind the AgNFs at the surface of the PAD.

❖ **Range studied: 1 to 10 mM**

No significant differences are observed.

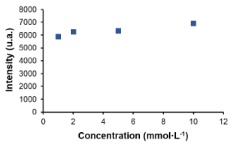

Figure 6. Intensity of the Raman peak of CV at 1183 cm⁻¹ in the range of 1 to 10 mM of ethylenediamine.

Crystal Violet

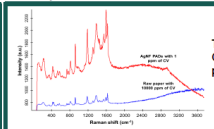

The intensity of the Raman signal of CV is increased when AgNFs are present.

Figure 7. Comparison of Raman and SERS spectra of CV deposited on raw paper and AgNF PAD, respectively.

Crystal Violet is used as model SERS probe for the first studies.

❖ **Range of concentration studied: 0.5 to 10 mg·L⁻¹**

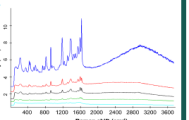

Figure 8. SERS spectra of crystal violet at different concentrations

Conclusions

I **A Silver-Nanoflower Paper-based Analytical Device** has been synthesized providing surface enhanced Raman scattering.

II SEM images show a **good coverage** of the surface of the PAD as well as a **well defined petal structure** of the silver nanoflowers.

III To anchor the AgNFs, the PADs previously modified by UV reduction of $AgNO_3$ to metallic silver were overnight incubated in a solution of **ethylenediamine.**

IV **A significant increase of the Raman signal** of crystal violet is obtained when compared to that in raw filter paper at much higher concentration.

Agradecimientos
The authors wish to thank Spanish Ministry of Economy, Industry and Competitiveness for funding project CTQ2017-83175-R. The authors also thank the Central Service for Research Support (SCAI) of the University of Córdoba for the service provided to obtain the SEM images.

Silver-Nanoflower Paper-based Analytical Device for Surface Enhanced Raman Spectroscopy

María del Carmen Díaz-Liñán, Ángela I. López-Lorente, Soledad Cárdenas, Rafael Lucena

Departamento de Química Analítica, Instituto Universitario de Nanoquímica (IUNAN), Universidad de Córdoba, Campus de Rabanales, Edificio Marie Curie Anexo, E-14071 Córdoba, España
q32dilim@uco.es

Introduction

Surface enhanced Raman spectroscopy (SERS) is a vibrational technique of increasing interest in contemporary analytical spectroscopy. A variety of SERS substrates have been prepared mainly based on the use of noble metal nanomaterials, among which gold and **silver nanoparticles** are included. Nanoparticles of different nature and geometries have been used in SERS, including spherical nanoparticles, nanorods, nanostars, among others.

Two enhancing mechanisms, namely **electromagnetic** and **chemical** are thought to contribute to the significant increase of the low interaction cross sections observed in vibrational spectroscopy. In order to boost this increase, **metal nanoparticles with sharped edges** have been employed as SERS enhancers, since they create a large number of the so called **"hot spots"** which lead to strong electromagnetic field confinement.

On the other hand, **conventional filter paper** has attracted attention in the last years thanks to the advantages of cellulose paper, i.e. easy handling, versatility, disposability and cost effectiveness, among others.

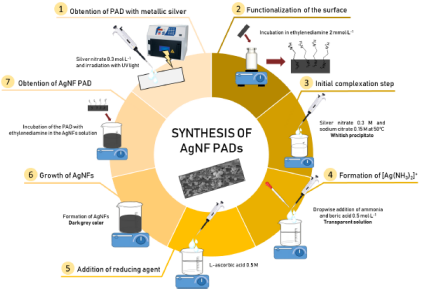

Figure 1. Paper strips modification and AgNFs synthesis processes

Optimization of experimental conditions

In order to obtain the highest peak intensity, the Raman **integration time** was evaluated.

❖ **Range: 1 to 180 seconds**

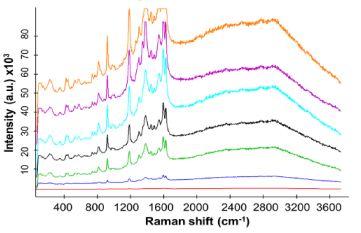

Figure 2. Raman spectra of crystal violet (CV) obtained at different integration times (CV concentration: 10 mol·L⁻¹)

The **irradiation time** was optimized by irradiating with UV light different paper strips after deposition of 20 µL of a 0.1 mol·L⁻¹ silver nitrate solution at different periods of time.

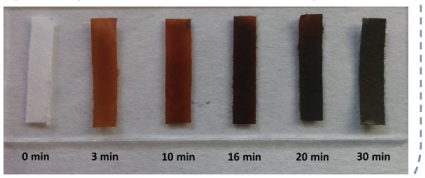

Figure 3. Paper strips after irradiation with UV light at different times

SEM characterization

The **surface of the Ag-NFs PADs** were characterized by SEM.
As can be seen in Figure 4(c), **the nanoparticles present multiple petals**, which increase the intensity of the peaks by acting as **"hot spots"**.

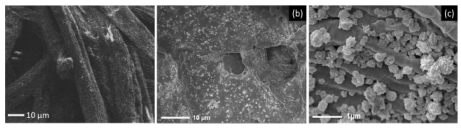

Figure 4. SEM images of (a) paper strip with metallic silver, (b) PAD with AgNFs on its surface and (c) AgNFs with defined petals anchored on PAD surface

Raman measurements and SERS effect

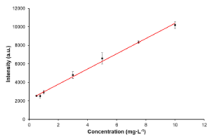

A calibration graph was built by drop casting different concentrations of CV onto AgNF PADs in the range of 0.5-20 mg·L⁻¹.
Concentrations above 10 mg·L⁻¹ resulted in saturation, so the linear range represented in Figure 5 was studied.

Figure 5.Calibration graph of AgNF PADs with CV at different concentrations

The intensity of the Raman signal of CV is increased when AgNFs are present.

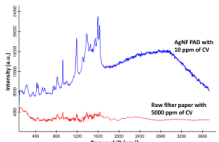

Figure 6. Comparison of Raman and SERS spectra of CV deposited on raw paper and AgNF PAD, respectively.

Conclusions

I **A Silver-Nanoflower Paper-based Analytical Device** has been synthesized providing surface enhanced Raman scattering.

II SEM images show a **good coverage** of the surface of the PAD as well as a **well defined petal structure** of the silver nanoflowers.

III To anchor the AgNFs, the PADs previously modified by UV reduction of $AgNO_3$ to metallic silver were overnight incubated in a solution of **ethylenediamine.**

IV **A significant increase of the Raman signal** of crystal violet is obtained when compared to that in raw filter paper at much higher concentration.

Acknowledgements
The authors wish to thank Spanish Ministry of Economy, Industry and Competitiveness for funding project CTQ2017-83175-R. The authors also thank the Central Service for Research Support (SCAI) of the University of Córdoba for the service provided to obtain the SEM images.

IUNAN IX NyNA 2019

P-150

SILVER NANOFLOWER-COATED PAPER FOR THE DETERMINATION OF KETOPROFEN VIA SURFACE ENHANCED RAMAN SPECTROSCOPY AND AMBIENT PRESSURE PAPER SPRAY MASS SPECTROMETRY

María del Carmen Díaz-Liñán, María Teresa García-Valverde, Ángela I. López-Lorente, Soledad Cárdenas, Rafael Lucena

Departamento de Química Analítica, Instituto Universitario de Nanoquímica (IUNAN), Universidad de Córdoba, Campus de Rabanales, Edificio Marie Curie Anexo, E-14071 Córdoba, España
q32dilim@uco.es

Introduction

Paper-based analytical devices (PADs) have gained great attention in the last years due to their numerous advantages, such as **low price, versatility and availability**[1]. Furthermore, its **easy handling** facilitates the coupling to different instrumental techniques. In this context, **a dual substrate for both SERS and ambient pressure paper spray mass spectrometry (PS-MS)** based on the modification of filter paper with **silver nanoflowers (AgNFs)** has been developed. The densely packed petals of the AgNFs led to a great amount of hot spots, resulting in an **enhancement of the Raman signal**. In addition, AgNFs also provided a **higher sensitivity on the PS-MS analysis** compared to bare paper and ny/Ag-paper, since this technique is based on a difference of potential[2].

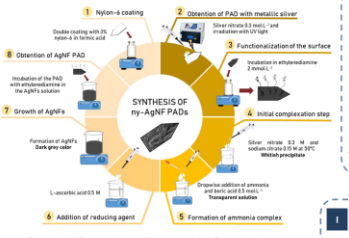

Figure 1. (a) Paper strips modification and AgNFs synthesis processes.

Results and discussion

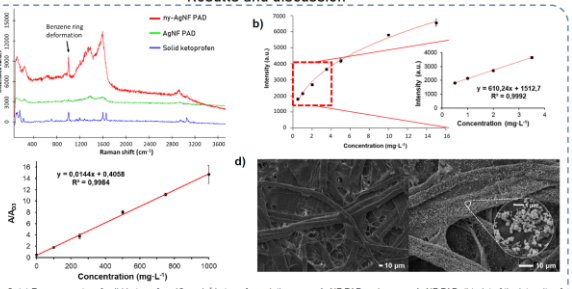

Figure 2. (a) Raman spectra of solid ketoprofen, 10 mg L^{-1} ketoprofen solution on an AgNF PAD and on a ny-AgNF PAD, (b) plot of the intensity of the band at 1000 cm^{-1} in the SERS spectrum of ketoprofen vs. concentration of aqueous standards, (c) relation of areas of ketoprofen standards and the isotope-labelled IS vs. concentration in saliva samples, and (d) SEM micrographs of raw filter paper (left) and ny-AgNF PAD (right).

Conclusions

I. **A Silver nanoflower-coated paper** has been synthesized providing SERS effect and improved sensitivity in PS-MS.

II. **Nylon-6 and ethylenediamine** ensured the surface availability of ketoprofen and acted as an anchor point for the AgNFs, respectively.

III. The AgNF PADs containing nylon-6 showed a **higher SERS effect** compared to those without it.

IV. ny-AgNF PADs were successfully employed for the **determination of ketoprofen in saliva spot samples.**

References

[1] Jiang, X.; Fan Z.H. *Annual Rev. Anal. Chem.*, **2016**, *9*, 203.

[2] Wang, H.; Liu, J; Graham Cooks, R.; Ouyang, Z. *Angewandte*, **2010**, *122*, 889.

P3

Determination of Drugs of Abuse in Saliva Samples via Dual-Template Molecularly Imprinted Paper and Direct Infusion Mass Spectrometry

Departamento de Química Analítica, Instituto Universitario de Nanoquímica (IUNAN), Universidad de Córdoba, Campus de Rabanales, Edificio Marie Curie Anexo, E-14071 Córdoba, España
q32dilim@uco.es

Introduction

The field of sample pretreatment is of high importance in order to suppress the so-called matrix effect derived from complex matrices, however, it is also the most time-consuming step of the analytical procedure. For this reason, this discipline has been deeply investigated in the last decades in order to create new strategies that allow rapid and reliable procedures. In this context, paper has emerged as a very promising material due to its multiple advantages, such as the possibility of retaining compounds on its cellulose fibers or the spontaneous fluidic transport based on its own capillary action. In addition, it is a highly available and cost-effective material that can be easily coupled to various instrumental devices thanks to its flexibility and portability; and also be chemically modified to broaden its application scope [1].

On the other hand, although the selectivity of the method is improved, chromatographic separation significantly increases the analysis time. Even so it is usually mandatory prior to mass spectrometry to avoid matrix effect problems. However, this step can be avoided by previously isolating the analytes from the interferences via the use of sorbents.

The design of a new sorbent is a tedious process in which selectivity must be deeply considered. In the last decades, the molecularly imprinting technology has been consolidated and numerous approaches concerning molecularly imprinted polymers (MIPs) have been published [2, 3]. These materials possess artificially generated recognition sites towards a control molecule or a structural-related analogue, thus being able to isolate a certain compound while getting rid of the interferences.

In this context, a dual-template molecularly imprinted paper has been developed for the determination of drugs of abuse in saliva samples by direct infusion mass spectrometry (DI-MS). The MIP paper was obtained by dip-coating the paper with a polymeric solution (nylon-6 in formic acid) containing the templates, i.e., cocaine (CO) and methamphetamine (MTA). When the solvent evaporates, the polymer chains rearrange surrounding the templates, leaving the empty cavities once the MIP is washed. The as-synthesized MIP paper showed a better performance compared to the non-imprinted polymer and exhibited better affinity towards the analytes than for 6-acetylmorphine. Also, since the extraction is performed in an Eppendorf tube, multiple samples can be extracted simultaneously, thus increasing the sample throughput.

Conclusions

I. A **dual template MIP paper** has been synthesized for the simple and rapid determination of CO and MTA via DI-MS.

II. The MIP papers showed **better adsorption ability** compared to the non-imprinted ones.

III. Since common filter paper is employed, the versatility of the material increases.

IV. **A high throughput** is achieved since multiple extractions can be performed simultaneously.

References

[1] E.W. Nery, L.T. Kubota, Sensing Approaches on Paper-Based Devices: A Review, Anal. Bioanal. Chem. 405 (2013) 7573-7595.

[2] M.C. Díaz-Liñán, A.I. López-Lorente, S. Cárdenas, R. Lucena, Molecularly Imprinted Paper-Based Analytical Device Obtained by a Polymerization-Free Synthesis, Sens. Actuators B Chem. 287 (2019) 138-146.

[3] P. Kadhirvel, A. Combes, L. Bordron, V. Pichon, Development and Application of Water-Compatible Molecularly Imprinted Polymers for the Selective Extraction of Carbamazepine from Environmental Waters, Anal. Bioanal. Chem. 411 (2019) 1525-1536.

Experimental procedure

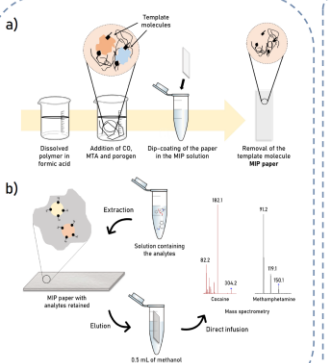

Figure 1. Scheme of a) synthesis of the MIP papers and b) extraction and determination of CO and MTA

Results and discussion

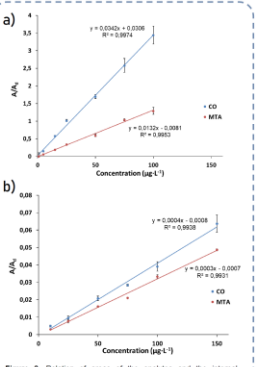

Figure 2. Relation of areas of the analytes and the internal standards vs. concentration after extraction from a) aqueous standards and b) diluted saliva samples.

ACRÓNIMOS

ABBREVIATIONS

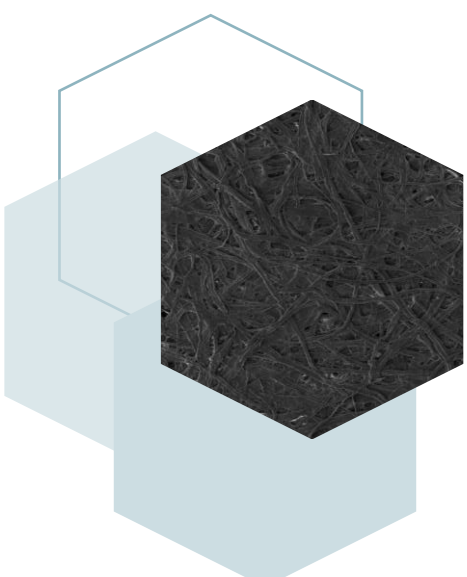

1OHP	1-hydroxypyrene/ 1-hidroxipireno
1PG	1-pyreneglucuronide/ 1-pireno glucurónido
2D	Two dimensional/ Bidimensional
3BPG	3-benzo(a)pyrene-glucuronide/3-benzo(a)pireno glucurónido
3D	Three dimensional/ Tridimensional
6-AM	6-acetylmorphine/ 6-acetilmorfina
8-HQ	8-hydroxyquinoline/ 8-hidroxiquinolona
AA	Amylamine/ Amilamina
Ab	Antibody/ Anticuerpo
ABTS	2' - azino - bis (3 – ethylbenzothiazoline - 6 - sulfonic acid) diammonium salt
AC	Analytical chemistry/ Química analítica
AFP	Alphafetoprotein/ Alfafetoproteína
AGM	Agmatine/Agmatina
AgNFs	Silver nanoflowers/ Nanoflores de plata
AgNPs	Silver nanoparticles/ Nanopartículas de plata
ANOVA	Analysis of variance/ Análisis de varianza
AOX	Alcohol oxidase/ Alcoholoxidasa
ATR-IR	Attenuated total reflection infrared/ Espectroscopía infrarroja de reflexión total atenuada
AuNPs	Gold nanoparticles/ Nanopartículas de oro
BA	Butylamine/ Butilamina
BAs	Biogenic amines/ Aminas biogénicas
BDD	Box-Behnken design/ Diseño factorial de Box-Behnken
BPA	Bisphenol A/ Bisfenol A
CAD	Cadaverine/ Cadaverina
CDs	Carbon dots
CE (Capítulo 1)	Counter electrode/ Electrodo auxiliar
CE	Capillary electrophoresis/ Electroforesis capilar
CEA	Carcinoembryonic antigen/ Antígeno carcinoembriónico

CFU	Colony forming units/ Unidades de formación de colonia
CID	Collision-induced dissociation/ Disociación inducida por colisión
CNMs	Carbon nanomaterials/ Nanomateriales de carbono
CNTs	Carbon nanotubes/ Nanotubos de carbono
CO	Cocaine/ Cocaína
CoPc	Cobalt phthalocyanine/ Ftalocianina de cobalto
COVID-19	Coronarivus disease/ Enfermedad del coronavirus
CTA	Cellulose triacetate/ Triacetato de celulosa
CTAB	Hexadecyltrimethylammonium bromide/ Bromuro de hexaldeciltrimetilamonio
CV (Capítulo 7)	Crystal violet/ Violeta cristal
CV	Cyclic voltammetry/ Voltametría cíclica
DAD	Diode array detector/ Detector de diodos en fila
DAP	1,3-diaminopropane/ 1,3-diaminopropano
DART	Direct analysis in real-time/ Análisis directo en tiempo real
DBS	Dried blood spots/ Muestras de sangre seca
DEA	Diethylamine/ Dietilamina
DESI	Desorption electrospray ionization/ Ionización por desorción mediante electrospray
DI	Direct immersion/ Inmersión directa
DI (Capítulo 5)	Direct infusion/ Infusión directa
DMA	Dimethylamine/ Dimetilamina
DMF	Dimethylformamide/ Dimetilformamida
DMFA (Capítulo 4)	Dimethylformamide/ Dimetilformamida
DNA	Deoxyribonucleic acid/ Ácido desoxirribonucleico
DPV	Differential pulse voltammetry/ Voltametría de pulso diferencial
dSPE	Dispersive solid phase extraction/ Extracción en fase sólida dispersiva
DSS	Dried saliva spots/ Muestras de saliva seca
DUADLLME	Derivatization ultrasound-assisted dispersive liquid-liquid

	microextraction/ Microextracción líquido-líquido dispersiva asistida mediante ultrasonidos y derivatización
E2	17β-Estradiol/ 17β-Estradiol
EA	Ethylamine/ Etilamina
EE2	Ethinylestradiol/ Etinilestradiol
EF	Enhancement factor/ Factor de incremento
EGb	Ginkgo biloba extract/ Extracto de ginkgo biloba
EIS	Electrochemical impedance spectroscopy/ Espectroscopía de impedancia electroquímica
ePADs	Electrochemical paper-based analytical devices/ Dispositivos analíticos basados en papel electroquímicos
ESI	Electrospray ionization/ Ionización por electrospray
ESM	Electronic Supplementary Material/ Material suplementario electrónico
ETA	Ethanolamine/ Etanolamina
Eu-DPA	Eu-dipicolinic acid/ Ácido Eu-dipicolínico
FD	Fluorescence detection/ Detection de fluorescencia
FID	Flame ionization detection/ Detección de ionización de llama
FMA	Fluorescein mercury acetate/ Acetato de mercurio fluoresceína
GAC	Green Analytical Chemistry/ Química analítica verde
GC	Gas chromatography/ Cromatografía de gases
GDME	Gas-diffusion microextraction/ Microextracción por difusión de gas
GO	Graphene oxide/ Óxido de grafeno
GOD	Glucose oxidase/ Glucosaoxidasa
HEA	Hexylamine/ Hexilamina
HF	Hollow fiber/ Fibra hueca
HF-LPME	Hollow fiber liquid phase microextraction/ Microextracción en fase líquida mediante fibra hueca
HILIC	Hydrophilic interaction liquid chromatography/ Cromatografía de

	líquidos por interacción hidrofílica
HIS	Histamine/ Histamina
HLPME	Headspace liquid-phase microextraction/ Microextracción en fase líquida en espacio de cabeza
HMDA	Hexamethylenediamine/ Hexametilendiamina
HMF	Hydroxymethylfurfural/ Hidroximetilfurfural
HPLC	High-performance liquid chromatography/ Cromatografía de líquidos de alta resolución
HPV	Human papilloma virus/ Virus del papiloma humano
HRP	Horseradish peroxidase/ Peroxidasa de rábano picante
IAC	Immunoaffinity chromatography/ Cromatografía de inmunoafinidad
IE	Immunoextraction/ Inmunoextracción
IL-UALLME	Ionic liquid-based ultrasound-assisted liquid-liquid microextraction/ Microextracción líquido-líquido basada en líquidos iónicos asistida por ultrasonidos
IMS	Ion mobility spectrometry/ Espectrometría de movilidad iónica
IR	Infrared/ Infrarrojo
IS (Capítulo 3)	Immunosorbent/ Inmunosorbente
IS	Internal standard/ Estándar interno
isoAA	Isoamylamine/ Isoamilamina
isoBA	Isobutylamine/ Isobutilamina
isoPA	Isopentylamine/ Isopentilamina
isoPPA	Isopropylamine/ Isopropilamina
LC	Liquid chromatography/ Cromatografía de líquidos
LCP	Liquid-crystal polymer/ Polímero de cristal líquido
LED	Light-emitting diode/ Diodo de emisión de luz
LIF	Laser induced fluorescence/ Fluorescencia inducida por láser
LOD	Limit of detection/ Límite de detección
LOQ	Limit of quantification/ Límite de cuantificación

LSPR	Localized surface plasmon resonance/ Resonancia del plasmón superficial
LSV	Linear sweep voltammetry/ Voltametría de barrido lineal
MA	Methylamine/ Metilamina
MAb	Monoclonal antibody/ Anticuerpo monoclonal
MBA	2-methylbutylamine/ 2-metilbutilamine
MEPS	Microextraction in packed sorbent/ Microextracction en sorbente empaquetado
MERS-CoV	Middle east respiratory syndrome coronavirus/ Síndrome respitatorio de Oriente Medio
MF	Morfoline/ Morfolina
MGF	Mesoporous graphene foams/ Espumas de grafeno mesoporoso
MIL-DLLME	Magnetic ionic liquid-dispersive liquid-liquid microextraction/ Microextracción líquido-líquido dispersiva con líquido iónico magnético
MIMs	Molecularly imprinted membranas/ Membranas impresas molecularmente
MINCMs	Molecularly imprinted nanocomposite membranes/ Membranas nanocomposite impresas molecularmente
MIPNPs	Molecularly imprinted polymer nanoparticles/ Nanopartículas impresas molecularmente
MIPs	Molecularly imprinted polymers/ Polímeros de impresión molecular
MNPs	Magnetic nanoparticles/ Nanopartículas magnéticas
MOF	Metal organic framework/ Estructura metal-orgánica
mPADs	Microfluidics paper-based analytical devices/ Dispositivos analíticos basados en papel microfluídicos
MS	Mass spectrometry/ Espectrometría de masas
MS/MS	Tandem mass spectrometry/ Espectrometría de masas en tandem
MSNs	Mesoporous silica nanoparticles/ Nanopartículas de sílice

	mesoporosa
MSPE	Magnetic solid phase extraction/ Extración en fase sólida magnética
MTA	Methamphetamine/ Metanfetamina
MTB	Mycobacterium tuberculosis/ Tuberculosis por mycobacterium
MWCNTs	Multi-walled carbon nanotubes/ Nanotubos de carbono multicapa
NIP	Non-imprinted polymer/ Polímero no impreso molecularmente
NPs	Nanoparticles/ Nanopartículas
ny	Nylon-6/ Nailon-6
OCT	Octopamine/ Octopamina
o-MWNTs	Oxidized multiwalled carbon nanotubes/ Nanotubos de carbono multicapa oxidados
OS	Oligosorbent/ Oligosorbente
o-SWNHs	Oxidized single-walled carbon nanohorns/ Nanocuernos de carbono monocapa oxidados
OTA	Ochratoxin A/ Ocratoxina A
PA	Propylamine/ Propilamina
PAA	Poly(acrylic acid)/ Poli(ácido acrílico)
PAb	Polyclonal antibody/ Anticuerpo policlonal
PADs	Paper-based analytica devices/ Dispositivos analíticos basados en papel
PAHs	Polycyclic aromatic hydrocarbons/ Hidrocarburos policíclicos aromáticos
PANI	Polyaniline/ Polianilina
PBS	Phosphate buffered saline/ Buffer fosfato salino
PD	Pyrrolidine/ Pirrolidina
PDA	Polydopamine/ Polidopamina
PEBA	Polyether-polyamide block copolymer/ Copolímero en bloque de poliéter-poliamida
PET	Poly(ethylene terephthalate)/ Poli(tereftalato de etileno)

PHE	Phenylethylamine/ Feniletilamina
PIL	Polymeric ionic liquid/ Líquido iónico polimérico
POC	Point-of-care/ Punto de atención
PP	Piperidine/ Piperidina
PS (Capítulo 1)	Paper-spray
PS	Polystyrene/ Poliestireno
PS-MS	Paper-spray mass spectrometry/ Espectrometría de masas con paper-spray
PTA-NH_2	2-aminopththalic acid/ Ácido 2-aminoftálico
PUT	Putrescine/ Putrescina
PVA	Poly(vinyl alcohol)/ Poli(vinilalcohol)
PVDF	Poly(vinylidene fluoride)/ Poli(fluoruro de vinilideno)
PVPP	Polyvinylpolypyrrolidone/ Polivinilpolipirrolidona
QDs	Quantum dots/ Puntos cuánticos
RACNTs	Restricted access carbon nanotubes/ Nanotubos de carbono de acceso restringido
RAMIPs	Restricted access molecularly imprinted polymers/ Polímeros impresos molecularmente de acceso restringido
RAMs	Restricted access materials/ Materiales de acceso restringido
RE	Reference electrode/ Electrodo de referencia
RGB	Red green blue color code/ Codificación de color rojo verde azul
RNA	Ribonucleic acid/ Ácido ribonucleico
RPLC	Reversed phase liquid chromatography/ Cromatografía líquida de fase reversa
RSD	Relative standard deviation/ Desviación estándar relativa
RSM	Response surface methodology/ Metodología de superficie de respuesta
S/N	Signal to noise ratio/ Relación señal-ruido
SCAI	Central service for research support/ Servicio central de apoyo a la investigación

SEM	Scanning electron microscopy/ Microscopía de barrido electrónico
SERS	Surface enhaced Raman spectroscopy/ Espectroscopia Raman amplificada en superficie
SLG	Single layer graphene/ Grafeno unilaminar
SPD	Spermidine/ Espermidina
SPE	Solid phase extraction/ Extracción en fase sólida
SPION	Superparamagnetic iron oxide nanoparticles/ Nanopartículas de óxido de hierro superparamagnético
SPME	Solid phase microextraction/ Microextracción en fase sólida
SPR	Spermine/ Espermina
SRM	Selected reaction monitoring/ Monitorización de la reacción seleccionada
SUPRASs	Supramolecular solvents/ Disolventes supramoleculares
SWASV	Square-wave anodic stripping voltammetry/ Voltametría de resolución anódica de onda cuadrada
SWCNHs	Single-wall carbon nanohorns/ Nanocuernos de carbono monocapa
SWCSV	Square-wave cathodic stripping voltammetry/ Voltametría de resolución catódica de onda cuadrada
SWV	Square wave voltammetry/ Voltametría de onda cuadrada
TFME	Thin-film microextraction/ Microextracción en capa fina
THF	Tetrahydrofuran/ Tetrahidrofurano
TRP	Tryptamine/ Triptamina
TYR	Tyramine/ Tiramina
UHPLC	Ultra-high performance liquid chromatography/ Cromatografía de líquidos de ultra alta resolución
USB	Universal serial bus/ Memoria USB
UV	Ultraviolet detection/ Detección ultravioleta
VSLLME	Vortex-assisted surfactant-enhanced emulsification liquid-liquid microextraction/ Microextracción líquido-líquido con emulsión

	amplificada mediante surfactante asistida por vórtex
WAC	White Analytical Chemistry/ Química analítica blanca
WE	Working electrode/ Electrodo de trabajo